1st International Mass Spectrometry Imaging Society Conference

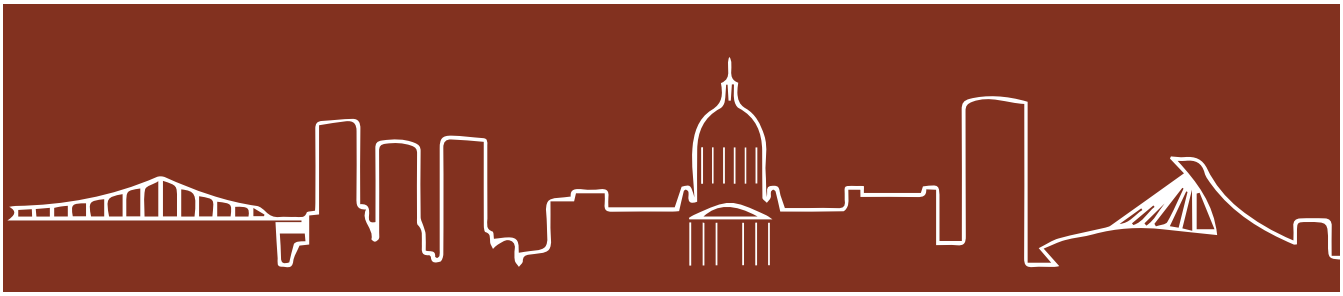

October 23-25, 2023.

Centre Mont-Royal, 2200 rue Mansfield, Montreal, QC Canada

2023

PROGRAM

1st International Mass Spectrometry Imaging Society Conference (IMSIS 2023)

October 23-25, 2023
Centre Mont-Royal, 2200 rue Mansfield, Montreal, QC Canada

WELCOME

Dear Friends and Colleagues,

We are delighted to welcome you to IMSIS 2023, the 1st Conference of the International Mass Spectrometry Imaging Society organized in Montreal, Quebec, Canada.

This is the first meeting of the of the newly formed International Mass Spectrometry Imaging Society which is comprised of the Mass Spectrometry Imaging Society (MSIS) (Europe) and the Imaging Mass Spectrometry Society (IMSS) (North America). As with the past jointly organized OurCon conferences, this conference is a global forum on mass spectrometry imaging research.

The environment of the event will be one of creativity, cutting edge technology, and scientific advancement. IMSIS 2023 plans to highlight the latest advances in the field of mass spectrometry imaging, promote research of students and new investigators, and acknowledge the top scientists who have helped to cultivate this innovative atmosphere over the years. it will offer a unique opportunity for scientific exchange, and plethora of accelerating networking opportunities for young scientists through lectures, posters, and impromptu meetings with leaders in the field.

We look forward to seeing you in Montreal at the Centre Mont-Royal!

Dr. Pierre Chaurand,
Université de Montréal,
Local Organizer
October 23, 2023

Co-organized with the International Mass Spectrometry Imaging Society:

Martina Marchetti-Deschmann, TU Wien
Malcolm R. Clench, Sheffield Hallam University
Liam McDonnell, FP Science
Tiffany Siegel, Boehringer Ingelheim Pharma GmbH
Christopher Anderton, Pacific Northwest National Laboratory
Peggi Angel, Medical University of South Carolina
Richard R. Drake, Medical University of South Carolina

1st International Mass Spectrometry Imaging Society Conference (IMSIS 2023)

October 23-25, 2023
Centre Mont-Royal, 2200 rue Mansfield, Montreal, QC Canada

AGENDA

*subject to change

Monday, October 23, 2023	
08:00	Registration Desk Opens All sessions take place in Mont-Royal I & II
08:30 - 11:30	**Workshop #1 - Bruker, pre-registration required** Mont-Royal I **User Meeting - Shimadzu, by invitation only** Mont-Royal II
11:30 - 12:00	Break - Plenary Room closed
12:00 - 13:00	**Lunch Workshop presented by Waters** Mont-Royal I & II 100 Lunches Available first come first serve; Lunch will also be available in the Foyer
WELCOME	
13:00 - 13:40	Plenary Lecture - **Malcolm R. Clench, Sheffield Hallam University** *Advances in mass spectrometry imaging 2000-2023*
13:40 - 15:20	**Session 1 - Instrumentation & Methods I (MALDI)** Chair: Shane Ellis, University of Wollongong
13:40 - 14:00	**Martin Dufresne, Vanderbilt University MSRC** *Sublimated/annealed aminated cinnamic acid analogues for high sensitivity sub 10 µm spatial resolution MALDI IMS of lipids in human tissues*
14:00 - 14:20	**Mengze Zhang, University of Zürich** *Toward hyper-multiplexed proteomics imaging by MALDI-IHC technology*
14:20 - 14:30	**Ian Anthony, Maastricht University** *Fast mass microscopy for 1,000-fold faster mass spectrometry imaging*
14:30- 14:40	**Andrej Grgic, Maastricht University** *Design and performance characterization of a novel MALDI-2-MSI ionization source with transmission and reflective mode capabilities*
14:40 - 14:50	**Matthew O'Rourke, The University of Technology Sydney** *Expanding peptide detection in MALDI MSI using ion mobility MS and matrix phase fractionation*
14:50 - 15:00	**Josiah Rensner, Iowa State University** *In-source hydrogen-deuterium exchange in MALDI-MSI to assist metabolite annotation*
15:00 - 15:10	**Peter Verhaert, ProteoFormiX** *High resolution mass spectrometry imaging (MSI) of neurotransmitters in (human) FFPE neuronal tissues without chemical derivatization: eventuality or utopia?*
15:10 - 15:20	Sponsored Talk: AmberGen **Presented by: John Gillespie,** *Latest Advancements in MALDI HiPLEX-IHC*

Monday, October 23, 2023, continued	
15:20 - 15:50	Coffee Break - Foyer with Posters & Exhibits
15:50 - 17:20	**Session 2 - Instrumentation & Methods II (SIMS)** Chair: Martina Marchetti-Deschmann, TU Wien
15:50 - 16:10	**Felicia Green, Rosalind Franklin Institute** *Enhancements in the use of SIMS for multi-omic biomolecular mass and structural analysis*
16:10 - 16:20	**Edith Sandström, Maastricht University** *Steps toward fast mass microscopy of immunolabelled samples*
16:20 - 16:40	**John Fletcher, University of Gothenburg** *SIMS and electrochemistry correlate dose dependent alterations on cells*
16:40 - 17:00	**Martin Metodiev, National Physical Laboratory** *Measuring spatial resolution of different mass spectrometry imaging modalities*
17:00 - 17:10	Sponsored Talk - IONOPTIKA **Presented by Kate McHardy** *Advances in, and applications of, Gas Cluster Ion Beam (GCIB) SIMS*
17:10 - 17:20	Sponsored Talk - SunChrom/Mass Tech **Presented by Gilles Frache, LIST** *Atmospheric Pressure MALDI coupled to Orbitrap(s), principle and applications*
17:20 - 19:00	**Session 3 - Instrumentation & Methods III (LDI, Ambient)** Chair: Yoichi Otsuka, Osaka University
17:20 - 17:40	**Daniel Simon, Imperial College of London** *Ambient laser desorption – REIMS with novel picosecond laser sources for sample preparation-free imaging*
17:40 - 18:00	**Michal Žalud, Masaryk University** *Detection and characterization of individual Au nanoparticles using SubAP LDI MSI*
18:00 - 18:20	**Arash Zarrine-Afsar, University Health Network** *On the concordance of molecular and morphometric cancer borders: insights from mass spectrometry imaging of cancer lipids*
18:20 - 18:30	**Christoph Bookmeyer, University of Tarragona** *Metal nanolayers combined with SPICI postionization for enhanced spatial metabolomics in the low mass range*
18:30 - 18:40	**Leonidas Mavroudakis, Uppsala University** *Identification and imaging of prostaglandin isomers utilizing MS3 product ions and silver cationization*
18:40 - 18:50	**Yoichi Otsuka, Osaka University** *Mass spectrometry imaging of single cells by tapping-mode scanning probe electrospray ionization*
18:50 - 19:00	Sponsored Talk - Shimadzu **Presented by M. Nazim Boutaghou** *Shimadzu: One-stop shop for your imaging needs*
19:00 - 22:00	**Opening Reception & Evening Poster Session #1** **4th Floor Foyer Mont-Royal I & II** **Even Poster Number presenters must be at their posters from 20:00 to 21:30**

Tuesday, October 24, 2023	
07:30	Registration Desk Opens
08:00 -08:40	Plenary Lecture - **Yasser Riazalhosseini, McGill University** *Spatial transcriptomics to understand molecular underpinnings of aggressive phenotypes in tumors*
08:40 - 10:20	**Session 4 - Lipids, Metabolites & Glycans** Chair: Richard Drake, Medical University of South Carolina
08:40 - 09:00	**Jayden Mckinnon, University of Wollongong** *Enhanced coverage and spatial resolution for the mass spectrometry imaging of small metabolites using MALDI-2*
09:00 - 09:20	**Stefania Alexandra Iakab, CeMOS - Center for Mass Spectrometry and Optical Spectroscopy** *(3D) Molecular snapshots of spheroids by mass spectrometry imaging*
09:20 - 09:40	**Keziah Liebenberg, Baylor College of Medicine** *Insights into metabolic alterations associated with resistance to immune checkpoint inhibitors in triple negative breast cancer utilizing DESI-MSI*
09:40 - 09:50	**Laurentiu Dabija, York University** *Assessment of MALDI matrices for phosphoinositide detection in mouse kidney models through matrix-assisted laser desorption ionization (MALDI) imaging techniques*
09:50 - 10:00	**Anthony Devlin, Rosalind Franklin Institute** *Mass spectrometry imaging of glycosaminoglycans: current progress and future prospects*
10:00 - 10:10	**Elizabeth Wallace, Medical University of South Carolina** *A MALDI MSI N-glycome atlas and analytic pipeline for human normal and cancer tissues*
10:10 - 10:20	Sponsored Talk - HTX Imaging **Presented by Alyson Black, PhD** *Advances in Sample Preparation for Ultra-High Spatial Resolution MALDI Imaging*
10:20 - 10:40	Coffee Break - Foyer with Posters & Exhibits
10:40 - 12:10	**Session 5 - Proteins and PTMs** Chair: Peggi Angel, Medical University of South Carolina
10:40 - 11:00	**Helen Cooper, University of Birmingham** *Native ambient mass spectrometry imaging: Applications in understanding amyotrophic lateral sclerosis*
11:00 - 11:10	**Matthew Briggs, The University of South Australia** *Integrating N-glycan and tryptic peptide MALDI mass spectrometry imaging with N-glycopeptide LC-MS/MS data for FFPE endometrial cancer tissue*
11:10 - 11:20	**Tana Palomino, North Carolina State University** *Preserving and predicting sialic acid content of N-linked glycans by IR-MALDESI*
11:20 - 11:30	**Jade Macdonald, Medical University of South Carolina** *Identification of unique extracellular matrix signatures that differentiate hepatocellular carcinoma by outcome*
11:30 - 11:50	**Andreas Roempp, University of Bayreuth** *Advances in MALDI imaging of tryptic peptides: improved spatial resolution in mammalian tissue and first results for plant proteins*
11:50 - 12:10	**Kevin Schey, Vanderbilt University** *Localization of membrane proteins and post-translational modifications in ocular tissues*

Tuesday, October 24, 2023, continued	
12:10 - 13:10	**Lunch Workshop presented by: Thermo Fisher Scientific;** *Focus your MSI-research: Coupling the power of high lateral and high mass resolution with AP-SMALDI5 AF ion source and Orbitrap Exploris MS* 100 Lunches Available first come first serve; Lunch will also be available in the Foyer
13:10 - 14:50	**Session 6 - Novel Biological Application** Chair: Shuichi Shimma, Osaka University
13:10 - 13:30	**Julia Haddow, University of Dundee** *Chagas' disease - tissue clearing and mass spectrometry to study parasite localisation and drug distribution in trypanosoma cruzi infected mouse tissues*
13:30 - 13:50	**Max Alexander Müller, Justus Liebig University Giessen** *Lipid signatures and inter-cellular heterogeneity of naïve and lipopolysaccharide-stimulated human microglia-like cells using AP-SMALDI MSI at 1.5 µm lateral resolution*
13:50 - 14:10	**Shadrack Mutuku, University of Wollongong** *Omics-scale quantitative mass spectrometry imaging of lipids using a multi-class internal standard mixture combined with MALDI and MALDI-2*
14:10 - 14:20	**Rachel Pryce, Université de Montréal** *A spatial multi-omics investigation into spinal cord remodeling in mouse mutant strains with altered myelin basic protein abundance*
14:20 - 14:30	**Gabor Toth, Uppsala University** *Correlation between oxylipin species and lesion formation in human multiple sclerosis revealed by silver-doped PA nano-DESI imaging*
14:30 - 14:40	**Bin Yan, National Physical Laboratory** *Uncovering metabolic signatures associated with the invasiveness of metastatic melanoma by DESI MSI*
14:40 - 14:50	Sponsored Talk - Aspect Analytics **Presented by Alice Ly** *Dedicated Software to Support High Throughput Spatial Multi Omics Applications*
14:50 - 16:20	**Session 7 - Pre-Clinical & Clinical Applications** Chair: Masaya Ikegawa, Doshisha University
14:50 - 15:10	**Per Andrén, Uppsala University** *Mass spectrometry imaging of brain signalling systems reveals abnormal alterations induced by parkinsonism and L-DOPA-induced dyskinesia*
15:10 - 15:30	**Gerard Baquer, Brigham & Women's Hospital, Harvard Medical School** *Understanding spatial relationships among cells and molecules in glioblastoma through multimodal imaging*
15:30 - 15:50	**Erin Seeley, University of Texas at Austin** *Mass spectrometry imaging reveals molecular changes associated with aging in pancreatic cancer*
15:50 - 16:00	**Jordan Hartig, Medical University of South Carolina** *Multi-fucosylated N-glycans detected by MALDI-MSI in tissues distinguish neuroendocrine prostate cancers from all stages of adenocarcinomas*
16:00 - 16:10	**Maiko Okamura, Doshisha University** *Deciphering Immunometabolism in delta-sarcoglycan deficient hamster with thoracic Mass Spectrometry Imaging (tMSI)*
16:10 - 16:20	**Laimdota Zizmare, Werner Siemens Imaging Center, University Hospital Tuebingen** *Combining MSI and ex vivo quantitative metabolomics with in vivo imaging to decipher molecular mechanisms of human breast cancer heterogeneity*
16:20 - 16:30	Sponsored Talk - Thermo Fisher Scientific **Presented by Maciej Bromirski, Sr. Project Manager, Thermo Fisher Scientific** *MS Imaging meets Orbitrap Technology*

Tuesday, October 24, 2023, continued	
16:30 - 16:50	Coffee Break - Foyer with Posters & Exhibits
16:50 -18:20	**Session 8 - MSI Data Analysis & Bioinformatics** Chair: Jeffrey M. Spraggins, Vanderbilt Universtiy
16:50 - 17:10	**Lukasz Migas, Delft University of Technology** *Qu-Cee: An automated quality control pipeline for cohort and 3D imaging mass spectrometry*
17:10 - 17:30	**Nico Verbeeck, Aspect Analytics** *Enabling integrative spatial multi-omics data analysis via dedicated data structures and interactive, web-based visualizations*
17:30 - 17:50	**Lalin Theverapperuma, Expert Intelligence** *Integration of topological data analysis with contrastive deep learning for molecular co-localization in mass spectrometry imaging*
17:50 - 18:00	**Alexandria Sohn, North Carolina State University** *A statistical approach to system suitability testing (SST) for mass spectrometry imaging*
18:00 - 18:10	**Sai Srikanth Lakkimsetty, Northeastern University** *Unsupervised co-registration of hematoxylin and eosin (H&E) stained microscopy images and mass spectrometry images (MSI) with feature filtering*
18:10 - 18:20	**Oliver Hale, University of Birmingham** *High-throughput m/z-to-mass deconvolution of protein complexes up to 145 kDa from native protein mass spectrometry imaging datasets*
18:20 - 19:20	IMSIS Board Meeting
19:20 - 22:00	**Evening Poster Session #2** **4th Floor Foyer Mont-Royal I & II** **Odd Poster Number presenters must be at their posters from 20:00 to 21:30.**

Wednesday, October 25, 2023	
07:30	Registration Desk Opens
08:00 -08:40	Plenary Lecture - **Livia Schiavinato Eberlin, Baylor College of Medicine** *Imaging metabolites and lipids in cancer tissues to help inform treatment options for patients*
08:40 - 10:10	**Session 9 - Xenobiotics, Kinetics, Toxicity** Chair: Malcolm R. Clench, Sheffield Hallam University
08:40 - 09:00	**Claire Villette, PIMS, IBMP, CNRS** *In situ localization of micropollutants, their transformation products and the associated stress response in plant leaves using MALDI-FTICR-imaging*
09:00 - 09:10	**Andrew Bowman, AbbVie** *Quantification of a potential pharmaceutical in a time course study of rat liver with mass spectrometry imaging*
09:10 - 09:30	**Peter Marshall, GSK** *Exploring ionizability and adduct formation of pharmaceutical compounds in MALDI and MALDI-2 Mass Spectrometry Imaging with machine learning*
09:30 - 09:40	**Sophie Pearce, Sheffield Hallam University** *Mass Spectrometry Imaging of an Osteosarcoma Tumour Model to Investigate Drug Induced Metabolic Response*
09:40 - 10:00	**Carolin Morawietz, Justus Liebig University** *Imaging of drugs and lipids in the parasite fasciola hepatica using high-resolution AP-SMALDI MSI*
10:00 - 10:10	**Mark Towers, Waters Corporation** *Increased level of detection of the drugs/metabolites biolocalisation with targeted DESI MRM TQ mass spectrometer*
10:10 - 10:40	Coffee Break - Foyer with Posters & Exhibits
10:40 - 12:00	**Session 10 - Microorganisms, Plants & Non-Mammalian Systems** Chair: Christopher Anderton, Pacific Northwest National Laboratory
10:40 - 11:00	**Nanna Bjarnholt, University of Copenhagen** *Exploring the potential for MALDI-2 post-ionization based visualization of lowly abundant phytohormones in plant tissues*
11:00 - 11:10	**Annika Mokosch, Justus Liebig University Giessen, Germany** *High-resolution AP-SMALDI imaging of endogenous neurotransmitters in infectious worm couples causing schistosomiasis (bilharzia)*
11:10 - 11:30	**Laura Sanchez, University of California, Santa Cruz** *A label free approach for relative spatial quantitation of c-di-GMP in microbial biofilms*
11:30 - 11:50	**Dusan Velickovic, Pacific Northwest National Laboratory** *4-APEBA on tissue chemical derivatization for enhanced MALDI MSI of carbonyls in environmental samples*
11:50 - 12:00	**Khaled Madhoun, University of Toronto** *Towards subcellular sampling via impulsive laser ablation coupled to mass spectrometry*
12:00 - 13:10	Luncheon Served - 4th Floor, Mont-Royal I &II Foyer

Wednesday, October 25, 2023, continued	
13:10 - 15:30	**Session 11 - Multimodal MSI** Chair: Marten Snel, University of Wollongong
13:10 - 13:30	**Martina Marchetti-Deschmann, TU Wien** *Correlating tissue biomechanics and molecular information – the combination of physiological AFM and MALDI MSI*
13:30 - 13:50	**Xander Spotbeen, KU Leuven** *Investigation of prostate cancer heterogeneity using a novel spatial multi omics pipeline integrating MS imaging and spatial transcriptomics*
13:50 - 14:10	Sponsored Talk - Bruker **Presented by Azad Eshghi, Field Applications Support Scientist** *Multimodal Imaging Analysis for Comprehensive Biological Information*
14:10 - 14:20	**Paul Trim, South Australian Health and Medical Research Institute** *MALDI-MSI lipidomics guided LCM proteomics on human prostate cancer biopsies: maximising the data from a single section.*
14:20 -14:40	**Laurine Lagache, PRISM - Inserm U1192** *New method machine process to unravel tissue biomarkers and validate it by multiplex MALDI IHC*
14:40 - 14:50	**Jens Soltwisch, University of Münster** *An integrated t-MALDI-2 ion source with In-source bright-field and fluorescence microscopy for direct correlative imaging at the cellular level*
14:50 - 15:00	**Gregory Vandergrift, Pacific Northwest National Laboratory** *Peak ambiguities and in-source fragmentation: how many peaks in mass spectrometry imaging experiments are biologically meaningful?*
15:00 - 15:10	**Isabeau Vermeulen, University of Maastricht** *Discovering the molecular secrets of epilepsy: multimodal molecular imaging in a focal cortical dysplasia animal model*
15:10 - 15:30	Sponsored Talk - Waters **Presented by Emrys Jones, Waters Corporation** *DESI MS imaging at the cellular level with nano-flow and multi-focus approaches*
15:30 - 16:00	Coffee Break - Foyer with Posters & Exhibits
16:00 - 17:30	**Session 12 - MSI Reporting & Standards** Chairs: Andreas Römpp, University of Bayreuth Lukasz Migas, Delft University of Technology Peggi Angel, Medical University of South Carolina
	Session Content TBA
17:30 - 17:45	Awards Presentation and Closing Remarks

UVic Genome BC
PROTEOMICS CENTRE

Providing service and support for research in the areas of mass spectrometry imaging, metabolomics, functional proteomics, and quantitative proteomics.

Proteomics – Biomarker Discovery & protein characterization

- Targeted Quantitation
- Untargeted Quantitation
- PTM Analysis
- Hydrogen-Deuterium Exchange (HDX)

MALDI Tissue Imaging

- Untargeted identification of Regions of Interest
- Targeted quantification of lipids, small molecules or peptides
- HiPLEX targeted protein localization via antibody probes

Metabolomics

- Untargeted analyses
- Targeted assays: >25 Pathway and Class specific multiplexed assays
- Customization available

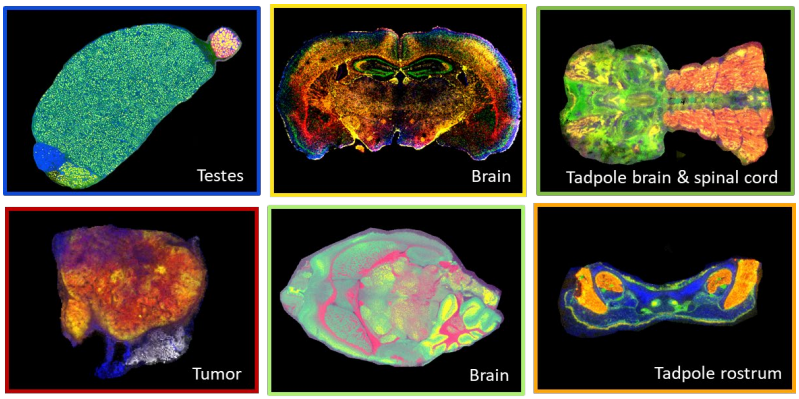

The UVic Genome BC Proteomics Centre is a not-for-profit analytical MS laboratory, offering fee-for-service, technology development and collaborative research opportunities to >150 global academic and industrial clients per year. For more information, visit us at www.proteincentre.com or contact us at info@proteincentre.com.

Supported by : Pacific Economic Development Canada | Canada
GenomeCanada GenomeBritishColumbia
University of Victoria

We wish to thank our Sponsors for their generous support of the 1st IMSIS Conference, Montreal, Canada 2023

PLATINUM

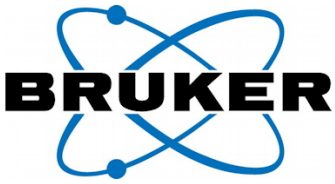

GOLD

SILVER

SPONSOR

MEDIA SPONSOR

Workshops

Bruker Breakfast Workshop **Monday October 23, 2023**

Mont Royal I

8:30 - 8:45 am Introduction and technology updates

Azad Eshghi, Ph.D., Field Applications Support Scientist, Bruker, Victoria, British Columbia, Canada

8:45 - 9:15 am Session 1: Advancements in MALDI-2: User stories

Peter Marshall, Ph.D., GSK

Benedikt Geier, Ph.D., Postdoctoral Researcher, Stanford University School of Medicine, California, USA

9:15 - 10:15 am Session 2: Applications in disease-based research

Kimberly Alonge, Ph.D., Assistant Professor, University of Washington, Seattle, Washington, USA

Kristina Schwamborn, Ph.D., Associate Professor, TU Munich, Munich, Germany

Laurence Florens, Ph.D., Director of Systems Mass Spectrometry, Stowers Institute for Medical Research, Kansas City, Missouri, USA

Masaya Ikegawa, Ph.D., Professor, Genomic Medical Sciences, Kyoto Prefectural University of Medicine, Kyoto, Japan

10:30 - 11:10 am Session 3: Trainee talks

Taylor Hulahan, Medical University of South Carolina

Tialfi Bergamin de Castro, Ph.D., Postdoctoral Researcher, University of Maryland, Baltimore, Maryland, USA

TBC

TBC

11:10 - 11:30 am Session 4: Future direction of research

Chris Anderton, Ph.D., Biogeochemical Transformations Team Lead & Mass Spectrometry Imaging Scientist, Pacific Northwest National Laboratory, Richland, Washington, USA

Ron Heeren, Ph.D., Distinguished Professor & Limburg Chair, Maastricht University, Maastricht, Limburg, Holland

https://www.bruker.com/en/landingpages/bdal/imsis.html

Waters Lunch Workshop **Monday October 23, 2023**

12:00-13:00

Mont Royal I&II

Dr. Mark Towers

From Discovery to Targeted MS Imaging with the New Targeted MS Imaging Solution with DESI XS and Xevo™ TQ Absolute

Discovery ToF based MS imaging offers the ability to directly detect, visualize, and quantify cellular and molecular events in situ, opening up huge possibilities to advance the understanding of biological systems and materials science. Direct MS analysis on a tissue or material's surface prevents compound-specific sample preparation, which can challenge the detection of certain molecules. The newly launched Waters targeted MS imaging system, based on DESI XS and the Xevo TQ Absolute, is at least five times more sensitive than discovery HRMS MS Imaging systems. This means that compounds can be accessed at lower levels than previously possible or even visualized for the first time. High sensitivity imaging mitigates the need for follow up analysis like laser capture microdissection LC-MS – saving time and cost of analysis. Gain confidence by bringing your molecules out of the weeds with the power of unparalleled sensitivity

Dr. Chloe Spencer

Mass Spectrometry Imaging in Pharmaceutics using DESI XS

Creating a realistic gastrointestinal tract model for drug absorption studies is challenging as the oral route consists of several different organs that differ in structure and environment which can be complex to sufficiently replicate. The extreme, fluctuating conditions and unique obstacles presented within each organ can have a profound effect on the active ingredient and could cause an oral drug to be released early if it has not been formulated correctly. It is often debated whether 2D cells, 3D cells, organoids, ex Vivo or in Vivo models are best-suited for drug absorption studies. However, what can be agreed upon is that a growing number of scientific studies are moving away from animal testing. With the now adapted QV600 milifluidics model, it is possible to perform drug absorption studies with either cultured cells or ex vivo tissue. Here, drug absorption studies have been carried out using atorvastatin with a mixture of different excipients to explore the effect they have on absorption in the ex vivo porcine small intestine. DESI imaging has been used to visualize the distribution of Atorvastatin on small intestine tissue sections when different amounts and combinations of excipients have been applied. LC-MS/MS has been used to quantify the amount of Atorvastatin that has been recovered from the tissue extracts and that has moved through the tissue.

Thermo Fisher Scientific Lunch Workshop **Tuesday October 24, 2023**

12:10-13:10

Focus your MSI-research: Coupling the power of high lateral and high mass resolution with AP-SMALDI5 AF ion source and Orbitrap Exploris MS

Plenary 1: Monday October 23 13:00-13:40

Mass Spectrometry Imaging: A Mature Technology?

Malcolm R Clench

Emeritus Professor of Mass Spectrometry, Sheffield Hallam University, UK

m.clench@shu.ac.uk

The origins of mass spectrometry imaging can be traced back 50 years to the use of SIMS to study semiconductor surfaces. However, it was the pioneering work of Berhard Spengler and Richard Caprioli in the 1990s applying MALDI to biological tissues that really alerted the scientific community to its potential. In this presentation advances in MSI over the last 30 years will be presented with a focus on instrumental developments. Applications from work carried at out at Sheffield Hallam in pharmacokinetics and dynamics along with examples of clinical, forensic, and agricultural application will be used to illustrate how these advances have been exploited and how they have led to the widespread adoption of MSI today. To conclude issues that still need to be addressed in MSI will be discussed along with potential solutions being presented in the literature.

Plenary 2: Tuesday October 24 8:00-8:40

Spatial transcriptomics to understand molecular underpinnings of aggressive phenotypes in tumors

Yasser Riazalhosseini, Ph.D.1,2

1Victor Phillip Dahdaleh Institute of Genomic Medicine, McGill University

2Department of Human Genetics, McGill University

The presence of mesenchymal-like cellular phenotypes in tumors with epithelial origins represents a de-differentiation process, known as epithelial-to-mesenchymal transition (EMT), which is commonly associated with aggressive cancers and poor outcomes. The current knowledge about molecular mechanisms that may drive EMT is primarily generated from experiments performed in vitro or in animal models, whereas studies on patient tumors have mainly used molecular profiling of bulk tumors, collecting data from a mixture of cells that co-exist in the tumor milieu. Therefore, high-resolution studies that precisely define molecular characteristics of different cellular phenotypes associated with EMT in patient tumors are missing. The advent of spatial omics technologies, including spatial transcriptome and proteome analyses, has provided new opportunities to address this gap. We have used spatial transcriptomic profiling to investigate molecular mechanisms that underline EMT features in kidney cancers. Specifically, we focused on renal cell carcinomas (RCC), the most common form of kidney cancer, that are affected by sarcomatoic or rhabdoid (S/R) de-differentation patterns. The presence of S/R features in RCC is associated with high risk of metastasis and poor survival. While preserving tissue context, we applied spatial whole human transcriptome profiling to areas exhibiting S/R or clear cell phenotypes within the same tumor specimens to generate phenotype-specific transcriptome profiles. Pathway and network analysis of genesets with upregulation in each area have revealed meaningful differences in cellular pathways which are active in each phenotype. These results will be presented at the conference.

Plenary 3: Wednesday October 25 8:00-8:40

Imaging Metabolites and Lipids In Cancer Tissues to Help Inform Treatment Options for Patients

Livia Eberlin

Baylor College of Medicine

Mass spectrometry imaging provides the unique and exciting opportunity to directly access the metabolic information from cancer tissues to not only investigate molecular changes happening within the tumor microenviroment but to also help inform treatment options for patients. In my seminar, I will discuss a few of my lab's recent developments and applications of DESI imaging in translational clinical studies in which we are leveraging the powerful metabolic information we acquire from cancer tissues using DESI to identify key genetic alterations that carry major implication to patient care, as well as to molecularly subtype cancer. Correlation between trends in metabolic and lipid expression and response to treatment including chemotherapy and immunotherapy will also be discussed. Key operational principles, depth of molecular data, and the analytical and diagnostic performance metrics will also be discussed to provide a critical assessment of our current capabilities with DESI imaging technology and potential uses within the context of routine clinical practice.

Andrén, Per
Uppsala University, Sweden

Tuesday October 24, Session 7, 14:50-15:10

Mass spectrometry imaging of brain signalling systems reveals abnormal alterations induced by parkinsonism and L-DOPA-induced dyskinesia

Introduction:

In the early stages of Parkinson's disease (PD), drug treatment is highly effective, but with disease progression involuntary motor complications, L-DOPA-induced dyskinesia (LID), become increasingly evident. There is a great need to define the molecular changes associated with PD patients that develop LID. We previously observed abnormal elevations of L-DOPA and its metabolite, 3-O-methyldopa, in the whole brain of LID animals. Furthermore, dopamine formation was spatially correlated with serotonin in specific layers of the hippocampus and cortex in LID. Abnormally truncated neuropeptides, i.e., dynorphins and tachykinins, correlated with dyskinesia severity and may constitute a functional compensatory mechanism for balancing the increased L-DOPA levels across the whole basal ganglia.

Method:

Using brain samples from an experimental Parkinson's disease (PD) model (MPTP, Macaca mulatta) with L-DOPA-induced dyskinesia (LID), we employed MALDI-MSI to comprehensively map different molecular species, such as (a) neurotransmitters and their metabolites, (b) neuropeptides, (c) metabolites, and (d) lipids in specific brain regions. We use multivariate analysis to investigate effects of PD and LID on the different molecular species in multiple brain regions and subregions. This strategy provides information about the dominant patterns of the neurotransmitter systems in each investigated brain region and emphasize brains region that are highly affected by PD and LID.

Results:

In the present study, utilizing tissue from the same individual animals, we observed reduced putaminal acetylcholine levels in PD and LID that persisted after L-DOPA treatment. LID showed decreases in metabolites crucial for brain homeostasis, including S-adenosylmethionine, glutathione, adenosine monophosphate, and acylcarnitines. The vasculature marker heme B was upregulated in LID, suggesting blood-brain barrier modifications and increased blood flow in the dyskinetic putamen. Additionally, we extensively imaged various lipid types, detecting specific distributions of sulfatide lipids in MPTP-lesioned brains. Hydroxylated sulfatides with polyunsaturated chains were depleted in motor-related regions, while non-hydroxylated sulfatides were elevated. Comparing LID with non-dyskinetic animals, plasmalogen phosphatidylcholines decreased, while polyunsaturated fatty acid-containing phospholipids increased in the internal segment of globus pallidus.

Novelty:

This study provides novel insights into signaling system dynamics during PD and LID.

Preliminary Data:

By comparing LID with similarly treated non-dyskinetic animals we found specific metabolic changes in specific brain regions.

Contributing Authors:

Theodosia Vallianatou, Ibrahim Kaya, Anna Nilsson, Reza Shariatgorji, Per Svenningsson, Erwan Bezard

Baquer, Gerard **Tuesday October 24, Session 7, 15:10-15:30**

Department of Neurosurgery, Brigham and Women's Hospital, Harvard Medical School, Boston, MA, USA., USA

Understanding Spatial Relationships Among Cells and Molecules in Glioblastoma through Multimodal Imaging

Introduction:

Glioblastoma (GBM) is an aggressive brain tumor characterized by extensive cellular and microenvironmental heterogeneity. Multiplexed imaging methods such as Cyclic Immunofluorescence (CyCIF) and single-cell transcriptome-imaging methods such as Multiplexed Error-Robust Fluorescence In Situ Hybridization (MERFISH), can map cell types, states, and interactions in complex diseases like GBM. However, additional molecular information is needed for a complete understanding of disease pathogenesis. Matrix-assisted laser desorption/ionization mass spectrometry imaging (MALDI-MSI) is a powerful platform for mapping the spatial distribution of proteins, lipids, metabolites, and other small molecules. However, instruments lack the necessary resolution to obtain robust single-cell information. To better understand the relationships among cells and molecules in GBM tissue, we developed workflows and protocols for collecting and co-analyzing MERFISH, CyCIF, and MALDI-MSI images.

Method:

Serial sections of fresh-frozen mouse and human GBM tissue were imaged by MALDI-MSI, CyCIF, and MERFISH using a 15T-solariX-FT-ICR, a RareCyte CyteFinder II microscope, and the MERSCOPE platform respectively. MSI datasets were pre-processed using SCiLS Lab and rMSIproc and annotated using METASPACE-ML. CyCIF images were pre-processed with MCMICRO and CyLinter, and clustered using UMAP/HDBSCAN. MERFISH were pre-processed with NS-Forest2, MERLIN, deepcell, and baysor. The resulting cell x gene matrix was Louvian clustered to identify cell types based on scRNA-seq-defined gene sets. MSI, CyCIF, and MERFISH images were registered using a projective transformation based on manual fiducials. Latent Dirichlet Association (LDA) probabilistic modeling was used to reduce cell populations into neighborhoods defined by multi-omic expression patterns (metabolomics, proteomics, and transcriptomics).

Results:

One key result of our work is the development and validation of protocols to extract, prepare, and analyze serial sections of multiple GBM biopsies of the same human specimen. To achieve this, we have optimized MALDI-MSI, CyCIF, and MERFISH protocols specifically for use with fresh-frozen tissue samples. Additionally, we have developed a robust pipeline to register the resulting images into the same coordinate space. For each sample, we obtain a multi-omic spatial dataset. With optimized protocols in place, we developed a computational framework to integrate information derived from the three complementary spatial omics techniques. The foundation of our integration lies in the use of Latent Dirichlet Association (LDA), a probabilistic modeling method that reduces complex mixtures of entities (in our case cells, transcripts, proteins, and metabolites) into recurrent topics (in our case multimodal neighborhoods). The LDA models are trained on 20-µm radius regions to yield multimodal neighborhoods that focus on the microenvironment of cells in physical contact. The resulting multimodal neighborhoods identify cells and molecules that recurrently appear together across the tissue, and can be used to generate and validate multiple hypotheses. As an example, we can identify the metabolic profiles of each cell type within the tumor according to its cellular environment. Our findings demonstrate the potential for MSI/CyCIF/MERFISH integration to reveal biologically relevant spatial relationships among cells and molecular entities in complex tissue microenvironments.

Novelty:

MALDI-MSI/CyCIF/MERFISH data integration provides complementary insight into cells and molecular entities comprising complex microenvironments in GBM tissue.

Preliminary Data:

We have acquired data on 5 GBM biopsy samples using the three modalities (MSI, CyCIF, and MERFISH).

Contributing Authors:

Gerard Baquer[1], Michael S. Regan[1], Sylwia Stopka[1], Jennifer Gantchev[1], Charles P. Couturier[1,2,3,4,5], Jia-Ren Lin[6,7], Sami Farhi[4], Chadi El Farran[4,5], Alex Shalek[3,4], Steven Tobochnik[1], Sandro Santagata[6,7,8] & Nathalie Y. R. Agar[1,8,9]

[1]Department of Neurosurgery, Brigham and Women's Hospital, Harvard Medical School, Boston, MA, USA.

[2]Institute of Medical Engineering and Sciences at MIT [3]Koch Institute at MIT

[4]Broad Institute of MIT and Harvard [5]Department of Cancer Biology, Dana-Farber Cancer Institute

[6]Laboratory of Systems Pharmacology, Harvard Medical School, Boston, MA, USA.

[7]Ludwig Center at Harvard, Harvard Medical School, Boston, MA, USA

[8]Department of Pathology, Brigham and Women's Hospital, Harvard Medical School, Boston, MA, USA

[9]Department of Radiology, Brigham and Women's Hospital, Harvard Medical School, Boston, MA, USA

Bjarnholt, Nanna
University of Copenhagen, Denmark

Wednesday October 25, Session 10, 10:40-11:00

Exploring the potential for MALDI-2 post-ionization based visualization of lowly abundant phytohormones in plant tissues

Introduction:
Plant hormones (phytohormones) are structurally diverse small molecules that regulate plant developmental processes such as seed germination, root and shoot branching, flowering time, and defense responses to herbivores, pathogens and abiotic stresses such as drought and cold. Correct activity depends on strict cell and tissue specific accumulation, and detection of phytohormone localization is hence crucial for understanding their mode of action and possible utilization in crop development. Today, this is achieved by cumbersome and/or indirect methods that may only be possible in model plants and few crops. Mass spectrometry imaging can alleviate this problem, but like other organisms, plants accumulate hormones in extremely low amounts. We therefore explored the potential of MALDI-2 post-ionization to enhance phytohormone detection in plant tissues.
Method:
With the Bruker timsTOF-fleX MALDI-2, we tested the ionization and response to MALDI-2 post-ionization in positive and negative mode of five different signalling compounds (indol-3-acetic acid (auxin), abscisic acid, jasmonic acid, zeatin, 6-benzyl-aminopurine) co-crystallized with six different matrices (2,5-dihydroxybenzoic acid (DHB), α-cyano-4-hydroxycinnamic acid (CHCA), caffeic acid (CA), norharmane (NOR), 1,5-diaminonaphthalene (DAN), 9-aminoacridine (9-AA)). A subset of compounds and matrices were chosen for further evaluation of the ion suppressing effect in plant extracts and for optimizing matrix application parameters phytohormone spiked plant extract droplets. Finally, matrix spraying parameters were optimized on tissue sections and the method used to detect auxin in a biological experiment. The identity of auxin was verified by tims (trapped ion mobility spectrometry).
Results:
In positive mode analysis of standards co-crystallized with matrix, the nitrogen containing compounds auxin, zeatin and 6-benzyl-aminopurine generally ionized well, mainly as [M+H]+ and also produced the strongest response to MALDI-2 post-ionization, whereas the two acids ionized weakly, mainly as [M+Na]+ that were not enhanced by MALDI-2, in accordance with literature. CHCA was the most versatile matrix, producing a good signal from most compounds, but DHB with auxin produced the strongest signal of all tested combinations. Interestingly, auxin was detected as the [M•]+ radical ion, and the intensity of this ion was increased 1000-fold by application of MALDI-2. In the negative mode, all compounds were generally ionized as [M-H]-, with only auxin failing to ionize with some matrices. MALDI-2 generally suppressed the signal in negative mode, with the ABA-NOR combination being the only to lead to a slightly increased signal. As expected, addition of plant extract suppressed ionization of compounds of interest in all cases tested, but the response to MALDI-2 post-ionization was unaltered. Parameters for spray application of matrix were initially optimized using pea or Arabidopsis leaf extract spiked with zeatin and DHB as matrix. However, when the optimized method did not yield results for pea stem tissue sections that are known to contain relatively high amounts of auxin and zeatin, the parameters were instead optimized on tissue sections using CHCA. Optimized spraying parameters and changed MALDI-2 settings finally allowed detection of auxin in pea stem sections. Stem segments were sampled from the top and bottom internodes of young pea plants that are known to be respectively high and low in auxin concentrations. In sections from the top segments, auxin was distributed across the whole tissue section, with the strongest signal intensity seen in the region of vascular bundles, whereas in the bottom internode auxin was more localized to the central pith, likewise co-localizing with the vasculature. The results are in agreement with proposed polar auxin transport in high auxin-producing regions such as shoot apical meristem or top(young) internodes, and in accordance with previously obtained results from transgenic plants expressing reporter genes or facilitating click chemistry reactions. This is the first example of direct analysis of phytohormone localization in plant tissue sections.
Novelty:
This results demonstrate the potential of MALDI-2 for faster and more accurate and versatile detection of phytohormone localization in plant tissues.
Preliminary Data:
No data are published and hence preliminary
Contributing Authors:
Nikola Micic, Stephanie conway, Elizabeth Dun, Mette Sørensen, Christine Beveridge, Brett Hamilton, Nanna Bjarnholt

Cooper, Helen
University of Birmingham, UK

Tuesday October 24, Session 5, 10:40-11:00

Native ambient mass spectrometry imaging: Applications in understanding amyotrophic lateral sclerosis

Introduction:
Native ambient mass spectrometry (NAMS) enables detection, identification and imaging of intact proteins in their native state directly from thin tissue sections. We have previously shown that NAMS is suitable for identification and imaging of protein assemblies (including membrane protein assemblies), endogenous protein-ligand complexes, and protein-drug complexes formed in vivo. Amyotrophic lateral sclerosis (ALS), also known as motor neuron disease, is a progressive and fatal neurodegenerative disease. Despite decades of research, the mechanisms underlying ALS remain unclear. Here, we apply native ambient mass spectrometry imaging to visualize the spatial distributions of proteins and their complexes in sections of brain and spinal tissue from the hSOD1G93A mouse model of ALS, and sections of human spinal cord taken post-mortem from ALS patients.
Method:
Brains and spinal cords from transgenic mice expressing human SOD1 (wild-type; hSOD1wt and G93A mutant; hSOD1G93A) were harvested and snap frozen before storage at -80 C. Brains were sectioned to 10 μm thickness and thaw mounted to glass slides. Sections of human spinal cord from sporadic ALS cases and controls were provided by the Sheffield Brain Tissue Bank (REC reference 19/SS/0029). MSI and in situ top-down protein analysis were performed using a home-built nano-DESI ion source attached to an Orbitrap Eclipse mass spectrometer. The solvent system was 200 mM aqueous ammonium acetate + 0.125% of the detergent C8E4. Nano-DESI pixels were 200x200 um for full section images, and 30x50 um for region-targeted, higher resolution imaging of specific CNS structures.
Results:
The hSOD1G93A mouse is a well-established model of ALS. Mutations in the metalloenzyme SOD1 are associated with ~20% of inherited forms of ALS and cause a toxic gain of function. Under physiological conditions, the human wild-type SOD1 (hSOD1wt) matures to form a non-covalently bound homodimer incorporating one zinc ion, one copper ion and one intramolecular disulfide bond per subunit. Human SOD1 dimers were analysed directly from transgenic mouse brain and spinal cord sections by nano-DESI. In situ top-down analysis identified SOD1 dimers containing 2, 3 and 4 (holo) metal ions. Native MSI of sagittal brain sections and coronal spinal cord sections revealed locations that were rich in metal-deficient hSOD1G93A complexes in the disease model, whereas holo-hSOD1G93A was distributed throughout disease and control samples. The relative abundance of dimers to monomers was consistent regardless of pathology. The results also showed that the dimer-destabilizing post-translational modification, glutathionylation, has limited influence on the spatial distribution of SOD1 dimers. In further work, native MSI of sections of human spinal cord from sporadic ALS cases was performed. A number of proteins and protein complexes whose spatial distributions correlate with ALS pathology were identified.
Novelty:
Application of native ambient mass spectrometry imaging of protein complexes provides insight into the molecular pathology associated with ALS.
Preliminary Data:
Native MSI of intact protein complexes in tissue sections from a mouse model of ALS, and human sporadic ALS cases.
Contributing Authors:
Oliver J. Hale Tyler R. Wells Richard J. Mead J. Robin Highley

Dufrense, Martin
Vanderbilt University MSRC, United States

Monday October 23, Session 1, 13:40-14:00

Sublimated/annealed aminated cinnamic acid analogues for high sensitivity sub 10 µm spatial resolution MALDI IMS of lipids in human tissues

Introduction:
Matrix-assisted laser desorption/ionization (MALDI) is the leading high spatial resolution (≤ 10 µm) imaging mass spectrometry (IMS) technology owing to its broad molecular coverage and ability to target selected molecular classes through a wide variety of sample preparations. Recent advancements in instrumentation led to the acquisition of sub 10 µm MALDI IMS datasets being more common. While these have resulted in high-quality IMS images, smaller pixel sizes can lead to a decrease in sensitivity. Here we propose the use of sublimated aminated cinnamic acid analogues (ACAA) followed by matrix annealing for 5 µm spatial resolution dual polarity MALDI IMS of lipids with high sensitivity.

Method:
1st and 2nd-generation ACAAs were provided by the Vanderbilt Institute of Chemical Biology Synthesis Core. Human tissue sections were cut at 6 or 10 µm thickness and thaw-mounted on ITO-coated glass slides. Thin layers of ACAA (≤0.25 µg/mm2) were sublimated on tissue using a custom-built aluminium apparatus (subliMATE), allowing the use of dry ice in the cold finger to reach -78°C making sample temperature inside the chamber more consistent during sublimation. On-tissue matrix crystal sizes were evaluated using scanning electron microscopy. IMS and MS/MS measurements were performed on a MALDI timsTOF Flex mass spectrometer in positive and negative ion modes at a spatial resolution of 5-10 µm.

Results:
ACAA compounds have been shown to be great candidates to replace common MALDI matrices for dual polarity MALDI IMS of lipids due to their reduced laser power requirement, their low toxicity, high sensitivity, and their near-perfect vacuum stability. This gives ACAA compounds an edge for both high spatial resolution MALDI IMS and high specificity imaging experiments (e.g., ion mobility or FTMS) that require longer acquisition times, often at elevated source temperatures (150°C) that can lead to loss of signal for commonly used matrices that degrade or sublime from the tissue surface over time. A new sublimation protocol for high spatial resolution MALDI IMS was developed by combining an ultra-thin amorphous matrix layer followed by an annealing step to induce crystallization increasing signal by 3-4 fold without inducing detectable analyte delocalization. Previously, we have demonstrated the use of 4-aminocinnamic acid for 5 µm spatial resolution MALDI IMS from Alzheimer's afflicted human brain tissue showing the intricate molecular distribution of gangliosides around β-amyloid deposits. We also demonstrated the use of 4-(dimethylamino)cinnamic acid for dual polarity 5 µm spatial resolution phospholipid MALDI IMS of human kidney and eye. In the case of the human kidney, we were able to annotate through exact mass ~120 lipids in positive mode and ~175 lipids in negative mode. From this point, we have synthesized a 2nd generation of ACAA compounds to expand both the molecular coverage and sensitivity by tailoring their absorption band to the wavelength of our MALDI laser (355 nm). This fine-tuning of the absorption band through the addition of selected functional groups allows an additional reduction in laser power leading to a further reduction of the spot size while increasing affinity for peptides, glycans, and proteins. This 2nd generation of ACAA compounds will be applied to our human tissue bank comprised of kidney, pancreas, brain, and eye.

Novelty:
Sublimated and annealed thin layer of 2nd generation ACAA matrices allow for high sensitivity 5 µm spatial resolution MALDI IMS

Preliminary Data:
5 um dual polarity MALDI IMS of lipids in human kidney, brain, eye, and pancreas

Contributing Authors:
Martin Dufresne[1,2], David M Anderson[1], Lukasz G Migas[3], Raf Van De Plas[3], Cody Marshall[1,4], Katerina Djambazova[1,4], Richard M Caprioli[1,2,5,6,7], and Jeffrey M Spraggins[1,2,4]

[1]Mass Spectrometry Research Center, Vanderbilt University, Nashville, TN
[2]Department of Biochemistry, Vanderbilt University, Nashville, TN
[3]Delft Center for Systems and Control, Delft University of Technology, Delft, Netherlands
[4]Department of Cell and Developmental Biology, Vanderbilt University, Nashville, TN
[5]Department of Chemistry, Vanderbilt University, Nashville, TN
[6]Department of Pharmacology, Vanderbilt University, Nashville, TN
[7]Department of Medicine, Vanderbilt University, Nashville, TN

Fletcher, John
University of Gothenburg, Sweden

Monday October 23, Session 2, 16:20-16:40

SIMS and Electrochemistry Correlate Dose Dependent Alterations On Cells

Introduction:
Proteasomal inhibitors have been utilized to create neurodegenerative models since aberrations on proteasome system is responsible for protein aggregates. On the other hand, some literature shows that low dose proteasomal inhibition can have neuroprotective effects. Lipids are dynamic regulatory factors on cells and changes in lipid profile affect neurotransmitter release dynamics and linked to neurodegeneration. To address the relationship between membrane lipid profile and neuroexocytosis upon proteasomal inhibition, a correlative study has been conducted with secondary ion mass spectrometry (SIMS) imaging and single cell amperometry. SIMS imaging was performed on chromaffin cells exposed to different doses of the UPS inhibitor lactacystin.

Method:
GCIB-SIMS was used to probe the membrane chemistry of chromaffin cells exposed to different doses of lactacystin. Co-cultured cells were subjected to electrochemical measurements to elucidate correlated changes in the dynamics of exocytosis. Bovine chromaffin cells we isolated from adrenal glands and cultured with different doses of lactacystin. SIMS analysis was performed using an Ionoptika J105 instrument fitted with a 40 kV gas cluster ion beam delivering CO2 clusters with a mean cluster size of 6000 molecules per cluster. To discover changes in the cell membrane following exposure. Single cell amperometry and in vivo impact electro cytometry were performed to monitor changes in neurotransmitter content and the dynamics of this release.

Results:
Gas cluster ion beam (GCIB)-SIMS was used to probe the membrane chemistry of chromaffin cells exposed to different doses of lactacystin. Co-cultured cells were subjected to electrochemical measurements to elucidate correlated changes in the dynamics of exocytosis. Bovine chromaffin cells we isolated from adrenal glands and cultured with different doses of lactacystin. SIMS analysis was performed using an Ionoptika J105 instrument fitted with a 40 kV gas cluster ion beam delivering CO2 clusters with a mean cluster size of 6000 molecules per cluster. To discover changes in the cell membrane following exposure. Single cell amperometry (SCA) and in vivo impact electro cytometry (IVIEC) were performed to monitor changes in neurotransmitter content and the dynamics of this release.

Novelty:
Combined MSI and echem measurements linking changes in lipid profile and exocytosis based resulting from UPS inhibition.

Preliminary Data:
Seperate low and high dose lipid changes detected potentially explaining contradictory literature.

Contributing Authors:
Inci Barut, Xiulan He, Erol Sener, Sanna Sämfors, Andrew G. Ewing, John S. Fletcher

Green, Felicia
Rosalind Franklin Institute, United Kingdom

Monday October 23, Session 2, 15:50-16:10

Enhancements in the use of SIMS for multi-omic biomolecular mass and structural analysis

Introduction:
Secondary Ion Mass Spectrometry (SIMS) is a powerful surface analysis technique that provides detailed chemical information about the surface and sub-surface regions of materials. However, low signals, particularly at high mass and at high spatial resolution, limit the technique's unique capability. Gas Cluster Ion Beam (GCIB) SIMS has shown to be excellent for the biological characterisation of hydrated frozen samples, achieving multi-omic imaging with sub-cellular resolution. This work show the use of GCIB-H2O to enhance SIMS sensitivity and demonstrate its use for the characterisation of cells and tissues.
Method:
TOF-SIMS analysis is performed on a J105 3D Chemical Imager instrument (Ionoptika Ltd.,UK) using a 70keV water gas cluster ion beam (GCIB-H_20) as the primary ion source with $(H_2O)_n$ clusters up to a size of n=30,000. The workflow for cell and tissue samples aims to keep them at near LiN_2 temperatures throughout the analysis. Tissue samples include frozen hydrated ape retinas and mouse hearts to study ATP in mitachondria. Examination and preparation of tissue and cell samples is performed with different standard methods in order to consider damage to the biological structure and suitability for SIMS analysis.
Results:
This work shows that the use of GCIB-H2O enhances the sensitivity and ability to detect intact, multiply-charged proteins in SIMS. This is possible for small proteins, such as Ubiquitin, (8565 Da) and Lyzozyme (14.3 kDa) and large enhancements in sensitivity to biomolecules can be seen between an Ar-GCIB and a H2O-GCIB primary ion beam. These are particularly large for some biomolecules, for example for ATP reaching up to x 9000 fold enhancement. These increases are higher in negative spectra and for frozen hydrated conditions. To study biological structure alongside biomolecular mass requires us to ensure native structure remains for mass spectrometry imaging (MSI). For MSI, tissue samples tend to come from frozen organs that are then cut to ~ 10 µm thickness using a cyrotome but this can introduce damage. Thicker samples could reduce this but with SIMS is the possibility of surface charging. We explore the damage effects on the proteins, lipids, metabolites and peptides in tissues caused by different sample preparation techniques. This will look at fragmentation and degradation of the near surface region with GCIB-H2O-SIMS analysis and MS/MS, and use depth profiling to look at the damage depth.
Novelty:
Instrumental improvements to inspire multi-omic biomolecular mass and structural analysis with GCIB-H2O-SIMS
Preliminary Data:
SIMS of multiply charged and intact species such as Lysozyme and Cytochrome C.
Contributing Authors:
Dr Sadia Sheeraz, Professor Nick Lockyer, Dr Felicia Green, Professor Zoltan Takats

Griffiths, Rian
The University of Nottingham, United Kingdom

Wednesday October 25, Session 9, 9:10-9:30

Tracking Drug Delivery In Vivo via Imaging Approaches

Introduction:
Too many drugs fail clinical trials because we cannot measure whether the drug is delivered to the right tissue, for the right duration, time, and correct dose. This project aims to address these challenges by developing an imaging workflow combining magnetic resonance imaging (MRI) for in vivo whole organ imaging and mass spectrometry imaging (MSI) for in vitro and ex vivo imaging of cell models and tissue sections. This will enable unbiased elucidation of drug distribution and endogenous metabolites in patient derived glioblastoma multiforme (GBM) samples. Our aim is to confirm drug-conjugate localisation via AP-MALDI MSI, to validate MRI data.

Method:
Synthesis: DOTA was coupled to Olaparib, deprotected and complexed. Salen complexes were synthesised by condensation (salicylic aldehyde with ethylene diamine), then complexed with salts. MRI data was collected (Bruker 7T MRI scanner) at 2 mm intervals. Relaxivity was determined at varying concentrations in HEPES buffer using 96-well plates. Custom routines allowed reconstruction in ImageJ. AP-MALDI: Drug/Salen 1mg/ml then 10mg/ml matrix (MeOH:H_2O, 3:2, v/v) were spotted onto target plates. Tissues were sectioned at 10um. Laser energy-4-8%, repetition rate-2000Hz. Data were acquired on a ThermoFisher Orbitrap Q-Exactive, full scan mode, 70000-140000 resolution (m/z400), m/z50−750, AGC target 1×106 charges, max injection 500ms, positive ionisation mode. MSMS (HCD): normalised CE20-40%, isolation +/-1.0 Th. Data were recorded for 1 minute, 1 microscan, and analysed in Xcalibur.

Results:
Olaparib is a therapy currently used for ovarian and fallopian tube cancers. However, it could have broader applicability as a therapeutic option; recently showing promise in oncology as a radiosensitiser. Contrast agent-tagged (MRI active) theranostic compounds that exhibit chemotherapeutic properties (Olaparib-DOTA) and small drug molecule mimics (salen complexes) were synthesised. Toxicity of synthesised compounds were determined via assays in patient derived GBM cell lines, IC50's was determined to be >100µM. MRI experiments show the relaxivity of an olaparib-DOTA complex comparable to the clinical standard (ProHance™). Salen complexes . Initial AP-MALDI experiments show that most of these compounds can be ionised in positive ion mode and CHCA matrix is optimal (vs DHB). Moreover, ionisation mechanisms were established with either [M+H]+ or M+ preferentially detected. The Olaparib-DOTA complex was tested in a 3D spheroid in vitro model, using patient-derived GBM cells, that exhibits tumour behaviour (hypoxic core). A medium (1% agarose) for spheroid suspension was optimised for MRI analysis, and samples treated with 0-100 µM tagged-drug, visualised via T1 scans. This was then sectioned for MSI validation experiments to determine penetration and whether the compound remains intact. In a separate approach, an excised murine brain was soaked in one of the synthesised salen compounds then imaged via MRI. This brain was subsequently sectioned and imaged via AP-MALDI. The salen compound provided good contrast via MRI and was found to be distributed homogenously through most brain tissue via MSI, with some evidence of accumulation in the fibre tract in the cerebellum.

Novelty:
i) Synthesis of Olaparib-DOTA, ii) synthesis of MRI-active small drug molecule mimics, iii) MSI to validate MRI-guided drug delivery.

Preliminary Data:
Synthesised compounds, tocixity data, MRI activity data, MS of sythesised compounds, MRI followed by MSI of treated tissue models.

Contributing Authors:
Charlotte Gidman, Ethan Harrup, Georgia Aspinall, Milo Hollingworth, Cameron Alexander, Ruman Rahman, Peter Harvey & Rian L. Griffiths

Haddow, Julia
University of Dundee, United Kingdom

Tuesday October 24, Session 6, 13:10-13:30

Chagas' disease - tissue clearing and mass spectrometry to study parasite localisation and drug distribution in Trypanosoma cruzi infected mouse tissues.

Introduction:
The drug development for Chagas' disease, a neglected tropical infection caused by the protozoan parasite Trypanosoma cruzi (T. cruzi), remains a significant challenge. Current treatments lack efficacy in the chronic stage and exhibit toxicity issues, necessitating research into new drugs. Despite development of several promising compounds, achieving a full, sterile cure remains elusive. Therefore, it is crucial to understand the underlying biology of the infection and explore potential causes for drug failures. Investigating the morphological stages of the parasite, particularly the existence and behaviour of dormant forms, as well as examining the patterns of drug distribution and parasite localisation following treatment is essential. Dormant parasites may remain unaffected by treatments and/or reside in areas with inadequate drug distribution.

Method:
The chosen method for 3D parasite localisation studies is CUBIC (Clear, Unobstructed Brain/Body Imaging Cocktails). It has been optimised for all target tissues, and a parasite strain expressing dual fluorescent/bioluminescent reporters has been selected. To identify parasite-specific phospholipids through mass spectrometry, high-resolution positive and negative ion electrospray MS was employed using an Advion Nanomate ion source on an Orbitrap XL. This approach aimed to distinguish literature-suggested parasitic phospholipid ions from host background signals. Lipid extracts from uninfected and T. cruzi-infected H9C2 cell cultures were compared to identify potential m/z values indicative of parasitic presence. For drug distribution studies, T. cruzi-infected animals received GSK1, and MALDI MS will be used to investigate its distribution within tissue slices.

Results:
A novel method has been developed to precisely localise the T. cruzi (CL Brener strain) parasites within organs of chronically infected mice. The optimised conditions enable effective clearance of tissues including brain, heart, kidney, intestines, liver, lung, lymph node, ovary, uterus, skeletal muscle, spleen, and stomach. The most compatible parasite strain for this approach is T. cruzi CL Brener expressing mScarlet fluorescent and Luciferase bioluminescent proteins. This method allows for the creation of 3D models of infected organs, revealing the exact parasite localisation after drug treatment. Simultaneously, another method of parasite localisation, involving lipid extraction and mass spectrometry analysis, has been explored. Specific m/z values have been investigated as potential indicators of parasitic presence. One promising molecule, plasmenyl-phosphatidylethanolamine - C36:2 plasmenyl-PE ($C_{41}H_{80}NO_7P$), has been identified as a promising parasitic marker. Further research aims to translate these findings onto a MALDI platform. Investigation of drug distribution is also crucial, as exemplified by GSK2 compound. Although, initial analysis of total brain homogenate suggested sufficient exposure to deliver a cure, treatment failed. Subsequent MALDI MS analysis on GSK2-treated brain slices revealed non-homogeneous distribution of the compound with multiple areas within the organ exhibiting insufficient drug concentrations to eliminate parasites, potentially explaining the failure. The focus is now on utilising infected animals treated with GSK1, a proteasome inhibitor that demonstrates efficacy in vitro but consistently fails to cure the disease in vivo. This compound presents an opportunity to investigate if inadequate tissue distribution contributes to treatment failures. In summary, a 3D visualisation method has been developed to localise parasites surviving drug treatment, while efforts continue to optimise biomarker research for MALDI MS analysis. The goal is to conduct experiments within a single animal, eliminating the need for multiple platforms to localise parasites and study drug distribution.

Novelty:
Research aims to advance understanding of T. cruzi infection and determine optimal properties of anti-chagasic compounds necessary for sterile cure.

Preliminary Data:
Potential biomarkers indicative of parasitic presence identified and whole-body drug distributions by MALDI MS imaging obtained.

Contributing Authors:
Julia Haddow, Rupa Nagar, Peter Marshall, Pablo Castanedo-Casado, Jaime De Mercado-Arnanz and Kevin Rea

Iakab, Stefania Alexandra
CeMOS - Center for Mass Spectrometry and Optical Spectroscopy, Germany

Tuesday October 24, Session 4, 9:00-9:20

(3D) Molecular Snapshots of Spheroids by Mass Spectrometry Imaging

Introduction:
Matrix assisted laser desorption/ionization mass spectrometry imaging (MALDI-MSI) is the go-to technique for describing in situ the molecular composition of biological samples. Organoids and spheroids are attractive samples for studying biological phenomena in human cells, and are becoming vital for drug screenings and clinical studies in terms of time and cost efficiency. Therefore, molecular snapshots provide valuable information for applications such as cell classification, biomarker discovery, and drug screenings. Here we developed a platform that allows high throughput and reliable detection of small molecules (in 3D) from spheroid models.

Method:
Spheroids were generated in house and flash frozen in a gelatin mold using HPMC-PVP as embedding medium. Sections were obtained at 12 and 20 µm thickness with a cryostat, and mounted on ITO coated slides. NEDC and DAN matrix were sprayed on the sections prior to MS acquisition. Bruker's timsTOFfleX was used in tims ON or OFF modes, at 20 µm lateral resolution. Data were preprocessed, analyzed and exported using SCiLS Lab (Bruker Daltonics), M2aia software was used to obtain 3D reconstructions and volume visualizations, and in house scripts were used in R language to further analyze the data.

Results:
Our in-house designed/manufactured 3D-printed metal casting molds enabled the embedding of several 3D culture samples in a precise and reliable sterical arrangement. Thus, sample preparation including harvesting, embedding and freezing of the spheroids has become reproducible, high throughput and, most importantly for 3D- reconstructions, reliable for obtaining consecutive sectioning. High quality imaging data was acquired in the ranges of small molecules (m/z 50-600 Da) and lipids (m/z 300-1200 Da), from which we were able to filter over 200 spheroid-associated molecules, which have been annotated using Metaboscape. Unsupervised multivariate data analysis (segmentation and principal component analysis) revealed multiple different spectral patterns, presumably corresponding to fibroblasts and cancer cells, as well as regions with mixed molecular fingerprints. PCA results suggested that the positioning of a specific cell type within a spheroid changed that cell type's molecular composition. the volcano plot results of all the possible unique combinations. Significant values were selected in volcano plots, by setting the adjusted p value threshold to 0.01 and the fold change threshold to 0.5. After annotating cell specific features, we obtained the stacked images from ~ 50 consecutive 20 µm thick sections. Region-specific features were the following: m/z 498.26 for the exterior layer, m/z 835.56 for the cancer cells and m/z 885.55 for the fibroblasts. Our 3D visualization workflow further proved that specific metabolites can be distinguished based on cell type and cell layer within a 3D cell culture model. The potential of our platform to identify markers for biological mechanisms unique to each cell type could be valuable for studying specific cellular signaling or metabolic interaction between cancer and fibroblast cells.

Novelty:
High-throughput spatial multi-omics data acquired from micron-scale samples reveal cell-specific metabolic fingerprints.

Preliminary Data:
Further work has been done to evaluate metabolic changes inside the different zones discovered within the bicultured spheroids

Contributing Authors:
Stefania-Alexandra Iakab, Florian Keller, Lars Gruber, Stefan Schmidt, James L. Cairns, Jasjot Singh, Frank Fischer, Richard Schneider, Rüdiger Rudolf, Carsten Hopf

Lagache, Laurine
PRISM - Inserm U1192, France

Wednesday October 25, Session 11, 14:20-14:40

New method machine process to unravel tissue biomarkers and validate it by multiplex MALDI IHC

Introduction:
Integrating machine learning tumour heterogeneity in the cancer diagnosis process is an essential issue to tackle the complexity of the pathology with precision and efficiency. Specific omic molecules identifications for each heterogeneous tumour subpopulations are especially important in order to characterize them in depth. In this way, distinguishing and detecting one clone from another, whatever the molecules analyzed, is an easy and fast process which can be carried out during the diagnosis. Moreover, protein information from each subpopulations are particularly interesting for drug discovery to tailor optimized therapy to the heterogeneous tumour.
Method:
The implementation of the concept was first optimized on rat brain. Lipid, protein and peptide MALDI mass spectrometry imaging (MSI) were performed on cerebellum area rat brain. A first MatLab script was developed to process imaging data, providing unsupervised clustering, independently for each data set. A second Python script provided the lipid, protein and peptide discriminant cluster ions. Microproteomic and MS/MS analysis were performed to identify the protein and lipid ions previously listed. In order to validate the identification of a subpopulation, a multiplex immunohistochemical (IHC) MALDI-MSI technique, using TAG mass technology, is being developed to identify specific biomarkers of the latter on tissue.
Results:
Multi MSI made it possible to demonstrate the presence of various heterogeneous subpopulations. 3 clusters were identified with the same spatial location for each images, whatever the molecule analysed, corresponding to the Granular Layer, Molecular Layer and the White Matter region of the cerebellum rat brain. Each cluster presents a specific localized lipid and protein network according the discriminant ions list delivered by our script. This purpose was verified experimentally thanks to localized microproteomic analysis and localized lipid analysis. This information will make it possible to produce a computer prediction model, which will make it possible to identify the presence of any cluster on any tissue according their specific molecular fingerprint, and validate it by machine learning. This protocol was also experimented on most complex tissues, as breast cancer tissues, showing same results. The multiplex immunohistochemical (IHC) MALDI-MSI technique make it well possible to visualize different biomarkers on the same image. In this way, the Granular Layer, Molecular Layer and the White Matter region of the cerebellum rat brain were observable at the same time by targeting a discriminant biomarker for each area.
Novelty:
multiplex immunohistochemical (IHC) MALDI-MSI
Preliminary Data:
Heterogenous clusters obersvations by omic MALDI MSI
Contributing Authors:
Laurine Lagache, Yanis Zirem, Alexandre Goossen, Zoltan Takats, Isabelle Fournier, Michel Salzet

Liebenberg, Keziah
Baylor College of Medicine, United States

Tuesday October 24, Session 4, 9:20-9:40

Insights into Metabolic Alterations Associated with Resistance to Immune Checkpoint Inhibitors in Triple Negative Breast Cancer Utilizing DESI-MSI

Introduction:
The use of immune checkpoint inhibitors (ICIs) is a promising strategy for the treatment of triple negative breast cancer (TNBC), for which treatment options are limited. Ongoing clinical trials have revealed, however, that only a small subset of patients showed durable responses to ICIs, while others acquired resistance. Treatment with ICIs is costly and accompanied by severe side effects, and it is therefore crucial to correctly identify patients who will benefit from treatment. There is mounting evidence that tumors can evade immune attack by metabolically suppressing the tumor microenvironment (TME) and hindering immune cell function. It is therefore important to consider the metabolic interplay occurring in the TME and its role in determining patient response and resistance to ICI treatment.

Method:
The Xiang Zhang laboratory at Baylor College of Medicine has established a series of murine TNBC models with sensitivity and acquired resistance to ICI treatment. The TNBC tissues were sectioned at 12 µm and analyzed using a Orbitrap Q-Exactive HF mass spectrometer (Thermo Scientific) suited with a DESI-MS imaging interface. DESI-MSI was performed using dimethylformamide and acetonitrile (ACN) as the solvent system in both the negative and positive ion modes. Images were obtained using a 200 µm spatial resolution. The tissue sections were then stained with hematoxylin and eosin (H&E) and distinct histological regions were annotated by a pathologist. Mass spectra correlating to regions of viable tumor were extracted and statistical analyses performed using significance analyses of microarrays (SAM).

Results:
DESI-MSI provides spatial lipid profiling of murine TNBC tissues with both sensitivity and resistance to combination ICI and chemotherapy treatment. It further provides delineation between the lipid profiles of tumor regions and regions of the TME, providing insights into metabolic interplay between these regions. The DESI-MSI method was optimized in both ion polarities for the detection of lipid species directly from TNBC tissue sections. A wide variety of lipid species were detected in both ion modes including cardiolipins, ceramides, fatty acids, phosphatidylserines, phosphatidylinositols, phosphatidylethanolamines, triacylglycerols, diacylglycerols and phosphatidylcholines. Although complex, the mass spectra obtained in both ion polarities presented trends that were characteristic of sensitive and resistant TNBC tissues. Statistical analyses with SAM revealed that triacylglycerols and arachidonic acid were significantly upregulated in TNBC tissues with resistance to ICIs, whilst phosphatidylcholines were upregulated in tissues with sensitivity to treatment. Furthermore, metabolic profiles before and after ICI treatment were compared allowing for the identification of treatment-induced alterations. Principle component analysis revealed a significant separation between TNBC tissues before and after treatment, indicating that chemotherapy combined with ICIs induces significant metabolic alterations within tumors. In future experiments, tandem MS experiments using high-energy collision dissociation will be conducted to elucidate the structural information regarding the identified upregulated triacylglycerol and phosphatidylcholine species. Immunofluorescence staining will be conducted on tissue serial sections following DESI-MSI analyses to correlate the spatial metabolic information with the location and identity of infiltrating immune cells. This will provide further insight into the cross-talk between tumor and immune cells in the TME. Further statistical analyses using logistic regression and the least absolute shrinkage and selection operator (LASSO) will be employed to develop classification models for the prediction of response to ICIs in TNBC tissues.

Novelty:
DESI-MSI of TNBC tissues allows spatial investigation of the metabolic alterations underpinning sensitivity and resistance to ICIs.

Preliminary Data:
DESI-MSI provides insights into lipid alterations underpinning ICI treatment response in TNBC and the metabolic impact of combination treatment.

Contributing Authors:
Keziah Liebenberg, Meredith Spradlin, Liqun Yu, Xiang Zhang, Livia Eberlin

Marchetti-Deschmann, Martina
TU Wien, Austria

Wednesday October 25, Session 11, 13:10-13:30

Correlating Tissue Biomechanics and Molecular Information – The Combination of physiological AFM and MALDI MSI

Introduction:
Degeneration of menisci is responsible for pain and loss of quality of life. 75 % percent of the dry weight of menisci are mainly collagens (type I-III, V, VI) and the most abundant collagens form supramolecular structures, the collagen fibrils. Collagen fibrils are the basic structural building blocks that provide mechanical stability to tissues from the nano- to the macroscale. To get an understanding of how collagens and proteins of the extracellular matrix influence degeneration and mechanical stability of menisci, a multimodal imaging approach was developed. We measured for the first time, biomechanical properties by AFM micro-indentation under biological conditions and proteomic changes by MALDI MSI on one tissue section to correlate molecular changes with mechanical tissue properties.

Method:
Cryosectioned human menisci (10 µm) were thaw-mounted on Poly-L-Lysin-coated microscopic slides. QPLM were collected to assess collagen fibre orientation. AFM (JPK BioAFM) microindentation analysis was conducted with a 10 µm sphere (1.5 nN setpoint) at physiological conditions (Ringer acetate buffer/protease inhibitors). Force maps at 50 µm spatial resolution were measured in ROIs, red-red to white-white zones. Salts/lipids were removed by washing (ethanol, water, Carnoy's solution) and samples were on-tissue digested. Trypsin/Lys-C, collagenases were applied by spraying (HTX Sprayer). After incubation at 37° C, α-cyano-4-hydroxycinnamic acid was also applied via spraying. Samples were measured on a MALDI-linTOF, a MALDI-TOF/TOF and 7T FTICR system (8030 Shimadzu, ultrafleXtreme/scimaX, Bruker) at 20 to 40 µm lateral resolution. Images were co-registered by SCiLS (Bruker).

Results:
The fibre orientation of degenerated menisci samples was determined via Quantitative polarized light microscopy (QPLM) to better understand mechanochemical properties determined by atomic force microscopy (AFM) and MALDI MSI before analysis. Fibre orientation plays a crucial rule in elasticity measurements. To determine tissue stiffness, AFM microintendation analysis was performed after cutting the material into 10 µm thin sections. To preserve physiological condition and prevent the tissue from degradation Ringer acetate buffer solution, which is containing only a limited amount of MS incompatible substances, was used and protease inhibitors added. Microintendation results revealed different properties for the different meniscis regions; the red-red, red-white and white-white zone were clearly distinguishable. The tissue sections were immediately washed after AFM analysis to remove salts and lipids before on-tissue digestion. While most of the human proteins are very well digested by Trypsin/Lys-C, collagen shows only a limited number of potential cleavage sites. Therefore, collagen on-tissue digestion as established in combination with Trypsin/Lys-C for sufficient peptide generation. After incubation the samples were washed, dried and subsequently covered with MALDI matrix. Via image co-registration of QPLC, AFM and MALDI MSI analysis we can show that, beside other proteins of the extracellular matrix, the spatial distribution of different collagen types is correlating with the indentation modulus. In regions with higher collagen intensity, like the white-white region, the indentation modulus is higher in comparison to regions with relatively low collagen availability, like the red-red region of human menisci. Our innovative combination of methods for tissue imaging allows for the first time to better understand the correlation of biomechanical properties and underling molecular changes on a µm-scale.

Novelty:
First time combination of MALDI MSI with AFM measurements under physiological conditions to assess tissue elasticity and molecular information.

Preliminary Data:
Correlation to collagen 1 distribution in tissue is additionally investigated by MALDI IHC.

Contributing Authors:
Martina Marchetti-Deschmann, Aleksandra Lebedeva, Martin Handelshauser, Orestis Andreotis, Philipp Thurner

Mckinnon, Jayden
University of Wollongong, Australia

Tuesday October 24, Session 4, 8:40-9:00

Enhanced Coverage and Spatial Resolution for the Mass Spectrometry Imaging of Small Metabolites using MALDI-2

Introduction:
Given the cell-to-cell metabolic heterogeneity observed in complex biological systems, there is a need to push spatial-omics techniques towards the single cell level. MALDI-MSI has taken tremendous strides towards elucidating altered metabolic states in biological tissue, however, the low ionisation efficiencies for many metabolites limits both analyte coverage and practical spatial resolution. Herein we have applied laser post-ionisation (MALDI-2) to enhance detection sensitivity and metabolite coverage allowing increased spatial resolution using oversampling.

Method:
Biological samples were prepared by applying napthyl ethylenedihydrochloride (NEDC) matrix by automatic spraying or sublimation prior to analysis by MALDI or MALDI-2. An intermediate pressure dual ion source (Spectroglyph, USA) fitted with a 349 nm UV laser was used to generate a MALDI plume before interception via a 266 nm PI laser Mass analysis was conducted using an Orbitrap Elite mass spectrometer (Thermo Fisher, Bremen) in the negative ion mode with a mass resolving power of 120 000 at m/z 400 (FWHM). Following analysis, the corresponding ion images were generated using the cheminformatics software LIPOSTAR, with metabolite annotations conducted via a false-discovery-rate approach through the METASPACE platform.

Results:
We first optimised ion source conditions to increase the detection of low mass metabolites. We observed a significant increase in the number and intensity of ion signals between m/z 100-1000 with an approximately 50% reduction in RF amplitude combined with a reduction in the ion source pressure from 7 to 4 Torr. The effect of reduced source pressure is hypothesised to arise via the faster mean velocity of ions and reduced radial diffusion as they traverse the gap between the two ion funnels. We also optimised the time delay between the MALDI and MALDI-2 laser pulses with an optimal delay time of 6 µs observed for low mass metabolites, in contrast to the 15-20 µs typically used for lipids. MALDI-2 doubled the number of ions observed in mouse kidney tissue and allowed the detection of a variety metabolites not observed using MALDI, e.g., arginine and uridine. When compared to existing kidney datasets on METASPACE, MALDI-2 detected 34 metabolites not previously reported in mouse or human kidney tissue. MALDI-2 was then applied to the analysis of metastasised breast cancer, revealing an up to 20-fold increase in tumour-specific ion signals, including 6 metabolites not detected at all using MALDI. Leveraging the increased sensitivity enabled by MALDI-2, we obtained rich metabolite spectra with a laser spot diameter of ~12 µm and step sizes as low as 5 µm, enabling metabolite imaging throughout kidney and cancer tissues at single cell scales.

Novelty:
MALDI-2 enhances detection of low mass metabolites allowing reduced pixel sizes using oversampling.

Preliminary Data:
MALDI-2 provides significant benefits for the imaging of small metabolites from both kidney and cancer tissues

Contributing Authors:
H.H.Milioli, C.Purcell, C.L.Chaffer, B.Wadie, T.Alexandrov, T.W.Mitchell and S.R.Ellis

Metodiev, Martin
National Physical Laboratory, United Kingdom

Monday October 23, Session 2, 16:40-17:00

Measuring spatial resolution of different Mass Spectrometry Imaging modalities

Introduction:
Spatial resolution in mass spectrometry imaging (MSI) is the minimal distance between two features such that those features are separated in an image. We previously developed an image formation model allowing parameters that influence spatial resolution to be studied. One such parameter, image blur, is generated by the size of the analytical probe, stage velocity, scan time, and material consumption effects. Image noise, which arises from the instrument detector and ion source fluctuations, also deteriorates resolution. Spatial resolution is therefore computed taking both into account, in a modality agnostic manner. This study presents a comparison of the resolution capabilities of different modalities with the goal of constructing an MSI modality "resolution ruler".

Method:
Gold, silver, polylactic acid, Fmoc-pentafluoro-L-phenylalanine, photoresist (AZ 52 14E) and irganox-1010 were prepared by vapour deposition (Angstrom Coater) or pipetting from solution. The number of characteristic peaks, intensity and signal-to-noise ratio distributions (SNR) determined from characteristic spectra were used as criteria to assess material performance. Tissue imaging data acquired with NanoSIMS (CAMECA), OrbiSIMS (Hybrid SIMS, IONTOF), MALDI and DESI qToF (Synapt G2-Si / Xevo G2-XS, Waters Corp) were used to calculate the resolution of those set ups. Resolution was calculated from the intersection of a modulation transfer function (MTF) and a noise power spectrum, which were obtained from step-edge-like features. Pixel sizes ranging from 117 nanometres to 100 micrometres were used.

Results:
The ability of different materials to act as a multimodal resolution standard was assessed using the criteria outlined in the methods section. The number of characteristic peaks was computed for each material and modality. The average intensity of a given peak and its image SNR were also calculated. The interquartile ranges of the intensity and SNR distributions were obtained thereafter. To estimate the performance of each material, these parameters were normalised and plotted on a spider graph. Where analysed by MALDI, gold and PLA exhibited many characteristic peaks, and their intensity and SNR distributions exhibited high median values and interquartile ranges. Most materials analysed by DESI performed poorly aside from PLA and photoresist (AZ 5214E) which showed enough characteristic peaks and a sufficient range of ion intensities. To evaluate resolution in multimodal MSI tissue data a global MTF was imposed on each image. This MTF was derived from sharp step edge features that satisfied a goodness of fit threshold, which allowed untrustworthy edges to be filtered out. This was done with the aid of the reduced chi-squared statistic. This approach showed good agreement when compared with ground truth silver step edge studies. As there are numerous ions detected in MSI analyses, resolution can be measured across all ions within each dataset. Thus, a given dataset is characterised by a resolution distribution. In order to estimate the resolution of an entire data cube, a median resolution is obtained, and bootstrapping is used to find a confidence interval. At a given pixel size, each modality was then assigned a median resolution value and an interquartile range. The median resolutions of NanoSIMS, OrbiSIMS, MALDI and DESI were computed to be 400nm, 40µm, 100µm and 450µm respectively. This allowed for the construction of an MSI modality "resolution ruler".

Novelty:
Comparing resolution performance of different MSI modalities. The ability to measure spatial resolution from tissue imaging experiments and a resolution standard.

Preliminary Data:
The median resolutions of NanoSIMS, OrbiSIMS, MALDI and DESI were computed to be 400nm, 40µm, 100µm and 450µm respectively.

Contributing Authors:
M. D. Metodiev, R. T. Steven, A. Christakopoulou, J. Bunch

Migas, Lukasz
Delft University of Technology, Netherlands

Tuesday October 24, Session 8, 17:00-17:20

Qu-Cee: An automated quality control pipeline for cohort and 3D imaging mass spectrometry

Introduction:
Matrix-assisted laser desorption ionization (MALDI) Imaging Mass Spectrometry (IMS) is a versatile analytical technique that spatially resolves the chemical composition of biological samples. IMS can concurrently detect hundreds of molecular species across multiple chemical classes from a single tissue section. While MALDI IMS is valuable in clinical tissue analysis, large-scale studies of cohorts (e.g. multiple samples from different patients) or 3-D studies (multiple samples from the same organ) can be hampered by non-biological variation introduced at the sample preparation or instrumental level. To assess and control for such variation, we developed Qu-Cee, an open-source library to track data quality using spectral and spatial metrics. By identifying and highlighting technical variation across IMS experiments, Qu-Cee helps control the robustness and reproducibility of IMS studies.
Method:
Qu-Cee is developed in Python and supports IMS data in vendor (Bruker .d), imzML, and custom formats via the imzy library. Human kidney and human eye samples were cryo-sectioned at 10 µm thickness and thaw-mounted onto indium-tin-oxide (ITO) slides. Either 2,5-Dihydroxyacetophenone or aminated cinnamic acid analogue matrix was sublimed onto the tissue surface using an in-house developed sublimation device. MALDI IMS data were acquired in both positive and negative (kidney) and positive polarities (eye) at 10 µm pixel size using a Bruker timsToF FleX (Bruker Daltonics) in QToF mode. Data analysis and visualisation were performed using in-house developed software.
Results:
Reporting of data quality controls (QC) is widely recognized and practised in various -omics fields. However, in the context of IMS studies, the incorporation of comprehensive QC has been relatively limited. Neglecting thorough QC measures can lead to observations influenced by technical variations, particularly in studies involving multiple sections from the same (e.g. 3-D) or different organs (e.g. patients). Moreover, long-term studies spanning weeks/months can introduce additional variations and outliers, which can significantly impact data interpretation and alter the study conclusions. Data pre-processing steps such as mass alignment, mass calibration, and inter-/intra-/batch-normalization can correct large data variations, reducing drift and bias in the downstream statistical and biological analyses. In this study, we apply Qu-Cee's workflow to assess the stability and reproducibility of MALDI-IMS data directly after acquisition and the influence of pre-processing steps. We demonstrate this in a 3-D experiment of the human eye (64 sections, positive mode) and a longitudinal study of human kidney samples investigating the effects of sample storage (96 datasets, 48 in each polarity). Qu-Cee facilitates the collection of spectral-, spatial-, and intensity-based metrics such as signal intensity variation, number of detected and common peaks, tentative identifications, peak widths, mass error, and others. The spectral quality measures provide insights into instrumental drift (e.g. mass shifts) and the efficacy of the pre-processing methods. Spatial measures shed light on differences in the sample morphology, while signal intensity-based metrics track the impact of no-/inter-/intra-/batch-normalization on data. All three metric types together enable Qu-Cee to generate a comprehensive dataset- and study-wide overview of IMS data variation, stability, and reproducibility, effectively identifying inconsistencies and outlier behaviour. Furthermore, we showcase the ability of the Qu-Cee workflow to assess the influence of pre-processing steps on data quality and provide early warnings about potential outlier datasets.
Novelty:
Automated quality control workflow for tracking variation across IMS experiments in cohort or 3-D studies and to uncover outlier datasets.
Preliminary Data:
We present automated quality control software for tracking of non-biological variation in a cohort and a 3-D studies.
Contributing Authors:
Lukasz G. Migas, Katerina V. Djambazova, David M. G. Anderson, Martin Dufresne, Ali Zahraei, Madeline E. Colley, Jeffrey M. Spraggins, and Raf Van de Plas

Morawietz, Carolin
Justus Liebig University, Giessen, Germany, Germany

Wednesday October 25, Session 9, 9:40-10:00

Imaging of Drugs and Lipids in the Parasite Fasciola hepatica using High-Resolution AP-SMALDI MSI

Introduction:
The parasite Fasciola hepatica (F. hepatica) causes fascioliasis, one of the neglected tropical diseases listed by the WHO.[1] Despite threatening humans and grazing animals across all inhabited continents, the flatworm has received little attention in research over decades. High-resolution atmospheric-pressure scanning microprobe MALDI MS imaging (AP-SMALDI MSI) enables molecular-level insights into physiology and metabolism of the parasite. As a result, the findings broaden the understanding of biochemical processes and drug operation mechanisms and might eventually even support the development of new treatment strategies.
Method:
Drug-treated or untreated F. hepatica were embedded in gelatin solution, cryosectioned, thaw mounted onto regular glass slides, and stored at −80 °C until MSI analysis. Before measurement, sections were thawed in a desiccator for 30 min and subsequently covered with matrix utilizing the SMALDIPrep pneumatic sprayer system (TransMIT GmbH, Giessen, Germany). Measurements were performed using an AP-SMALDI5 AF ion source, including a 3D autofocusing system (TransMIT GmbH), coupled with a Thermo Scientific Q Exactive HF instrument[2] (Thermo Fisher Scientific, Bremen, Germany). Analyses were conducted in an m/z range of 250−1000 at pixel sizes down to 7 µm in positive- or negative-ion mode. The Mirion software package[3] and the LIPIDMAPS[4] database were used for data analysis and lipid annotation[5,6], respectively.
Results:
Triclabendazole (TCBZ), Imatinib, and the drug candidate Schl-33.292 were detected in sections of individually treated F. hepatica specimens. While TCBZ and Imatinib signals were already detected in the worm after 20 min of exposure, Schl-33.292 was not found to be present before 12 h of exposure. At the incubation time of initial detection, TCBZ was exclusively detected in the outer surface (tegument) of the parasite, whereas Schl-33.292 was only found in the intestine. These findings point towards tegumental and oral drug uptake routes, respectively. During further incubation, the drugs spread into other tissues, such as gastrodermis and reproductive organs, as well. Furthermore, signals of predicted Imatinib and Schl 33.292 metabolites were present in the MSI data, spatially superimposed with the signals of the parent drugs. By imaging sections of the untreated parasite, we investigated the endogenous lipids present in the parasite's most relevant organs regarding host contact and reproduction (i.e. gastrodermis, tegument, ovary, testes) and revealed signals of lipid species that accumulate or even specifically occur in these organs. This points to a specific lipid composition of the different pathogen tissues. In combination with information obtained from histological staining, these lipid markers also enabled precise localisation of the aforementioned drug compounds within the tissue section.
[1] WHO, Integrating neglected tropical diseases into global health and development: fourth WHO report on neglected tropical diseases. Geneva, Switzerland, 2017. [2] R. A. Scheltema, J.-P. Hauschild et al., Mol. Cell. Proteomics 2014, 13, 3698. [3] C. Paschke, A. Leisner et al., J. Am. Chem. Soc. 2013, 24, 1296. [4] E. Fahy, M. Sud et al., Nucleic Acids Res. 2007, 35, W606-12. [5] C. M. Morawietz, H. Houhou et al., Front. Vet. Sci. 2020, 7, 611270. [6] C. M. Morawietz, A. M. Peter Ventura, C. G. Grevelding, S. Haeberlein, B. Spengler, Parasitol. Res. 2022, 121, 1145.
Novelty:
Uncovering spatial distributions and metabolic pathways of various compounds in the parasite F. hepatica using high-resolution AP-SMALDI mass spectrometry imaging.
Preliminary Data:
Experiments show that AP-SMALDI MSI is a suitable method for investigating F. hepatica's lipid distribution and pharmacokinetics.
Contributing Authors:

Carolin M. Morawietz (1,5), Stefanie Gerbig (5), Parviz Ghezellou (1), Georg Rennar (3), Kerstin Strupat (4), Martin Schlitzer (3), Christoph G. Grevelding (2), Simone Haeberlein (2), Bernhard Spengler (1,5)

(1) Institute of Inorganic and Analytical Chemistry, Justus Liebig University, Giessen, Germany (2) Institute of Parasitology, Justus Liebig University, Giessen, Germany (3) Institute of Pharmaceutical Chemistry, Philipps University, Marburg, Germany (4) Thermo Fisher Scientific (Bremen) GmbH, Bremen, Germany (5) TransMIT GmbH, Giessen, Germany

Müller, Max Alexander
Justus Liebig University Giessen, Deutschland

Tuesday October 24, Session 6, 13:30-13:50

Lipid signatures and inter-cellular heterogeneity of naïve and lipopolysaccharide-stimulated human microglia-like cells using AP-SMALDI MSI at 1.5 µm lateral resolution

Introduction:
Microglia are non-neuronal cells, residing in the brain and spinal cord, often referred to as the immune cells of the central nervous system. Their involvement in several neurodegenerative diseases has been implicated recently, and multiple morphologically different phenotypes of microglia fulfilling discrete functions have been described. However, morphology is not the sole descriptor of cell status, which is rather based on complex biological processes. Lipids, as examples for bioactive molecules, can give vital insights into a cell's metabolic status or its response to a changing environment. Here, we attempted to characterize, statistically evaluate and localize the lipid signatures in human microglia-like cells and their response upon inflammatory stimulation with a lateral resolution of down to 1.5 µm.

Method:
Microglia-like cells were differentiated from human embryonic stem cells on glass slides and stimulated with lipopolysaccharide (LPS). Atmospheric-pressure scanning microprobe matrix-assisted laser desorption/ionization mass spectrometry imaging (AP-SMALDI MSI) was employed using a prototype ion-source based on an AP-SMALDI5 AF system (TransMIT GmbH, Giessen, Germany), capable of a lateral resolution of 1.5 µm, coupled to a high-resolution orbital trapping mass spectrometer (Q Exactive, Thermo Fisher Scientific (Bremen) GmbH, Germany). Multiple sample-preparation and matrix-application protocols employing 2,5-dihydroxybenzoic acid or 9-aminoacridine were evaluated and optimized for positive- and negative-ion mode, respectively, employing an ultra-fine pneumatic spraying system (SMALDIPrep, TransMIT). Data was evaluated using Mirion, Perseus or self-written Matlab scripts and lipid annotation was based on database research employing accurate mass measurements using LipidMAPS.

Results:
First, sample preparation workflows were optimized for flash-frozen cells and cells fixed with paraformaldehyde (PFA). It was observed that flash-frozen cells were best suited for in-depth lipidomics research, while fixation with PFA for 1 minute better preserved the morphology of the cells and was therefore used for high-lateral-resolution AP-SMALDI MSI experiments. A lateral resolution of down to 1.5 µm pixel size was achieved while preserving the morphology of the cells on a micrometer scale compared to microscopy results. It was possible to differentiate cell lines and LPS-activation status based on population-based lipidomics results from AP-SMALDI MSI at 5 µm lateral resolution using statistical models. Especially triglyceride species were found to be increased upon inflammatory stimulation in individual cells. High-lateral-resolution AP-SMALDI MSI with sub-cellular resolution down to 1.5 µm pixel size was then applied to better resolve the heterogeneous lipid distributions between naïve and LPS-stimulated cells in positive-ion mode. The increase in triglyceride species abundances was assigned to lipid droplets, which were heterogeneously distributed on a single-cell level but were overall increased upon stimulation. While this would have been observable with fluorescence staining techniques and is in line with previous results, our method allowed for the first time to investigate the molecular composition of lipid droplets and their inflammatory-induced changes on a molecular level while simultaneously resolving their heterogeneous distribution. Further, phospholipid-based heterogeneity was characterized and used to differentiate otherwise undistinguishable microglia cells into multiple well-resolved phenotypes using a statistical approach or MS images of selected phospholipids. Especially, a reproducibly heterogeneous expression of some phosphatidylinositol species differing only by fatty-acid unsaturation between genetically identical microglia cells, which is unaffected by inflammatory stimulation, was found in negative-ion mode and visualized at 2 µm lateral resolution, while other phospholipid species with similar fatty-acid compositions were not affected.

Novelty:
Sub-cellular lipid heterogeneity and inflammatory response in human microglia-like cells was visualized on a molecular level using AP-SMALDI MSI.

Preliminary Data:
Microglia cells were successfully investigated at 1.5 or 2 µm pixel size in positive- or negative-ion mode using non-oversampling AP-SMALDI-MSI.

Contributing Authors:
Max A. Müller[1,6], Norman Zweig[1], Kerstin Strupat[5], Bernhard Spengler[1,6], Maria Weinert[2], Sven Heiles[1,3,4]
[1]Institute of Inorganic and Analytical Chemistry, Analytical Chemistry, Justus Liebig University Giessen, 35392 Giessen, Germany
[2]Department of Brain Sciences, Imperial College London, Hammersmith Hospital, London, W12 0NN, United Kingdom
[3]Leibniz-Institut für Analytische Wissenschaften - ISAS - e.V., 44139 Dortmund, Germany
[4]Faculty of Chemistry, University of Duisburg-Essen, 45141 Essen, Germany
[5]Thermo Fisher Scientific (Bremen) GmbH, Bremen, Germany
[6]TransMIT GmbH, Giessen, Germany

Mutuku, Shadrack
University of Wollongong, Australia, Australia

Tuesday October 24, Session 6, 13:50-14:10

Omics-Scale Quantitative Mass Spectrometry Imaging of Lipids using a Multi-Class Internal Standard Mixture combined with MALDI and MALDI-2

Introduction:
Although the demonstration of quantitative-MSI (Q-MSI) has been reported in numerous studies, these have been limited to either a single analyte or analyte class. Here we have aimed to overcome this limitation by developing an internal standard (IS) lipid mixture representing 13 lipid classes with concentrations optimised for measurement of endogenous signal intensities obtained from brain tissue. Using both MALDI and MALDI-2 mass spectrometry imaging (MSI) for pixel-wise normalisation of each lipid species signal to the corresponding IS lipid class, this approach enabled Q-MSI of over 200 lipid species in mouse brain tissue. By performing the analyses using both an Orbitrap and Q-TOF mass analyser, this study also investigates the influence of mass resolving power on the accuracy of Q-MSI.

Method:
C57BL/6N mouse brains were cryosectioned (Leica Biosystems) and mounted on ITO-coated slides (Delta Technologies). The optimised 13-lipid IS mixture (MSI Splash, AVANTI Polar Lipids) was diluted 1:10 in LC-MS-grade methanol and deposited onto tissue sections using a TM-Sprayer (HTX Technologies). MALDI matrices were applied using the TM Sprayer: norharmane for negative- or DHB for positive- mode analysis. MSI was conducted using regular MALDI (negative mode) and laser post-ionisation MALDI-2 (positive mode) on both an Orbitrap Elite (Thermo Fisher) equipped with a reduced pressure ESI/MALDI ion source (Spectroglyph), and a timsTOF fleX MALDI-2 (Bruker). Detected lipids were normalised against their respective IS reference peaks, and m/z images plotted with a ±3 or ±12 ppm theoretical mass window of the chosen species.

Results:
We first generated a curated lipid target list across 13 lipid classes to determine the IS signal each m/z value should be normalised to. Q-MSI of lipids covered 3 orders of magnitude ranging from ~0.1-200 pmol/mm2 in dynamic range and enabled correction of class-specific ionisation efficiencies. For example, in negative-ion mode after IS normalisation, PE and PS lipid species had the highest concentrations whereas using conventional total-ion-current normalisation, PI and SHexCer yield the highest signal intensities. IS normalisation also revealed subtle changes in distribution compared to the original ion images, for example elevated levels of PI 38:4 and PS 36:2 within the hindbrain. IS normalisation also corrected for image artefacts commonly observed using MALDI-2 that are thought to be caused by slight laser alignment drift or topographical artefacts interfering with the post-ionisation laser. Post-MSI haematoxylin and eosin stained sections were co-registered with MSI data, where hindbrain, midbrain, prefrontal cortex, basal ganglia and cerebellum regions were annotated to enable comparison of absolute lipid content for >200 unique sum-composition lipid species within each brain region. Q-MSI results were largely in agreement with reported concentrations obtained following homogenisation and lipid extraction, providing confidence the IS was accounting for both class-specific extraction and ionisation across the tissue. The robustness of the method was evaluated by independent experiments in two laboratories on biological replicates using timsTOF and Orbitrap mass spectrometers operated with a ~4-fold difference in mass resolution power. There was a strong overall correlation in the Q-MSI results obtained using the two approaches with outliers mostly rationalised by isobaric interferences that are only resolved with the Orbitrap system (e.g., PI 38:3 and the more abundant PI 38:4[13C2] or the higher sensitivity of one instrument particularly for lipids detected at low intensity. These data provide insight into how mass resolving power can affect Q-MSI values.

Novelty:
This work demonstrates the ability to perform Q-MSI on over 200 lipid species, greatly expanding the ability of MSI to investigate regional changes in lipid metabolism.

Preliminary Data:
Proof of concept has been demonstrated with mouse brain tissue using MALDI and MALDI-2 on two MSI instrument platforms.

Contributing Authors:
Shadrack M. Mutuku[1], Michiel Vandenbosch[2], Maria José Q. Mantas[3], Nathan H. Patterson[3], Tucker Hallmark[4], Marc Claesen[3], Ron M. A. Heeren[2], Nathan G. Hatcher[5], Nico Verbeeck[3], Kim Ekroos[6] and Shane R. Ellis[1]
[1]Molecular Horizons and School of Chemistry and Molecular Bioscience, University of Wollongong, Wollongong, NSW, Australia; [2]Maastricht MultiModal Molecular Imaging (M4I) Institute, Division of Imaging Mass Spectrometry, Maastricht University, Maastricht, Netherlands; [3]Aspect Analytics NV, Genk, Belgium; [4]Avanti Polar Lipids, Alabama, USA; [5]Merck & Co., Inc., 770 Sumneytown Pk, West Point, PA, 19486, USA; [6]Lipidomics Consulting Ltd., Esbo, Finland

Verbeeck, Nico
Aspect Analytics, Belgium

Tuesday October 24, Session 8, 17:20-17:40

Enabling integrative spatial multi-omics data analysis via dedicated data structures and interactive, web-based visualizations

Introduction:
Rapid advances in spatial omics technologies are enabling detailed molecular analyses in tissue context. Parallel to advancement of individual spatial omics technologies, integration of multiple spatial omics readouts to obtain a holistic multi-omics view has become desirable. Owing to its unique ability to target certain classes of analytes, such as drugs and metabolites, mass spectrometry imaging (MSI) is one omics technology that when combined with other spatial omics can bring insightful integrated information. However, spatial-multi-omics data analysis is a daunting bioinformatics task with few guideposts. The data is typically acquired on serial sections, at different spatial resolutions, in a variety of different data formats and requires expertise across multiple domains to obtain the best results from each individual technology.

Method:
In this work, we present a suite of bioinformatics tools dedicated to enabling spatial multi-omics data analysis. The software enables efficient integration and joint visualization of readouts from different assays, as well as multiple common downstream multimodal analysis pipelines. Our approach towards enabling spatial multi-omics data analysis consists of multiple steps. First, we provide accurate, non-rigid image registration to translate between serial sections' coordinate systems. Second, several data integration approaches are provided to create an integrated data structure across assays of different spatial resolutions. This data structure acts as a foundation for downstream data analysis and overall joint visualization. Finally, we provide examples of downstream analysis, including spatial correlation between analytes across assays, multi-omics tissue segmentation and differential expression analysis.

Results:
We illustrate the broad applicability of our approach and the associated data visualizations via several spatial multi-omics use-cases which combine MSI with complementary assays. MALDI-1 and -2 measurements, performed using a Bruker timsTOF fleX on human brain tissue sections with 5 micrometer spatial resolution in the lipid mass range, were combined with multiplexed immunofluorescence microscopy, performed on the same section using a Leica Sted. This workflow is geared towards extracting molecular profiles of individual cells from the multimodal data. Several Imaging Mass Cytometry (IMC) readouts on the same section were stitched together and compared with MALDI-IHC (using a Bruker rapifleX) for a lymph node sample. In this study, serial sections were analyzed using IMC and MALDI-IHC to investigate the correspondence and difference between both assays for readouts of equivalent antibodies. Delineating precipitating Alzheimer pathology in vivo and the associated molecular and cellular response via a trimodal approach consisting of stable isotope-encoded MS peptide imaging, spatial transcriptomics (using a NanoString GeoMx DSP) and immunofluorescence microscopy. Data were acquired from control and diseased animal model tissue sections using DESI MSI (Waters Synapt G2-si) for lipid analysis and the GeoMx DSP (Nanostring) for spatial transcriptomics to better understand how representative these models reflect disease. The lipid acquisition was performed in an untargeted manner across the full section, whilst the spatial transcriptomics were focused on specific regions, known to convey response relevant to neurological disease pathology. In this use-case, we combine lipid and transcriptomic outputs to obtain a more comprehensive understanding of the biological pathways involved. For each use-case, a web-based, interactive spatial multi-omics data visualization will be constructed. Moreover, the aforementioned use-cases illustrate that the integrated spatial multi-omics data structures at the heart of our approach support a wide range of downstream data analyses.

Novelty:
We provide a framework to integrate MSI data with other spatial omics, addressing the need for spatial multi-omics bioinformatics solutions.

Preliminary Data:
The proposed software has proven capabilities to integrate and jointly display data across a variety of popular spatial omics assays.

Contributing Authors:
Nathan Heath Patterson[1],*, Baruch Berger[1],*, Wanqiu Zhang[1,2], Phuong Thao Tran[1], Maria José Q. Mantas[1], Bart De Moor[2], Tim Hendriks[3], Elias Wieland[3], Pieter Goossens[3], Eva Cuypers[3], Ron Heeren[3], M. Reid Groseclose[4], Fang Xie[4], Jörg Hanrieder[5,6], Maciej Dulewicz[5], Jack Wood[5,7], Junyue Ge[6], Michael Eyres[8], Philippa Hart[8], Irma Berrueta Razo[8], Gayle Marshall[8], Alice Ly[1], Nico Verbeeck[1], Marc Claesen[1]
Author affiliations:
[1]Aspect Analytics NV, C-mine 12, 3600 Genk, Belgium
[2]STADIUS Center for Dynamical Systems, Signal Processing and Data Analytics, Department of Electrical Engineering (ESAT), KU Leuven, Kasteelpark Arenberg 10, 3001 Leuven, Belgium
[3]Maastricht MultiModal Molecular Imaging Institute (M4i), Maastricht University, Universiteitssingel 50, 6229 ER Maastricht, The Netherlands
[4]GSK, Collegeville, PA, USA
[5]Department of Psychiatry and Neurochemistry, Sahlgrenska Academy, University of Gothenburg, Mölndal, Sweden
[6]Department of Neurodegenerative Disease, Queen Square Institute of Neurology, University College London, London, United Kingdom
[7]Department of Neuroscience, Physiology and Pharmacology, University College London, London, United Kingdom
[8]Medicines Discovery Catapult, Alderley Park, Cheshire, United Kingdom
* These authors contributed equally.

Roempp, Andreas
University of Bayreuth, Germany

Tuesday October 24, Session 5, 11:30-11:50

Advances in MALDI imaging of tryptic peptides: improved spatial resolution in mammalian tissue and first results for plant proteins

Introduction:
On-tissue digestion offers the possibility to extend the range of proteins that can be analyzed by mass spectrometry imaging. Digestion makes larger proteins accessible which cannot be detected directly on tissue in top-down approaches. Spatial resolution is limited by trypsin application and not by instrumental parameters such as laser focus. Conditions for sample preparation need to be balanced carefully in order avoid migration of tryptic peptide and yet provide efficient enzymatic digestion. The vast majority of studies uses trypsin for application to mammalian tissue. On-tissue digestion of proteins in plant tissue has not shown before. This study aims at a) higher spatial resolution and reproducible results in mammalian tissue and b) the first MALDI images for on-tissue digestion of plants.

Method:
Lipids and salts were removed from tissue by a series of washing steps. Digestion was performed by spraying trypsin sequentially on tissue using a semi-automatic pneumatic spraying device. Between each spray, tissue sections were placed inside a digestion chamber at 37°C. Sections were incubated for 120 min after the last spray. 2.5-DHB matrix was applied using a pneumatic spraying device. MS imaging was performed using an AP-SMALDI5-AF (TransMIT, Giessen, Germany) ion source attached to a Q-Exactive-HF (Thermo Scientific, Bremen, Germany). Tryptic peptides were identified by matching imaged m/z peaks to peptides which were identified in complementary LC-MS/MS measurements of an adjacent tissue sections using in silico digestion of proteins. All MS measurements were based on accurate mass (<3 ppm RMS).

Results:
Trypsin spray application was investigated and optimized to achieve high spatial resolution MS imaging of tryptic peptides in fresh-frozen mammalian tissue. We were able to image tryptic peptides in mouse brain sections at 10 µm pixel size with high mass resolution (R > 100000 FWHM) and mass accuracy (RMSE < 3 ppm). These results were confirmed in a number of replicates in order to show the reproducibility of our workflow. As in our previous study (DOI: 10.1007/s00216-018-1199-z), multiple application cycles of trypsin with intermediate incubation proved to be crucial to obtain these results. Interestingly, peptide intensities and number of identified proteins were not significantly reduced at 10 µm pixel size. In a parallel effort we adopted our MALDI imaging workflow to plant samples. Chickepea was chosen as a model system because of its high protein content. The sectioning and trypsin application process were adopted and resulted in MALDI images of tryptic peptides at 65 µm pixel size. Different distributions that correlated with plant structures such as seed coat and cotyledon were observed. Identification of proteins was based on at least two peptides that were detected with accurate mass and showed matching distributions. As a first application of our workflow we imaged tryptic peptides of abrin, a toxic protein present in crab's eye vine. We were able to show the distribution of abrin in the seed and discuss these results with regard to the severity of intoxication in case of ingestion of crab's eye vine seeds. This approach of on-tissue digestion in plant tissue opens up new possibilities for MALDI imaging of protein analysis ranging from developmental biology to food safety.

Novelty:
On-tissue digestion of proteins: reproducible 10 µm imaging in mammalian tissue and the first images in plant sections.

Preliminary Data:
Proteins identified by accurate mass measurements of multiple tryptic peptides in mouse and plant tissue.

Contributing Authors:
Andreas Roempp, Bastian Jahreis, Oliver Wittek

Sanchez, Laura
University of California, Santa Cruz, USA

Wednesday October 25, Session 10, 11:10-11:30

A label free approach for relative spatial quantitation of c-di-GMP in microbial biofilms

Introduction:
Cyclic dimeric guanosine monophosphate (c-di-GMP) is a universally important second messenger which regulates exopolysaccharide production, virulence, antimicrobial tolerance, chemotaxis, cell morphology, and cell cycle control across nearly all bacterial phyla. Cyclic dimeric guanosine monophosphate is synthesized by diguanylate cyclases (DGCs) and hydrolyzed by phosphodiesterases (PDEs). The regulatory role of c-di-GMP is particularly important in biofilm-forming bacteria, as evidenced by the high number of DGC and PDE enzymes present in the genomes. Biofilms are known to have heterogeneous structure and chemical gradients which change dynamically over time and influence the regulation of DGC and PDE enzymes. Accurate and sensitive techniques for detecting c-di-GMP and related compounds are needed in order to better understand chemical gradients in biofilms.

Method:
All MALDI-qTOF analyses were performed using a Bruker timsTOF fleX mass spectrometer. We optimized ionization of c-di-GMP by testing individual and mixtures of MALDI matrices which have been shown to improve nucleotide ionization including CHCA, DHB, THAP, and HPA. We selected matrices which enhanced c-di-GMP ionization while also allowing for untargeted analysis of small molecules. The agar biofilm colonies were prepared by applying MALDI matrix using a sieve method to determine the c-di-GMP concentrations on an agar biofilm colony of V. cholerae (O1 El Tor A1552) using MSI. We validated our MSI technique using a fluorescent riboswitch in Vibrio cholerae and we further applied the MSI detection of c-di-GMP to the symbiotic organism V. fischeri and Pseudomonas aeruginosa PA14.

Results:
Two model Vibrio cholerae El Tor strains to compare c-di-GMP production in a strain which is well-established as an overproducer of c-di-GMP. The V. cholerae O1 El Tor A1552 wild type strain produces a smooth phenotype when grown on LB agar, while the V. cholerae O1 El Tor A1552 rugose variant produces a wrinkly phenotype on LB agar due to an excess of biofilm production. The V. cholerae rugose variant used here has been well-established as a biofilm producer due to the activity of the DGC vpvC, which has a single nucleotide polymorphism in the V. cholerae wt strain, rendering it inactive. Our initial results using the V. cholerae wt and rugose variants showed that c-di-GMP can be detected as both m/z 689.09 [M-H]- and m/z 711.09 [M+Na-2H]- . Both adduct ions of c-di-GMP show related distribution in the ion images of the wt and rugose variant V. cholerae strains, and the presence of these adducts is confirmed by the use of a c-di-GMP chemical standard applied by the dried droplet method to a piece of LB agar, which was prepared for MSI using the sieve method with 1:1 CHCA:DHB. When comparing the c-di-GMP distribution between the wt and rugose variant strains, we see that the rugose variant produces higher concentrations of c-di-GMP along the edge of the colony, whereas the wt strains tend to produce c-di-GMP more diffusely throughout the colony. We applied this MSI approach for c-di-GMP detection to V. cholerae strains over time to observe how spatial changes in c-di-GMP production develop in wild-type V. cholerae and the rugose variant.

Novelty:
We present an MSI technique for the detection of c-di-GMP in bacterial biofilm colonies grown on solid agar media.

Preliminary Data:
The c-di-GMP levels in the wild-type V. cholerae, P. aeruginosa, and V. fischeri were measured using MSI.

Contributing Authors:
Catherine S. McCaughey, Michael A. Trebino, Allyson McAtamney, Ruth Isenberg, Mark J Mandel, Fitnat H. Yildiz, Laura M Sanchez

Schey, Kevin
Vanderbilt University, USA

Tuesday October 24, Session 5, 11:50-12:10

Localization of Membrane Proteins and Post-Translational Modifications in Ocular Tissues

Introduction:
Spatially regulated protein localization is important for protein function and tissue organization. Post-translational modifications (PTMs) provide additional dimensions of protein regulation in spatial and temporal patterns. Membrane proteins represent a major protein class and are major drug targets; however, their physiochemical properties make them a challenging target for imaging mass spectrometry (IMS). In addition, very few IMS studies have imaged modified proteins, many of which are present in low abundance. We have developed a method to localize membrane proteins and their modified forms by IMS and have applied this method to demonstrate differential membrane localization in ocular tissues including the lens and the retina.

Method:
Cryostat sections were obtained from human retina or anterior, posterior, or equatorial regions of fresh frozen or fixed bovine lenses. Washing protocols were performed to retain insoluble, membrane or cytoskeletal proteins. Imaging mass spectrometry (IMS) combined with on-tissue trypsin digestion was used to visualize spatial distributions of proteins and PTMs. 2,5-Dihydroxybenzoic acid (DHB) was used as MALDI matrix and IMS was performed using either a Bruker SolariX 15T FT-ICR mass spectrometer or a Bruker RapiFlex instrument. Laser capture microdissection (LCM) of specific lens regions (anterior/posterior suture and equator regions) followed by LC-MS/MS analysis using either data-dependent acquisition (DDA) or data-independent acquisition (DIA) was performed for in-depth proteomic study, identification of IMS signals and validation of IMS results.

Results:
IMS analysis of sections collected in lens equatorial regions revealed cytoskeletal and membrane remodeling in the narrow region of lens cortex. IMS analysis of sections collected in anterior or posterior regions of the lens showed increased expression of adherens junction (membrane) proteins ARVCF and CDH2, but decreased gap junction proteins Cx50 and Cx46 at the suture branches. Phosphopeptide imaging showed increased phosphorylation of multiple proteins, such as AQP0, alpha B crystallin, CP49, filensin and connexin 50, in the lens inner cortex region. Age-related truncation and deamidation were also detected modifications and demonstrated regional specificity. Proteomic analysis of regions collected by LCM complemented and confirmed the IMS results and provided a rich database of region-specific lens protein expression, including, for the first time, in lens sutures. Comparison of anterior and posterior proteomes of bovine lenses showed a significant increase of proteins involved in oxidative stress regulated ubiquitination, protein degradation and vesicle-mediated transport in anterior region of the lens, whereas increased expression of proteins related to glycolysis and gluconeogenesis was observed in the posterior region. Correspondingly, glucose transporter GLUT1, GLUT3 and monocarboxylate transporter SLC16A3 were found significantly increased in the interior and posterior region of the lens, as seen by IMS. Such localization may play a role in establishing the lens microcirculation system.

Novelty:
IMS methods were developed to measure distributions of low abundance, hydrophobic transmembrane proteins and PTMs in ocular tissues.

Preliminary Data:
none

Contributing Authors:
Zhen Wang, Lee Cantrell

Scott, Alison
University of Maryland, Baltimore, United States

Tuesday October 24, Session 4, 8:40-9:00

Identification of sex-dependent biomarkers of fMRI-active brain regions in a rat model of comorbid pain hypersensitivity using MSI

Introduction:
Chronic pain conditions affect over 100 million people in the United States. Chronic overlapping pain conditions that include temporomandibular disorder (TMD) and irritable bowel syndrome (IBS) are predominant in women and are exacerbated by stress. The overlapping nature of these conditions, sex-dependence, and stress linked mechanisms of these conditions make adequate treatment difficult. We used a rat model of comorbid pain to induce chronic visceral pain hypersensitivity (CPH). This model consists of masseter muscle inflammation followed by stress and recapitulates the pain associated with TMD and IBS. To gain insights in to the sex-dependency of this model, we evaluated brain activity by functional magnetic resonance imaging (fMRI) and during colorectal distention followed by MSI.

Method:
Rats were injected with complete Freund's adjuvant into both masseter muscles followed by restraint stress for 2 hours/day for 4 days alternating nose-up or nose-down at a 45° angle in 15-minute blocks. Colorectal distention was performed during fMRI collection (Bruker BioSpec 7T). Scans were collected at baseline, 1, and 7 weeks. Brains were dissected and colons collected from cecum to anus, opened along the mesenteric line, and Swiss-rolled in 4% gelatin. Cryosections were prepared (12um) from section depths referenced to Bregma values. Sections were prepared for MSI with norharmane matrix using previously established conditions (HTX M5). Negative ion mode lipid data was collected at

Results:
CPH persisted longer in females (at least 7 weeks) than it did in males (resolved after 1 week). One week after stress, several candidate subregions of interest were identified as having greater activity in females over males. These included the prelimbic cortex (PrL), insula (Ins), caudate putamen (CPu), nucleus accumbens (NAc), anterior cingulate cortex (ACC), thalamus (Th), and hippocampus (Hipp). Since the bulk of these regions are dispersed throughout the brain, we developed a targeted sectioning strategy based on the Bregma locations of each. A standard brain matrix produced suboptimal brain slices to target our specific regions of interest (too many discarded sections between each area). A custom brain matrix was 3D printed to generate fMRI-targeted subregions for cryosectioning. We produced 6 subsections (A-F) of the brain in the coronal axis for cryosectioning and all discarded sections were counted to estimate Bregma depth for each collected section based on the brain matrix reference point. We collected 12 sections from each subregion. Subregions active during the pain stimulus by fMRI were then evaluated by matrix-assisted laser desorption/ionization MSI for lipids (n=3). A custom algorithm was used to identify the closest brain atlas reference and encircle uniformly sized brain subregions on the post-MSI Nissl image for analysis, these were termed functional regions of interest (fROIs). Three fROIs were present in the B subregion and 11 differential ions were identified within the ACC fROI alone. The most striking differences were phosphatidylglycerol (PG) lipids with greater intensity in male ACC than female; however, a panel of lipids showed greater intensities in female ACC. Similar results were observed in the NAc and Ins fROIs.

Novelty:
We identified sex-dependent differential lipid signatures within brain functional regions active during IBS-like pain stimuli in a comorbid pain model.

Preliminary Data:
Using this approach, we identified a panel of region-specific and sex-dependent lipid changes that are being evaluated for mechanistic links to pain-stimulated brain activity.

Contributing Authors:
Alison J. Scott[1], Joyce T. Da Silva[2,3], Abena Ntiamoah[1], Shelby Hanson[2,3], Luis G. Hernandez[2,3], David A. Seminowicz[4], Ohannes Melemedjian[2,3], Robert K. Ernst[1], and Richard J. Traub[2,3]
1. Dept. of Microbial Pathogenesis, University of Maryland School of Dentistry, Baltimore, MD, USA
2. Dept. of Neural and Pain Sciences, University of Maryland School of Dentistry, Baltimore, MD, USA
3. UM Center to Advance Chronic Pain Research, Baltimore, MD, USA
4. University of Western Ontario, London, ON, CA

Seeley, Erin
University of Texas at Austin, USA

Tuesday October 24, Session 7, 15:30-15:50

Mass Spectrometry Imaging Reveals Molecular Changes Associated with Aging in Pancreatic Cancer

Introduction:
Aging is one of the most important risk factors for pancreatic ductal adenocarcinoma (PDAC) with the typical median age of onset in the 70s at the time of diagnosis. However, a subset of patients experiences disease onset much earlier, especially among women, without any known genetic predisposition. The increasing recognition of age-associated pancreatic cancer incidence necessitates understanding diverse molecular changes associated with variations in age of onset and gender. Mass spectrometry imaging allows for detection of hundreds of biomolecules from tissue sections without target-specific reagents and multiple classes of analytes can be analyzed from the same section using sequential imaging. Here, we seek to interrogate molecular differences between early and typical onset pancreatic cancer as well as any gender-specific differences.

Method:
FFPE tissue sections were dewaxed with xylene before being coated with DAN matrix using an HTX M5 Sprayer. Metabolite images were collected in negative ion mode using a Bruker timsTOF fleX MALDI QTOF mass spectrometer. After image collection, matrix was removed and PNGase F digestion was performed on the same section before coating with CHCA matrix and N-glycan image collection. Subsequent to N-glycan imaging, matrix was removed and tryptic digestion was performed on the same section before coating with CHCA and peptide image collection. All images were collected at 20 µm resolution. Finally, the imaged sections were H&E stained for histological evaluation. Image visualization was performed using SCiLS Lab and metabolite and glycan identification were carried out using MetaboScape.

Results:
In this study we sought to understand molecular differences between early onset PDAC (< 55 year) versus typical onset (>75 year) as well as any gender differences. Sequential imaging of the same tissue section allows us to maximize data coverage and perform direct co-registration of different classes of molecules to each other. Preliminary analysis focused on imaging tumor samples from two early onset and two elderly patients, one male and one female in each age group. Metabolite imaging revealed higher abundance of taurine and palmitic acid in samples from elderly patients, while more guanine was detected in samples from early onset patients. Cytosine and uracil were slightly more abundant in male patients than female patients with higher abundance in the early onset patient. Glycan imaging showed more abundant signal for Hex5dHex1HexNAc4 and an unknown glycan at m/z 2056.743 in tumor tissues from female patients. Hex5HexNAc 2 was most abundant in the sample from the elderly female patient. Finally, tryptic digest imaging was performed on the sections. From these data, we found an unknown peptide at m/z 958.572 to be more abundant in the elderly patients, as was actin. An unidentified peptide at m/z 1240.267 was almost exclusively detected in the early onset male patient. Histone H2A displayed similar abundance across all samples, while an unidentified peptide at m/z 1487.674 was more prevalent in the samples from elderly patients. Work is on going to replicate these results in additional samples and to identify more of the molecules detected in these imaging studies. We also plan to integrate these MSI results with other spatial-omics technologies, including spatial transcriptomcis. The results gleaned from this work will aid in our understanding of how the aging process impacts dynamic changes of multi-analytes in pancreatic cancer.

Novelty:
Determination of molecular differences in pancreatic cancer with different ages and genders by sequential imaging of metabolites, N-glycans, and peptides.

Preliminary Data:
Numerous small metabolites, glycans, and peptides detected by sequential MSI in PDAC biopsies correlating with age and/or gender.

Contributing Authors:
Jimin Min, Jared K. Burks, Paola A. Guerrero, Anirban Maitra

Simon, Daniel
Imperial College London, UK

Monday October 23, Session 3, 17:20-17:40

Ambient Laser Desorption – REIMS with novel picosecond laser sources for sample preparation-free imaging

Introduction:
We present our work coupling a picosecond λ = 3 µm laser source to a Laser Desorption – Rapid Evaporative Ionisation Mass Spectrometry (LD-REIMS) ambient imaging platform. The aim of this work was to explore whether superior sampling efficiency and resolution could be achieved for sample preparation free Mass Spectrometry Imaging (MSI) by using novel laser sources.

Method:
A Xevo G2-XS QToF (Waters) mass spectrometer equipped with a prototype REIMS source was used. A home-built 3D motorized XYZ stage coupled with focusing optics was used for the laser desorption workflow. Two different mid-IR sources were compared: a nanosecond pulse duration OPOTEK Opolette 2940 Optical Parametric Oscillator (OPO) operating at 20Hz with λ = 2.94 µm, and a prototype λ ~ 3 µm picosecond Optical Parametric Amplifier (OPA) delivering 200 nJ pulses, equipped with a pulse picker capable of delivering arbitrary combinations of pulses picked from a fundamental 500 kHz pulse repetition rate. 10 µm thick, fresh frozen pork liver and mouse brain samples were used for MSI.

Results:
Ablation spot sizes of around 5-10 µm were achieved using the OPA, compared with ≥ 20 µm for the OPO. The minimum number of pulses required for observable MS signal (SNR > 3) was ~50 (individual pulse energy 200 nJ). No MS signal, or visible desorption was observed when delivering only single pulses to the sample. Inter pulse spacings greater than 2 µs resulted in a sharp decrease in the MS signal. An imaging comparison was performed on mouse brain sections using the OPO and OPA, imaging at 20 µm raster size, with the MS operating at 10 Hz. Similar ion signal intensity was seen across the metabolic and lipidomic ranges for both laser sources despite a significantly reduced volume of tissue being ablated by the OPA. MSI has also been performed with 10 µm raster size with the OPA. 10 µm raster imaging enabled observation of features related to individual cell nuclei in MSI images, indicating subcellular resolution is possible with this technique. Pulse picking experiments suggest the laser desorption is photothermal. Further studies facilitated by the experimental imaging platform are required to understand and optimise this laser tissue interaction for MSI applications. LD-REIMS is an emerging tool that allows the sample prep-free characterisation of tissues based on metabolic and lipidomic profiles. With appropriate laser sources, it may be applied to numerous applications, from high resolution – single cell imaging to in vivo diagnostics.

Novelty:
Highest lateral resolution 3 µm-laser based MSI of sample preparation free tissue in ambient conditions.

Preliminary Data:
10 µm spot size and pixel size ion images generated from mouse brain and colorectal adenoma samples.

Contributing Authors:
Ronan Battle[1], Daniel Simon[1,2], Yuchen Xiang[1], Kenneth Robinson[2], Stefania Maneta-Stavrakaki[1], Lauren Ford[1], Robert Murray[1], Josephine Bunch[3] and Zoltan Takats[1,2]

[1]Imperial College London, London, United Kingdom

[2]Rosalind Franklin Institute, Harwell, United Kingdom

[3]National Physical Laboratory, London, United Kingdom

Spotbeen, Xander
KU Leuven, Belgium

Wednesday October 25, Session 11, 13:30-13:50

Investigation of Prostate Cancer Heterogeneity Using a Novel Spatial Multi Omics Pipeline Integrating MS Imaging and Spatial Transcriptomics.

Introduction:
Complex human diseases such as solid cancers are typically characterised by a high degree of inter- and intra-patient heterogeneity posing major challenges in current cancer treatment. This heterogeneity is reflected in molecular alterations in the diverse cell types composing the tumour ecosystem and manifests at all levels of the gene regulatory cascade. Mapping this molecular heterogeneity and understanding their intricate connections require the integration of multiple spatial technologies. Here, we applied a novel spatial multi-omics (SMOx) strategy combining in situ lipidomics via mass spectrometry imaging (MSI), spatial transcriptomics (ST) and single nuclei RNA sequencing (snRNAseq) to gain unprecedented insights into the cellular and molecular heterogeneity of prostate cancer (PCa).
Method:
Prostate tumour and matched normal 6mm biopsy cores were collected from 8 previously untreated high-risk PCa patients undergoing radical prostatectomy at University Hospitals Leuven (Belgium). Immediately after surgery, the biopsy cores were embedded in carboxymethylcellulose (CMC) and snap frozen in pre-cooled isopentane. ST (Visium, 10X Genomics) and MSI analysis (MALDI with laser post-ionisation (MALDI-2) on an Orbitrap Elite mass spectrometer, Thermo Fisher Scientific) were performed on neighbouring frozen tissue sections (10 µm). These sections were H&E stained and reviewed by expert uropathologists. Single nuclei-RNA sequencing (snRNA-seq) (Chromium, 10X Genomics) was conducted on matched homogenised tissue sections for spot deconvolution. A novel SMOx bioinformatics pipeline (Aspect Analytics NV) was used to integrate the data from the various platforms.
Results:
Using specific routines for co-registration, pixel to spot alignment, and integrated analysis of MSI and ST data with unsupervised dimensionality reduction, we identified lipid and transcript profiles that colocalised with specific histological areas defined by uropathologists, including tumour, benign, transforming prostatic intraepithelial neoplasia (PIN) and stromal areas. Based on lipid-transcript associations we were able to assign unique lipid profiles to each histopathological state. Subsequent deconvolution of the multi-omic spots by integrating snRNA-seq data, not only allowed the identification and localisation of discrete subpopulations of cells but also facilitated the association of unique lipid profiles to these cell types, while retaining the spatial information. This integrated analysis enabled automated molecular pathological annotation with high confidence and enabled the detection of diseased regions not readily apparent by classical histopathology. Moreover, our integrated SMOx approach revealed novel molecularly different histological features in PIN and tumour areas. These include a spatial association between subregions of PIN and club cells, a distinctive epithelial cell population which recently have been shown to promote prostate tumorigenesis. Additionally, we identified molecular lipid-transcript signatures unique to high-grade tumour cells exhibiting a cribriform growth pattern, an adverse prognostic indicator associated with more aggressive disease behaviour, increased risk of metastasis and worse patient outcome. These findings highlight the unique potential of an integrated spatial and single cell multi-omics analysis pipeline to provide unprecedented insight into the molecular heterogeneity of prostate cancer.
Novelty:
We applied a novel SMOx pipeline allowing the spatial integration of MSI and ST data and their deconvolution based on snRNseq data.
Preliminary Data:
Using the novel SMOx pipeline we identified cell type-specific molecular signatures and generated unprecedented insight in the intra-tumoral heterogeneity of PCa.

Contributing Authors:

Xander Spotbeen[1], Wanqiu Zhang[2,3]; Tassiani Sarretto[4,5]; Fabio Socciarelli[6]; Sebastiaan Vanuytven[7,8]; Sam Kint[7,8]; Katy Vandereyken[7, 8]; Jose Ignacio Alvira Larizgoitia[8, 9]; Gabriele Partel[9]; David Wouters[8,9]; Jakub Idkowiak[1], Vincent De Laat[1], Maria Mantas[3]; Thomas Gevaert[10]; Wout Devlies[10, 11]; Steven Joniau[10, 12]; Massimo Loda[6]; Bart De Moor[2]; Thierry Voet[7,8]; Alejandro Sifrim[8, 9]; Shane Ellis[4, 5]; Marc Claesen[3]; Nico Verbeeck[3]; Johannes V. Swinnen[1]

[1]Laboratory of Lipid Metabolism and Cancer, KU Leuven and Leuven Cancer Institute (LKI), Leuven, Belgium;
[2]STADIUS Center for Dynamical Systems, Signal Processing and Data Analytics, Department of Electrical Engineering (ESAT), KU Leuven, Leuven, Belgium;
[3]Aspect Analytics NV, Genk, Belgium;
[4]Molecular Horizons and School of Chemistry and Molecular Bioscience, University of Wollongong, Wollongong, Australia;
[5]Illawarra Health and Medical Research Institute, Wollongong, Australia;
[6]Department of Pathology, Weill Cornell Medical College, New York, NY;
[7]Laboratory of Reproductive Genomics, Department of Human Genetics, KU Leuven, Leuven, Belgium;
[8]KU Leuven Institute for Single Cell Omics (LISCO), KU Leuven, Leuven, Belgium;
[9]Laboratory of Multi-omic Integrative Bioinformatics, Department of Human Genetics, KU Leuven, Leuven, Belgium;
[10]Department of Urology, University Hospitals Leuven, Leuven, Belgium;
[11]Laboratory of Molecular Endocrinology Laboratory, KU Leuven, Leuven, Belgium;
[12]Department of development and regeneration, KU Leuven, Leuven, Belgium

Theverapperuma, Lalin
Expert Intelligence, United States

Tuesday October 24, Session 8, 17:40-18:00

Integration of Topological Data Analysis with Contrastive Deep Learning for Molecular Co-localization in Mass Spectrometry Imaging

Introduction:
Mass spectrometry imaging (MSI) combines spatial and molecular data for understanding biological tissues. Molecular co-localization identifies correlated spatial distributions among ion images, providing insights into tissue heterogeneity and intricate biochemical pathways. Previous research demonstrates the use of deep learning for unsupervised clustering of ion images. In this approach, we present a novel framework that integrates Topological Data Analysis (TDA) methods to address the issue of molecular co-localization. TDA offers robust and global features pertaining to multidimensional data, which can overcome some limitations of unsupervised clustering. Specifically, we employ the Mapper algorithm for clustering. This approach offers a robust, and mathematically principled framework, yielding initial improvements of 1.98% and 2.01% in mean Spearman and Kendall correlation coefficients, respectively.
Method:
For our approach, we first utilized a pre-trained, state-of-the-art deep-learning CNN encoder trained on optical images. We then retrained it using contrastive self-supervised learning with unlabeled ion images from the dataset mentioned below, yielding lower dimensional and robust representations crucial for subsequent steps. To determine the optimal number of clusters and other hyperparameters, we employed the Mapper algorithm from TDA. The Mapper algorithm also helps us to understand the high-level structure of ion images and their patterns. The obtained clusters were compared against previous deep-learning approaches using ColocML rankings and measurements.
Results:
The initial findings of our framework demonstrate encouraging outcomes. The utilization of Topological Data Analysis (TDA) proves to be a resilient approach in mitigating the impact of noise that may afflict the mass spectrometry images acquired within any laboratory setting. Moreover, the incorporation of contrastive training enables the deep learning model to effectively capture the spatial context derived from an extensive range of biological specimens. It is worth noting that the contrastive learning framework removes the necessity for expert annotated labels, which are often unavailable and expensive for most mass spectrometry data sets. Our approach provides a 1.98% and 2.01% improvement in mean Spearman and Kendall correlation coefficients respectively, for the ranking agreement with the gold standard target-comparison dataset over the prior studies done on the same standard dataset.
Novelty:
A framework combining contrastive learning, and topological data analysis (TDA) for molecular co-localization in MSI images.
Preliminary Data:
We used the dataset of (Beque et al., 2021), and the gold standard for molecular co-localization (Ovchinnikova et al., 2020).
Contributing Authors:
Leiver Campeón, Mihira Kasun, Pasindu Tennakoon, Lalin Theverapperuma.

Velickovic, Dusan
Pacific Northwest National Laboratory, United States

Wednesday October 25, Session 10, 11:30-11:50

4-APEBA on tissue chemical derivatization for enhanced MALDI MSI of carbonyls in environmental samples

Introduction:
Carbonyls have numerous physiological roles in environmental samples: regulating plant growth and development, harvesting energy, protection, membrane fluidity, etc. Insight into their localization is vital to understand those processes at cell-specific level. MALDI MSI is one of the most utilized techniques for unveiling cell-specific molecular signatures. Still, current MALDI-MSI workflows are not sensitive enough to map many physiologically important carbonyls due to their low abundance, poor ionization, tissue suppression, instrument mass cut-offs, etc. On-tissue chemical derivatization (OTCD) bypass these challenges by introducing a readily ionizable functional group to the analyte. Herein, we synthesized 4-(2-((4-bromophenethyl)dimethylammonium)ethoxy) benzenaminium dibromide (4-APEBA) and optimized its deposition for enhanced MSI of carbonyls in several environmental samples: plant roots, interacting soil microbes, and rhizosphere models.
Method:
All samples (cryosections of Populus trichocarpa exposed to drought, co-culture of B. subtilis and Fusarium sp. on agar plate, P. trichocarpa inoculated Rhizochips that mimic soil-like environment) were derivatized with independent deposition of 6 mg/mL 1-ethyl-3-(3-dimethylaminopropyl)carbodiimide (EDC) and 2 mg/mL 4-APEBA using a HTX M5 sprayer in optimized conditions: 4 cycles each, 3 mm space tracking, nozzle velocity 1,200 mm/min, 10 PSI N2, and 25 µL/min flow rate. DHB matrix was subsequently sprayed and MALDI-MSI was performed using 12T FTICR-MS (Bruker Daltonics) at 25 to 200 µm step size, mass resolution ~110k at m/z 400, and in the m/z range 100-1,000. Datasets were submitted to METASPACE for automated annotation using a chemical mass shift of 4-APEBA against the KEGG database.
Results:
To expand the scope of measurable molecules by MSI, we developed an OTCD workflow using 4-APEBA. This also provided confident identification of several dozen elusive phytocompounds, including several phytohormones, which have various roles within stress responses and cellular communication. The superiority of 4-APEBA is established in comparison to other DAs with (1) broad specificity towards carbonyls, (2) low background, and (3) introduction of bromine isotopes, where the latter two facilitate confident bioinformatic annotation. Furthermore, metabolites of opposite polarities and different hydrophobicity can be detected within a single imaging analysis. The introduction of bromine isotopes, in combination with the METASPACE bioinformatic framework, revealed more than 300 small molecules in the poplar root cross-section. Some phytocompounds, including shikimate, malonaldehyde, oxalate, and plant growth hormone ACC, show characteristic temporal, cell-specific, and growth regime-dependent trends. In B.subtilis/Fusarium sp. co-culture model, we spatially resolved ~ 300 metabolites containing carbonyl-groups, many of which were previously undetectable from colonies grown on agar due to the agar suppression effects. Spatial patterns observed indicate possible extracellular or intercellular processes of the metabolites and their up or down-regulation during microbial interaction. The unique dual-step chemistry of our approach allowed us to bring additional confidence in accurate carbonyl identification, especially when multiple isomeric candidates were possible. Within the inoculated plant in Rhizochips, a wide variety of exuded and pooled metabolites can be seen within the primary root structures, hairs, and the secondary root tip. Aliphatic carboxylic acids, amino acids, reactive aldehydes, and free fatty acids could be simultaneously detected. 4-APEBA approach enhances the depth of metabolic profiling, where many glyoxylate and citric acid cycle components can be noted and traced, and hot spots of microbial activity can be visualized.
Novelty:
4-APEBA OTCD was optimized for MSI workflow, and it outperformed other carbonyl derivatization agents by its performance.
Preliminary Data:
4-APEBA introduces confidence in MSI metabolite annotation, isomer, and isobar resolving, enabling sensitive simultaneous detection of molecules with opposite polarity.
Contributing Authors:
Dusan Velickovic, Kevin Zemaitis, Vivian Lin, Christopher Anderton, Jayde Aufrecht, Robert Stanley, Arunima Bhattacharjee, Amirhossein Ahkami.

Villette, Claire
PIMS, IBMP, CNRS, France

Wednesday October 25, Session 9, 8:40-9:00

In situ localization of micropollutants, their transformation products and the associated stress response in plant leaves using MALDI-FTICR-imaging

Introduction:
Micropollutants and emerging organic contaminants have been widely studied in terms of persistence, removal, human risk assessment, toxicology, etc. Mass spectrometry imaging (MSI) offers the possibility to follow the fate of a single pesticide in a plant leaf or a drug in the whole body of an animal, organ by organ. However, the admissibility of chronic low doses of complex mixtures for the ecosystem has not been assessed. How do micropollutants diffuse in the environment? How do living organisms cope with a chronic exposure to low doses of diverse micropollutants? Is there a cocktail effect or a chance for hormesis? To answer these questions, we studied different compartments of the environment: water, sludge and spontaneous plants (Populus nigra, Salix alba).
Method:
A combination of mass spectrometry imaging (MSI) and targeted and nontargeted liquid chromatography coupled to mass spectrometry (LC-MS) was used to get a large-scale profiling of the three compartments of the environment. Water, sludge and plant leaves from the same square meter at the outlet of treated wastewater facility were sampled. Leaves from P. nigra and S. alba were analyzed in non-targeted MALDI-MSI to localize micropollutants. Transformation products were predicted using known biotranformation rules and searched for in the imaging data. The plant response to micropollutants accumulation was visualized in the tissues and further investigated with the targeted analysis of pigments and hormones which are described as plant stress markers.
Results:
The diversity of micropollutants at the exit of a wastewater treatment facility was described, as well as their diffusion in different compartments of the environment: water, sludge and poplar leaves. Six classes of micropollutants from anthropogenic origin (personal care products, industry toxics, drugs, pesticides, phthalates, other toxics) were detected in all samples, revealing their diffusion in living organisms. A further analysis of plant leaves using MSI showed the accumulation of micropollutants in the outer tissues of the leaves, which is not correlated to the physico-chemical properties of the stored micropollutants. This reveals active processes occurring in plant leaves to manage the accumulation of exogenous and potentially toxic molecules. This storage is coupled to a stress response, for example a chlorophyll degradation product was detected in MSI. The response from the plant was further described by quantifying pigments and determining the hormonal profile of the leaves, with an increase of stress related compounds. The ability of the plants to manage micropollutants by biotransformation was also revealed. The implementation of a control plant on the same study site enforced the conclusions, assessing the impact of a chronic exposure to low doses of a mixture of micropollutants on plants.
Novelty:
We demonstrated that plants can support a chronic exposure to micropollutants, which they store and transform despite a stress response.
Preliminary Data:
Micropollutants, their transformation products and the plant response were localized in leaf tissues by MALDI-MSI.
Contributing Authors:
Claire Villette, Julie Zumsteg, Loïc Maurer, Adrien Wanko, Dimitri Heintz

Žalud, Michal
Masaryk University, Czech Republic

Monday October 23, Session 3, 17:40-18:00

Detection and characterization of individual Au nanoparticles using SubAP LDI MSI

Introduction:
We present a laser desorption/ionization mass spectrometry imaging (LDI MSI) method for the detection of individual gold nanoparticles (AuNPs) and discuss key parameters affecting the measured signals, such as laser fluence and particle diameter. AuNPs with different diameters were examined, and an average signal intensity generated by a single NP depending on its diameter was estimated. The NP size determines the detection efficiency as larger NPs generate higher ion counts.

Method:
Tiny droplets (65 pL) containing a certain number of AuNPs were deposited on predefined Si and glass substrate positions using a piezoelectric dispenser. The deposited spot arrays were then examined using a scanning electron microscope (SEM) for NP counts. Then, mass spectrometry imaging (MSI) was performed using a SubAP dual MALDI/ESI ion source (MassTech Inc., USA) and orbital tap (Q-Exactive Plus, Thermo Fisher Scientific Inc., Germany). Gas-phase reactions and ionization processes were utilized to enhance the signal and detect the released Au+ ions. The MSI measurements required specific ion injection time, laser pulse frequency, and pixel sizes. The obtained data were analyzed using a self-made Python script.

Results:
The sample preparation phase played a crucial role, where NPs of specific diameters (20, 40, 50, 60, and 100 nm) were deposited on glass slides for SubAP LDI MS/MSI and on Si substrates for NP counting using SEM as the reference method. Gas-phase reactions involving xylene and Au+ ions in the SubAP ion source resulted in amplified signals; individual NPs with a diameter of 40 nm or more could be detected. Using SEM as the reference method, average detection efficiency was determined for all NPs; it increased from 19 % for 40 nm AuNPs to up to 84 % for 100 nm AuNPs. Furthermore, the developed method was used to detect individual NPs on the surface of porcine brain homogenate tissue. The detection rate of 30 % was achieved for deposited NPs with a signal intensity of (1.4 ± 0.4) thousand ion counts. Overall, our study highlights the potential of SubAP LDI MSI for the sensitive detection of single AuNPs, providing insights into their size-dependent detection efficiency and signal intensity.

Novelty:
Individual AuNP detection using SubAP LDI MSI for sensitive tissue imaging.

Preliminary Data:
AuNP detection efficiency up to 84 % on the glass slide and 30 % on the homogenate tissue.

Contributing Authors:
Michal Žalud, Vadym Prysiazhnyi, Antonín Bednařík, Jan Preisler

Zarrine-Afsar, Arash
University Health Network, Canada

Monday October 23, Session 3, 18:00-18:20

On the concordance of molecular and morphometric cancer borders: insights from mass spectrometry imaging of cancer lipids

Introduction:
Spatially resolved ambient mass spectrometry imaging methods have gained popularity to characterize cancer sites and their borders using molecular changes in the lipidome. This utility, however, is predicated on metabolic homogeneity at the border, which would create a sharp molecular transition at the morphometric borders.
Method:
We subjected murine models of human medulloblastoma brain cancer to mass spectrometry imaging using two ambient methods of desorption electrospray ionization mass spectrometry DESI-MS and picosecond infrared laser mass spectrometry PIRL-MS, two techniques that provides a direct readout of tissue molecular content in a spatially resolved manner.
Results:
We discovered a distance-dependent gradient of cancer-like lipid molecule profiles in the brain tissue within 1.2 mm of the cancer border, suggesting that a cancer-like state progresses beyond the histologic border, into the healthy tissue. The results were further corroborated using orthogonal liquid chromatography and mass spectrometry (LC-MS) analysis of selected tissue regions subjected to laser capture microdissection. LC-MS/MS analysis for robust identification of the affected molecules implied changes in a number of different lipid classes, some of which are metabolized from the essential docosahexaenoic fatty acid (DHA) present in the interstitial fluid.
Novelty:
Caution must be exercised in interpreting multimodal imaging results stipulated on a coincidental relationship between metabolic and morphometric borders of cancer, at least within animal models used
Preliminary Data:
Metabolic molecular borders are thus not as sharp as morphometric borders, and mass spectrometry imaging can reveal molecular nuances not observed with microscopy.
Contributing Authors:
Michael Woolman, Lauren Katz, Georgia Gopinath, Taira Kiyota, Claudia M. Kuzan-Fischer, Isabelle Ferry, Mark Zaidi, Kaitlyn Peters, Ahmed Aman, Trevor McKee, Fred Fu, Siham Amara-Belgadi, Craig Daniels, Brad G. Wouters, James T. Rutka, Howard J. Ginsberg, Chris McIntosh, and Arash Zarrine-Afsar

Zhang, Mengze
University of Zürich, Switzerland

Monday October 23, Session 1, 14:00-14:20

Toward hyper-multiplexed proteomics imaging by MALDI-IHC technology

Introduction:
Highly multiplexed proteomic imaging is critical for understanding complex biological systems. While several antibody-based technologies have achieved high multiplexity, none of them allow for >50-protein detection in an "all-in-one staining and imaging" experiment. Recent advancements in the field of MALDI-MS imaging have provided us with a novel approach to exceed that limit, namely, using UV-cleavable peptide tags as reporters to label antibodies and reveal the protein distributions based on the MALDI imaging (G. Yagnik, et al). Despite the great potential, preliminary works mainly focus on proof-of-concept, and only 12-plex results were demonstrated. To maximize its multiplexity potential, here, we aim to further extend the peptide-tagged antibody panel to >150-plex with a focus on the tumor and the microenvironment.
Method:
Extensive efforts have been invested in antibody validation. To validate antibody specificity, both labeled and unlabeled versions of antibody were tested against marker-positive and -negative tissues using single-plex immunofluorescence microscopy (IF). Consequently, the IF-validated antibodies will be tested by MALDI imaging at 20µm resolution. MALDI imaging sample preparation and data acquisition methods were correspondingly refined based on different markers and tissues.
Results:
We designed a panel of 166 markers, including a wide range of immune, tumor, tumor microenvironment (TME), neurology, cell state, and pathway-specific markers. To date, we have successfully labeled and validated over 100 antibodies using IF and MALDI imaging. More than 75% of these antibodies generate specific signals with a satisfactory signal-to-noise ratio. Additionally, we have refined the MALDI imaging sample preparation workflow, resolving issues like polymer contamination, salt adduct, low sensitivity markers, and intensity variation caused by matrix deposition and MS acquisition. Using optimized protocols, we have stained and imaged healthy tissues (tonsil, colon, kidney, etc.) and various tumor samples (breast cancer, ovarian cancer, melanoma, ccRCC, etc.). To ensure the quality of MALDI-based proteomics imaging, we developed a quality control (QC) pipeline in the R environment. This pipeline analyzes tissue staining images for signal-noise distribution, spatial arrangement, mean-variance comparison, and signal-noise separation. Subsequently, the ion images of QC-ed markers were subjected to single and multi-variance analysis to discover the captured tissue structure at the spatial resolution of 20µm and 50µm. Our ultimate goal is to apply this technology to study clinical tumor samples, acquiring mesoscale tissue information through hyper-multiplexed MALDI imaging experiments. By uncovering high-dimensional molecular features correlated to histopathologies, we aim to enhance patient stratification and precision medicine.
Novelty:
The first time the method allows >100-plex proteomics imaging in a single all-in-one staining and imaging experiment
Preliminary Data:
We have so far validated >100 antibodies, and successfully imaged and analyzed several tissues at 20µm and 50µm resolution.
Contributing Authors:
Mengze Zhang, John Abbey, Dr. Pierre Bost, Prof. Dr. Bernd Bodenmiller

Anthony, Ian
Maastricht University, Netherlands

Monday October 23, Session 1, 14:20-14:30

Fast mass microscopy for 1,000-fold faster mass spectrometry imaging

Introduction:
Mass spectrometry imaging (MSI) of biological samples at high spatial resolutions is slow compared to other imaging technologies such as fluorescence microscopy. We recently developed fast mass microscopy (FMM), a MSI technique capable of imaging approximately half a standard microscope slide (8.5 cm2) in under 30 minutes with 900 nm2 pixels.[1] This is ~1,000 to 10,000x faster than microprobe-mode MSI. Despite high imaging speed, our implementation of FMM had some limitations for adoption in place of more standard MSI and microscopy workflows. These included large data sizes and processing times, non-standard data formats, a secondary ion mass spectrometry (SIMS)-only implementation, and poor mass resolution. Herein, we demonstrate improvements and innovations in FMM for adoption for standard MSI and microscopy workflows.
Method:
The FMM used in this study is a modified TRIFT-II-based mass spectrometer (Physical electronics, Inc, (PHI) Chanhassen, MN, USA) equipped with a C60+ ion beam (Ionoptika, UK), a 3rd harmonic Nd:YLF laser at 349 nm (Spectra-Physics, USA), and a Timepix3-based detector (TPX3CAM, Amsterdam Scientific Instruments (ASI), NL). Custom software in combination with WinCadence 5.2.0.1 control software (PHI) and the SoPhy software package (SoPhy 1.6.6, ASI) were used to control the instrumentation and data processing was completed using in-house software. New encoders with modern readout electronics (National Instruments, USA) were installed to enable more accurate image construction at high stage speeds.
Results:
Some major limitations for widespread appeal and adoption of FMM in standard MSI and microscopy workflows are addressed: Mass resolution: Mass resolution has been effectively doubled (from ~100 to >200 m/Δm50% at m/z 400) due to adjustments in primary ion pulse length, time walk correction, and the use of a faster scintillator in the detection unit. Further mass resolution improvements and improvement strategies should also be possible. SIMS-only implementation: A newly developed, custom laser interface allows for FMM-LDI imaging. In principle, this interface should also allow for FMM-MALDI of biological tissue samples and (as the C60+ ion beam was not removed) multimodal SIMS+MALDI analyses. Data analysis: The large size of images (hundreds of GB and potentially larger) initially prohibited some common data analysis such as standard principle component analysis (PCA). Our implementation of an incremental PCA (IPCA) algorithm has proven reliable, extremely fast (10-1000 times faster than commercial MSI software capable of PCA), and able to analyse the FMM data. Additionally, as a new technology FMM can itself be improved in throughput. A limitation to the imaging throughput were due to the inaccuracy of interpolation required for stage position estimation. New encoders were integrated into the FMM that allow precise position of the stage at each time-of-flight cycle. Preliminary tests show promise that these encoders will ensure the imaging speed is limited only by the stage motors' top speeds. Taken together, and with the promise of future integration with improvements in targeted MSI labelling approaches, these series of improvements represent major steps to the positive disruption of MSI and other biological imaging workflows. [1] A. Körber, J. D. Keelor, B. S. R. Claes, R. M. A. Heeren, I. G. M. Anthony, Anal. Chem., 2022, 94, 14652–14658.
Novelty:
FMM is a promising technique with a unique implementation that has been advanced in numerous ways.
Preliminary Data:
Improvements demonstrated: doubling mass resolution, FMM-LDI, demonstrated 10-1000 x faster PCA, and stage position accuracy down to ~500 nm.
Contributing Authors:
Ian G. M. Anthony [1], Aljoscha Körber [1], Kasper Krijnen [1], Edith Sandström [1], Ron M. A. Heeren [1]

Bookmeyer, Christoph
Metabolomics Interdisciplinary Laboratory, University of Tarragona, Spain

Monday October 23, Session 2, 18:20-18:30

Metal nanolayers combined with SPICI postionization for enhanced spatial metabolomics in the low mass range

Introduction:
MALDI-MSI has evolved as the standard technique for visualizing the distributions of numerous classes of biomolecules in tissue sections, but its sensitivity towards some analyte classes is restricted by, e.g., low ionization efficiencies, ion suppression effects, and interfering background signals for low-weight compounds. To address these limitations, postionization (PI) techniques have been introduced to majorly overcome ion suppression effects, whereas matrix-free surface-assisted LDI (SALDI) has been reported to enable the analysis of metabolites in the lowest mass range. Here, we combine two promising techniques for comprehensive spatial metabolomics on an elevated-pressure dual-ion funnel mounted to an Orbitrap-MS: Single-Photon-Induced Chemical Ionization (SPICI) was recently shown for efficient postionization similar to MALDI-2 but with more degrees of freedom, e.g., without the necessity of matrix interaction. Our combination with Au/Ag nanolayers for SALDI-PI-MSI can majorly extend the range of detectable compounds while producing only minute background.

Method:
The SPICI postonization module consists of a set of shielded Kr-lamps (PKR106-6-14, Heraeus; emission lines: 117/124 nm) operated at 13.56 MHz, as recently shown. The vacuum ultraviolet (VUV) lamps are pulsed in synchronization with the ablation laser to achieve efficient secondary ionization. The module was placed in a Spectroglyph dual-ion funnel MALDI/ESI injector mounted for the first time on a novel Exploris Orbitrap MS. Thin tissue sections were coated with Au/Ag nanolayers by sputtering or with an organic matrix by sublimation. Optionally, a dopant (i.e., acetone) was introduced via a capillary to affect the ionization pathways. Technical parameters like the in-source N2 buffer gas pressure, extraction voltages, and laser repetition rate were optimized for an increased signal intensity for lipids and low molecular weight compounds.

Results:
We selected a set of mammal tissue sections as a test system to explore the performance characteristics and application ranges of our SALDI/MALDI-SPICI-MSI method. Lipidomics: As for the case of matrix-assisted LDI-MSI, many classes of endogenous lipids like glycerophospho- and sphingolipids exhibit a strong boost in signal intensity by up to three orders of magnitude by SPICI when ablated from tissue sections coated with metal nanolayers. This is further proof of the suggested gas-phase reactions initiated by the VUV excitation that yield soft and comprehensive ionization independent of an interaction of the means of postionization with the chosen matrix. For polar and mid-polar lipids, the effect is generally similar to laser-based MALDI-2-MSI and found for both ion modes. However, distinct differences between the two different matrices are notable and will be discussed. Low-molecular-weight compounds: In contrast to classic MALDI matrices, our metal nanolayers produce only a negligible intensity of background signals. This allows for the detection of numerous metabolites in the small mass range below 400 Da. By systematic parameter optimization, we could majorly increase the signal intensity for numerous small-weight compounds such as, e.g., cholesterol and other sterols, compounds of several metabolomic pathways, or neurotransmitters. The combination with SPICI postionization further boosts the signal intensity of numerous compounds by up to two orders of magnitude and augments the analytical depths of the analysis. We used our method for the spatial metabolic and lipidomic analysis of exemplary tissue sections from bovine and mouse brain, liver, and pancreas.

Novelty:
We present the first combination of SALDI substrates with soft postionization at elevated pressure. This allows for extended spatial metabolomics and lipidomics of complex biological/clinical samples.

Preliminary Data:
Matrix-free postionization boosts signals for metabolites by up to three orders of magnitude, which could not be ablated or detected before with matrix-based postionization of complex tissue sections.

Contributing Authors:
Christoph Bookmeyer, Maria Garcia-Altares, Pere Rafols, Oscar Yanes, Xavier Correig

Bowman, Andrew
AbbVie, United States

Wednesday October 25, Session 9, 9:00-9:10

Quantification of a Potential Pharmaceutical in a Time Course Study of Rat Liver with Mass Spectrometry Imaging

Introduction:
Quantitative biodistribution of drugs is important in many aspects of drug development including toxicology, pharmacology, metabolism, target engagement, biomarkers, clearance, and PK. Quantification of pharmaceuticals metabolites from biological matrices is a well-developed science using fluid-based methodologies. However, biofluids are at best approximations of the concentrations of analytes of interest within tissue. Tissue homogenization and extraction can provide specific, quantitative data, but destroys spatial information and treats organs as single compartments. Mass spectrometry imaging provides drug and/or endogenous compound distribution across tissue, allowing physiological changes in tissue to be compared to localized distribution and accumulation. One potential flaw in most MSI experiments is the lack of quantification. Adding quantification to MSI can provide valuable correctional information for determining toxicological findings.

Method:
Male Sprague-Dawley rats were co-dosed with ABT-515 (an HCV protease inhibitor) and ritonavir at 100 mg/kg/day and 15 mg/kg/day, respectively, for 5 days. Rats were sacrificed and their livers harvested at 6, 24, 48, 72, and 96 hours after final dose. Livers were sectioned at 12 µm thickness. A quantification standard was produced using homogenized naïve male rat liver, spiked with 0, 5, 15.8, 50, 158, and 500 µg/g ABT-515. Both set of standards and one liver section were mounted onto a single slide and coated with 2,5-dihydroxyacetophenone as a MALDI matrix. Samples were then analyzed in tandem with standards on a timsTOF fleX (Bruker Daltoniks). Quantification curves and ion images were then generated using LipostarMSI and Pyxis (Molecular Horizon).

Results:
ABT-515 was being investigated as an HCV protease inhibitor. We found in the MSI data that there was a higher abundance of ABT-515 in the epithelia of the bile ducts above that found in the surrounding hepatocytes. Additionally, hematoxylin and eosin staining of the liver tissue found neutrophil infiltration around the bile ducts after 5 days of dosing, which is a noted inflammatory and immunological response in peripheral tissues. As a noted side effect of the sectioning process, we found that samples that had been sectioned and stored at -80 °C for 2 months had lower than expected amounts of ABT-515 compared to samples that were sectioned and analyzed within 1 week. The addition of the quantification standard, however, corrects for this signal decay so long as the standard and tissue were stored in the same conditions.

Novelty:
Mass spectrometry imaging was used to analyze and corroborate the inflammatory response to a pharceutical compound as noted by pathology.

Preliminary Data:
ABT-515 accumulates in bile ducts preferentially to hepatocytes early (6-24 hours) but shares similar abundance and clearance later (48-96 hours).

Contributing Authors:
Andrew P. Bowman, Wayne R. Buck, Junhai Yang, and David S. Wagner

Briggs, Matthew
The University of South Australia, Australia

Tuesday October 24, Session 5, 11:00-11:10

Integrating N-Glycan and Tryptic Peptide MALDI Mass Spectrometry Imaging with N-Glycopeptide LC-MS/MS Data for FFPE Endometrial Cancer Tissue

Introduction:
Endometrial cancer is a gynaecological cancer that originates from the uterus in adult women. While the cancer is still confined to the uterus, the 5-year survival rate is 95%. However, this rate drops to 17% when the cancer metastases. During metastasis, epithelial cells undergo epithelial-mesenchymal transition (EMT) and increase their resistance to apoptosis by altering the extracellular matrix (ECM). ECM proteins play an imperative role in cell health as they provide the scaffold upon which cells and tissues are built. Hence ECM proteins influence almost all cellular processes, including cell differentiation, proliferation, and motility. The majority of ECM proteins are known to be heavily glycosylated, most commonly N-glycosylated whereby glycans are attached to asparagine residues on proteins (i.e., glycoproteins).

Method:
Previously, our group has employed MALDI mass spectrometry imaging (MSI) using axial TOF instruments to spatially map N-glycans and tryptic peptides across formalin-fixed paraffin-embedded (FFPE) ovarian and endometrial cancer tissue sections. In this study, we have spatially mapped N-glycans and tryptic peptides across FFPE endometrial cancer tissue sections (n=3), including primary tumour and lymph node metastasis sections from the same patients, using Bruker's latest timsTOF fleX MS system. Furthermore, our group established an in-situ tandem mass spectrometry (MS/MS) fragmentation protocol which can be implemented post-MALDI-MSI analysis to structurally characterise and confirm cancer-specific N-glycans and tryptic peptides. Lastly, our group has integrated a traditional N-glycopeptide LC-MS/MS method which complements this aforementioned N-glycan and tryptic peptide MALDI-MSI data.

Results:
It was determined that multiple N-glycans and tryptic peptides spatially localised to primary tumour relative to lymph node metastasis, and vice versa. For example, all oligomannose N-glycans were found to be predominantly in primary tumour relative to lymph node metastasis and adjacent stroma, whereas the complex-type N-glycan, (Hex)5(HexNAc)4, was specifically localised to lymph node metastasis. However, upon further analysis, it was discovered that the addition of fucose to (Hex)5(HexNAc)4 resulted in spatial localisation to the stroma adjacent to the primary tumour. Furthermore, the integration of N-glycopeptide LC-MS/MS data with N-glycan and tryptic peptide MALDI-MSI data also proved to be beneficial for validating the spatial results that were reported while for obtaining a deeper molecular understanding of endometrial cancer progression. For example, the type III collagen glycopeptide (ASQNITYHCK) was characterised by LC-MS/MS and confirmed to present several oligomannose N-glycans, consistent with the same structures observed by MALDI-MSI in primary tumour.

Novelty:
This preliminary study combines complimentary MS techniques, N-glycan and tryptic peptide MALDI-MSI and N-glycopeptide LC-MS/MS, to better understand endometrial cancer.

Preliminary Data:
With this preliminary result, we can better understand endometrial cancer and its progression from primary tumour to lymph node metastasis.

Contributing Authors:
Matthew T. Briggs, Parul Mittal, Manuela Klingler-Hoffmann, Gurjeet Kaur, Martin K. Oehler, Peter Hoffmann

Dabija, Laurentiu
York University, Canada

Tuesday October 24, Session 4, 9:40-9:50

Assessment of MALDI Matrices for Phosphoinositide Detection in Mouse Kidney Models Through Matrix-Assisted Laser Desorption Ionization (MALDI) Imaging Techniques

Introduction:
Phosphatidylinositols (PIs) and phosphoinositides (PIPs) play pivotal roles in cellular functions, with their irregularities implicated in various diseases. Though adept at mapping molecules, matrix-assisted laser desorption/ionization mass spectrometry imaging (MALDI-MSI) struggles with phosphoinositides due to their low abundance. This study optimizes matrix selection and thickness for enhanced phosphoinositide detection in mouse kidneys using MALDI-MSI. Hence, common MALDI matrices, 9AA, DAN, CMBT, and DHA were evaluated with varying thicknesses. 9AA, DAN, and DHA produced high-intensity images of PI distributions while CMBT rendered lower intensities but achieved the detection of PIPs alongside 9AA. Thus, a DAN, 9AA, and CMBT matrix mix may boost phosphoinositide mapping, facilitating further research and disease pathology studies

Method:
20 µm kidney tissue sections were cut and thaw-mounted onto indium tin oxide slides (ITO). Each matrix, 9AA, DHA, DAN, and CMBT, was applied using a custom-built sublimation apparatus. Following specific time intervals (dependent on the matrix type), the matrix was heated, sublimed, and deposited onto the sample. MALDI-MSI experiments were performed with a Q-Exactive mass spectrometer (Thermo Fisher Scientific, San Jose, CA, USA) equipped with a Spectroglyph MALDI ion source (Spectroglyph LLC, Kennewick, WA, USA). Data acquisition parameters included a nominal mass resolution setting of 70,000 at m/z 400, a maximum injection time of 200 ms, an m/z range of 250 – 1200, and a spatial resolution of 50 µm for negative ion polarity

Results:
Under the experimental conditions, PI molecular species were identified within the m/z range of 800-950, with PI diacyl (18:0/20:4) at m/z 885.5493 being the most common. The matrices had varying levels of success in detecting and visualizing PIs. DAN matrix provided the best images, except for one PI compound, with distinct kidney features. CMBT matrix could capture most PIs, though some compounds were missing and the image quality was lower compared to DAN. However, kidney features were still visible. The 9AA matrix was unique as it managed to capture all targeted PIs, albeit some at lower intensities. DHA resulted in high-intensity images for all but three undetected PIs. Beyond PIs, the study also mapped phosphoinositides (PIP, PIP2, and PIP3). Interestingly, despite its lower intensity in PI mappings, the CMBT matrix detected four phosphoinositides. Meanwhile, the 9AA matrix detected one PIP compound. However, DAN and DHA failed to detect any phosphoinositides. In summary, while 9AA, DAN, and DHA matrices provided high-intensity images of PI distributions, only 9AA was able to visualize all PIs. The CMBT matrix had a lower intensity for PIs, but it could detect additional phosphoinositides. This study aids in optimizing the experimental conditions for detecting PIs in kidney tissues

Novelty:
Detecting phosphoinositides using MALDI-MSI

Preliminary Data:
DAN, 9AA, and DHA detected most PIs with high-intensity images, while CMBT and 9AA detected both PIP and PIP2 compounds.

Contributing Authors:
Maryam Yousefi-Taemeh, Ergi Duli, Mathieu Lemaire, Demian R Ifa

Devlin, Anthony
Rosalind Franklin Institute, United Kingdom

Tuesday October 24, Session 4, 9:50-10:00

Mass spectrometry imaging of glycosaminoglycans: current progress and future prospects.

Introduction:
Glycosaminoglycans (GAGs) are an essential class of polysaccharides which possess vital structural, adhesion and signalling roles in mammals and other organisms. GAGs are analytically challenging as they are characterised by a disaccharide repeat which may be variably sulphated and total chain lengths can reach sizes in the MDa. Furthermore, GAGs are structural isomers of each other, possessing isomeric carbohydrate linkages and sulphation which form the basis of their varied activities. The level of each type of GAG and the sulphation found within are indicative of cellular activities and pathology progression and hence act as an exciting probe into the nature of the tissue microenvironment.
Method:
On-section enzymatic digestion of targeted GAGs, followed by MALDI-MSI using a Bruker tims-TOF flex to spatially resolve target GAGs, including CS and DS. Analysis of full-length standards, including heparin, CS-A, CS-C and the proteoglycan decorin, using MALDI, DESI, SIMS and LD-REIMS to study future native (derivatisationless) GAG analysis of tissues.
Results:
Post enzymatic-treatment, GAG disaccharides were yielded and imaged. The disaccharides were localised to relevant tissue structures, including the brush border of hepatic veins. Through the use of TIMS, matrix peaks isobaric to GAG disaccharides were removed and isomeric CS-A and CS-C were detected in situ. Following this, preliminary evidence for native GAG disaccharide detection was demonstrated through analysis of whole GAG chains, including heparin, CS-A, CS-C and the GAG containing proteoglycan decorin, yielding GAG fragments. Preliminary data, showing GAG fragments yielded natively, in situ are also demonstrated. A discussion around using various instrumentation, including a novel TIMS-FTICR for future analysis will also be undertaken. Following on from this, we demonstrated that labile sulphate loss can be tracked with ion mobility profiles, allowing identification of parent ions from fragmented ions.
Novelty:
Multi GAG images and identification of parent ions after labile sulphate loss using ion mobilities.
Preliminary Data:
Isomeric GAG disaccharide detection in situ, both after enzymatic digestion and natively.
Contributing Authors:
Kenneth Robinson, Dani simon, Anna Simmonds, Felicia Green, Zoltan Takats

Grgic, Andrej **Monday October 23, Session 1, 14:30-14:40**

M4i, Maastricht MultiModal Molecular Imaging Institute, Maastricht University, The Netherlands

Design and performance characterization of a novel MALDI-2-MSI ionization source with transmission and reflective mode capabilities

Introduction:

As MALDI-MSI pushes spatial resolution towards the low-micron regime by using transmission geometry optics (t-MALDI), increasing demands are placed on developing new ion optical systems, to ensure the limited amount of material is efficiently detected. Laser post-ionization, (MALDI-2) improves the sensitivity of t-MALDI, but requires elevated source pressure and thus suitable ion optics. We have developed a new ionization source based on intermediate pressure ion optics, instead of a conventional ion funnel, to maximize transmission. In this new setup, ions from the MALDI/MALDI-2 plume are captured in a flow of gas laminarized inside a RF ion guide. Here, we present the design and optimization of this new ionization source, and evaluate its performance in both reflective and t-MALDI geometries for tissue imaging.

Method:

An OrbitrapTM EliteTM mass spectrometer (Thermo Fisher Scientific GmbH, Bremen, Germany) was heavily modified, to accept the novel t-MALDI-2 ionization source. The system features both reflection and transmission geometry optics, the latter realized with a 50x objective (Mitutoyo, Japan) placed beneath the sample holder. The sample stage consists of three attocube linear stages, for precise positioning at nanometer resolution. A wavelength tunable OPO laser (Ekspla NT230) was used for MALDI-2. The parameters of the new ionization source, including sample positioning, rastering, sample visualization, laser triggering, and voltage settings are all controlled by software developed in C# language. Tissue samples were coated with a matrix using sublimation. Data visualization was performed using Lipostar MSI (Molecular Horizon Srl, Italy).

Results:

Extensive ion optics and computational fluid dynamics simulations were carried out, to optimize the design of the ionization source in terms of the ion transfer efficiency of ions and neutrals from the sample surface into the RF ion guide. A system of DC lenses enable the direct injection of ions produced by single-step or two-step laser desorption ionization processes into downstream ion optics. The design is gas dynamically optimized, to maintain laminar flow conditions, and minimize ion losses driven by turbulent flows. Different pressure conditions were simulated, identifying an optimum pressure regime in the range of 10 - 15 mbar, allowing lossless ion transfer from the sample surface to the RF ion guide. The higher-pressure regime has also placed new demands in downstream optics. In this new geometry, the S-lens configuration has been replaced by an ion funnel with an axial DC gradient. Initial experiments on mouse brain and kidney tissue have demonstrated high signal-to-noise detection of lipids, in both reflective and transmission operating mode, the latter enabling laser ablation marks with diameters of approx. 2 µm. Following initial optimization using MALDI, the system was coupled with MALDI-2 to further increase ion yields and lipid coverage.

Novelty:

First report of a MSI ionization source for high ion transmission and sensitivity using a lamiarized low pressure gas flow.

Preliminary Data:

Images at 2 µm spatial resolution acquired with the novel MALDI-2-MSI ion source.

Contributing Authors:

Benjamin Bartels, Alexander Lekkas, Diamantis Kounadis, Elias Panagiotopoulos, Dimitris Papanastasiou, Ron M. A. Heeren, Shane R. Ellis

Hale, Oliver
University of Bimingham, UK

Tuesday October 24, Session 8, 18:20-18:30

High-throughput m/z-to-mass deconvolution of protein complexes up to 145 kDa from native protein mass spectrometry imaging datasets

Introduction:
Protein mass spectrometry imaging (MSI) with electrospray-based ambient ionization techniques, such as nanospray-desorption electrospray ionization (nano-DESI), generates datasets in which each pixel corresponds to a mass spectrum populated by peaks corresponding to multiply-charged protein ions. The signal associated with each protein is split among the multiple charge states. Protein MSI under native-like conditions, i.e., non-denaturing conditions where protein quaternary structure is retained, typically uses mass resolving powers which do not provide isotopic resolution in order to improve signal-to-noise ratio. Here, we developed a new feature set for UniDec, open-source software originally developed for rapid deconvolution of complex native MS spectra. We modified the high-throughput module, MetaUniDec, to deconvolve native MSI datasets and transform m/z-domain image files to the mass-domain.

Method:
MSI of protein complexes up to 144 kDa in molecular weight was performed using a home-built nano-DESI ion source attached to an Orbitrap Eclipse mass spectrometer (Thermo Scientific, San Jose, CA). A targeted MSI method used proton transfer charge reduction (PTCR) to produce a charge-reduced series for m/z-selected homodimers of creatine kinase (CKB, ~85 kDa) in mouse brain. Broadband MSI experiments analysed soluble and membrane protein complexes with M.W. approx. 10 – 144 kDa in brain, spinal cord and eye lens. New functionality was added to MetaUniDec to process imzML files. The m/z spectrum associated with each pixel was automatically deconvoluted to a mass spectrum. The processed data were output as a mass-domain imzML file for downstream visualisation.

Results:
The deconvolution workflow was initially tested using targeted PTCR analysis of CKB homodimers. The 17+ charge state (approx. m/z 5010) was isolated and charge reduced by reaction with perfluorophenanthrene anions in the linear ion trap. The product ions were distributed in charge states 16+ – 13+. An m/z-domain imzML file was created from Thermo raw files, then imported and processed in MetaUniDec. Deconvolution was performed at a rate of approx. 10 spectra/s. Ion images at each charge state of CKB were validated with respect to the mass image by cosine similarity scoring (all >94% similar). The mass images produced for homodimeric CKB by MetaUniDec and our original, manual processing method were visually indistinguishable (cosine similarity score: 98.1%). Further validation of the workflow was performed with untargeted experiments scanning up to m/z 8000. Generally, signal-to-noise ratio is poorer in these experiments and the spectra are much more complex. Despite this, mass images were generated for protein complexes including a/y-enolase (heterodimeric, ~94.3 kDa), glucose-6-phosphate isomerase (homodimeric, ~125.4 kDa) and glyceraldehyde-3-phosphate dehydrogenase (homotetrameric, ~144 kDa). Furthermore, the presence of a single phosphorylated subunit in the integral membrane protein complex aquaporin-0 (homotetrameric, ~113.1 kDa) was resolvable in the deconvoluted spectrum. Previously, confirmation of this PTM had required additional higher mass resolving power experiments. Native protein MSI enables highly precise and accurate protein complex mass measurement in parallel to the recording of spatial information, but the data are challenging to interpret for the non-specialist. Mass information is readily interpretable by users of established protein biology tools, such as SDS-PAGE. Transformation of m/z data into the mass domain provides greater accessibility to non-specialists. MetaUniDec is free and open source and will help drive adoption of native protein MSI methodology.

Novelty:
Automated per-pixel deconvolution of native protein mass spectrometry imaging datasets from the m/z to mass-domain.

Preliminary Data:
MSI spectra of proteins up to 144 kDa in molecular weight have been deconvoluted by the MetaUniDec workflow

Contributing Authors:
Oliver J. Hale (1) Helen J. Cooper (1) Michael T. Marty (2) (1) School of Biosciences, University of Birmingham, Edgbaston, Birmingham, B15 2TT, UK. (2) Department of Chemistry and Biochemistry and Bio5 Institute, University of Arizona, 1306 E University Blvd, 85721, Tucson, AZ, USA

Hartig, Jordan
Medical University of South Carolina, United States of America

Tuesday October 24, Session 7, 15:50-16:00

Multi-fucosylated N-glycans detected by MALDI-MSI in tissues distinguish neuroendocrine prostate cancers from all stages of adenocarcinomas

Introduction:
The current 5-year survival rate for late-stage prostate cancer is 32.3%. Late-stage prostate cancer is characterized by the development of distant metastases, androgen deprivation therapy resistance, and neuroendocrine differentiation. These are challenging conditions for treatment, highlighting an urgent need for novel predictors of prostate cancer progression. Using a panel of neuroendocrine prostate cancer (NEPC) tissues in comparison to earlier stage prostate adenocarcinoma (PCa) tissues, the N-glycan compositions for each tumor type were determined by MALDI-MSI. Aberrant glycosylation has been classified as a hallmark for PCa incidence and progression. Fucosylation, the addition of one or more fucose sugars to N-glycans, has been associated with aggressive PCa. However, the structures of specific fucosylated glycans and their association with PCa patient outcome is poorly defined. To explore the role that fucosylated N-glycans may play in the development of lethal PCa and NEPC, independent tissue cohorts were evaluated for levels of fucosylation, linked with immunohistochemistry of NEPC tissue markers, and correlated with patient outcomes and other clinical data.

Method:
Formalin-fixed paraffin-embedded (FFPE) tissues and FFPE tissue microarrays (TMA) were obtained from Washington University and University of Texas Health Science Center at San Antonio. A full tissue panel (n=14) of primary and metastatic prostate cancer tissues with phenotypic small cell neuroendocrine histology, 5 neuroendocrine tumors from lung and ileum, and a series of 33 prostate adenocarcinoma were tested that ranged from Gleason scores 6-10. Slides were stained by IHC for androgen receptor (AR), chromogranin A (CgA), and synaptophysin (SYN). A subset of tissues were stained for a fucose antigen, anti-Lewis Y antibody. Tissue microarrays representing 125 primary PCa adenocarcinoma samples, clinically defined for non-disease recurrence (n=75) and recurrence (n=50) outcomes, were also evaluated by N-glycan MSI. FFPE tissues and TMA slides were prepped for N-glycan MSI using established methods by digestion with peptide N-glycosidase (PNGase F) (PNGase F PRIME, N-Zyme Scientifics) followed by CHCA matrix using an HTX M3 sprayer. MALDI MSI was done on either a Bruker timsTOF fleX or 7T Solarix MALDI-FTICR instruments. Images were processed for statistical analysis via SCiLS Lab Software version 2023c. Fucose scoring was performed by quantifying the number of multi-fucosylated N-glycan structures within each tumor core as determined by a database of 53 possible structures.

Results:
NEPC and PCa tissues were assessed by N-glycan IMS, and over 125 glycan structures were detected. A notable trend of highly fucosylated N-glycans were detected in NEPC tissues relative to other PCa tissues such that a panel of 53 fucosylated glycans that contained at least 2 fucose residues was identified for use as a fucose scoring system. For each tissue, a value of +1 was added for each fucosylated N-glycan detected. N-glycans common to all tumors that were singly fucosylated or high mannose content were not included in the score. In the NEPC versus PCa adenocarcinoma tissues, the average fucose score (FS) for NEPC tissues was 25, and 9 for PCa. Intensity values of IHC staining for AR, Syn and CgA were plotted versus FS for each tissue. Strong correlation of high FS with high Syn and CgA staining tissues was observed, and AR negative expression. Tissues with robust fucose targeted Lewis Y antigen staining co-localized with high FS glycans, Syn and CgA staining. This is consistent with high FS reflecting known NEPC markers. A tissue with mixed NEPC and PCa adenocarcinoma histology confirmed the distinct glycosylation patterns of these two prostate tumor types. The recurrence and non-recurrence outcome TMA samples were also scored for the 53 fucosylated N-glycans. Using the cumulative FS scores for each sample, the FS score values did not reflect initial stage or Gleason grade of the tumors, nor serum levels of PSA at the time of prostatectomy. The FS score could predict those individuals who were most likely to have disease recurrence (I.e., higher FS scores). Future directions involve further characterization of the N-glycome of additional tissue cohorts in order to predict the presence of prostate cancer that can be expected to metastasize, develop androgen therapy resistance, and/or develop neuroendocrine differentiation in order to improve patient treatment routes and overall patient outcome.

Novelty:
This study provides novel insight into the N-glycan profiles of the most lethal forms of prostate cancer tumors and provides a basis for using N-glycans to predict disease recurrence.

Preliminary Data:
Previous studies worked towards profiling the N-glycome of tissues derived from patients following a prostatectomy procedure with the goal of predicting recurrence and metastasis.

Contributing Authors:
Jordan Hartig Joseph Ippolito Kaitlyn Bejar Robin Leach Peggi M. Angel Richard R Drake

Lakkimsetty, Sai Srikanth
Northeastern University, United States

Tuesday October 24, Session 8, 18:10-18:20

Unsupervised co-registration of hematoxylin and eosin (H&E) stained microscopy images and mass spectrometry images (MSI) with feature filtering

Introduction:
Mass spectrometry imaging techniques which allow for a spatially resolved identification of molecules provide insight into molecular features of different tissue regions. Since it is not possible for a pathologist to identify pathologically relevant regions on mass spectrometry images, an alignment of microscopy images and mass spectrometry images is needed to transfer the annotations between the modalities. This integration of image modalities also corrects the histological deformities arising from proximal tissue sections, tissue preparation and tissue handling. Unsupervised coregistration techniques for MSI and H&E images do exist but they are not comprehensive enough to handle idiosyncratic attributes of the images pairs such as global and local deformities, differing aspect ratios, the presence of background and appropriate feature filtering.
Method:
We propose an improved framework that handles multimodal coregistration and specifically addresses the idiosyncratic attributes of MSI. We tackle the multivariate nature of the MSI by initially employing statistical filtering of the features using unsupervised spatial shrunken centroids algorithm from the R package, Cardinal (which reduces the noise and improves the contrast); followed by summarizing the MSI using t-SNE. The framework allows for user selected removal of background in images of both modalities to improve the registration accuracy. The framework automatically performs an initial translation and affine coregistration so the local deformable coregistration starts from an advantageous initial state. The framework is publicly available as a R package, msireg (https://github.com/sslakkimsetty/msireg) and tested on MacOS and Linux.
Results:
We demonstrate the framework's performance using various performance metrics (Dice coefficient and displacement vector field jacobian determinant) and visual inspection. We evaluated the proposed framework on three public datasets. The coregistration led to an improvement, for the three datasets on average, of 5% in Dice coefficient. The displacement field jacobian det showed very little (<1.5%) of image folding (an artifact resulting from improper registration). The proposed framework is also tested for coregistration of TMA arrays.
Novelty:
Feature filtering in pre-processing of MSI for noise reduction and a comprehensive framework for coregistration of MSI and microscopy images.
Preliminary Data:
The proposed framework is tested on three datasets: mouse bladder (AP-MALDI), and two human tissue specimens of colorectal cancer (MALDI-TOF).
Contributing Authors:
Kylie A. Bemis, Andreas Weber, Melanie C. Föll, Olga Vitek

Macdonald, Jade
Medical University of South Carolina, US

Tuesday October 24, Session 5, 11:20-11:30

Identification of Unique Extracellular Matrix Signatures that Differentiate Hepatocellular Carcinoma by Outcome

Introduction:
Hepatocellular carcinoma (HCC) is one of the few cancers that has a rising incidence in the US. Despite research directed toward improved treatments, HCC's immense heterogeneity has made discovery of a universally effective treatment difficult, highlighting the need for a biomarker to stratify patients. Ninety percent of HCC cases arise in the background of cirrhosis, a pathological thickening and deposition of collagenous extracellular matrix (ECM). Despite its role in HCC progression, there has been little research on how ECM proteins change on the translational and post-translational level. This project leverages mass spectrometry imaging and a novel proteomic approach to quantify the distribution of extracellular matrix peptides throughout and around hepatocellular tumors and correlate peptides to clinical outcomes.

Method:
HCC tumors were subtyped into worse outcomes (S1, n = 12) or better outcomes (S3, n = 24) by Dr. Yujin Hoshida using transcriptomic data. In preparation for spatial proteomics, collagenase locally digested ECM proteins on-tissue. CHCA matrix was applied prior to matrix-assisted laser/desorption ionization mass spectrometry (MALDI MS) data acquisition on a timsTOF fleX (Bruker Daltonics). Tissues were subsequently prepared for liquid chromatography tandem mass spectrometry (LC-MS/MS) on an Orbitrap Fusion™ Lumos™ Tribrid™ Mass spectrometer (ThermoFisher Scientific) to elucidate peptide sequences and post translational modifications. Pathological annotations on H&E-stained tissues were used to colocalize MS images and export peptide peak intensities from tumor regions in SCiLS Lab. Statistical analysis and data visualization was performed in GraphPad Prism.

Results:
Since 1980, hepatocellular carcinoma (HCC) incidence has tripled, while mortality has doubled in the US. Despite a surge of excellent research directed at diagnostic markers, there is no clear answer as to why, in a fraction of individuals, the disease results in an aggressive clinical phenotype with high mortality. Collagen deposition and other extracellular matrix (ECM) composition play a role throughout the course of HCC, yet the translational and post-translational association with outcome remains largely undefined. Dr. Yujin Hoshida previously modeled HCC by transcriptomic patterns into three molecular subtypes (S) that differentiate clinically. Notably, S1 & S2 are characterized by poor outcomes, while S3 is characterized by favorable outcomes. To date, there are no investigations on the pathological ECM proteome contributing to subtype outcomes. Here, we hypothesize that ECM variation at the translational and post-translational modification (PTM) level represents a novel, clinically significant contributor to HCC endpoints. HCC tissues subtyped as S1 or S3 were used to investigate ECM proteomic patterns relative to pathological annotation and outcome. ECM-targeted imaging mass spectrometry (IMS) spatially mapped collagen peptide domains relative to pathology and by HCC subtypes. Proteomic sequencing by LC-MS/MS and IMS identified that many altered peptides were post-translationally modified and from trypsin-resistant triple helical regions of fibrillar collagens. Collagen peptide PTM variations were uniquely linked to pathologist-annotated fibrosis, cirrhosis, and tumor regions. S1 largely showed unique peptide signatures in tumor while S3 showed unique signatures in fibrosis. Multiple collagen peptides could distinguish between subtype pathology by area under the receiver operating curve (AUROC) ≥ 0.7, p-value <0.01. Specific collagen domains that bind integrins were spatially localized to bridging fibrosis. Additionally, fibrinogen peptides localized primarily to S1 tumors and could differentiate S1 and S3 tumors (AUC > 0.8). Overall, this study shows that ECM peptides may distinguish hepatocellular carcinoma characterized by outcome.

Novelty:
This novel proteomics approach leverages enzyme specificity and MALDI-IMS to spatially profile ECM peptides that differentiate by clinical outcomes.

Preliminary Data:
Our results suggest localization of extracellular matrix peptides and post-translational modification status could provide important insight on patient outcomes.

Contributing Authors:
Harrison Taylor, Mengjun Wang, Andrew DelaCourt, Jake Griner, David Lewin, Christin Edge, Atsushi Ono, Hiroshi Aikata, Takashi Nakahara, Kazuaki Chayama, Noato Kubota, Noato Fujiwara, Fahmida Rasha, Cesia A. Marquez, Richard R. Drake, Yujin Hoshida, Anand S. Mehta, Peggi M. Angel

Madhoun, Khaled
University of Toronto, Canada

Wednesday October 25, Session 10, 11:50-12:00

Towards subcellular sampling via Impulsive Laser Ablation Coupled to Mass Spectrometry.

Introduction:
Understanding the spatial correlations between protein expressions, concentration fluctuations, and biological functions within living cells will provide unique insights into the Physics driving biological processes. The scientific goal of creating a "molecular map of the cell" requires subcellular resolution, full molecular collection, detection, and proper analysis of all the biomolecular signatures in the sample of study. Impulsive laser coupled mass spectrometry is a powerful tool for studying protein distributions within single cells.

Method:
The study exploits the well-understood and fast development of Drosophila melanogaster embryos allowing for real-time observation of cell differentiation from a single cell to a fully formed organism. There is already a substantial body of data on proteome expressions measured every 2 hours during development of the embryo that provides a detailed library of the cell's building blocks; however, this information lacks spatial relationships. A novel laser ablation method is used to drive ablative phase transitions faster than nucleation growth to give completely intact subcellular voxels. A raster scan is performed on a single Drosophila embryo to determine the spatial distribution of the proteins. The extracted biomolecular species are then processed in state-of-the-art liquid chromatography with tandem orbitrap mass spectrometry.

Results:
In this study, we have achieved subcellular dissection of the drosophila embryo, enabling the mapping of the developmental proteoform. Using the LC-MS/MS of laser ablated segments, we have identified over 2100 unique proteins in a single cell in the early embryonic development of Drosophila embryo.

Novelty:
This research introduces a novel laser ablation method coupled to LC-MS/MS for subcellular mapping of biochemical pathways in cell functioning.

Preliminary Data:
described in results.

Contributing Authors:
Khaled Madhoun, Alexander Wainwright, Stuart Hayes, Temitope Tosin Abiola, Manoel L. da Silva-Neto, Samansa Maneshi, Jiaxi Peng, Aaron Wheeler, Tony Harris, Dwayne Miller

Mavroudakis, Leonidas
Uppsala University, Sweden, Sweden

Monday October 23, Session 2, 18:30-18:40

Identification and imaging of prostaglandin isomers utilizing MS3 product ions and silver cationization

Introduction:
Prostaglandins (PGs) are important eicosanoids involved in physiological processes such as inflammation and pregnancy. The pleiotropic effects of PG isomers and their differential expression from cell types impose the necessity for studying individual isomers locally in tissue to understand molecular mechanisms. For example, the isomers PGE2 and PGD2 exhibit opposing effects in regulation of food intake, sleep, and ischemic injury. Mass spectrometry (MS) based analytical workflows for differentiating PG isomers typically require homogenization, which masks spatial information. However, knowing the location of PG isomers in tissue is important to reveal their action mechanisms. Here, we describe a new method that combines a prediction model with silver-doped PA nano-DESI MSI in MS3 to image isomeric PG species in thin tissue sections.

Method:
Standard solutions of individual PGs in with 10 ppm Ag+ were analyzed with direct infusion (DI) MS using an Orbitrap Velos to identify characteristic product ions from each isomer in MS2 and MS3. The identified product ions were validated using liquid chromatography (LC) MS analysis of a complex extract from rat brain. Prediction models were trained by analyzing standard solutions containing various proportions of the isomers PGE2, PGD2 and Δ12-PGD2 using DI-MS on an Orbitrap IQ-X. For improved signal-to-noise ratio, the linear ion trap was used for acquiring MS3 spectra. Pneumatically assisted (PA) nano-DESI was used for mass spectrometry imaging (MSI) in MS3. The developed prediction model was used to map isomeric PG distributions in a mouse uterine tissue section.

Results:
Cationization of PGs with silver ions drastically enhances the sensitivity compared to deprotonated, protonated and sodiated ions, and produces more informative MSn spectra. High resolution MS2 of [PG + Ag]+ showed characteristic product ions related to loss of AgH and fragmentation in the acyl chain, where other adducts mainly showed loss of water. In MS3, PGE2 and Δ12-PGD2 produce unique characteristic product ions at m/z 331.0096 and 341.0301, respectively. Furthermore, product ions at m/z 333.2060 are generated from all isomers, PGE2, PGD2 and Δ12-PGD2, after neutral loss of AgH. However, the abundance of m/z 333.2060 is distinctly different between the isomers, which enabled its use in the prediction model. The prediction model was trained with high quality MS3 spectra of mixtures of PGE2, PGD2 and Δ12-PGD2 standards acquired using a linear ion trap. Following, the model was created using the fractional abundance of each product ion. Specifically, the model predicted the abundance of PGE2 based on the abundance of the product ion m/z 331 while Δ12-PGD2 was predicted from the abundance of m/z 331 and 341. Finally, PGD2 was predicted as the remaining isomer of the three. The prediction model was tested and cross-validated using standard solutions and chemically complex samples. Overall, the predictions showed high robustness and accuracy (RMSE < 5 % for each isomer). The method was applied to data acquired from a mouse embryo implantation site at day 8 of pregnancy using PA nano-DESI MSI in MS3. The results show distinct localizations of each PG isomer around the anti-mesometrial pole and the luminal epithelium at different abundances. Specifically, PGE2 and Δ12-PGD2, a degradation product of PGD2, were most abundant in the tissue while PGD2 was the least abundant. These results demonstrate for the first time distributions of three different PG isomers in thin tissue sections.

Novelty:
First results of isomeric prostaglandin distributions with mass spectrometry imaging, enabled using a prediction model of MS3 product ions.

Preliminary Data:
The three prostaglandin isomers have different abundances in tissue with Δ12-PGD2 being the most abundant in the anti-mesometrial pole.

Contributing Authors:
Leonidas Mavroudakis, Ingela Lanekoff

Mokosch, Annika
Justus Liebig University Giessen, Germany, Germany

Wednesday October 25, Session 10, 11:00-11:10

High-resolution AP-SMALDI imaging of endogenous neurotransmitters in infectious worm couples causing schistosomiasis (bilharzia)

Introduction:
The parasitic flatworm Schistosoma mansoni causes schistosomiasis, which affects several hundred million people worldwide. In S. mansoni infection, a worm couple produces approximately 300 eggs daily, many of which lodge in host tissues causing schistosomiasis pathology. Neurotransmitters appear to play an important role in the development and fertility of female worms. Investigating their occurrence and distribution in worms with different mating status is an important subject in defining potential drug targets.

Method:
We studied the distribution of neurotransmitters in mature S. mansoni couples, immature worms and genetically altered worms. Before measurement, samples were derivatized with 2,4,6-trimethylpyrylium tetrafluroborate (TMP)[1] to enable the detection of neurotransmitters. On-tissue derivatisation and matrix application were performed on a high-resolution pneumatically asssisted spraying device (SMALDIPrep, TransMIT GmbH, Giessen, Germany). Samples were analysed by atmospheric-pressure scanning microprobe MALDI mass spectrometry imaging (AP-SMALDI MSI). Sections were prepared using a cryotome. Imaging experiments were performed using an AP-SMALDI5 AF ion source (TransMIT GmbH) coupled to a high-resolution orbital trapping mass spectrometer (Thermo Scientific Q Exactive HF, Thermo Fisher Scientific (Bremen) GmbH, Bremen, Germany).

Results:
Imaging of neurotransmitters is challenging due to poor ionizability. Ionization-enhancing on-tissue derivatization is an inevitable approach for MALDI MSI. We have tested different concentrations of TMP to achieve the best possible result for derivatization of the investigated neurotransmitters. Other possible derivatization reagents were also tested, but were found less efficient or less reproducible. In the control worms, various neurotransmitters were detected after TMP derivatization. Signal intensities in mating couples were found to be significantly higher in males than in females. No neurotransmitters were detected in immature females. This supports the reported hypothesis of a male-dominated factor involved in female maturation.[2] Preliminary results of MSI measurements of genetically modified worm couples, in which the neurotransmitter-producing gene was silenced, indicated a signal at the m/z value of the downregulated neurotransmitter, unexpectedly with no significant difference to control couples, suggesting the presence of two isomeric forms of the neurotransmitter which cannot be distinguished without tandem MS approaches. We are therefore currently testing dedicated derivatization reagents, which form distinguishable products.

[1] Shariatgorji, M. et al., Neuron, 2014, 84, 697-707.
[2] Li, X. et al, Front. Cell. Infect. Microbiol., 2023, 13:1173557

Novelty:
On-tissue chemical derivatization allowed to visualize the spatial distribution of various neurotransmitters in Schistosoma mansoni using high-resolution AP-SMALDI MSI analysis.

Preliminary Data:
Our methodology is useful for sensitive, simultaneous metabolite imaging, including neurotransmitters.

Contributing Authors:
Annika S. Mokosch[1], Parviz Ghezellou[1], Xuesong Li[2], Stefanie Gerbig[3], Kerstin Strupat[4], Simone Haeberlein[2], Christoph G. Grevelding[2], Bernhard Spengler[1,3]

Affiliations
[1]Institute of Inorganic and Analytical Chemistry, Justus Liebig University Giessen, Giessen, Germany
[2]Institute of Parasitology, BFS, Justus Liebig University Giessen, Giessen, Germany
[3]TransMIT GmbH, Giessen, Germany
[4]Thermo Fisher Scientific (Bremen) GmbH, Bremen, Germany

Okamura, Maiko
Doshisha University, Japan

Tuesday October 24, Session 7 16:00-16:10

Deciphering Immunometabolism in delta-sarcoglycan deficient hamster with thoracic Mass Spectrometry Imaging (tMSI)

Introduction:
J2N-k hamster (J2N-k), which has a defective δ-sarcoglycan (δ-SG) encoding gene, have been considered as a suitable Dilated Cardiomyopathy (DCM) model. From our previous study, inflammatory pathologies were also noticeable on skeletal muscle as well as myocardium of J2N-k, which has not been observed in its healthy control J2N-n hamster (J2N-n). In the current study, we have adopted a method, thoracic mass spectrometry imaging (tMSI), which allows us to achieve simultaneous visualization of global metabolomic landscape in the thoracic cavity of the hamsters. The multidimensional data obtained from tMSI allowed us to formulate a hypothesis how δ-SG deletion affects both skeletal muscle and myocardium in terms of immunometabolism in time and spatially resolved manner.

Method:
J2N-k and its healthy control J2N-n, each from 4 to 8 weeks of age were fed for the experiment. Frozen transverse sections of J2N-k and J2N-n were prepared by whole animal sectioning. Hematoxylin and Eosin staining was performed. Mass spectrometry Imaging (MSI) using iMScope QT was performed according to the standard method. The matrix used is 9-Aminoacridine (9-AA). IMAGEREVEAL (Version 1.30.0.11507) was used for image and statistical analysis. Uniform Manifold Approximation and Projection (UMAP; in-house) analysis, region of interest (ROI) analysis, and principal component (PC) analysis were used for statistical analysis. Fluorescence-Activated Cell Sorting (FACS) was performed for elucidating immunological phenotype of the immune cells from both hamsters after checking cross reactivity among species. Immunohistochemistry was performed with anti-S100A9 antibody.

Results:
As we have developed a direct thoracic sectioning method, histopathologic and metabolic microenvironments of the heart as well as multiple organs within the thoracic cavity has been enabled. In a single thoracic tissue section, multiple organs besides heart and skeletal muscles such as bone marrow, thymus, lymph node, smooth muscle, esophagus, trachea, lung, spinal cord, adipose tissue, arteriovenous blood vessels and blood were included to be analyzed for both histology and MSI. The most important finding of the current study was that, while myocardium of J2N-k from 5 to 9 weeks of age shows several pathological hallmarks such as inflammation and calcification as expected, skeletal muscle from J2N-k hamsters at around 4 weeks of age has been necrotic and inflammatory. Even from the earlier stage at 4 weeks of age of J2N-k, we found inflammatory features on skeletal muscle in advance while heart pathology seems quiescent. Here we adopt tMSI to define metabolites unique to inflammatory area for both skeletal muscle and myocardium of J2N-k. Segmentation analysis was performed based on the acquired data using machine learning methods and UMAP as a dimension reduction algorithm. Definitive metabolic compartment was successfully extracted for inflammatory foci both in skeletal muscle and myocardium and unique metabolites were also identified. Most important finding was that those metabolomic profiles and metabolites in skeletal muscle and myocardium were consistent with the one from bone marrow, thymus and circulating blood, respectively. Furthermore, myeloid related proteins were expressed both in inflammatory foci in skeletal muscles as well as in the bone marrow of J2N-k hamsters which can be attributed to myeloid cell related immune reaction in situ.

Novelty:
Metabolomic landscape of J2N-k hamster was visualized with tMSI and unique metabolite was detected for both inflammatory tissues and circulation.

Preliminary Data:
Both skeletal muscle and myocardial involvement of J2N-k hamster are impacted with unique metabolite obtained by tMSI strategy.

Contributing Authors:
Maiko Okamura, Shinichi Yamaguchi, Takushi Yamamoto, Ryo Inoue, Laura Yuriko González – Teshima, Keisuke Hakamada, Inori Shintani, Takashi Tsuji, Kisaki Amemiya, Kenji Minatoya, Hidetoshi Masumoto, Satoru Noguchi, Ichizo Nishino, Hatsue Ueda, Masaya Ikegawa

O'Rourke, Matthew
The University of Technology Sydney, Australia

Monday October 23, Session 1, 14:40-14:50

Expanding Peptide Detection in MALDI MSI using Ion mobility MS and matrix phase fractionation

Introduction:
Peptide analysis from formalin fixed paraffin embedded (FFPE) tissue in MALDI MSI is often overlooked due to difficulty with sample preparation and a lack of automated MS/MS acquisition. Peptides are also more difficult to ionize than smaller molecules such as lipids and metabolites due to their relative large size. The end result is that peptide-based experiments only achieve detection of the top 50-100 peptides. In situ MS/MS is also generally not achievable, due to an inability to perform a parent ion scan and subsequent MS/MS on selected ions in a Top N style method. This results in a reliance on intact mass rather than MS/MS to attempt to identify peptides. All of these issues make peptides an challenging target for MSI based experiments, despite the fact that understanding peptides can provide the basis for novel therapeutic target detection, biomarker discovery and mapping molecular changes to physiology. Here we describe our approach that can detect a significantly higher population of peptides and provide sequence information in-situ in a single experiment. This is achieved using a combination of on tissue matrix-based peptide enrichment and ion mobility HDMSe MALDI mass spectrometry.

Method:
FFPE tissues are serially sectioned and mounted to nitrocellulose coated, ITO coated glass slides. Paraffin and formaldehyde crosslinks are removed using our well published methods, followed by on tissue digestion with trypsin. Next, samples are dry coated, by sublimation, with one of multiple peptide specific matrices. Samples are then recrystallized enabling proper embedding of surface peptides with the matrix crystals, before being analysed using a Synapt XS MALDI Ion Mobility QTOF-MS. Data acquisition is performed using HDMSe which incorporates ion mobility with DIA acquisition resulting in separation of intact peptides in the gas phase followed by immediate fragmentation. Data is then deconvoluted to match drifted ions back to the accompanying MS2 spectra thereby providing the peptide sequence.

Results:
Our sample preparation methods focus on using simple chemistry and basic equipment to allow for non-delocalizing digestion and matrix coating. SEM analysis of matrix application has shown that crystal size is uniform and homogenous without spaces between crystals. Comparison to other spraying based methods also shows that analytes do not delocalize meaning that the achievable resolution is much higher. Our previous work using different matrices and pH conditions results in different populations of ionized species, with very little overlap between sample preparation conditions. A normal experiment will produce ~150 detected ions, however by using different matrices in negative and positive mode, we are able to generate 150 ions per matrix per ionisation mode. The end result of an experiment using 4 matrices, at two pH levels, in both negative and positive modes result in 16 x 150 detected species or around 2,400 detected molecules.

Novelty:
This is the first reported workflow for using HDMSe for peptide detection and identification together with using multiple matrices at varied conditions.

Preliminary Data:
Our early efforts show total efficacy of the described method, demonstrating that limits to molecular detection can be overcome with parallel experiments.

Contributing Authors:
*Matthew B O'Rourke1,2, *Sam T Gould1,2, Matthew P Padula2,3, **Philip Hansbro1,2 1 Centre for Inflammation, Centenary Institute, Camperdown, NSW, 2050, Australia 2 School of Life Sciences, Faculty of Science, University of Technology Sydney, Ultimo, NSW, 2007, Australia 3Proteomics, Lipidomics and Metabolomics Core Facility, Faculty of Science, University of Technology Sydney, Ultimo 2007, Australia

Otsuka, Yoichi
Osaka University, Japan

Monday October 23, Session 2, 18:40-18:50

Mass spectrometry imaging of single cells by tapping-mode scanning probe electrospray ionization

Introduction:
The systematic analysis of various molecular constituents in a cell is crucial for comprehending fundamental biological concepts and realizing practical applications in the life sciences. Mass spectrometry imaging allows for the visual representation of the distribution of various components in biological tissues comprised of cells. We have been developing a tapping-mode scanning probe electrospray ionization (t-SPESI) technique. In t-SPESI, a capillary probe with a microscale aperture delivers a minute amount of solvent to the tissue surface while oscillating vertically. This facilitates the extraction-ionization process in an atmospheric pressure environment. We present the implementation of a new t-SPESI unit aimed at elevating the spatial resolution of imaging and providing the results of MSI of HeLa cells.
Method:
For MSI of single-cell, precise positioning of both the cell and the probe's tip is crucial. To achieve this, we have designed and developed a t-SPESI unit that can be integrated into an inverted fluorescence microscope. The new system uses feedback control of the height of the t-SPESI unit to maintain the amplitude constant. To prepare the specimens, HeLa cells grown on glass substrates were labeled with fluorescent dyes, fixed with glutaraldehyde, and rinsed with ammonium acetate. Fused silica capillary probes with 2-3 um opening apertures were used. DMF/MeOH 1/1 v/v, 0.1% formic acid was used as the solvent. PC 25:0 was added as an internal standard for lock mass correction. Xevo G2-XS QTOF mass spectrometer was used.
Results:
The new t-SPESI system allows us to observe individual cells as bright-field and fluorescent images and verify the liquid bridges formed at the probe's tip during the measurement. We also investigated the effect of the configuration of the MS Inlet on the ion intensity to introduce ions into the mass spectrometer with high efficiency. Heated stainless steel tubes of the same length with inner diameters of 2.2 mm or 1.3 mm were connected to the MS to measure sodium iodide ions generated by ESI, and the results showed that the inlet with smaller inner diameters increased the intensity of the cluster ions. Mass spectrometry imaging of HeLa cells was performed at a sampling pitch of 2um, and multiple phospholipids localized in the cells were successfully visualized. In the presentation, we will discuss the details of the cellular lipid alterations resulting from gene regulation of glycolipid synthesis in HeLa cells.
Novelty:
An extraction-ionization method using femtoliter solvents was developed for high spatial resolution mass spectrometry imaging of HeLa cells.
Preliminary Data:
Multimodal imaging (fluorescence, ion, topography) of HeLa cells was performed. Localization of cellular lipids was visualized in ion imaging.
Contributing Authors:
Yoichi Otsuka, Kazuya Kabayama, Ayane Miura, Koichi Fukase, Michisato Toyoda

Palomino, Tana
North Carolina State University, USA

Tuesday October 24, Session 5, 11:10-11:20

Preserving and Predicting Sialic Acid Content of N-Linked Glycans by IR-MALDESI

Introduction:
5-N-acteylneuraminic acid (Neu5Ac) is a sialic acid that plays several roles in both physiological and pathological processes; however, due to their labile nature they are difficult to analyze using mass spectrometry since many ionization methods deposit large amounts of internal energy. As a result, chemical derivatization is required to prevent the loss of sialic acid since their lability could lead to incorrect annotations. IR-MALDESI is a soft ionization technique that can preserve sialic acid residues and detect intact glycans without the use of chemical derivatization. Additionally, IR-MALDESI can predict sialic acid content by using the isotopic pattern of chlorine. We also report a three-fold increase in brain N-sialoglycan detection using IR-MALDESI compared to MALDI-MSI.

Method:
Formalin-fixed paraffin-embedded human kidney and mouse brain sections were prepared by tissue washing, antigen retrieval, and PNGase F enzymatic digestion to expose N-linked glycans and subsequently analyzed in negative ion mode using IR-MALDESI MSI. An Orbitrap Exploris 240 mass spectrometer was coupled to IR-MALDESI and used for data collection using a mass range of 500 – 2000 m/z. Glycan annotations were made using GlyConnect, an experimental database. Ion heatmaps were generated and processed using MSiReader.

Results:
A discrete pattern to predict the degree of sialylation using the theoretical isotopic pattern of chlorine was determined using IR MALDESI. The number of sialic acids on an N-linked glycan equals the charge state minus the number of chloride adducts, or z - #Cl-. The source of chloride adducts is predicted to be the hydrochloric acid present in the citraconic acid buffer used for antigen retrieval. N-linked glycans were detected as doubly- and triply-charged ions, and this rule accurately predicts the number of sialic acids for all glycans detected. Most studies in the MSI field rely solely on accurate mass measurements to characterize N-linked glycans; however, there are many pitfalls to only using accurate mass. The chloride adduction rule generates confident glycan annotations and compositions beyond accurate mass, further improving the capability of IR-MALDESI to study sialylated N-linked glycans. Kidney tissue N-glycans were used as a proof-of-concept to validate the sialic acid prediction. IR-MALDESI was then used to analyze and spatially resolve N-linked glycans within brain tissue. 132 glycans were structurally characterized, and more than 50% of these glycans were sialylated, which is 3-fold higher than sialylated glycans previously detected in the brain using MALDI. This is also the first MSI study to report sulfated glycans in rodent brain. These sulfated glycans were localized to the myelin-enriched corpus callosum region. Myelination plays an important role in axonal functions; therefore, the localization of the sulfated glycans demonstrates the significance of using spatially resolved glycans to study disease pathology.

Novelty:
IR-MALDESI characterizes and spatially resolves N-linked glycans while preserving and predicting sialic acid content without the use of chemical derivatization.

Preliminary Data:
Section thickness optimization for tissue glycan imaging was performed alongside representing the distinct spatial regulation of brain N-linked glycans.

Contributing Authors:
Juhi Samal, Judy Chen, Tatiana Segura, David C. Muddiman

Pearce, Sophie
Sheffield Hallam University, United Kingdom

Wednesday October 25 Session 9, 9:30-9:40

Mass Spectrometry Imaging of an Osteosarcoma Tumour Model to Investigate Drug Induced Metabolic Response

Introduction:
Mass Spectrometry Imaging of an osteosarcoma 3D cell culture model to investigate drug induced metabolic response. Through spatially resolved analysis, we investigated the molecular distribution across treatment naïve, treatment resistant and acutely treated tumour models, to inform mechanisms of drug resistance and the development of novel therapeutics for refractory osteosarcoma. The work aims to demonstrate the clinical translatability of the tumour model and the suitability of MSI methodology in early pharmaceutical drug discovery research. High mass resolution techniques were employed, including Desorption Electro Spray Ionisation (DESI) Multi-Reflecting Time-of-Flight Mass Spectrometry Imaging, Imaging Mass Cytometry and Matrix Assisted Laser Desorption Ionisation Immunohistochemistry (MALDI-IHC), to assess the interplay between metabolic and cellular pathways in response to refractory disease and therapeutic intervention.
Method:
Osteosarcoma tumour models were developed by the culture of Multi-Cellular Tumour Spheroids (MCTS) and subjected to targeted cytotoxic treatments. Negative Desorption Electro Spray Ionisation (DESI)- Multi-Reflecting-Quadrupole-Time-of-Flight Mass Spectrometry Imaging of the osteosarcoma tumour models was performed using the SELECT SERIES MRT, DESI XS System (Waters Corporation, Wilmslow, UK). Endogenous metabolite DESI-MSI was also performed using an Orbitrap Q-Exactive Mass Spectrometer (Thermo Fisher Scientific, Germany). MALDI-IHC Mass Spectrometry Imaging was performed using a Rapiflex TOF MS (Bruker Daltonics, Bremen, Germany), following antibody probing with photocleavable mass-tags (PC-MTs) (AmberGen Inc., Massachusetts, US). Imaging Mass Cytometry by Time-of-Fight identified metal tagged antibodies at sub-cellular 1um spatial resolution by acquisition on the Hyperion Imaging System (Fluidigm Standard BioTools).
Results:
MS Images have revealed distinct localisation of lipids and metabolites within osteosarcoma multi-cellular tumour spheroids. MSI Segmentation clustering pattern analysis has identified a distinct outer proliferative region, quiescent, and necrotic core region of the osteosarcoma tumour model, reflecting the microenvironment of an in-vivo tumour. Metabolic response following cytotoxic drug dosage was analysed by DESI MSI whereby significant molecular changes were identified. A group of molecules displayed significant increased abundance within the tumour models upon dosage with chemotherapy drug doxorubicin. Whilst, conversely, given molecules including small mass metabolites, displayed decreased abundance in treated models. These DESI-MSI data reveal understanding of the tumour model endogenous response to drug treatments and potential mechanisms of drug resistance. Dose dependent discriminatory analysis by Principal Component Analysis presented significant separation of molecular composition between untreated and a range of chemotherapy drug doses. High capabilities were observed from The Multi-Reflecting Time-of-Flight analyser, able to achieve fourth order energy focusing to produce resolving powers over 200 000 FWHM and sub-ppm mass accuracy, by employment of the effective 48m path length and planar, gridless ion mirrors. The DESI XS high performance sprayer demonstrated high reproducibility across tumour model replicates, providing capability to analyse response to treatment, whilst reaching 15um spatial resolution. A drug induced reduction in proliferation was identified by MALDI IHC, with a photocleavable mass tag Ki67 probe localised at 10um spatial resolution. Subcellular protein localisation analysis by IMC at 1um spatial resolution, utilizing metal tagged antibodies, demonstrated an agreed reduction in cellular proliferation. MSI of in-vitro 3D tumour models, offers the capability to assess the interplay of metabolic and cellular pathways in response to refractory disease and therapeutic interventions, without the need for animal testing. It provides improved clinical translatability, thereby elucidating potential strategies for pharmaceutical research.
Novelty:
Analysis of chemotherapeutic intervention by DESI-MRT-MSI of osteosarcoma tumour models. The application of MALDI-IHC to a 3D cell culture model.
Preliminary Data:
A drug induced reduction in proliferation was identified by MALDI IHC, IMC and complimented by increased abundances by DESI MSI.
Contributing Authors:
Sophie M. Pearce; Neil A. Cross; David P. Smith; Malcolm R. Clench; James I. Langridge; Emmanuelle Claude; Lucy E. Flint; Gregory Hamm; Richard J. A. Goodwin; Laura M. Cole

Pryce, Rachel
Université de Montréal, Canada

Tuesday October 24, Session 6, 14:10-14:20

A spatial multi-omics investigation into spinal cord remodeling in mouse mutant strains with altered myelin basic protein abundance

Introduction:
Myelin basic protein (MBP) is responsible for connecting the lipid layers of the myelin sheath. It is believed to be a limiting factor in the production of myelin. The inability to properly construct myelin greatly decreases the efficiency of nerve conduction and occurs in several neurodegenerative diseases, such as multiple sclerosis. It is hypothesized that MBP dysregulation may be an important factor in the genesis of these diseases, prompting the production of mouse models that are genetic mutants for the Mbp gene`s enhancer region. These mutants produce between 160-8% of wild-type Mbp mRNA, which results in major reconstruction of the mouse spinal cord. The shiver mouse which is not expressing the Mbp gene was also investigated.
Method:
The relative abundance and distribution of MBP were measured within the spinal cord using mass spectrometry imaging (MSI) to differentiate between the grey and white matter. Sections were first digested overnight with trypsin before analysis by MALDI MSI. A reporter MBP tryptic peptide was used to measure relative MBP abundance within the white matter across the mutant cohort. After determining that the genetic changes greatly affected the abundance of MBP, other potential molecular changes were considered. As cholesterol makes up 44% of the lipid component of myelin, it was monitored using silver-assisted LDI MSI. Changes in phospholipid abundance were also investigated using dual polarity MALDI MSI. MSI was performed at 50 µm (MBP, Cholesterol) or 75 µm (phospholipids) spatial resolution.
Results:
In 90-day old mice, levels of MBP were shown to range from 120-8% of the wild-type, corresponding to a range from 122-25% Mbp mRNA in these mice. A strong correlation was therefore seen between the amount of Mbp mRNA and the amount of MBP detected. Cholesterol levels remained stable for the single mutation knockouts (122-64 % Mbp mRNA) but reduced significantly in the double (38% Mbp mRNA) and triple (25% Mbp mRNA) knockouts (by 27 and 32% respectively), falling to about 40% of WT cholesterol levels in the white matter of the shiver mouse (0% Mbp mRNA). Interestingly, a slight increase in cholesterol levels was observed in the grey matter of the triple-knockout mouse and the shiver negative control. For phospholipids, significant changes were detected in both the white and grey matter with decreasing Mbp mRNA expression. For example, PC(36:3) increased 6-fold in the white matter, whereas PA(44:9) decreased to about 10% of the wild-type levels in the white matter. PE(P-40:6), which is localized to the grey matter, increased 3-fold. Overall, about 80 lipid species showed distinctive variation trends with decreasing Mbp mRNA expression, many of which are statistically significant. The sum of these results demonstrates that alterations in MBP abundance leads to the extensive remodeling of both the spinal cord white and grey matter. These results may also shed valuable insights into the onset and development of demyelination neurologic disorders.
Novelty:
A multimodal MSI approach was used to monitor the molecular consequences of Mbp gene alteration within the spinal cord.
Preliminary Data:
Significant molecular changes linked to Mbp gene alteration indicate extensive remodeling of the spinal cord.
Contributing Authors:
Rachel Pryce[1], Hooman Bagheri[2], Alan C. Peterson[2] and Pierre Chaurand[1]
(1) Department of Chemistry, Université de Montréal, Montreal, Quebec, Canada
(2) Department of Neurology and Neurosurgery, McGill University, Montreal, Quebec, Canada

Rensner, Josiah
Iowa State University, United States

Monday October 23, Session 1, 4:50-15:00

In-Source Hydrogen-Deuterium Exchange in MALDI-MSI to Assist Metabolite Annotation

Introduction:
Metabolite annotation in complex biological samples is complicated by the presence of isomers and isobars. This limitation is exacerbated in mass spectrometry imaging because chromatography is often incompatible with MSI. Ion mobility spectrometry combined with MSI has become a powerful tool to address this issue, but requires TOFMS. As an additional tool for isomer differentiation, especially for MALDI-Orbitrap, we have developed gas phase hydrogen-deuterium exchange (HDX) by introducing D2O vapor directly into an intermediate pressure MALDI source. By combining with deuterated matrix and heated ion source, we achieved highly efficient (75-85%) HDX up to 17 labile hydrogens. The number of labile hydrogens in metabolites can be accurately determined, allowing elimination of incorrect structural isomers and increased confidence in database annotations.
Method:
An intermediate pressure (~9 Torr) MALDI source (Spectroglyph) paired with an Orbitrap Q-Exactive HF (Thermo) was used for analysis. D2O vapor produced by bubbling nitrogen gas through a sealed bottle of D2O was introduced into the MALDI source. Reaction efficiency was improved by heating the MALDI source before analysis to remove any surface adsorbed H2O and by using deuterated MALDI matrix. MALDI matrices were deuterated through in-solution HDX by dissolving in deuterated solvent and was applied to tissues using sublimation or aerosol spraying. MALDI-HDX-MSI is applied to surface and middle layers of duckweed fronds as well as rat heart tissue sections. Control samples were annotated using METASPACE and the annotations were compared to the observed number of exchanged deuterium atoms.
Results:
MALDI-MSI of Lemna minor (duckweed) fronds and Rattus norvegicus (rat) heart tissue sections were first obtained without HDX and annotated with METASPACE using the BraChem database and HMDB, respectively. The number of labile hydrogen atoms was counted for all metabolite annotations with an FDR of 20% and compared to HDX measurements. This allows us to narrow down potential metabolite annotations by filtering out those with different numbers of labile hydrogen atoms. 2,5-dihydroxyacetophenone (DHAP) was used as a matrix in positive ion mode. Deuterated DHAP was applied to heart samples using a TM Sprayer and sublimated onto duckweed samples. When combined with gas phase HDX, the matrix deuteration efficiency was calculated as ~94% for both TM spray and sublimation. For maltopentaose deposited on duckweed fronds, up to 17 HDX was observed with ~73 % HDX efficiency. Similarly, HDX efficiency of 73-85% is obtained for on-tissue metabolites in duckweed. A slightly lower efficiency of 60-75% is obtained for metabolites in rat tissue. For negative ion mode analysis of rat hearts using N-(1-naphthyl)-ethylenediamine dihydrochloride we similarly measure a labeling efficiency of 94% for the matrix and an efficiency of 55-75% for on-tissue metabolites. Further optimization is needed for more confident application to animal tissue, but even at the current efficiency the maximum exchange is clearly distinguishable, allowing confident determination of the number of labile hydrogen atoms. Crucially, this method can be used reliably with different matrices in diverse samples and is amenable to both sublimation and aerosol spraying. One example of this approach is the flavonoid [C26H28O14+K]+, m/z 603.111. The BraChem database has 6 structural isomers with varying numbers of labile hydrogens. Ten HDX is observed, reducing the number of possible annotations to 2. This helps determine which structures are actually present, and could be combined for other methods for greater specificity.
Novelty:
Highly efficient in-source gas phase HDX is developed for increasing confidence in metabolite annotation in MALDI mass spectrometry imaging.
Preliminary Data:
Reaction efficiency improvements will be made for animal tissue samples and steps will be taken to automate data analysis.
Contributing Authors:
Josiah J. Rensner and Young Jin Lee

Sandström, Edith
M4i, Maastricht University, Netherlands

Monday October 23, Session 2, 16:10-16:20

Steps toward fast mass microscopy of immunolabelled samples

Introduction:
Mass spectrometry imaging in combination with immunohistochemistry (MSI-IHC) enables multiplexing and imaging >40 targeted tags compared to the 4-7 possible with immunofluorescence microscopy[1]. However, time saved by multiplexing MSI-IHC can be lost due to long imaging times at high spatial resolutions. Fast mass microscopy (FMM) is a recently developed, microscope-mode MSI technique that can provide 1,000-10,000 times faster imaging than microprobe-mode MSI[2]. FMM-IHC would greatly increase the viability of large-scale, high spatial resolution screenings of multiplexed immunostained samples. For such an undertaking, FMM requires a series of improvements and validations that, for examples, increase speed and accuracy of stage movements, reduce data processing time, and validate the observation of the IHC tags. Here we demonstrate these improvements and validation tests.

Method:
The BioTrift instrument used is based on the TRIFT II mass microscope (Physical electronics, Inc, (PHI) Chanhassen, MN, USA) equipped with a C60+ ion beam (IOG C0-20S, Ionoptika, Chandler's Ford, UK) and a Timepix3 camera (TPX3CAM, Amsterdam Scientific Instruments, Amsterdam, NL). Linear encoders were added for faster stage coordinate readout. Custom software in combination with WinCadence 5.2.0.1 control software (ULVAC PHI) and the SoPhy software package (SoPhy 1.6.6, ASI) were used to control the instrumentation and data processing was completed using in-house scripts.

Results:
To move towards the full potential of FMM for immunohistochemistry sample analysis, incremental improvements have been made to the instrumentation. One of the main limitations for reaching the full capacity in imaging speed (beyond ~600,000 pixels per second) was the unreliable collection of stage coordinates required for correct image reconstruction. This was improved by the introduction of high-speed linear encoder readouts programmed using LabVIEW (National Instruments, Austin, TX, US) in collaboration with IDEE, Maastricht University, NL, which were able to record the precise stage coordinates throughout each image run. Another limitation affecting the quality of the analysis was the physical stability (specifically the rotation) of the dedicated camera. A more stable mounting system for the TPX3CAM detector has been developed and included in the instrumentation set-up to be used for the screening of immunostained samples. The feasibility of FMM-MSI of lanthanide labels (such as those used in Multiplexed Ion Beam Imaging, MIBI) was investigated with analysis of lanthanide solutions (Ho, Gd) spotted on clean slides as well as sprayed on flash-frozen mouse brain tissue (thickness 12 µm). The same experiments were conducted using a separate instrument, a NanoTOF II (PHI) with a liquid metal ion source (LMIG) (Bi3+) for comparison. The preliminary results show that both instruments can distinguish between metal sprayed and unsprayed areas on tissue, but FMM requires no pre-sputtering of the surface in contrast to the analysis with ToF-SIMS. These promising results will be extended to include more lanthanide solutions for evaluation of the method before expanding to metal-tagged antibodies and high throughput screening of patient samples.

[1] M. Angelo, S. C. Bendall, R. Finck, M. B. Hale, C. Hitzman, A. D. Borowsky, R. M. Levenson, J. B. Lowe, S. D. Liu, S. Zhao, Nature medicine, 2014, 20, 436–442.
[2] A. Körber, J. D. Keelor, B. S. R. Claes, R. M. A. Heeren, I. G. M. Anthony, Anal. Chem., 2022, 94, 14652–14658.

Novelty:
FMM is a unique technique with large advantages over microprobe-mode MSI that can enable high throughput imaging of immunolabelled samples.

Preliminary Data:
Instrument modifications have enabled faster imaging of lanthanides sprayed on tissue and pave the way for high throughput screening studies.

Contributing Authors:
Edith Sandström, Mariya Shamraeva, Kimberly Garcia, Pascal Huysmans, Paul Laeven, Ron M. A. Heeren, Sebastiaan Van Nuffel, Ian G. M. Anthony

Sohn, Alexandria **Tuesday October 24, Session 8, 18:00-18:10**

North Carolina State University, United States of America

A Statistical Approach to System Suitability Testing (SST) for Mass Spectrometry Imaging

Introduction:

Mass spectrometry imaging (MSI) elevates the power of conventional mass spectrometry (MS) to multi-dimensional space, elucidating both chemical composition and localization. Similar to other MS platforms, variability is inherent to MSI; however, the field lacks any robust quality control (QC) and/or system suitability testing (SST) protocols to monitor inconsistencies during data acquisition attributed to sample preparation, system/instrument conditions, or otherwise. To satisfy this demand in the community, we propose an adaptable QC/SST approach with five analyte options amendable to the source of interest (e.g., DESI, MALDI, MALDI-2, IR-MALDESI). Selected data metrics will be analyzed by principal component analysis (PCA) to develop an informative and statistics-based SST scoring system that will guide the researcher to either troubleshoot or continue data acquisition. Please consider for presentation in the "MSI reporting & standards" session. Thank you!

Method:

An equimolar mixture (15 µM) of caffeine, emtricitabine, propranolol, fluconazole, and fluoxetine was prepared in 50% MeOH and sprayed across plain glass slides with a TM-sprayer. Slides were analyzed with an applied ice matrix by IR-MALDESI-MSI coupled to an Orbitrap Exploris 240 in positive mode from m/z 100-500 with a resolving power of 240,000FWHM at m/z 200. A fixed injection time of 15 ms was used, as AGC was disabled. The laser (2970 nm) applied 2.2 mJ/burst with a diffractive optical element. Under optimal instrumental conditions, 118 regions-of-interest (ROI) containing 400 voxels were collected. MSiReader v2 was used to extract relevant data to construct the SST scoring system in RStudio. Follow-on experiments will include collecting 118+ ROIs under compromised conditions.

Results:

Across three days, 46, 47, and 25 ROIs were collected (118 total) on an instrument in optimal condition. While considering existing QC criteria and features unique to MSI, we included the following metrics to develop the statistical model: mass measurement accuracy (MMA), monoisotopic peak abundance, monoisotopic peak detection frequency (DF), isotopic peak DF (C13 and S34), spectral accuracy by atom counting, and percent relative standard deviation (%RSD) of the monoisotopic peak abundance. These are each reflective of system suitability or experimental protocol to aid the researcher in troubleshooting measures. The output of the scoring system results in a final SST score that describes the state of the system. This score is the summation of individual, analyte-based SST scores normalized to the number of compounds used (score range of 0-1), rendering this approach amendable to any number of species utilized. MMA acts as a preliminary filter, where if any analyte is detected at an average MMA >1 ppm, the researcher is immediately advised to troubleshoot. Otherwise, individual SST scores are calculated for each analyte where: 1) the experimental value for each metric will be compared against a statistically determined “ideal value”, 2) PCA analysis assigns a weight to each metric as a function of relevance to variance in the data, and 3) the weighted metric scores will be summed to provide the individual SST score. Individual analyte scores are added and subsequently divided by the number of species used in the model to yield a final SST score. A cutoff for the final SST score will be determined (e.g., 0.80) and implemented on an ROI basis, ultimately advising the researcher to continue analysis or otherwise. Follow-on experiments will include collecting ROIs from a compromised instrument, acting as a testing dataset, to evaluate the reliability and reproducibility of this SST protocol.

Novelty:

Establish a first of its kind statistics-based QC/SST scoring system for MSI techniques to monitor variability and system suitability.

Preliminary Data:

118 ROIs were collected, analyzing five QC compounds, serving as the training set to develop the SST-scoring framework by PCA.

Contributing Authors:

Alexandria L. Sohn*, Russell R. Kibbe*, Olivia E. Dioli*, Emily C. Hector, Hongxia Bai, Kenneth P. Garrard, David C. Muddiman *These authors contributed equally to this work.

Soltwisch, Jens **Wednesday October 25, Session 11, 14:40-14:50**
University of Münster, Germany

An Integrated t-MALDI-2 Ion Source with In-source Bright-field and Fluorescence Microscopy for Direct Correlative Imaging at the Cellular Level

Introduction:
Transmission-mode MALDI combined with laser-induced postionization (t-MALDI-2) enables MS imaging (MSI) at sub-cellular resolution and pixel sizes down to about 1 µm. To advance the method further, a precise co-registration of optical microscopy and t-MALDI-2-derived MSI data is pivotal. Here we present the integration of slide-scanning microscopy into a t-MALDI-2-MS imaging ion source. By using the same closed-loop piezo-actuated sample stage and microscope objective for material ejection and optical microscopy, both modalities are inherently co-registered with sub-micron fidelity. The ion source was coupled to a state-of-the-art QTOF analyzer system (timsTOF fleX MALDI-2) enabling high-speed data acquisition. We demonstrate the capabilities of our correlative imaging method with selected tissue samples and cell cultures.
Method:
A timsTOF-fleX MALDI-2 instrument (Bruker) was heavily modified to integrate a piezo-actuated XYZ-stage and an UV-transmitting objective in transmission-mode geometry. Using the standard smartbeam laser, ablation marks of ~1 µm width were produced on the sample. A dielectric mirror enables the parallel use for digital optical microscopy. An LED ring-light was used for bright-field illumination. Fluorescence images were recorded by inserting filter sets (excitation and emission filter, dichroic mirror) into the beam path. Excitation light was generated by fiber-coupled LEDs. Python-based software was used for autofocusing, acquisition and stitching. Overlays were generated using flexImaging (Bruker) and SCiLS Lab (SCiLS/Bruker). Tissue sections (7 10 µm thick) and cell cultures (grown directly on glass slides) were coated with different MALDI matrices using sublimation.
Results:
The integrated multi-modal ion source records bright-field and fluorescence microscopy images as well as high lateral resolving power t-MALDI-2-MSI. Here we present MALDI-2-MSI measurements of tissue sections and cultured cells with pixel sizes as low as 1 µm x 1 µm and microscopy slide scanning with 50x magnification of the same sample. By utilizing the absolute positional accuracy (< 40 nm) of the closed loop stage, MS and optical images are both recorded at the same spatial coordinate inside the ion source and are therefore intrinsically co-registered with a position error < 1 µm. This omits the need for fiducial markers or subsequent external co-registration. Because optical images are recorded using samples readily prepared for MALDI, dedicated matrix application and staining protocols were developed to be compatible with MSI as well as optical microscopy. Well-prepared samples allowed for the analysis at cellular to sub-cellular resolution in both modalities. The potential of the method is demonstrated with murine tissue samples, which were coated with HABA matrix using a sublimation protocol. Laser-postionization (MALDI-2) critically increases analytical sensitivity and chemical depth of the MSI analysis. In mouse cerebellum, small-scale features of the granular layer, the Purkinje cell layer and the white matter regions are all well resolved in the t-MALDI-2 data as well as bright field and fluorescence microscopy. Next to tissue sections, we will demonstrate the analysis of cell cultures with sub-cellular resolution and direct co-registration of optical microscopy data. Using automated cell segmentation algorithms based on fluorescence images of nuclei, cell lumen, and membrane specific stains, regions of interest for single cells or small groups of cells can be automatically generated for subsequent MSI measurements. By omitting the empty regions between cells, measurement time was decreased by about a factor of five, depending on the population density and cell size.
Novelty:
Integration of cellular resolving power MALDI-MSI with bright-field and fluorescence microscopy in one instrument for inherent co-registration
Preliminary Data:
Recording of bright-field and fluorescence microscopy and MSI images from cells and tissue with sub-cellular resolving power and sub-micron co-registration.
Contributing Authors:
Jens Soltwisch,1 Alexander Potthoff,1 Marcel Niehaus,2 Sebastian Bessler,1 Jan Schwenzfeier,1 Jens Höhndorf,2 Klaus Dreisewerd1 1: Institute of Hygiene, University of Münster, Germany 2: Bruker Daltonics GmbH & Co. KG, Bremen, Germany

Toth, Gabor **Tuesday October 24, Session 6, 14:20-14:30**

Department of Chemistry, BMC Uppsala, Uppsala University, Sweden

Correlation between oxylipin species and lesion formation in human multiple sclerosis revealed by silver-doped PA nano-DESI imaging

Introduction:

During multiple sclerosis, the immune system attacks the myelin cover of the nerve cells causing deteriorated signal transduction. This increased immune activity results in lesion formation throughout the white matter, however, in some cases remyelination occurs in order to restore normal nerve cell functions. Oxylipins are believed to be important modulators in multiple sclerosis, especially due to their regulating activities in inflammation and immune activity. However, their extremely low abundance poses challenges for mass spectrometry imaging (MSI). We aimed to explore oxylipin alterations in human multiple sclerosis brain sections along with non-targeted full lipidomic profiling. Thus, different multiple sclerosis lesion types, adjacent normal-appearing white matter, and control tissue were analyzed using pneumatically assisted nanospray desorption electrospray ionization (PA nano-DESI) MSI.

Method:

Fresh frozen human brain samples were obtained from 2 multiple sclerosis patients and 2 non-neurological controls. Lesion types were identified by histological staining. The PA nano-DESI probe comprised of two fused silica capillaries (50 µm i.d., 150 µm o.d.) and the solvent was 0.1% formic acid in acetonitrile:methanol 9:1 doped with 10 ppm AgNO3 and internal standards. A Thermo Scientific IQ-X mass spectrometer was used at 120 000 mass resolution (Δm/m, at m/z 200), and alternating scans of m/z 200-1100 and m/z 425-470 were acquired. The samples (around 16x14 mm) were moved under the probe by an XYZ stage, generating pixels of ~25 x 150 µm. The data was evaluated with the in-house developed i2i MATLAB application.

Results:

Targeted analysis of the oxylipin species 15-HETE, LTB4, and PGE2 was performed with quantitative MSI in SIM mode. The results show that both 15-HETE and LTB4 species are elevated in remyelinating lesions compared to normal-appearing white matter with fold changes between 3–6. A slight increase was also observed in chronic lesions. On the other hand, PGE2 showed ca. 2-fold decrease in both chronic and remyelinating lesions, while arachidonic acid had increased activity in highly immune-active border regions and non-uniform expression in the various lesions. This suggests increased inflammatory activities in the remyelinating lesions and border regions through both LOX and COX. Non-targeted imaging of several lipid classes was simultaneously performed. The results show a decreased abundance of several lipids in the lesion, including monoacylglycerols (e.g. MG(18:0), MG(20:4), MG(22:6)), diacylglycerols (e.g. DG(34:1), DG(36:2)), and plasmalogens (e.g. PC(O-34:2), PC(O-36:2)). In the border regions surrounding remyelinating lesions, we observed increased abundance of all detected MGs and decreased intensities of sphingomyelins. Moreover, the accumulation or depletion of lipid species was found to be highly dependent on the fatty acyl chains. For example, PC(32:0) is increased in remyelinating lesions but PC(36:1) is decreased. These results are further corroborated with the accumulation or depletion of specific free fatty acids. Finally, the chemical distributions in non-neurogical control tissues were uniform, overall suggesting that the distinct lipid aberrations originate from multiple sclerosis pathology. We aim to further validate the presented preliminary results on a larger cohort to uncover the underlying biological mechanisms.

Novelty:

Silver-doped PA nano-DESI imaging revealed alterations of oxylipins and neutral lipids in human chronic and remyelinating lesions from multiple sclerosis.

Preliminary Data:

Oxylipins, neutral lipids, and fatty acyl chains are highly involved in lesion formation and together contribute to multiple sclerosis pathology.

Contributing Authors:

Gábor Tóth, Jelle Y. Broos, Gijs Kooij, Ingela Lanekoff

Towers, Mark **Wednesday October 25, Session 9, 10:00-10:10**

Waters Corporation, United Kingdom

Increased level of detection of the drugs/metabolites biolocalisation with targeted DESI MRM TQ mass spectrometer

Introduction:

Typically, DMPK studies are performed using LC/MS with electrospray. However, as tissues are homogenised the molecular localisation information is lost. Conversely, DESI MSI allows the determination of small molecule distribution directly from tissue. TOF based MSI has commonly been demonstrated for untargeted discovery analyses. However, there is an increasing need for methods that enhance specificity for the detection of low-level analytes considering tissue complexity and the decreasing amounts of available analytes when moving to ever increasing spatial resolution. There is a also a need to visualise previously inaccessible therapeutic level drug dosages and the products generated by the biotransformation of the drug which are present at even lower levels. Tandem quadrupole (TQ) MS are renowned for their sensitivity and specificity in targeted applications using MRM modes of acquisition. Here a DESI source was used in combination with a triple quadrupole mass spectrometer. Limits of detection (LOD's) for several pharmaceutical compounds spotted on control tissue section were determined at different speeds of acquisition as well their distributions and metabolites in dosed tissue sections.

Method:

Several pharmaceutical compounds such as chloroquine, gefitinib, olanzapine, theophylline etc.. were dissolved in MeOH and diluted in 50:50 MeOH: H2O at various concentration to generate a dilution series that was spotted onto control porcine tissue sections to evaluate and compare quickly their LODs. In the case of dosed tissue, drugs were administrated to mice or rats by intravenous administration and organs were collected at different time points and stored at -80C until sectioning at 18 µm using a cryostat. MSI experiments were carried out using a DESI XS source mounted on a tandem quadrupole mass spectrometer in positive and negative ionisation mode. All experiment were performed multi reaction monitoring (MRM) mode. DESI High-Performance sprayer conditions were set at 1-2 µl/min, 95:5 MeOH: water v/v, with a N2 nebulising gas pressure was set at 10-15 psi and capillary voltage set between 0.55 to 0.8 kV allowing a focused spray. The samples were imaged at different pixel sizes from 15 up to 75 µm and a range of acquisition speeds from 5 Hz up to 50 Hz.

Results:

Pharmaceutical compound, chloroquine, was spotted on a control porcine liver tissue section from 0.003 µM up to 30 µM in a 10 fold dilution series. One series was imaged at a speed of 10 pixels per second (Hz) with two MRM transitions for chloroquine (320.2 > 142.17 and 320.2 > 274.1) and MRM transitions for protonated PC (34:6) (782.55 > 184) which led to a dwell time of 21 ms per MRM transition per pixel. A second series was acquired with only two of the MRM transitions at 50 Hz, leading to a dwell time of 6 ms. For both acquisition speeds, chloroquine was detected from the 0.3 µM spot with s S/N=14. Further pharmaceutical compound dilution series such as a mix solution of propranolol, olanzapine, erlotinib, moxifloxacin, terfenadine and irinotecan was DESI imaged at 10 Hz. LODs were determined between 0.02 µM and 0.25 µM. Calibration curves were generated by drawing regions of interest (ROIs) for each spot and average intensities were plotted vs. amount per spot. For all compounds the calibration curves shown linearity superior as R2 of 0.99. Drug dosed studies were conducted with different pharmaceutical compounds. For example a DESI MSI experiments were performed in targeted MRM mode using the DESI TQ MS. MRM transitions for the metabolites were obtained from previous UPLC MS/MS studies and transferred onto the DESI TQ MS. Only gefitinib and M11 metabolite standards were used to optimised and confirming the transition parameters. Gefitinib and 16 metabolites' MRM transitions were set and imaged, as well as potassiated lipid PC (34:1). Out of 16 metabolites, ten were detected in livers from dosed mice but not in the control tissue. Gefitinib, M7, M9, M10, M11, M12 and M14 concentrations were maximal at 0.5h, declining thereafter, whereas metabolites M1, M2, M6 and M13 reached their maximum concentrations at 3h post dosing.

Novelty:

Therapeutic level drug discovery studies with increased level of detection the biolocalisation of drugs and their metabolites using a targeted DESI MRM TQ system.

Preliminary Data:

DESI Targeted MRM imaging for drug studies on tissue

Contributing Authors:

Emmanuelle Claude, Nyasha Munjoma, Ian Wilson, Joanne Ballantyne

Trim, Paul
South Australian Health and Medical Research Institute, Australia

Wednesday October 25, Session 11, 14:10-14:20

MALDI-MSI lipidomics guided LCM proteomics on human prostate cancer biopsies: maximising the data from a single section.

Introduction:
Current dual source instruments offer a significant advantage in performing multimodal data collection. We used a Bruker timsTOF fleX™ for spatial analysis of lipids and proteins from the same tissue section. MALDI MSI spatial lipidomics was performed on cryosections from human prostate cancer (PCa) biopsies, the unique lipid signatures of different cellular populations allowed for spatial segmentation. Comparison of lipidomics MSI data between ITO and PEN membrane slides was evaluated, PEN membrane slides resulted in reduced signal intensity, but coverage of lipids and their localisation were maintained resulting in no obvious difference in image segmentation. Segmentation-based tissue regions were excised by laser capture microdissection (LCM) followed by bottom-up proteomics, identifying 5524 protein groups. Pathway analysis revealed PCa specific alterations.

Method:
Human PCa biopsies (n=13) were cryo-sectioned onto ITO, PEN membrane and glass slides. ITO and PEN slides were spray-coated with αCHCA using a SunCollect sprayer. Lipid imaging was performed at 20 µm raster size using a Bruker timsTOF flex™ instrument. MALDI data quality was assessed between ITO and PEN slides to confirm suitability of PEN slides for MALDI imaging. Slides were scanned post-acquisition. Bruker region mapper tool was used to convert ROI co-ordinates (Stromal tissue and cancer, benign epithelia) to LCM co-ordinates. Co-registration of the MALDI and LCM images was performed with high accuracy. ROIs were excised for in-solution tryptic digestion bottom-up proteomics on the same instrument. Nano LC-PASEF workflow was used, data processed using DIA-NN.

Results:
Evaluation of ITO vs PEN slides using a list of commonly detected lipid ions showed a decrease in signal intensity for several species, however, importantly segmentation of the tissue using hierarchical clustering resulted in matched segmentation between the two slide types. Further analysis of m/z features was conducted using the SCiLS lab feature finder tool. Comparison of the data showed PEN membrane slides, although not ideal, are suitable for MALDI imaging. MALDI segmentation data was used to define spatial distributions of 3 distinct tissue types, cancerous epithelial (CE), benign epithelial (BE) and stroma (STR). These ROIs were also confirmed by matching to a pathologist annotated H&E section. Using Bruker's region mapper tool, the co-ordinates of the ROIs for each tissue were exported to a Zeiss PALM Robo LCM system, optimum co-registration of regions were achieved using the laser ablation pattern and SCiLS lab image for each tissue, resulting in near perfect accuracy. Bottom-up proteomics data was processed using DIA-NN with MBR and identified 5524 unique proteins across all samples already imaged by MALDI MSI. Principle component analysis produced clear separation of the 3 tissue types with 30.4% and 11.6% of the data variance explained by PC1 and PC2 respectively. 74 proteins were significantly increased, and 107 proteins were significantly decreased in the CE samples compared to the BE samples. Pathway analysis comparing CE to BE detected significantly down regulated expression of proteins involved in the immune response, consistent with prostate cancer being immunologically cold, as well as upregulation of proteins produced by genes regulated by transcription factor MYC, a major driver of prostate cancer tumorigenesis.

Novelty:
Lipidomics guided spatial proteomics on single tissue section and instrument, using commercially available software. Identification of cancer specific protein signatures.

Preliminary Data:
Spatially resolved lipidomic and proteomic data from human PCa tissue. Evaluation of effect of microscope slide type on data quality.

Contributing Authors:
Paul J Trim*, Jacob XM Truong, Sushma R Rao, Feargal J. Ryan, Lisa M Butler, Marten F Snel

Vandergrift, Gregory
Pacific Northwest National Laboratory, United States

Wednesday October 25, Session 11, 14:50-15:00

Peak Ambiguities and In-Source Fragmentation: How Many Peaks in Mass Spectrometry Imaging Experiments are Biologically Meaningful?

Introduction:
Expanding molecular coverage and confident molecular annotation in mass spectrometry imaging (MSI) has been a long-standing challenge. Means to address these issues have included multi-modal ionization approaches and data capture/processing pipelines with increasingly high mass resolution capabilites. Despite this, two key questions are often overlooked: to what extent are MSI features the composite of multiple molecular features (peak ambiguities), and to what extent are the observed MSI features artificial (in-source fragmentation)? These questions are investigated here using nanospray desorption electrospray ionization (nano-DESI) and matrix assisted laser desorption ionization (MALDI) modalities with 21 Tesla Fourier Transform ion cyclotron resonance MS (21T FTICR MS). Additionally, the possible contributions to in-source fragmentation from a post-ionization event with MALDI (i.e., MALDI-2) are investigated.
Method:
Nano-DESI and MALDI MSI experiments were performed on a hybrid Velos Pro 21T FTICR MS equipped with a Window Cell. The 21T FTICR-MS has parallel data acquisition (DAQ) platforms including the internal FT Ultra DAQ, and an external DAQ within a FTMS Booster X3. Sagittal rat brain sections were used for the nano-DESI/MALDI comparison and mounted directly on glass or ITO-coated glass slides, respectively. For MALDI-2 analyses, lipid standards (mixed with matrix at 1:10 ratio; DHB for positive ion mode and NEDC for negative ion mode) were spotted individually onto Bruker IntelliSlides and analyzed via three different MALDI modes using a Bruker timsTOF fleX MALDI-2 instrument: conventional MALDI-1, MALDI-1 with an additional 15% laser power, and MALDI-2 (266 nm laser).
Results:
Peak ambiguities in mammalian lipidome MSI were investigated using nano-DESI and MALDI with 21T FTICR MS. Absorption mode data (aFT) was collected for both ionization modes, resulting in ultrahigh mass resolution datasets (≥613k at m/z 760, 1.536 s transients). Ambiguities were assessed by collating the observed mass splits (i.e., the difference in m/z between neighboring peaks) across all pixels from each MSI experiment; histograms of the mass splits observed via both ionization modalities showed several intense populations as low as 2.4 mDa (corresponding to sodium adduct ambiguity) which importantly require a mass resolving power >600k (at m/z 750) to be baseline resolved. The need for ultrahigh mass resolving power to mitigate amiguity is furthermore showcased via experimentally observed 4.6 mDa mass splits (potassium adduct ambiguity) for m/z >1000, which requires the use of advanced FTICR MS platforms to be observed. In-source fragmentation was interrogated next for various MALDI strategies. For the analysis of select lipid standards (phosphatidylcholine, phosphatidylserine, cardiolipin, and sphingomyelin subclasses), MALDI-2 was found to not increase the extent of in-source fragmentation for pathways that were already observed within MALDI-1. However, an increased number of lipid-derived species (i.e., fragments) were observed with MALDI-2 compared to MALDI-1 for the analyses of individual lipid standards. The origin of these species was computationally investigated for phosphatidylserine lipids in negative ion mode using density functional theory (DFT). Preliminary results revealed electrons in a lowest occupied molecular orbital (LUMO) feature a 4.7625 eV ionization energy (corresponding to 260.33 nm transition). Given the 266 nm laser used for MALDI-2 analyses, we postulate that some of the unique molecular species observed may be the result of in-source fragmentation from excess energy imparted by the MALDI-2 post ionization event. Current efforts involve DFT calculations for additional lipid species and correlation with experimental results for lipid standards.
Novelty:
An experimental assessment of lipid ambiguities and a critical assessment of MALDI-2 post-ionization events.
Preliminary Data:
Peak ambiguities and in-source fragmentation are ubiquitous in MSI and should be carefully considered in final data interpretation and application.
Contributing Authors:
Gregory W. Vandergrift; Will Kew; Kevin J. Zemaitis; Jessica K. Lukowski; Hoshin Kim; Amity Andersen; Dušan Veličkovic; Young Ah Goo; Ljiljana Paša-Tolić; Christopher Anderton

Verhaert, Peter
ProteoFormiX, Belgium

Monday October 23, Session 1, 15:00-15:10

High resolution Mass Spectrometry Imaging (MSI) of neurotransmitters in (human) FFPE neuronal tissues without chemical derivatization: eventuality or Utopia?

Introduction:
Sample preparation is a crucial aspect in MSI. Since formaldehyde fixation and paraffin embedding (FFPE) involve steps in which many biomolecules are being chemically crosslinked and others are abundantly extracted from the sample, FFPE processed tissues have long been considered of little use for MSI. Previous MSI analyses failed to yield sufficient sensitivity for the detection of certain classes of low abundant and/or poorly ionizable biomolecules in FFPE material. Revisiting the same samples with recent generation high performance mass spectrometers does allow successful top-down mass spectrometry imaging of biologically relevant signaling molecules in histological sections, especially when short deparaffination times and precise matrix application conditions are observed. Our latest analyses suggest that also neurotransmitters can be imaged in FFPE sections.
Method:
Homo sapiens FFPE tissues (neuronal tissues producing well-known neuropeptides as well as other cerebral tissue areas) are procured directly from tissue banks, fully compliant with ethical and GDPR regulations. The nonapeptides oxytocin and vasopressin serve as 'positive controls' for human secretory peptide MSHC. An automated sprayer (HTX M5) is employed for consistent MALDI matrix (DHB) application on regular glass microscope slides containing 5 micron thick deparaffinated histological sections [see Paine et al. (2018) Anal. Chem. 90:9272-9280]. High resolution mass spectrometry (HRMS) data are acquired by LTQ Orbitrap Velos and Exploris 480 (ThermoFisher) systems equipped with an atmospheric pressure MALDI source (AP MALDI ng UHR, MassTech). Data are analyzed using HistoSnap (ProteoFormiX), Mozaic QR (Spectroswiss), Lipostar (Molecular Discovery) and MetaSpace (EMBL).
Results:
In analogy to immunohistochemistry the MSI method, which employs direct (top-down) MS for biomolecule localization in histological sections, is called mass spectrometry histochemistry (MSHC). MSHC of human FFPE tissues allows routine biomolecule imaging with high mass accuracy (<1-2 ppm) at 20 micron lateral resolution on a Velos, down to 5 micron pitch using an Exploris 480. Multi-gigabyte data (recorded in full profile acquisition mode) from sections of nonapeptide peptide synthesizing hypothalamic neurosecretory perikarya demonstrate that MSHC is a single cell resolving technology. Whereas the older generation Velos Orbitrap system often lacks the sensitivity to allow for the second isotopologue of a neuropeptide to be detected in the smallest pixels achievable (10x10 micron), the latest generation HRMS (Exploris 480) instrument yields full isotopic pattern in a single 5x5 micron pixel mass spectrum.
Interestingly, MSHC data sets from human cerebral cortex sections indicate that the Exploris 480 system may directly (i.e., without the requirement for chemical derivatization) detect various neurotransmitters, including acetylcholine [M]+, dopamine, DOPA, hydroxydopamine, norepinephrin, serotonin, and histamine [M+H]+. can be detected with sub-ppm mass accuracy (1st isotope). However, the very low neurotransmitter concentrations and the consequent extremely low quantities in a probed sample volume of a mere 5x5x5 µm3, do not allow full isotopic profile revelation. Since MSHC makes the vast numbers of clinically well-documented human materials archived in tissue banks accessible for disease biomarker discovery research, time is ripe to employ this method to some of the well characterized FFPE samples representing neurodegenerative diseases which until today lack unambiguous molecular disease biomarkers. Studies with Prof. D. Swaab (Netherlands Brain Institute) and Prof. D. Thal (Leuven University Neuropathology Laboratory) are underway.
Novelty:
Detection of neuropeptides and (underivatized) neurotransmitters in human FFPE tissues by (top-down) Mass Spectrometry Histochemistry
Preliminary Data:
Detection of neuropeptides and (underivatized) neurotransmitters in human FFPE tissues by (top-down) Mass Spectrometry Histochemistry
Contributing Authors:
Peter Verhaert, Maureen Feucherolles, Gilles Franche

Vermeulen, Isabeau **Wednesday October 25, Session 11, 15:00-15:10**

Maastricht Multimodal Molecular Imaging Institute (M4i), University of Maastricht, Netherlands

Discovering the Molecular Secrets of Epilepsy: Multimodal Molecular Imaging in a Focal Cortical Dysplasia Animal Model

Introduction:

Focal cortical dysplasias (FCD) represent a crucial contributor to refractory epilepsy, affecting pediatric and adult populations. Characterized by localized cortical lesions, FCD results from abnormal brain development (in utero) due to genetic mutations. We successfully established an FCD mouse model to examine the functional consequences of these mutations in depth. We have applied Mass Spectrometry Imaging (MSI), enabling us to explore mouse brain's lipidome and proteome. The combination of this methodology with human transcriptomics experiments, allowed us to investigate the interplay between genetic mutations and molecular changes of FCD. This research unveils hidden complexities of FCD at a molecular level, thereby deepening our understanding of the disease. Moreover, our findings provide a step towards the development of novel therapeutic strategies.

Method:

Fresh-frozen mouse brain sections were sprayed with norharman matrix (HTX-TM sprayer) and analyzed at 20 µm raster size on a tims-ToF (Bruker). Data dependent acquisition (DDA) was performed on Orbitrap Elite hybrid ion trap for lipid identification. Lipid data analysis was performed in Scils and Lipostar. Fluorescence images were taken with a Leica SP8 STED. Laser capture microdissection of the FCD region was performed using a Leica LMD 7000 instrument. LMD samples were trypsin-digested and further processed for LC-MS/MS peptide analysis on a Ultimate 3000 UHPLC system coupled to a Q-Exactive (Thermo). Protein identification was performed in Proteome Discover. Surgical resections of brain tissues (cortex) from FCD 2b and age-matched postmortem samples were used for performing bulk transcriptomics.

Results:

A combination of fluorescence imaging and mass spectrometry imaging (MSI), unveil significant disruptions in neuronal migration and distinct alterations in lipid distribution within the FCD-affected region. Notably, MSI analysis revealed a substantial decrease in sulfatides and phosphatidylserines (PS), key lipids involved in crucial brain myelination processes. In addition, our integration of fluorescence imaging and MSI facilitated the precise outlining and incorporation of the FCD region for proteomic analysis. This proteomic analysis provided compelling evidence of a marked reduction in the glial cells' capacity to form an insulating layer around neuronal cell bodies and axons within the FCD region. This observation highlights a potential disruption in the critical process of neuronal insulation, which may contribute to the pathogenesis of FCD. Moreover, our comparative analysis between the protein pathways identified enrichment of Gene Ontology pathways related to myelination in both the FCD-affected mouse model and human FCD transcriptomic, reinforcing the translational relevance of our animal model. This alignment of findings across species strengthens our understanding of the functional consequences arising from somatic mutations in FCD. These significant discoveries not only enhance our comprehension of the intricate molecular mechanisms underlying FCD but also hold promise for the identification of novel therapeutic targets. Furthermore, our study serves to validate the animal model employed, establishing its utility for future investigations in epilepsy research and the exploration of innovative treatment strategies. Overall, our study exemplifies the power and potential of a multimodal approach that seamlessly integrates fluorescence imaging, MSI, and MSI-guided proteomics in the early stages of target identification within the drug development pipeline and combine this with human validation.

Novelty:

Multimodal spatial omics approach to investigate molecular changes in brain lipidome and proteome with a strong correlation to human transcriptomics.

Preliminary Data:

MSI reveals FCD mouse lipidome and proteome changes linked to brain myelination with similar findings in human transciptomic data.

Contributing Authors:

Natalia Rodriguez, Liesbeth François, Delphine Viot, Patrick Barton, Berta Cillero-Pastor, and Ron M.A. Heeren

Wallace, Elizabeth
Medical University of South Carolina, United States

Tuesday October 24, Session 4, 10:00-10:10

A MALDI mass spectrometry imaging N-glycome atlas and analytic pipeline for human normal and cancer tissues

Introduction:
N-glycosylation is an abundant post-translational modification of most cell-surface proteins. The presence of N-glycans aid in crucial cellular functions like protein folding, protein localization, cell-cell signaling, and immune detection. As different tissue types display different N-glycan profiles, changes in N-glycan compositions occur in tissue-specific ways when cells become cancerous. However, no comparative atlas resource exists for documenting changes in the N-glycomes of multiple normal and cancerous human tissue types. The goal of this study was to create such an atlas and to demonstrate the usefulness of code to analyze MALDI-MSI data efficiently and accurately in a way that can be used in graphing pipelines or analytic tools.

Method:
We used MALDI mass spectrometry imaging (MSI) to look at two custom formalin-fixed paraffin-embedded (FFPE) tissue microarrays (TMAs) containing fifteen tissue types. For each patient tissue, there were samples of both normal and tumor tissues. Using established MALDI MSI workflows and existing N-glycan databases, the N-glycans present in each tissue core were spatially profiled and peak intensity data compiled for comparative analyses. A multi-enzymatic approach allowed for further information on structural composition, using EndoF3 to confirm core fucose and stabilization chemistry to distinguish sialic acid linkages. Analysis was performed using R and functions were written for in-depth analysis, starting with Bruker's SCiLS program to create a data analysis pipeline. Data will also be available in METASPACE.

Results:
The most abundant glycans seen in every tissue were the biantennary glycan with a core fucose at 1809.64 m/z and the same glycan structure without a core fucose at 1663.58 m/z, with triantennary, bisected, and sialylated forms of these glycans making up most of the top glycans across the tissues. High mannose glycans tended to be elevated in cancer, as did polylactosamine, multiantennary, and paucimannose glycans. Biantennary and hybrid glycans tended to be lower in cancer, and glycans containing an N-Acetylglucosamine (GlcNAc) bisect varied by tissue type with no clear trend. We also observed that multiantennary glycans with a core fucosylation in particular tended to be increased in cancer, though no overall changes in core fucosylation proved significant. We also looked at sialylation in depth and observed that, although there were no strong overall trends for α2,3 vs. α2,6 linkage abundance changes between normal and cancer, when one type of linkage was high in the normal, it was low in cancer, and vice versa. Additionally, we noted that α2,3 linked sialic acids were more abundant in tissues overall. All of these results were analyzed and graphed using custom code in R. Overall, this study has demonstrated key trends in cancer and shown the overall trends of glycan structures in different tissue types and their cancer. It also demonstrates the use of our code to analyze data from SCiLS in an efficient pipeline for streamlined analysis and consistent graphing.

Novelty:
An atlas like this has not been created before. We have created and demonstrated code for efficiently analyzing MALDI-IMS data.

Preliminary Data:
This study reports structural information on a wide scale for both normal tissue types and cancers in those tissues.

Contributing Authors:
Elizabeth N. Wallace1, Connor A. West1, Grace Grimsley1, Colin T. McDowell1, Xiaowei Lu1, Evelyn Bruner2, Kiyoko F. Aoki-Kinoshita3; Anand S. Mehta1, Peggi M. Angel1, and Richard R. Drake1 1Medical University of South Carolina, Department of Cell & Molecular Pharmacology & Experimental Therapeutics, Charleston SC 2Medical University of South Carolina, Department of Pathology and Laboratory Medicine, Charleston SC 3Soka University, Department of Bioinformatics, Tokyo, Japan

Yan, Bin
National Physical Laboratory, UK

Tuesday October 24, Session 6, 14:30-14:40

Uncovering metabolic signatures associated with the invasiveness of metastatic melanoma by DESI MSI

Introduction:
The treatment of melanoma is challenging due to its high metastatic potential and therapy resistance. Although previous studies of melanoma found that its invasive front (IF) is enriched in cells with high metastatic potential and in vitro cell line studies revealed unique metabolite signatures of these cells, whether the invasive front of melanoma tumour harbours similar metabolic features has not been directly confirmed under tissue environment. In this work, DESI MSI is employed to perform spatial omics of melanoma tissue and isolated cells from tissue specific regions to characterize molecular composition of the IF versus tumour body (TB), aiming to reveal regional altered metabolic pathways characterising highly invasive melanoma cells which could provide important information for treatment, diagnosis and prognosis.

Method:
Melanoma tumours were collected from mice injected with Yale University Mouse Melanoma (YUMM) 1.7 cells carrying high invasive potential. The tumour tissues were cryo-sectioned using the CryoStar™ NX70 microtome to 10 µm thin layers which were thaw mounted onto superfrost glass slides for MSI measurements. In addition, YUMM1.7 cell pellets isolated from melanoma distal invasive front (DIF) and tumour body (TB) were prepared for MSI studies using the method of either HPMC /PVP embedding and cryo-sectioning, or deposition of resuspended solution. DESI MSI measurements were performed on a Waters Xevo G2-XS QTof instrument, with the sprayer solvent of 95:5 Methanol/Water and the pixel size set at 50 µm and 100 µm for tissue and cell pellets study, respectively.

Results:
Unsupervised interpretation and histological annotation assisted statistical analysis of DESI MSI data of melanoma tissue have revealed a variety of metabolites and lipids that differentiate the tissue regions of invasive front and tumour body. The metabolite and lipid signatures associated with the tissue edge and centre regions were observed in the multivariate analysis using PCA or NMF. Tissue segmentation of melanoma tumour were achieved through statistical classification by k-means or tSNE method. With the assistance of histological annotations, the regions of highly invasive DIF, less aggressive TB, as well as the proximal invasive front (PIF) were manually defined by the combination of tSNE clusters. For both MSI segmentation and histological annotation determined regions of interest, ROC and t-test univariate analysis were performed to identify biomarkers showing statistical differences between DIF and TB. In addition, DESI MSI of cell pellets isolated from tumour DIF and TB regions has also determined similar regional omics features. Nevertheless, it's worthy to note that the number of metabolites and lipids showing regional difference was much smaller in cell pellets studies, and the statistical differences between DIF and TB were more pronounced in tissue measurements for commonly identified biomarkers. It indicates that spatial omics measurement directly on tissue could uncover intrinsic molecular features of metastatic melanoma better than MSI study of cell pellets, which oversimplifies the complex tumour microenvironment. Besides, although the preparation method of embedding and sectioning led to more uniform distribution of cells on surface, the deposition of resuspended solution discovered more metabolites and lipids distinguishing the TB from the DIF. Though the underlying mechanism has not been investigated, partially it could be attributed to the heterogeneous molecular distribution between different cell pellet sections.

Novelty:
Identification of regional altered metabolic features characterising highly invasive melanoma cells may provide valuable information for diagnosis, treatment, and prognosis

Preliminary Data:
Histological annotation assisted MSI tissue clustering and univariate analysis to investigate spatial metabolic features of metastatic mouse melanoma tumours

Contributing Authors:
Bin Yan1, Janella Marie de Jesus1, Rory Steven1, Vittoria Graziani2, Eva Crosas Molist2, Oscar Maiques2, Victoria Sanz-Moreno2, & Josephine Bunch1,3, 1. National Centre of Excellence in Mass Spectrometry Imaging, National Physical Laboratory, Teddington TW11 0WL, UK 2. Centre for Tumour Microenvironment, Barts Cancer Institute, Queen Mary University of London, Charterhouse Square, London, EC1M 6BQ, UK 3. Faculty of Medicine, Department of Metabolism, Digestion and Reproduction, Imperial College London, South Kensington Campus, London SW7 2AZ, UK

Zizmare, Laimdota **Tuesday October 24, Session 7, 16:10-16:20**
Werner Siemens Imaging Center, University Hospital Tuebingen, Tuebingen, Germany

Combining MSI and ex vivo quantitative metabolomics with in vivo imaging to decipher molecular mechanisms of human breast cancer heterogeneity.

Introduction:
Malignant tissue growth progression and mutation status have a direct impact on therapeutic outcomes. Altered glucose metabolism is a known hallmark of cancer and is routinely studied in vivo by [18F]FDG positron emission tomography (PET) and magnetic resonance (MR) approaches. These in vivo techniques however provide only limited information on tumor metabolism and heterogeneity. Within a multimodal explorative study linking human in vivo PET-MR imaging with molecular ex vivo analysis by NMR spectroscopy-based metabolomics and RNA microarray, the ongoing investigation has shown promising metabolic differences between luminal A and B breast cancers. Based on the preliminary results, we further wanted to investigate the spatial metabolome alterations to uncover differences not only between tumor types but also tumor center and periphery.
Method:
Snap-frozen punch-biopsies of tumor center, periphery and native breast tissue control of 36 patients were selected representing luminal A and B, and HER 2 genotypes. Mass spectrometry-based metabolomic imaging using rapiFlex and timsTOF MALDI allowed obtaining spatially resolved metabolite and lipid distribution information, accompanied by breast cancer antibody panel and histology staining. Further ex vivo correlations were made with nuclear magnetic resonance (NMR) spectroscopy-based metabolomics and RNA microarray-based transcriptome readout. The in vivo and ex vivo correlation was investigated using initially obtained patient [18F]FDG PET-MR imaging data of tracer standard uptake value (SUV) distribution in the patient tumor center and periphery.
Results:
Tumor metabolomic heterogeneity was visually and quantitatively linked to the luminal A/B and HER 2 tumor subtypes. As tumors with an activated metabolic switch towards lipid metabolism are resistant to neoadjuvant chemotherapy and reluctant to immune-based therapies, additional biomarker and metabolic event characterization is of high importance. [18F]FDG uptake confirmed that glucose metabolism was dominant in the center of the tumor, while it was lower in the tumor periphery. Similarly, the obtained metabolomics and transcriptomics results, specifically lipid and growth-related metabolites, indicated clear metabolic differences between the luminal A and B subtypes in both the center and periphery of the tumor. Lipid metabolic pathways were more enriched in tumor periphery based on the gene expression analysis. Elevated levels of acetate were characteristic to the luminal B tumor periphery, which is a crucial precursor of lipid metabolism. Serine concentrations were increased in the luminal B tumor periphery as an important one-carbon donor leading tumor growth. The overall metabolic activity of luminal B subtype was higher compared to luminal A. This study illustrates the importance of ex vivo validation that provides increased sensitivity and detail otherwise unavailable in vivo. MSI provides unique opportunity to decipher molecular and cellular metabolic changes that should be considered for everyday preclinical and clinical routines alongside classical histology. The tumor microenvironment of aggressively growing cancers with a unique metabolome and lipidome can be subject to the development of refined PET tracers, molecular treatment targets and improved guidelines for personalized tumor resection. Our comprehensive dataset and in vivo – ex vivo detailed correlation analysis can strengthen future patient diagnosis, aid the recognition of ongoing molecular events in vivo, and lead to improved therapy monitoring.
Novelty:
Patient tumor center/periphery vs genotype co-correlation with in vivo metabolic imaging and ex vivo spatial, quantitative metabolomics and transcriptomics
Preliminary Data:
Mass spectrometry imaging provided additional lipid and metabolite information on metabolic differences between tumor periphery and center.
Contributing Authors:
Laimdota Zizmare, Laura van der Vloet, Qianlu Yang, Anna Fischer, Brigitte Gückel, Annet Duivenvoorden, Heike Preibsch, Tim-Colin Schade, Georgy Berezhnoy, Isabeau Vermeulen, Sisi Deng, Annette Staebler, Andreas D. Hartkopf, Bernd. J. Pichler, Christian la Fougère, Markus Hahn, Irina Bonzheim, Konstantin Nikolaou, Michiel Vandenbosch, Ron M. A. Heeren, Christoph Trautwein

Bruker **Wednesday October 25, Session 11, 13:50-14:00**

Azad Eshghi, Ph.D

Field Applications Support Scientist, Bruker, Victoria, British Columbia, Canada

Multimodal Imaging Analysis for Comprehensive Biological Information

Waters **Wednesday October 25, Session 11, 15:10-15:20**

Dr. Emrys Jones

DESI MS imaging at the cellular level with nano-flow and multi-focus approaches

Mass spectrometry imaging (MSI) continues to gain momentum as the breadth of applications and range of techniques continue to expand. Whilst the push to higher and higher spatial resolutions has, to a certain extent, been tempered by the over-riding requirement to obtain the greatest information depth in a sensible time frame, biology is still best studied on the cellular level. Here we present a DESI based workflow that allows for coarse pixel size low-damage initial scan that is used to direct higher spatial resolution images to only the areas where they are required. In this way, images at or below 10-micron spatial resolution can be obtained without the prohibitive time and data burden of untargeted imaging of the whole sample.

Ionoptika **Monday October 23, Session 2, 17:00-17:10**

Kate McHardy

Advances in, and applications of, Gas Cluster Ion Beam (GCIB) SIMS

Work with Gas Cluster Ion Beam (GCIB) SIMS represents a small subset of SIMS applications, but interest is growing in the use of these gentle ion beams for SIMS on soft materials such as biological tissues and polymers. Ionoptika's J105 is the only SIMS instrument developed specifically for the use of Gas Cluster Ion Beams as the primary ion beam, meaning that the cluster sizes achievable are unique to the instrument. The advantages of such large clusters include: low fragmentation of high AMU species, higher sensitivity to high AMU species, the ability to use various beams and real-life non-flat samples without sacrificing mass resolving power or mass accuracy, and excellent depth resolution.
Here we discuss some of the applications of GCIB SIMS from lipidomics to drug research and introduce recent advances in GCIB technology, such as Ionoptika's water cluster ion beam.

Aspect Analytics **Tuesday October 24, Session 6, 14:40-14:50**

Alice Ly, PhD

Dedicated Software to Support High Throughput Spatial Multi Omics Applications

Different technologies are increasingly being used in tandem to spatially profile and characterize various molecular families, such as combining mass spectrometry imaging for lipids with spatial transcriptomics or multiplexed immunofluorescence. However, these techniques generate tens to hundreds of gigabytes of complex data in a single experiment, creating a critical bottleneck in data analysis. Dedicated software to manage, integrate, visualize and QC these technologies is required.

Aspect Analytics provides software solutions to support spatial multi omics research across a range of different techniques, applications and user bases. Our platform supports a variety of spatial multi omics applications by bridging the gap between algorithmic development in bioinformatics research and enterprise-grade platforms. Examples of our work on spatial multi omics integration will be presented in this talk.

HTX Imaging **Tuesday October 24, Session 4, 10:10-10:20**
Alyson Black

Advances in Sample Preparation for Ultra-High Spatial Resolution MALDI Imaging

As interest grows in ultra-high spatial resolution and single cell MALDI MS Imaging, sample preparation techniques from HTX Imaging are continuing to evolve to support this scientific need. This talk will highlight the use of the HTX M3+ Sprayer and of the HTX SubliMATE for uniform matrix coating with ultra-small crystals for the highest possible spatial resolution MALDI imaging.

The HTX M3+ Sprayer uses a combination of temperature, solvent chemistry, and velocity control to produce aerosolized droplets of matrix solution that quickly dry when coating samples. Quick drying spray methods are used to produce small matrix crystals for MALDI Imaging down to 5 microns. The HTX M3+ Sprayer also features a high level of automation for streamlined operation, with software-controlled cleaning to improve instrument performance.

For ultra-high spatial resolution imaging, sublimation produces the smallest possible matrix crystals as a solvent-free method. The HTX SubliMATE, developed with Vanderbilt University, increases the reproducibility and simplicity of the sublimation process for ultra-high spatial resolution sample preparation, with crystal sizes below 1 micron. Controlled heating and cooling with the HTX SubliMATE decrease the variability of sublimation cycles, leading to uniform matrix coating that can be reproduced across users and laboratories

Ambergen **Monday October 23, Session 1, 15:10-15:20**
John Gillespie
AmberGen® is a biotechnology company and producer of Miralys™ spatial biology imaging solutions.

Miralys™, also known as MALDI HiPLEX-IHC, is a new breakthrough method for imaging targeted intact proteins within a MALDI Imaging Mass Spectrometry workflow that has unique capabilities. Introduced in 2022, it has gained significant traction in a short period of time. It is currently being used to study tissues and conduct DMPK studies for a wide range of disease states including many types of cancer, neurodegenerative diseases, and infectious diseases.

Benefits include:

- Drug/target co-localization on the same tissue section, using a single workflow and instrument.
- The ability to produce images that co-register small molecule lipids and metabolites as well as the intact targeted proteins.
- The product's combination of fast, targeted, protein imaging (scan time as short as 45 min for a 1cm^2 section), ultra-high plex (10 to 100+), wide viewing area (up to 25 x 75 mm), and multi-modal capability make it an ideal technology for doing initial scans to identify regions of interest for later deep-dive analysis.
- Miralys™ requires no dedicated instrument, and minimal investment to start using. It is used on MALDI Mass Spec Imaging instruments that your institution most likely already owns, such as the industry-leading instruments from our partner, Bruker Corporation.

In our talk we will introduce several new enhancements to our Miralys product line.

Thermo Fisher Scientific **Tuesday October 24, Session 7, 16:10-16:20**

Maciej Bromirski, Sr. Project Manager

MS Imaging meets Orbitrap Technology

Mass spectrometery imaging (MSI) techniques combined with Thermo Scientific Orbitrap detection is very attractive for various life science applications due to the High Resolution Accurate Mass (HRAM) capabilities with ease-of-use of Orbitrap instrumentation. Several ion source techniques, such as MALDI, nanoDESI, SIMS, MALDESI are capable of MS Imaging by their nature - have been coupled to Orbitrap instrumentation.

In this talk we briefly report about Atmospheric Pressure (S)MALDI technique solutions coupled to Orbitrap technology. Perspectives from the 'sample to image' workflow are provided when coupled with MassTech's AP-MALDI UHR source or TransMIT's AP-SMALDI5AF source - both for MSI applications - particularly in metabolomics and lipidomics.

Sun Chrom/ MassTech **Monday October 23, Session 2, 17:10-17:20**

Maureen Feucherolles, Jean R. N. Haler, Tina B. Angerer, William Le, Jérôme Bour, Gilles Frache

Atmospheric Pressure MALDI coupled to Orbitrap(s), principle and applications

The interest in Mass Spectrometry Imaging (MSI) has been growing over the years and increasingly demanding (biomedical) applications are being investigated. Yet, Matrix-Assisted Laser Desorption/Ionization (MALDI) MSI instrumentation need to provide both precise localization, and unambiguous identification for (bio-)molecular ions. The presented experimental set-up takes benefit of the High-Resolution Accurate Mass measurement provided by the Orbitrap technology, combined with Atmospheric-pressure MALDI ionization, allowing for high resolution MSI in both mass and space.

The latest generation Orbitrap Exploris 480 (Thermo Scientific) coupled to a APMALDI UHR ion source (Masstech) has been used to evaluate the improved sensitivity and scan rate over APMALDI coupled to former generation LTQ/Orbitrap Elite set-up.

Several applications will be presented including polymers, peptides test samples and biological tissue sections for imaging. Lipid distributions in biological tissue sections were evaluated. Matrix application was performed using pneumatic sprayer (Sunchrom). Data visualization and interpretation was achieved using Multimaging (Imabiotech) and Lipostar (Molecular Horizon). Several imaging modes are presented with lateral resolutions down to 5 micrometres. Achievable sensitivity, image acquisition speed and potential for both targeted and untargeted MSI methods are discussed.

Masstech APMALDI UHR Orbitrap MSI offers an alternative to dedicated MALDI MS instrumentations. The presented setup allows to add imaging capabilities to existing high-end Orbitrap LC/MS systems, and users can switch from MSI to LCMS configuration within minutes. The improved performances of latest generation Orbitraps as well as improved method development workflows opens new perspectives for a wide range of applications.

SCHIMADZU **Monday October 23, Session 3, 18:50-19:00**

M. Nazim Boutaghou

Shimadzu: One-Stop Shop for Your Imaging Needs

At ASMS 2022, Shimadzu Corporation released its full solution for MALDI-based MS Imaging (MSI). From matrix deposition to data processing, Shimadzu provides high-end equipment to meet your imaging needs. Shimadzu Corporation is the only instrument manufacturer that provides solutions that support all three phases of MSI experiments: Matrix Deposition, Data Acquisition and Image Processing and Analysis.

Our matrix deposition solutions comprise dry and wet deposition. The iMLayer Aero is a robust sprayer that has proven to provide sensitivity and pixel resolution down to 10 um. The iMLayer is our high-end sublimator that will make sub-cellular 5 um imaging routine as it combines laser measurement for matrix deposition thickness. The iMScope QT is our flagship AP-MALDI QTOF instrument specifically designed for MS imaging. It combines an optical microscope for precise scan area determination and an AP-MALDI source with a laser that can fire at a speed up to 20 KHz and offers a class-leading 50 pixels/s acquisition speed. Next to our high-performance MALDI-QTOF is a MALDI-TOF instrument that comes in a compact format (small size) and at a compact price. This entry-level instrument is packed with high-end features and is ideal for any MSI experiment, such as method optimization, image screening, and teaching MALDI and MALDI-based MS Imaging.

Since imaging is not just about beautiful images but rather about meaningful images, Shimadzu released IMAGEREVEAL, a vendor-neutral image processing software that will extract meaningful results out of your gigabyte result files.

Bruker **Wednesday October 25, Session 11, 13:50-14:00**

Azad Eshghi, Ph.D

Field Applications Support Scientist, Bruker, Victoria, British Columbia, Canada

Multimodal Imaging Analysis for Comprehensive Biological Information

Waters **Wednesday October 25, Session 11, 15:10-15:20**

Dr. Emrys Jones

DESI MS imaging at the cellular level with nano-flow and multi-focus approaches

Mass spectrometry imaging (MSI) continues to gain momentum as the breadth of applications and range of techniques continue to expand. Whilst the push to higher and higher spatial resolutions has, to a certain extent, been tempered by the over-riding requirement to obtain the greatest information depth in a sensible time frame, biology is still best studied on the cellular level. Here we present a DESI based workflow that allows for coarse pixel size low-damage initial scan that is used to direct higher spatial resolution images to only the areas where they are required. In this way, images at or below 10-micron spatial resolution can be obtained without the prohibitive time and data burden of untargeted imaging of the whole sample.

Ionoptika **Monday October 23, Session 2, 17:00-17:10**

Kate McHardy

Advances in, and applications of, Gas Cluster Ion Beam (GCIB) SIMS

Work with Gas Cluster Ion Beam (GCIB) SIMS represents a small subset of SIMS applications, but interest is growing in the use of these gentle ion beams for SIMS on soft materials such as biological tissues and polymers. Ionoptika's J105 is the only SIMS instrument developed specifically for the use of Gas Cluster Ion Beams as the primary ion beam, meaning that the cluster sizes achievable are unique to the instrument. The advantages of such large clusters include: low fragmentation of high AMU species, higher sensitivity to high AMU species, the ability to use various beams and real-life non-flat samples without sacrificing mass resolving power or mass accuracy, and excellent depth resolution.
Here we discuss some of the applications of GCIB SIMS from lipidomics to drug research and introduce recent advances in GCIB technology, such as Ionoptika's water cluster ion beam.

Aspect Analytics **Tuesday October 24, Session 6, 14:40-14:50**

Alice Ly, PhD

Dedicated Software to Support High Throughput Spatial Multi Omics Applications

Different technologies are increasingly being used in tandem to spatially profile and characterize various molecular families, such as combining mass spectrometry imaging for lipids with spatial transcriptomics or multiplexed immunofluorescence. However, these techniques generate tens to hundreds of gigabytes of complex data in a single experiment, creating a critical bottleneck in data analysis. Dedicated software to manage, integrate, visualize and QC these technologies is required.

Aspect Analytics provides software solutions to support spatial multi omics research across a range of different techniques, applications and user bases. Our platform supports a variety of spatial multi omics applications by bridging the gap between algorithmic development in bioinformatics research and enterprise-grade platforms. Examples of our work on spatial multi omics integration will be presented in this talk.

HTX Imaging **Tuesday October 24, Session 4, 10:10-10:20**
Alyson Black

Advances in Sample Preparation for Ultra-High Spatial Resolution MALDI Imaging

As interest grows in ultra-high spatial resolution and single cell MALDI MS Imaging, sample preparation techniques from HTX Imaging are continuing to evolve to support this scientific need. This talk will highlight the use of the HTX M3+ Sprayer and of the HTX SubliMATE for uniform matrix coating with ultra-small crystals for the highest possible spatial resolution MALDI imaging.

The HTX M3+ Sprayer uses a combination of temperature, solvent chemistry, and velocity control to produce aerosolized droplets of matrix solution that quickly dry when coating samples. Quick drying spray methods are used to produce small matrix crystals for MALDI Imaging down to 5 microns. The HTX M3+ Sprayer also features a high level of automation for streamlined operation, with software-controlled cleaning to improve instrument performance.

For ultra-high spatial resolution imaging, sublimation produces the smallest possible matrix crystals as a solvent-free method. The HTX SubliMATE, developed with Vanderbilt University, increases the reproducibility and simplicity of the sublimation process for ultra-high spatial resolution sample preparation, with crystal sizes below 1 micron. Controlled heating and cooling with the HTX SubliMATE decrease the variability of sublimation cycles, leading to uniform matrix coating that can be reproduced across users and laboratories

Ambergen **Monday October 23, Session 1, 15:10-15:20**
John Gillespie
AmberGen® is a biotechnology company and producer of Miralys™ spatial biology imaging solutions.

Miralys™, also known as MALDI HiPLEX-IHC, is a new breakthrough method for imaging targeted intact proteins within a MALDI Imaging Mass Spectrometry workflow that has unique capabilities. Introduced in 2022, it has gained significant traction in a short period of time. It is currently being used to study tissues and conduct DMPK studies for a wide range of disease states including many types of cancer, neurodegenerative diseases, and infectious diseases.

Benefits include:

- Drug/target co-localization on the same tissue section, using a single workflow and instrument.
- The ability to produce images that co-register small molecule lipids and metabolites as well as the intact targeted proteins.
- The product's combination of fast, targeted, protein imaging (scan time as short as 45 min for a 1cm^2 section), ultra-high plex (10 to 100+), wide viewing area (up to 25 x 75 mm), and multi-modal capability make it an ideal technology for doing initial scans to identify regions of interest for later deep-dive analysis.
- Miralys™ requires no dedicated instrument, and minimal investment to start using. It is used on MALDI Mass Spec Imaging instruments that your institution most likely already owns, such as the industry-leading instruments from our partner, Bruker Corporation.

In our talk we will introduce several new enhancements to our Miralys product line.

Thermo Fisher Scientific **Tuesday October 24, Session 7, 16:10-16:20**

Maciej Bromirski, Sr. Project Manager

MS Imaging meets Orbitrap Technology

Mass spectrometery imaging (MSI) techniques combined with Thermo Scientific Orbitrap detection is very attractive for various life science applications due to the High Resolution Accurate Mass (HRAM) capabilities with ease-of-use of Orbitrap instrumentation. Several ion source techniques, such as MALDI, nanoDESI, SIMS, MALDESI are capable of MS Imaging by their nature - have been coupled to Orbitrap instrumentation.

In this talk we briefly report about Atmospheric Pressure (S)MALDI technique solutions coupled to Orbitrap technology. Perspectives from the 'sample to image' workflow are provided when coupled with MassTech's AP-MALDI UHR source or TransMIT's AP-SMALDI5AF source - both for MSI applications - particularly in metabolomics and lipidomics.

Sun Chrom/ MassTech **Monday October 23, Session 2, 17:10-17:20**

Maureen Feucherolles, Jean R. N. Haler, Tina B. Angerer, William Le, Jérôme Bour, Gilles Frache

Atmospheric Pressure MALDI coupled to Orbitrap(s), principle and applications

The interest in Mass Spectrometry Imaging (MSI) has been growing over the years and increasingly demanding (biomedical) applications are being investigated. Yet, Matrix-Assisted Laser Desorption/Ionization (MALDI) MSI instrumentation need to provide both precise localization, and unambiguous identification for (bio-)molecular ions. The presented experimental set-up takes benefit of the High-Resolution Accurate Mass measurement provided by the Orbitrap technology, combined with Atmospheric-pressure MALDI ionization, allowing for high resolution MSI in both mass and space.

The latest generation Orbitrap Exploris 480 (Thermo Scientific) coupled to a APMALDI UHR ion source (Masstech) has been used to evaluate the improved sensitivity and scan rate over APMALDI coupled to former generation LTQ/Orbitrap Elite set-up.

Several applications will be presented including polymers, peptides test samples and biological tissue sections for imaging. Lipid distributions in biological tissue sections were evaluated. Matrix application was performed using pneumatic sprayer (Sunchrom). Data visualization and interpretation was achieved using Multimaging (Imabiotech) and Lipostar (Molecular Horizon). Several imaging modes are presented with lateral resolutions down to 5 micrometres. Achievable sensitivity, image acquisition speed and potential for both targeted and untargeted MSI methods are discussed.

Masstech APMALDI UHR Orbitrap MSI offers an alternative to dedicated MALDI MS instrumentations. The presented setup allows to add imaging capabilities to existing high-end Orbitrap LC/MS systems, and users can switch from MSI to LCMS configuration within minutes. The improved performances of latest generation Orbitraps as well as improved method development workflows opens new perspectives for a wide range of applications.

SCHIMADZU **Monday October 23, Session 3, 18:50-19:00**

M. Nazim Boutaghou

Shimadzu: One-Stop Shop for Your Imaging Needs

At ASMS 2022, Shimadzu Corporation released its full solution for MALDI-based MS Imaging (MSI). From matrix deposition to data processing, Shimadzu provides high-end equipment to meet your imaging needs. Shimadzu Corporation is the only instrument manufacturer that provides solutions that support all three phases of MSI experiments: Matrix Deposition, Data Acquisition and Image Processing and Analysis.

Our matrix deposition solutions comprise dry and wet deposition. The iMLayer Aero is a robust sprayer that has proven to provide sensitivity and pixel resolution down to 10 um. The iMLayer is our high-end sublimator that will make sub-cellular 5 um imaging routine as it combines laser measurement for matrix deposition thickness. The iMScope QT is our flagship AP-MALDI QTOF instrument specifically designed for MS imaging. It combines an optical microscope for precise scan area determination and an AP-MALDI source with a laser that can fire at a speed up to 20 KHz and offers a class-leading 50 pixels/s acquisition speed. Next to our high-performance MALDI-QTOF is a MALDI-TOF instrument that comes in a compact format (small size) and at a compact price. This entry-level instrument is packed with high-end features and is ideal for any MSI experiment, such as method optimization, image screening, and teaching MALDI and MALDI-based MS Imaging.

Since imaging is not just about beautiful images but rather about meaningful images, Shimadzu released IMAGEREVEAL, a vendor-neutral image processing software that will extract meaningful results out of your gigabyte result files.

P-1

Abbey, John
University of Zurich, Switzerland

Data processing pipeline for highly multiplexed MALDI-imaging data

Introduction:
The development of highly multiplexed proteomic imaging technologies has enabled tissue characterisation of healthy and diseases tissue on a level previously unobtainable. One such technology, MALDI-imaging achieves ultra-high plex targeted staining in conjuction with Photocleavable Mass Tags (PCMTs). The concurrent development of adequate statistical and computational tools is essential to unlock the immense amounts of data that are produced by such technologies. In par ticular, there is a great need for efficient and robust data processing protocols so that high quality data is generated; an essential step before image analysis. This work presents such a data pre-processing and processing pipeline for MALDI-imaging data, as well as quality control statistics to test the quality and reliability of the data.
Method:
The raw data are first pre-processed according to the standard Cardinal pre-processing procedures of TIC normalisation, spectral smoothing and baseline reduction. The pre-processed data then undergo peak detection, where noise is estimated using a robust median adaptive deviation (MAD) peak picking algorithm. From here, a novel method is implemented, involving first clustering detected peaks that correspond to the same molecular species (due to technical mass shift or isotopic peaks), followed by matching of these metapeaks to the expected m/z locations of the peptide mass tags. The pipeline also allows for detection of peaks arise due to adduct ion formation.
Results:
The data processing pipeline enables robust signal quantification for targeted MALDI-imaging experiments. This can be evaluated using spatial and image-level quality control statistics. Spatial QC statistics involve computing Geary's C autocorrelation score, as well as variogram modelling. On the image-level, mean-variance correlation analysis as well as Gaussian mixture modelling (GMM) can be implemented to assess the quality of the generated ion images. Further analysis that is supported by the pipeline includes dimensionality reduction techniques, such as PCA, NMF and UMAP, as well as pixel-clustering methods and community detection algorithms such as Louvain and Leiden clustering.
Novelty:
Peak processing pipeline involving generation of metapeaks to account for signal loss due to mass shift and isotopic peaks.
Preliminary Data:
Ion images, QC plots, clustering methods, dimensionality reduction.
Contributing Authors:
Mengze Zhang

P-2

Amer, Sara
Purdue University, United States

Evaluation of organic dye and porphyrin-based photosensitizers for online singlet oxygen based isomer-resolved mass spectrometry imaging of lipids

Introduction:
Coupling of nanospray desorption electrospray ionization (nano-DESI) and singlet oxygen (SO) reaction has proven valuable in the field of isomer-resolved mass spectrometry imaging (iMSI). In the presence of a photosensitizer, lipids are converted online to lipid hydroperoxides (LOOHs). Upon CID, unique fragments are produced that pinpoint the location of C=C bonds within the structure in real-time. Previous work by our group used different PSs for positive and negative ionization mode to reduce spectral interferences. Efforts have been made to discover a singular compound that will allow for LOOH formation and identification in both analysis modes. Herein, we evaluate the applicability of several porphyrins as potential candidates for a universal photosensitizer.

Method:
Frozen 12 µm-thick sections of wild type (WT) mice brain tissues were used for the analysis. Nano-DESI MSI experiments were performed on a Q-Exactive HF-X mass spectrometer. The working solvent composed of methanol:H2O in a 9:1 ratio was spiked with several internal standards of different lipid classes, including d8-arachidonic acid, LPE 17:1, LPG 17:1, LPS 17:1 and LPI 17:1, and 20 uM of the selected photosensitizer- tetraphenylporphyrin (H2TPP), zinc tetrephenylporphyrin (ZnTPP), or tetrakis 4-carboxyphenyl porphyrin (TCPP). SO was generated by focusing a violet laser (405 nm) on the nanospray capillary. MS/MS imaging experiments were performed for a targeted list of unsaturated lipids from different lipid classes.

Results:
In this study, we explore several porphyrins as candidates for the universal PS for lipid isomer identification in both positive and negative ionization modes. While each of the porphyrins studied has a high quantum yield ($\Phi>0.6$), they ionize differently. For example, ZnTPP was deemed a poor candidate because it ionizes well in positive mode and upon laser irradiation is photoactive and increases in ionization, overtaking the mass spectrum. In contrast, H2TPP and TCPP ionize poorly in both positive and negative modes. For these porphyrins, ionization in positive mode further decreases during tissue analysis, posing no interference. Reaction between SO and C=C bonds in unsaturated lipids generates LOOH species. CID of LOOH in the gas phase generates diagnostic fragment ions indicative of the C=C location in the unsaturated lipid. Lipid extracts undergoing SO conversion show a prominent conversion of PCs and PEs in positive mode. In addition, free fatty acids, as sodium adducts, have also shown to convert to their respective LOOH. For example, FA 16:1;O2 was identified in positive mode at m/z 309.2036 and upon CID produced fragments at m/z 179.0679 and 235.1305, indicative of Δ7 and Δ11 isomers, respectively. Upon nano-DESI line scans of sample tissue, only the Δ7 isomer is identified indicating that these isomers may have spatial significance. In negative mode, a plethora of mono- and polyunsaturated lipids belonging to classes of PAs, PSs, PEs, PIs, and PGs were converted to their respective LOOH and isomeric positions were identified. The advantage of negative mode analysis is the identification of the LOOH acyl chains upon CID due to their neutral losses. For the LOOH of PG 34:1 (m/z 779.4749), it can be confirmed that the acyl composition is 16:0/18:1 due to the loss of the 18:1 hydroperoxide acyl chain.

Novelty:
Online singlet oxygen-based nano-DESI is achieved in both positive and negative ionization mode for positional isomers of multiple lipid classes.

Preliminary Data:
Performance of different photosensitizers for singlet oxygen reaction-based isomer-resolved nano-DESI analysis of lipids.

Contributing Authors:
Sara Amer; Manxi Yang; Miranda Weigand; Emerson Hernly; Daisy M Unsihuay Vila; Mushfeqa Iqfath; Julia Laskin

P-3

Anderson, David
Vanderbilt University, USA

Imaging Technologies for Constructing 3D Multimodal Lipid Atlases of the Human Eye

Introduction:
The human ocular globe has evolved to handle remarkably complex visual tasks. It subserves vision at light levels ranging from starlight to sunlight, and its supporting tissues and vasculature regulate plasma-delivered lipophilic essentials for vision. While the anterior portion of the globe is responsible for focusing light onto the neural retina, there are multiple cell types and anatomical regions responsible for achieving this effectively. The neural retina is comprised of many specialized cell types, including five types of neurons: photoreceptors, bipolar cells, ganglion cells, horizontal cells, and amacrine cells that are responsible for photon absorption, signal transduction, and signal transmission via the optic nerve to the visual cortex of the brain. The optic nerve head is the point at which all the ganglion cell fibers leading from the neural retina coalesce to traverse the sclera into the optic nerve towards the visual centers of the brain. During this transition the axonal bundles change from unmyelinated to myelinated fibers as they pass through the lamina cribrosa. To map the distribution of lipids present in these cells in three dimensions using MALDI IMS and microscopy, methods have been extensively developed. As data reconstruction for 3D experiments is critical for high quality registration and volume reconstruction of high yield of quality sections throughout these regions, the methods employed for this analysis were essential for generating 3D atlases

Method:
A whole human ocular globe was fresh frozen on liquid nitrogen vapor in 15% fish gelatin. The globe was then dissected into anterior and posterior portions. The posterior region was trimmed up to the point of the optic nerve where 63 serial sections (7 lost sections) at 10 µm thickness were cut and thaw mounted onto ITO coated slides. Sections from the anterior segment and fovea were gathered separately. Autofluorescence (AF) microscopy images were acquired prior to IMS analysis. 2,5-Dihydroxyacetophenone (2,5-DHA) and 4-Dimethylaminocinnamaldehyde (DMACA) using was applied using a in house designed custom sublimation device. Data were acquired at 5-10 µm pixel size in positive and negative ion mode.. Data were acquired using a Bruker timsTOF Flex in QTOF mode. All 3-D image reconstruction and analysis were performed using in-house tools.

Results:
Data acquired with a 10 micron pixel size from 63 serial sections collected spans 700 µm of the optic nerve head from a 31-year-old donor. Each 2-D tissue image is comprised of ~200,000 pixels totaling approximately 12.6 million pixels and 2.7TB of data for all 63 sections. Data show lipids have specific localizations to several anatomical features, including the localization of specific lipids include the myelinated axons (m/z 760.56) as they proceed towards the laminar cribosa before becoming unmyelinated depicted by m/z 781.62 and 820.52 observed at the lamina cribrosa. Spatial localizations from signals corresponding to the varying cell types of the inner and outer retina, such as the ganglion cells (m/z 766.57) and the photoreceptors (m/z 828.55) were also observed throughout the tissue adjacent to the optic nerve head. Once overlaid, the fully constructed 3-D molecular image enables the visualization of various lipids to highlight the specific substructures in the optic nerve head and surrounding neural retina and how they vary throughout this important region of the ocular globe. Data obtained from anterior segment sections with a 5-micron pixels size starts to reveal subtleties of lipid distributions at the cellular level in the pigmented and non-pigmented cells of the ciliary processes along with the endothelial and epithelial layers on the exterior and interior of the cornea. Notably, data from the neural retina show localizations to the subcellular level of the photoreceptors and the single-cell layer of the RPE. Dissecting the fresh frozen ocular globe into anatomically relevant smaller regions provides high-quality sections with preserved morphology and improved section-to-section reproducibility. Mapping and visualization of molecular distributions in 3-D space by means of IMS provides atlases with remarkable chemical specificity. The availability of such detailed spatio-chemical information allows for new biomedical and multidisciplinary questions to be addressed, across the range of anatomical features necessary for healthy vision.

Novelty:
A novel pipeline for 3-D biomolecular multimodal tissue imaging enables the construction of high-resolution lipid images of human eye.

Preliminary Data:
3D MALDI IMS combined with microscopy elucidates the molecular composition of discrete retina layers at a cellular and subcellar level.

Contributing Authors:

Posters

Jeffrey D. Messinger, Dongfeng Cao N, Madeline Colley, Ellie L Pingry, Heath Patterson, Ankita Kotnala, Lukasz Migas, Raf Van de Plas, Richard M. Caprioli, Christine A. Curcio, Kevin L. Schey, and Jeffrey M. Spraggins

P-4

Anderton, Christopher
Pacific Northwest National Laboratory, United States

Molecular cartography of human organs: recent advances in multimodal imaging and omics approaches to map the molecular universe of tissues

Introduction:
There is an increased emphasis on creating molecular atlases of human organs, due in part, to the idea that these maps can help realize the potential of precision medicine by revealing critical cells, pathways, and targets for novel therapies for disease. Our team is part of a number of consortia aiming to map the human kidney and human lung. Here, we have developed and optimized a number of matrix-assisted laser desorption/ionization mass spectrometry imaging (MALDI-MSI)-based spatial metabolomics, lipidomics, and N-glycomics assays that we use in concert with clinically common imaging methods, MS-based bulk omics methods, and other spatially resolved and single cell omics and imaging-based assays employed by our collaborators within these consortia.
Method:
Fresh frozen and formalin-fixed paraffin-embedded (FFPE) tissues were used for MALDI-MSI-based spatial omics assays. Kidney biopsy and nephrectomy samples were obtained from the University of Michigan and tissue recruitment sites. Human lung tissue was obtained from the University of Rochester LungMAP Biorepository for Investigation of the Lung (BRINDL). Sectioning, matrix application (HTX M5-Sprayer), and high mass resolution MALDI-MSI analysis was performed (Bruker FTICR-MS) on tissue sections. For spatial N-glycomics, peptide-N-glycosidase F (PNGase F) was applied with the TM-Sprayer (HTX technologies). All imaging data was converted to imzML and uploaded to METASPACE for putative annotations. Metabolomics and lipidomics annotations were confirmed via LC-MS/MS analysis. Autofluorescence- and histochemical-based microscopy was performed to correlate kidney and lung tissue features to the MSI data.
Results:
As part of these efforts, we have created best practices for tissue handling, developed quality control and quality assurance metrics, and established metabolite, lipid, and N-glycan markers for different compartments within the human kidney and lung. Of note, we recently developed and optimized methods for inflation, embedding, and multi-omic and MALDI-MSI analysis of human lung tissue (Lukowski et al., Front. Mol. Biosci. 2022). Two of our more major advancements with MALDI-MSI permitted us to explore N-glycosylation changes within human kidney and lung cells and tissue functional units during disease progression. Specifically, these advancements were: (1) the creation of a N-glycan database (NGlycDB), which can be utilized by researchers worldwide for annotating and visualizing N-glycan mass spectrometry imaging results across all sample types in METASPACE (Veličković et al., Anal. Chem. 2021), and (2) the ability to control the relative humidity during enzymatic retrieval, which minimizes N-glycan delocalization across the tissue (Veličković et al., JASMS 2022). As part of the Kidney Precision Medicine Project (KPMP), we have analyzed over 550 human kidney sections from 56 biopsy samples acquired from different patients to date. By correlating MALDI-MSI data generated from our tissue interrogation site (TIS) with regional proteomics and single-cell RNA sequencing data of tissue generated at other KPMP TISs from the same patient, we were able to validate metabolite, lipid, and N-glycan markers for podocytes. Within the LungMAP and The Human BioMolecular Atlas Program (HuBMAP) consortia, our team has imaged tissue from healthy lung and those with bronchopulmonary dysplasia (BPD). We found that specific lipids and proteins localize to structures including, for example, bronchioles and submucosal glands. Our MALDI-MSI findings correlate closely with those of multimodal microscopy combining high lateral resolution stimulated Raman scattering, second harmonic generation, and two-photon fluorescence.
Novelty:
Multimodal analyses coordinately identify key molecular species and compositional changes within distinct functional features of the human kidney and lung.
Preliminary Data:
Coordinated MALDI-MSI-based assays permit mapping of a broad range of biomolecules in human kidney and lung tissue.

Contributing Authors:
Dušan Veličković1, Brittney Gorman1, Kisurb Choe1, Geremy Clair1, Joshua N. Adkins1, Zhi Li2, Lingyan Shi2, Ravi Misra3, Gloria Pryhuber3, Theodore Alexandrov4, Kumar Sharma5,6 1Pacific Northwest National Laboratory, Richland, WA, USA; 2University of California San Diego, San Diego, CA; 3Department of Pediatrics, University of Rochester Medical Center, Rochester, NY, USA; 4Structural and Computational Biology Unit, European Molecular Biology Laboratory, Heidelberg, Germany; 5Center for Renal Precision Medicine, Division of Nephrology, Department of Medicine, The University of Texas Health San Antonio, TX, USA; and 6Audie L. Murphy Memorial VA Hospital, South Texas Veterans Health Care System, San Antonio, TX, USA

P-5

Baquer, Gerard
Department of Neurosurgery, Brigham and Women's Hospital, Harvard Medical School, Boston, MA, USA, USA

Enhancing Metabolome Coverage through Matrix Annotation using Stable-Isotope-Labeled MALDI Mass Spectrometry Imaging

Introduction:
Matrix-assisted laser desorption ionization mass spectrometry imaging (MALDI-MSI) enables the spatial resolution of metabolites on tissue. However, the matrix introduces spectral interferences that hamper data processing and narrow metabolome coverage. In this study, we demonstrate the use of isotopic labeling to discover and annotate matrix adducts in MALDI-MSI. Our approach enables the removal of matrix signals, facilitating the interpretation of tissue morphology, improving metabolite annotation confidence, and extending metabolome coverage.

Method:
Starting from 13C6 labeled salicylic acid 13C6-DHB was synthesized in 2 steps: (1) selective electrophilic bromination of the 5th position with N-bromosuccinimide in acid media and, (2) Cu-mediated Ullmann-type hydroxylation. For matrix annotation 4 consecutive sections (10µm) were prepared (2x DHB and 2x 13C6-DHB). For validation, 20 sections were prepared with different matrices (DHB, Au, 9AA, NEDC, and Norharmane). MALDI-FTICR-MSI was performed on a 12T solariX with a CombiSource (m/z range 100-1000 Th, 100 µm step-size). All samples were registered into the same coordinate space to enable spatial correlation of analytes across samples. Matrix signal annotation was performed with rMSIcleanup by exploiting (1) the labeling-induced m/z shift, and (2) the preserved spatial distribution.

Results:
We propose a SIL-MALDI-MSI workflow to enhance untargeted metabolomics. By synthesizing 13C6-DHB and exploiting their known m/z shift and preserved spatial distribution we can annotate all matrix signals. To ensure confident annotation we introduce a novel FDR estimation paradigm based on decoy matrices and m/z shifts. Using this approach, we show that matrix signals represent 17.7% of all ions (SNR>5) of which 90% (16% of all ions) correspond to analyte-matrix adducts. We demonstrate that matrix signals negatively affect MALDI-MSI untargeted metabolomics. By removing these signals, dimensionality reduction algorithms like UMAP can better emphasize biologically and anatomically relevant structures. Additionally, excluding matrix signals improves the annotation of small molecules using automated tools like METASPACE. This removal results in a higher number of annotations with increased confidence (lower FDR). Furthermore, we annotate the analyte-matrix adducts against HMDB, significantly expanding metabolite coverage. In conclusion, by using SIL matrices and a specialized computational method we liberate MALDI-MSI from the challenges associated with matrix signals, and ultimately enhance confidence and coverage in untargeted metabolite annotation.

Novelty:
Annotation of matrix signals through SIL-MALDI-MSI enhances metabolite annotation and coverage.

Preliminary Data:
Complete manuscript preprint: https://doi.org/10.1101/2023.06.28.546946 . Data availability: https://doi.org/10.17632/ms3365kb5p.1.

Contributing Authors:
Gerard Baquer 1,#,*,^, Miguel Bernús 2,#, Lluc Sementé 1, René van Zeijl 3, Maria García-Altares 1,*, Bram Heijs 3,4, Omar Boutureira 2, Xavier Correig 1,5,6, Pere Ràfols 1,5,6 1 Department of Electronic Engineering, University Rovira i Virgili, Tarragona, Spain 2 Department of Analytical Chemistry and Organic Chemistry, Universitat Rovira i Virgili, Tarragona, Spain. 3 Center of Proteomics and Metabolomics, Leiden University Medical Center, Leiden, the Netherlands 4 The Novo Nordisk Foundation Center for Stem Cell Medicine (reNEW), Leiden University Medical Center, the Netherlands 5 Spanish Biomedical Research Center in Diabetes and Associated Metabolic Disorders (CIBERDEM), Madrid, Spain 6 Institut D'Investigacio Sanitaria Pere Virgili (IISPV), Tarragona, Spain # These authors contributed equally to this work ^ Current Address: Department of Neurosurgery, Brigham and Women's Hospital, Harvard Medical School, Boston, MA, USA. *Correspondence: Gerard Baquer, Department of Electronic Engineering, University Rovira i Virgili, Tarragona, Spain. Email: gerard.baquer@alumni.urv.cat Maria García-Altares, Department of Electronic Engineering, University Rovira i Virgili, Tarragona, Spain. Email: maria.garcia-altares@urv.cat

P-6

Bednařík, Antonín
Faculty of Science, Masaryk University, Brno, Czech Republic, Czech Republic

Metal Oxide Laser Ionization MS Imaging of Fatty Acids and their Double Bond Positional Isomers

Introduction:
In metal oxide laser ionization mass spectrometry (MOLI MS), metal oxides assist the generation of ions as an inorganic matrix. Many metal oxides, for example CeO2, have catalytic properties and can efficiently cleave ester bonds of mono-, di-, triacylglycerides, and phospholipids producing free fatty acid (FA) ions under UV laser irradiation. This can be efficiently used for mapping the distribution of FAs in MOLI MS imaging. In this work, we have coupled MOLI MS imaging with on-tissue reaction of unsaturated FAs with ozone to estimate content of FA isomers in tissue.
Method:
MOLI MS and MS imaging experiments were realized with CeO2 nanopowder using vacuum time-of-flight (TOF) mass spectrometer in negative mode. Metal oxide methanol suspensions (10 mg.ml-1) were sprayed onto the samples by airbrush pistol with 0.15 mm needle positioned 9 cm above the sample. After covering sample with metal oxide layer, first MS image was recorded followed by on-tissue derivatization of unsaturated lipids with ozone. Samples were exposed to high-concentration ozone atmosphere (7 g of O3 per hour) for 2 min. Excess O3 in the exhaust gas was quenched by an iodine/thiosulphate solution. After derivatization, second MOLI MS imaging was carried from the same tissue section.
Results:
First, the standards of FA 18:1 (Δ9) and FA 18:1 (Δ11) were analyzed using CeO2 prior and after reaction with ozone. Signal at m/z 281.3 completely disappeared after the reaction and four intense peaks corresponding to aldehyde (A) and carboxyl (C) fragments of ozonides from carboxyl end (α-end) and methyl end (ω-end) of the FA emerged. FA 18:1 (Δ9) provided peak at m/z 157.1 attributed to carboxyl fragment ion [M-H]- originating from the methyl end (Cω) and peaks at m/z 171.1 (Aα) and 187.1 (Cα) from the carboxyl end. The fourth peak at m/z 143.1 is likely a result of CO2 neutral loss from Cα ion at m/z 187.1. The same fragmentation pattern was observed also for FA 18:1 (Δ11) with Cω, Cα – CO2, Aα and Cα [M-H]- ions at m/z 129.1, 171.1, 199.1 and 215.1, respectively. To evaluate relative abundance of FA 18:1 (Δ9) and (Δ11) isomers in the sample, ratio of Aα (Δ11)/Cω (Δ9) fragments 199.1/157.1 was chosen, as it provided linear response. MOLI MS images of mouse brain and human colorectal carcinoma tissues recorded prior and after reaction with ozone revealed sharp distribution of major FAs (FA 16:0, FA 18:0, FA 18:1, FA 20:1 and FA 20:4). Unsaturated FA signals were strongly dominated by FA 18:1 and the signal of species which would provide the fragments at the same m/z values was negligible. The content of FA 18:1 (Δ11) 20±3%, 18±3% and 13±2% was estimated in the molecular layer of cerebellum, cortex gray matter and white matter, respectively. In colorectal carcinoma tissue, tumor showed increased abundance of monousaturated FA 18:1 and FA 20:1 and relative low signals of polyunsaturated FAs. The content of FA 18:1 (Δ11) isomer was estimated to 4.3±1.1% and 3.3±1.1% in tumor and healthy tissues.
Novelty:
MOLI MS imaging method using CeO2 for mapping of FAs pool down to isomer level in biological samples.
Preliminary Data:
MOLI MS images of FAs in mouse brain and human colorectal carcinoma tissues.
Contributing Authors:
Monika Koktavá, Jan Valášek, Dominika Bezdeková, Vadym Prysiazhnyi, Barbora Adamová, Petr Beneš, Jarmila Navrátilová, Michal Hendrych, Petr Vlček, Jan Preisler

P-7

Bergamin de Castro, Tialfi
Department of Microbial Pathogenesis, University of Maryland, School of Dentistry, United States

N-glycan signature of activated neutrophil region of S. aureus skin infection mouse models

Introduction:
Staphylococcus aureus, the primary cause of skin infections, has emerged as a significant public health concern due to the rise of antibiotic-resistant strains. In humans, the inhibition of tumor necrosis factor (TNF) has been associated with an elevated risk of S. aureus infections. Neutrophils (PMNs) are the primary cells expressing the TNF receptors TNFR1 and TNFR2 and activate the immune system. TNFR1, including PAD4+/+ (peptidylarginine-deiminase-4) induces the synthesis of NETs (neutrophil extracellular traps) which is related to host defense. Biologic and structural alterations in the cell membrane, like N-glycans and PAD4-/-, have been related to increased skin infections. The aim of this study is to compare the N-glycans signature in PMN regions between WT, TNFR1, TNFR2 and PAD4+/+ groups using MALDI-MSI.
Method:
An in vivo mouse model skin infection was used whereby activated TNFR1, TNFR2 deficient, PAD4 deficient, and wildtype (WT) mice were intradermally injected with S. aureus. The slides were dewaxed and rehydrated prior to antigen retrieval using citraconic buffer and heated for 30 minutes. After cooling and drying in desiccator, 0.1µg/µl of PNGaseF was applied and the slides were incubated in a humid chamber for 16 hours. A solution of 7mg/mL of CHCA (50% ACN/0.1% TFA) was sprayed using a HTX M5. The MSI was performed in positive mode in a timsTOF Flex with 50µm of spatial resolution. SCiLS software was used to analyze the MSI data and perform the ROC test. An AUC ≥ 0.700 was considered significant.
Results:
We used METASPACE database to identify 71 N-glycans. Analyzing the PMN region between the groups, we found a higher intensity in 933.317m/z (Hex:3 HexNAc:2), 1298.4492m/z (Hex:4 HexNAc:3), 1664.5682m/z (Hex:4 HexNAc:4 Pent:1 Me:1) and 1810.6261m/z (Hex:4 HexNAc:4 dHex:1 Pent:1 Me:1) in WT comparing to TNFR2. There was no difference between the WT and TNFR1. However, PAD4 had two specific N-glycans in higher intensity than WT, TNFR1 and TNFR2 groups, 1679.5553m/z (Hex:5 HexNAc:4) and 1825.6132m/z (Hex:5 HexNAc:4 dHex:1). The opposite was observed for 933.317m/z (Hex:3 HexNAc:2), 1136.3963m/z (Hex:3 HexNAc:3) and 1298.4492m/z (Hex:3 HexNAc:3) which were more intense in TNFR1 than in PAD4. Besides that, the comparison between TNFR1 and the knockout TNFR2 showed higher intensity of 933.317m/z (Hex:3 HexNAc:2), 1136.3963m/z (Hex:3 HexNAc:3), 1298.4492m/z (Hex:4 HexNAc:3) and 1664.5682m/z (Hex:4 HexNAc:4 Pent:1 Me:1) in TNFR1. Our preliminary conclusion is that the knockout TNFR2 has lower diversity of N-glycans expressed than the WT, which leads to a non-protective factor against S. aureus and, even with no significant difference between TNFR1 and the WT, specific N-glycans are related to TNFR1 and PAD4, showing a specific signature linked to NETs synthesis during the infection and a protective factor.
Novelty:
We identified differential N-glycan signatures of the functional aspects (NET formation, migration) of neutrophils responding to S. aureus infection.
Preliminary Data:
We found specific N-glycans in higher intensity comparing the knockout groups, which can be related to S. aureus -specific neutrophil functions.
Contributing Authors:
Tialfi B. de Castro; Abena Ntiamoah; Christine Youn; Meng-Jen Wu; Nathan K. Archer; Alison Scott

P-8

Birsan, Alex
Waters Limited, Canada

MSI Quantify: A micro-app for the automated processing of quantitative mass spectrometry imaging data

Introduction:
Mass spectrometry imaging (MSI) is a rapidly-developing molecular-imaging modality that maps the spatial distribution of thousands of analytes across a sample. Absolute quantification is a challenge in the analysis of complex mixtures with MSI, due to ionization-efficiency variations, matrix effects, and the lack of appropriate standards. Typical quantitative experiments use a dilution series of tissue spotted with known concentrations of the compound of interest. A calibration curve is then constructed from these regions, mapping the signal intensity of the mass of interest to the concentration of the drug. A new micro-app called MSI Quantify is presented which uses unsupervised machine learning to assist in the data-processing workflow associated with these experiments, including automated dilution-region detection and model fitting.

Method:
MSI Quantify is a web application with a user-friendly graphical user interface (GUI). The application and GUI were both written in Python using Streamlit, an open-source framework for building web applications with Python. Python was chosen due to its clean syntax, object-oriented structure, and integration with third-party numerical and statistical packages that enable common processing tasks in MSI. MSI Quantify currently accepts input from the MassLynx RAW file-format, as well as pre-processed and peak-picked data in a custom text-based format.

Results:
MSI Quantify provides the user a number of useful tools for quantitative MSI data analysis. The app first allows for custom image display of a given mass of interest for visualization of the dilution spot series. These regions can be manually annotated and segmented using common shapes (circles, ellipses, etc.). The regions can also be automatically detected using a custom image-segmentation routine that projects the mass data into a lower-dimensional subspace using manifold learning, followed by density-based clustering of the pixels into groups with similar spectral profiles. This typically results in the calibration spots being grouped as a single cluster – once that cluster is identified, the spots are then individually labeled. Alternatively, the app provides a semi-supervised approach, where the user clicks a pixel inside and outside of each spot and the app clusters all pixels within a given radius into two groups based on similarities with the two selected pixels. These automated approaches select tighter, more accurate edges around the spots, which improves the accuracy of the data used for construction of the calibration curve. Once the user inputs the concentration for each spot (or the absolute quantity of the compound if the pixel area and thickness are provided), the target mass spectrum is summed across each region (with the option to normalize using the total ion current or the spectrum associated with a standard), and this value is fit to a linear, exponential, logarithmic or power-law model to construct the calibration curve. After the calibration curve is constructed, it is used to predict the concentration of the compound in a separate region or dataset. Note that MSI Quantify can also accept tissue segmentation maps output from the Waters MSI Segmentation microapp to predict the concentrations of the target compound across automatically identified tissue regions of interest.

Novelty:
A new application was developed that allows for rapid processing of quantitative MSI data with automated region selection routines.

Preliminary Data:
A new micro-app called MSI Quantify is presented which uses unsupervised machine learning to assist in the data-processing workflow

Contributing Authors:
Scott Trinkle, Emmanuelle Claude, Alex Birsan, Emrys Jones, Mark Towers, Richard Chapman

P-9

Bollwein, Christine
Institute of Pathology, Technical University of Munich, Germany

Proteomic and N-Glycan in-situ Characterization of Small Blue Round Cell Tumors

Introduction:
Morphological characterization of small blue round-cell tumors (ewing sarcoma, rhabdomyosarcoma, neuroendocrine carcinoma, acute lymphoblastic leukemia, nephroblastoma, neuroblastoma) is challenging, and routine immunohistochemistry (IHC) is often insufficient to define the tumor. Glycosyltransferases enzymatic activity and gene expression are altered in various pathophysiological situations, namely in tumor development. In this study, we have characterized the protein/ peptide and N-Glycan content of the tumors utilizing matrix-assisted laser desorption/ionization (MALDI) mass spectrometry imaging (MSI) to better comprehend the molecular signatures of each tumor subtype.
Method:
Samples from small blue round-cell tumors (SBRCT, n = 26) were assembled in a tissue microarray: ewing sarcoma (EWS, n = 5), rhabdomyosarcoma (RMS, n = 5), neuroendocrine carcinoma (NEC, n = 5), acute lymphoblastic leukemia (ALL, n = 5), nephroblastoma (NEPB, n = 3), and neuroblastoma (NEUB n = 3). The specimens were subjected to on-tissue enzymatic digestion, utilizing N-glycosidase F and trypsin, followed by matrix application (α-cyano-4-hydroxycinnamic acid). Samples were analyzed utilizing MALDI-TOF mass spectrometry. Subsequently, the matrix was removed, the section was stained by hematoxylin and eosin for histopathological annotation. Data analysis was performed using SCiLS Lab (Bruker) and statistical analysis was performed on R.
Results:
MSI data was employed for the training and validation of classification algorithms . Random forest classification yielded over 96% accuracy. From the analysis of feature extraction, it was possible to establish correlation between some molecular features and tumor subtypes (Hex4dHex1HexNAc5, could be associated with NEPB, while Hex3dHex1HexNAc5 is overexpressed in NEPB and NEUPB). From the receiver operating characteristic – area under the curve analysis (ROC-AUC) analysis we found that Hex5HexNAc4 was a discriminating feature between EWS and RMS; and Hex4dHex1HexNAc5 and Hex3dHex1HexNAc6, were found to be differently expressed between NEPB and NEUB subtypes. In this study, we show that N-Glycan imaging is an auspicious methodology to assist in the stratification of different small blue round-cell tumors.
Novelty:
Mass spectrometry imaging is a robust tool to assist in the definition of SBRCT using molecular features.
Preliminary Data:
Peptides and N-Glycans, such as Hex4dHex1HexNAc5 and Hex3dHex1HexNAc5, could be associated with different SBRCT subtypes.
Contributing Authors:
Christine Bollwein1, Juliana P. L. Gonçalves1, Wilko Weichert1,2, Kristina Schwamborn1,* 1. Institute of Pathology, School of Medicine, Technical University of Munich, Trogerstraße 18, 81675 Munich, Germany 2. German Cancer Consortium (DKTK), Partner Site Munich, 80336 Munich, Germany

P-10

Bottomley, Heather
University of Exeter, United Kingdom

Improved detection of tryptic peptides from tissue sections using Desorption electrospray ionisation mass spectrometry imaging (DESI-MSI).

Introduction:
DESI-MSI is an ambient ionisation technique used frequently for the detection of lipids, small molecules, and drug targets. Previously, DESI had only limited use for the detection of proteins and peptides in tissue, due to the setup and needs around deconvolution of data resulting in a small number of species being detected at lower spatial resolution. We know that there are differences in the ions detected using DESI and matrix-assisted laser desorption/ionization (MALDI) for other molecules, so we sought to identify whether this extends to proteomic species. Here, we present the use of DESI for the detection of large numbers of tryptic peptides from mouse and rat brain tissue sections, with enhanced spatial resolution when compared to previous DESI-MSI studies.

Method:
The images were obtained with DESI using a Waters pre-commercial heated inlet (approx. 450°C) to the mass spectrometer (Waters, Synapt G2-si). Further, ion mobility separation was applied in a traveling wave ion guide with nitrogen gas to resolve spectral overlap of peptide ions and improve the detection of multiply charged species. Other DESI optimisation included the sprayer nozzle position and respective source geometries. The images acquired had a resolution of 100 µm for the rat brain sections and 50 µm for the mouse brain sections. The tryptic peptides observed were filtered against LC-MS generated (Thermo Exploris 240) proteomic target lists for consecutive sections of both the mouse and rat brain sections, allowing tentative protein assignment for each peptide ion image.

Results:
Tryptic peptides were detected with DESI at precise locations in the mouse and rat brain tissue sections. These peptides were assigned protein IDs using a proteomic target list, generated from LC-MS of homogenised tissue. This allows for further interpretation of peptide function, which is of great importance when considering possible application areas of the method (e.g. biomarker discovery/monitoring). Large numbers of peptides and corresponding proteins were detected for both tissues using DESI. There was an increase in the number of detected peptide ions when comparing DESI to MALDI. The corresponding number of proteins tentatively assigned were similar for DESI and MALDI, due to the detection of both singly and multiply charged peptide ions for the same protein by DESI. However, DESI showed a small increase in identified proteins. Therefore, the benefit of using DESI to find a greater number of tryptic peptide ions has been demonstrated, due to the improved detection of multiply charged species. Those peptides detected through DESI that showed precise localisation were compared to the same peptides found using matrix-assisted laser desorption/ionization (MALDI). This indicates that DESI could corroborate those tryptic peptides found in MALDI or could be used as an alternative to MALDI where needed. Some spatially localised peptides ions were observed in DESI that were not found in the MALDI replicates; these were typically multiply charged peptides with a low mass to charge ratio. Further investigation is required to fully understand how many more proteins this allows to be identified, or how much these additional ions bolster protein ID from MS imaging experiments. To allow this comparison, MALDI acquisition was conducted using consecutive tissue sections and the same conditions as for DESI (with the obvious addition of a chemical matrix for ionisation).

Novelty:
Enhanced detection of many tryptic peptides acquired using DESI-MS imaging, with the addition of proteomic target list confirmation.

Preliminary Data:
The benefit of using DESI-MSI to find a greater number of localised tryptic peptide ions has been demonstrated.

Contributing Authors:
Heather Bottomley, Dr Jonathan Phillips, Dr Philippa Hart

P-11

Brown, Dalton
Johns Hopkins AIMS Core, United States of America

Statistical Heterospectroscopy of MALDI Imaging and NMR Spectroscopy Data for Evaluation of Breast Tumor Models

Introduction:
Matrix Assisted Laser Desorption/Ionization Time of Flight (MALDI-TOF) Mass Spectrometry Imaging (MSI) generates extensive peak lists with spatial encoding, yet identifying analytes by tandem mass spectrometry (MS/MS) is time-consuming. Proton High Resolution Nuclear Magnetic Resonance (1H-HR-NMR) spectroscopy conversely provides analyte identification and quantitative information, but no spatial information. Both of these technologies are powerful in their own right. Combining these two complementary approaches will significantly enhance our knowledge gained. Further, the combination of these two modalities is potentially quite powerful in the identification of pathways which are not easily detected in both modalities. Here we have developed Statistical Heterospectroscopy (SHY) of 1H-HR-NMR and MALDI-TOF MSI, supplementing the lack of spatial resolution of H1-HR-NMR with spatially resolved MALDI imaging data while adding 1H-HR-NMR based analyte identification.
Method:
Standards as detailed below were prepared in 50% ACN with 0.1% TFA and spotted on an MTP 384 target plate. Spectra were collected on a Bruker RapifleX MALDI TOF/TOF instrument in reflectron positive ion mode with 300 shots per pixel and a 20 µm laser for m/z 40-1000 Da. Similar solutions were prepared in deuterated water for NMR experiments. Proton spectra were collected with a 5-mm TXI probe on a Bruker Avance-III 750 MHz NMR spectrometer with 8 scans. MDA-MB-231 and SUM159 cells were also grown under standard conditions and separated for dual phase extraction or to be spun down to a cell pellet which was made into a block with M-1 embedding matrix and cryosectioned at 10um thickness. MDA-MB-231 and SUM159 tumor xenografts were produced in athymic nude mice and cryosectioned at 10um thickness. Interleafed sections were collected for dual phase extraction. Spectra were binned in Topspin for NMR data. MALDI imaging spectra was exported from FlexImaging and background subtracted in mMass. Both spectra were exported as .txt files. These .txt files were imported into MATLAB where water peak subtraction was performed and negative values were set to zero. NMR spectra were fit to a cubic spline with resolution 0.001ppm while MS spectra was binned in histograms with 1Da width. Datasets were unit sum normalized before calculating the Pearson correlation coefficients for each paired m/z and ppm. These coefficients were then plotted to a contour plot for visualization.
Results:
SHY has previously been reported for UHPLC data correlated with NMR data, however, no code has been published to allow others to use this method. We have built a MATLAB based software which allows for the correlation of the spectral domain of MALDI imaging data with NMR spectroscopy data. To test our new software, we have acquired NMR, MALDI target plate, and MALDI imaging data from a set of standards, including glutamine, glutamate, phenylalanine, taurine, and a 1:1:1:1 mixture of all four components. These standards were measured by both 1H-HR-NMR and on a MALDI target plate. Spectra were binned to the same size using 32768 data points and imported into MATLAB for analysis. We are currently testing the homebuilt software with these data sets. We have also grown SUM159 and MDA-MB-231 cells and harvested tumor xenografts from athymic nude mice. We have chosen these two tumor models as they are well studied models of triple negative breast cancer. Currently, triple negative breast cancer has no targeted treatment options and has the highest rate of mortality in breast cancer patients. These tumors have been cryosectioned for MALDI imaging with interleafed samples taken for dual phase extraction for NMR spectrometry. We have begun measuring these tumors using both modalities. For MALDI imaging experiments, we are measuring tumor sections using negative ion mode from m/z 0-500 Da to detect metabolites including lactate, taurine, and amino acids, among others. We are using positive ion mode from m/z 400-1000 Da to measure phospholipids. For NMR spectroscopy, we are measuring both the aqueous phase containing water-soluble metabolites and the organic phase containing phospholipids. We will bin and correlate these data in our new software to investigate the similarities and differences in both small molecules and lipids in our two triple negative breast cancer tumor models.
Novelty:
First application of Statistical Heterospectroscopy (SHY) on MALDI target plate/imaging data with NMR spectroscopy data.
Preliminary Data:
Contributing Authors:
Dalton Brown, Zuriel Erikson Joven, Natalie Dillman, Ethan Yang, Cole Johnson, Sofia Nackuchima, Kristine Glunde, and Caitlin Tressler

P-12

Castellani, Maria Elena
University of Oxford, United Kingdom

Development of a High Throughput Microscope Mode Secondary Ion Imaging Mass Spectrometer

Introduction:
Secondary Ion Mass Spectrometry (SIMS) is a surface-analysis mass-spectrometric technique in which a primary ion beam irradiates a solid sample, hence releasing secondary ions that are then collected by a mass analyser. SIMS is one of the key ionisation techniques in Mass Spectrometry Imaging (MSI), in which a primary ion beam is used to visualize the spatial distribution of the sample, thus considerably expanding the analytical sensitivity of conventional mass spectrometry. By coupling a defocussed primary ion beam with stigmatic ion optics and a position-sensitive detector, SIMS imaging can be performed in microscope mode. In this work, we combined a pulsed ion extraction technique, Pulsed Extraction Delayed Acceleration (PEDA), and multi-mass ion imaging, with a fast CMOS detector with high time resolution, thus allowing for the simultaneous analysis of large sample areas with high mass and spatial resolution resolution.
Method:
A defocussed beam of C60+ ions, produced by a primary ion gun initially developed for microprobe mode SIMS imaging, was combined with novel extraction optics and a multichannel-plate/phosphor screen detector assembly. Optimal voltage conditions for each component were obtained via simulations with SIMION, an ion trajectory software, using a Genetic Algorithm (GA). A secondary electron detector was used to acquire beam profile images and to ensure that the beam defocussed in a uniform manner. The spatial resolution was tested by recording microscope mode MS images of Rhodamine B samples sprayed through a metal grid using a Pixel Imaging Mass Spectrometry (PImMS) camera, which is equipped with a fast time-stamping device with time resolution of 12.5 ns. Hence, PImMS is capable of recording not only intensity information, but also time of flight. The mass resolution was instead tested on metal samples by measuring the leading edge of a reference mass peak, recorded using both a photomultiplier tube and the PImMS camera.
Results:
Coupling of microscope mode SIMS imaging with secondary ion mass spectrometry and pulsed extraction of the secondary ions.
Novelty:
A highly defocussed C60+ primary ion beam was achieved by lowering the voltage on a focussing lens stack on the ion gun. The beam profile was studied via secondary electron imaging, which showed that the ion beam maintained an even coverage over several m
Preliminary Data:
Contributing Authors:
Contributing Authors: M. Elena Castellani,1,2 Yifeng Jia,1 Anya Eyres,1 Natasha Smith,1 Michael Burt,1 Josephine Bunch, 2 Zoltan Tákats 2, Mark Brouard 1 and Felicia Green 2
Affiliations: 1. Department of Chemistry, University of Oxford, Chemistry Research Laboratory, Oxford, OX1 3TA
2. Rosalind Franklin Institute, Harwell Campus, Didcot, OX11 0QX

P-13

Cologna, Stephanie
University of Illinois Chicago, USA

MALDI-MSI mapping of lipids in Niemann-Pick disease, type C: Exploring potential treatments

Introduction:
Niemann Pick disease, type C (NPC) is a fatal, autosomal recessive, lysosomal storage disorder that is characterized by progressive cerebellar neurodegeneration. NPC is caused by mutations in either the NPC1 or NPC2 genes which result in their respective protein dysfunction and inability to traffic cholesterol out of the lysosome. Following cholesterol storage, a cascade of events occur which ultimately results in cell death. Currently there is no FDA-approved therapy for NPC disease. However, 2-hydroxypropyl-beta-cyclodextrin (HPBCD) and gene therapy strategies are currently being investigated. In the current work, we utilize MALDI mass spectrometry imaging to understand the lipid distribution profile of mice with NPC1 disease, as well as those treated with these experimental therapies.
Method:
HPBCD treatment was administered by intraperitoneal injection (4000 mg/kg HPBCD or PBS) every other day following weaning and until euthanasia (7 weeks). AAV9 gene therapy was administered via retro-orbital injection (1.21e11 vector genomes/mouse) at weaning and mice were euthanized at 10 weeks old. Brain tissue was harvested and flash frozen. The brains were sectioned in the sagittal direction to a 10µm thickness, and then thaw mounted onto a stainless steel MALDI plate. Matrix was applied using a home-built sublimation system onto the samples in a uniform coating. Lipids were imaged in both positive and negative mode from 500-1600m/z using a Sciex 4800 MALDI-TOF/TOF. All images were processed using MSiReader.
Results:
Prior studies in multiple animal models have shown that lipids other than cholesterol are altered in brain tissue from NPC1 mouse models. For example, bioactive sphingolipids such as ceramides and gangliosides have been reported as altered and have also shown unique spatial distributions in the cerebellum of mutant animals. In the current study, we further investigated these lipids owing to their involvement in signaling pathways and regulation of biological functions. For example, ceramides are known to induce apoptotic cell death and are increased in NPC1 brain areas such as the cerebellum where a well-documented patterned loss of Purkinje cells occurs. Whether the neuronal cell death seen in NPC1 is caused by an accumulation of ceramides or an accumulation of ceramides is present because of the ongoing neuronal cell death is currently unknown. In the MSI analysis of animals treated with HPβCD, we observe ceramide accumulation decreases significantly in the mutant brain while the drug induces no change in wild type mice. This effect is most striking in the cerebellum. Similar results are seen with gangliosides, GM2 and GM3, in the NPC1 brain. That is, untreated mutant animals have elevated ganglioside levels whereas HPBCD treatment appears to normalize ganglioside levels and distribution. Interestingly, ganglioside accumulation is also reduced in treated mutant animals across the brain. Currently, our work is focused on defining lipid distribution changes in mice that have received NPC1 gene therapy treatment. This will give us the opportunity to see how different treatments affect lipid accumulation in NPC1 with particular focus on the central nervous system.
Novelty:
This work highlights changes in lipid distribution within the brain of Npc1 mutant mice following therapeutic intervention.
Preliminary Data:
Candidate therapies for NPC1 disease show altered brain lipid distributions.
Contributing Authors:
Dominick Pierre-Jacques, Nigina Khamidova, Cristin D. Davidson, William J. Pavan, Stephanie M. Cologna

P-14

Cousineau, Samantha
University of Western Ontario, Canada

Mass Spectrometry Imaging of Brain Fatty Acids and Behavioral Studies on Prenatal Cannabis Exposure and Omega-3 Fatty Acid Diet Supplementation

Introduction:
Fatty acids (FAs), including omega-3 and omega-6 FAs such as docosahexaenoic acid (DHA) and arachidonic acid (AA), play crucial roles in brain health and development. Deficiencies in FAs have been linked to cognitive impairments and psychiatric disorders like Alzheimer's, schizophrenia, and mood disorders. The legalization of cannabis has led to increased use, but the long-term effects of prenatal cannabis exposure (PCE) on neurodevelopment remain unclear. Given the interaction between the endocannabinoid system (ECS) and FA pathways in the brain, we hypothesized that prenatal exposure to Δ9-tetrahydrocannabinol (THC) might disrupt fetal neurodevelopment but could be mitigated by omega-3 supplementation. This study presents behavioural and mass spectrometry imaging data on the effects of PCE and omega-3 supplementation.
Method:
The study involved four treatment groups: vehicle vs. THC with control diet (VEHCT/THCCT) and vehicle vs. THC with omega-3 diet (VEHN3/THCN3). Pregnant Wistar rats were exposed to THC from gestational day (GD) 7 to GD22. Omega-3 diets were provided ad libitum from GD5 to postnatal day (PD) 21. Behavioral assessments were conducted on male and female offspring at adolescence (PD45) and adulthood (PD120). Mass spectrometry imaging (MSI) using the novel matrix 1,6-diphenyl-1,3,5-hexatriene (DPH) was performed to measure FA levels in the prefrontal cortex (PFC), nucleus accumbens (NAc), and hippocampus (HIPP), while minimizing lipid fragmentation.
Results:
At PD120, THCCT offspring (both male and female) exhibited decreased social motivation and memory, long-term recognition, and spatial working memory, with male THCCT also showing increased anxiety compared to VEHCT. Omega-3 supplementation in THCN3 males reduced anxiety levels and prevented deficits in social motivation, memory, and spatial working memory caused by THC exposure. In THCN3 females, deficits in social memory and spatial memory were prevented, but some deficits in social motivation and long-term recognition memory persisted. MSI data showed DHA deficits in the PFC, NAc, and HIPP of THCCT offspring at PD21. By PD120, female THCCT showed increased DHA levels in the PFC and NAc but low levels in the HIPP, suggesting possible functional deficits in this region. The ECS's primary receptor had higher expression in the female HIPP, implying its increased susceptibility to PCE. Male THCCT offspring continued to exhibit deficits in all brain regions at PD120, while female offspring showed limited sex-specific ability to normalize DHA levels by adulthood. Omega-3 supplementation significantly increased DHA levels in both male and female brains, with females showing higher levels. Female THCN3 exhibited prevention of DHA deficits throughout the brain except for the HIPP, while the effect of the omega-3 diet on DHA levels in male THCN3 was less pronounced. Overall, omega-3 supplementation prevented behavioural and fatty acid changes caused by PCE, with sex-specific mechanisms influencing results in females.
Novelty:
MALDI MSI study on the effect of PCE and omega-3 supplementation on fatty acid levels in brain
Preliminary Data:
The use of exogenous lipid standard (PC 17:0-17:0) is being investigated for monitoring lipid fragmentation. Ongoing work optimizes deposition conditions.
Contributing Authors:
Samantha L. Cousineau; Mohammed H. Sarikahya; Marta De Felice; Aleksandra Doktor; Daniel B. Hardy; Steven R. Laviolette; Ken K.-C. Yeung

P-15

Dillman, Natalie
Johns Hopkins University, USA

Characterization of a Humanized Mouse Model for Organophosphate Poisoning and Detection of Countermeasures via MALDI-MSI

Introduction:
Organophosphate (OP) poisoning most commonly occurs due to contact with OP pesticides or nerve agents. OP chemicals inhibit the enzyme acetylcholinesterase (AChE), causing a buildup of the neurotransmitter acetylcholine in the synapses of the body and resulting in the hallmark symptoms of a cholinergic crisis. Typical treatment includes a combination drug therapy of a reactivator which displaces the OP from the active site of AChE and thereby regenerates the active enzyme, and an anticholinergic drug which works in opposition to the pro-cholinergic effects of the poisoning. Studying OP poisoning is difficult because common small animal research models (e.g., mice, rats, guinea pigs) have serum carboxylesterase, which contributes to these animals' resistance to OP poisoning. In contrast, humans and nonhuman primates do not express serum carboxylesterase. In addition, though AChE serves the same function in all animals, differences in amino acid sequence can cause the enzyme to react differently in response to small molecule therapies intended to regenerate the active enzyme. A novel genetically modified mouse strain (KIKO) has been recently developed in which the gene expressing serum carboxylesterase is interrupted so that a functional protein is not expressed (Es 1 KO) and the gene expressing acetylcholinesterase has been altered to express the amino acid sequence of the human form of the same protein (AChE KI).
Method:
KIKO mice were injected with 1 LD50 of OP nerve agent or water as a vehicle control. After one to three minutes, animals were injected with 35 mg/kg the currently fielded reactivator countermeasure for OP intoxication. After fifteen minutes, or upon death, brains of the animals were removed and frozen on liquid nitrogen vapors. Tissue was cryosectioned at 10-micron thickness onto ITO slides. After cryosectioning brains were imaged in positive ion mode at 50-micron pixel size with THAP (10mg/mL in 70% MeOH) on a Bruker RapifleX ToF/ToF. Data was analyzed in SCiLS lab.
Results:
Data from the above experiments confirms the presence of increased acetylcholine in OP-exposed animals, regardless of treatment status. This result is expected as OP binds to the AChE within the brain leading to an increase in acetylcholine. More interestingly, we were able to detect reactivator (m/z 137) within the brain of both exposed and unexposed animals. Currently, it is debated if reactivator is able to enter the brain of OP-exposed animals. Our data suggests a small amount of reactivator is able to enter the brain, regardless of OP exposure. Our data also suggests reactivator does not equally enter the brain of both male and female animals. Preliminary data shows more 2-PAM enters the brains of female animals than male animals, regardless of exposure status. Further, we find there to be more acetylcholine present in male brains than female brains of OP exposed animals, indicating that sex may play a role in toxicity of OP exposure. We did not observe any changes beyond an increase in acetylcholine and the penetrance of reactivator in the brains in the imaging run, indicating no change on phospholipids as a result of OP-intoxication within fifteen minutes of exposure. We are currently repeating these experiments including the use of an anticholinergic, which is part of the currently fielded cocktail. We are also increasing our time point from 15 minutes to 30 minutes.
Novelty:
This study, which utilizes sensitive and advanced MALDI-MSI methods, could characterize KIKO mice as a functional model for OP countermeasure development and a tool for disorders that involve AChE.
Preliminary Data:
Data suggest that this study may establish whether standard medical countermeasures are able to cross the blood brain barrier to interact with inhibited acetylcholinesterase in the brain.
Contributing Authors:
Crawford R. A., Dillman N., Carriero, S., Wadsworth, B., Cadieux, C. L., Tressler C.

P-16

Cressman, Erik
MD Anderson Cancer Center, USA

Early experience with tumors generated in the Oncopig characterized by Mass Spectrometry Imaging and Computed Tomography

Introduction:
Large animal cancer models are valuable due to greater similarities to human anatomy and physiology, yet they are uncommon, logistically complex, and costly. The inherent multiplexed nature of mass spectrometry imaging lends itself as a valuable, high-yield tool for in-depth characterization in such circumstances.
Method:
Under an approved protocol, hepatic tumors were generated in 9 transgenic Oncopigs using published methods by inoculation with adeno viral vector. Tumors were allowed to grow for 2-4 weeks (n=3/gp) with weekly CT imaging (non-contrast, arterial phase, portal venous phase) to monitor tumor growth using a Siemens Edge scanner. Animals were subsequently euthanized and samples were collected for analysis. A Waters Synapt G2 was utilized in both positive and negative modes and molecular ion images were correlated with adjacent H&E sections.
Results:
Tumors were successfully initiated in the liver of all 9 animals, although volumes were somewhat inconsistent. On triple-phase CT imaging, tumors were low attenuating masses with mild contrast enhancement around the margins, but showed little to no enhancement within the tumors themselves. At necropsy, tumors were pale yellowish white in color and very friable. Some central necrosis was observed, particularly in the 4-week group. Histology and immunohistochemistry demonstrated inflammatory masses consisting predominantly of neutrophils, macrophages, and T-cells with no definitive evidence of carcinomas. Several distinctive patterns were noted among the molecular ion images: 1) liver parenchyma only, 2) tumor only, 3) necrotic center only, 4) liver parenchyma and tumor but not necrotic center. These features correlated well with respect to how conspicuous they were when compared to conventional staining and were also congruent with CT images.
Novelty:
First report correlating mass spectrometry and CT imaging to study such features in this animal model.
Preliminary Data:
Although model refinement appears necessary, MSI data may provide distinct mass biomarkers specific to immune cells and necrosis.
Contributing Authors:
Danielle Stolley PhD, Maria Sophia Stenkamp, Natalie Wall Fowlkes DVM, PhD, Erin H. Seeley, PhD, Steven Parrish, Erik Cressman PhD MD FSIR

P-17

Cuypers, Eva
University Maastricht - M4i, Netherlands

Survival prediction of glioblastoma patients based on REIMS and MALDI-MSI molecular profiling

Introduction:
Glioblastomas (GBM) are highly aggressive brain tumors with poor median survival of 12-14 months. However, this survival rate is very unpredictable and can range from less than 1 month up to more than 2 years. The high recurrence rate of GBMs can partially be attributed to inadequate margin delineation during surgery, leading to incomplete removal of cancer cells and subsequent regrowth. Rapid evaporative ionization mass spectrometry (REIMS) was earlier developed to serve as an intraoperative technique, capable of recognizing the chemical differences between tissue types within seconds and thus providing real-time information about margin status. However, within these GBM patients, the wide spread of overall survival and recurrence remains highly unpredictable and is not always related to inadequate margin delineation.
Method:
In this research, we present a REIMS based molecular database that separates short (1-11 months), mid (12-19 months) and long term (21+) GBM survivors. Interesting differentiating m/z values and their spatial distributions are further investigated by MALD-MSI (using a Bruker rapifleX, 30X30um spot size, negative and positive mode). MS/MS based identification, relative quantification and ROC analysis is performed to investigate the significance of potential biomarkers.
Results:
Our data showed tissue based prognostic value by separating samples based on various survival rates. The loading plots and averaged spectra showed sufficient alignment, further validating the REIMS based model's efficacy and providing valuable insights into the main discriminators contributing to the classification. These discriminators and thus potential biomarkers are identified. Their spatial distribution within the tumor tissue sections is shown, leading to a better understanding and potential future therapy response prediction.
Novelty:
We show survival rate prediction is possible for GBM patients based on their molecular profiles.
Preliminary Data:
Molecular based survival rate prediction, including differentiating biomarkers ID's and their spatial distribution, is shown.
Contributing Authors:
Eva Cuypers(1), Angeliki Birmpili(1), Tim Hendriks(1), Steven De Vleeschouwer(2) (1)Maastricht MultiModal Molecular Imaging Institute (M4i), Universiteitssingel 50, 6229 ER, Maastricht, The Netherlands (2)Neurosurgery Department, University Hospitals Leuven; Laboratory for Experimental Neurosurgery and Neuroanatomy, Department of Neurosciences

P-18

Desyaterik, Yury
University of North Carolina at Chapel Hill, United States

Enhancing Quantification Accuracy of Antiretroviral Drugs through Signal Averaging with a Q Exactive Mass Spectrometer and a New-Generation External Data Acquisition System

Introduction:
Mass spectrometry imaging (MSI) is a powerful technique for measuring the spatial distribution of biologically significant compounds in tissues. Analyte sensitivity can be a significant limitation in MSI applications because of the small sample amount probed at each pixel. While signal averaging can be used to increase sensitivity, integrated instrumental noise thresholding in routine Orbitrap-based imaging applications may also remove relevant peak information close to the limit of detection. Here, we investigate whether MSI analyte sensitivity toward antiretrovirals (ARVs) can be increased by averaging the Orbitrap transient signals, which can be recorded through integration of an external data acquisition system.
Method:
A high-performance data acquisition system (FTMS Booster X2, Spectroswiss) was coupled to the preamplifier outputs of a Q Exactive Plus Orbitrap (Thermo Fisher Scientific), allowing FTMS transients to be directly recorded in parallel with the RAW mass spectra acquisition. MSI analysis was performed using an infrared matrix-assisted laser desorption electrospray ionization (IR-MALDESI) source coupled to the mass spectrometer. Nonhuman primates were dosed for 10 days to steady state with 4-drug ARV regimens (emtricitabine + tenofovir with either efavirenz + raltegravir or maraviroc + atazanavir). Imaging of thaw-mounted 10 µm genital tract tissue sections was conducted in positive ionization mode using full MS acquisition with a resolution of 140,000 at m/z 200. Orbitrap mass spectra were processed with MSiReader (MSI Software Solutions), and transients were analyzed with Mozaic software (Spectroswiss). Quantification of ARVs in consecutive tissue sections was performed using standard LC-MS analysis.
Results:
Existing procedures of Orbitrap data-handling currently prevent effective signal averaging of peaks near the limit of detection. First, the abundance of Orbitrap signals below an internally defined threshold in the raw data is zeroed to reduce the resulting data file size. Second, while there are existing capabilities for up to 10 consecutive mass spectra to be discretized into microscans for averaging, this may disproportionally compromise spatial resolution in one scanning dimension depending on sequence of data acquisition. Microscan averaging is also performed for the entire spectrum, leading to loss of spatial resolution for all peaks unilaterally. A more effective approach involves recording the complete spectra, including noise, and averaging the signals of adjacent pixels only for compounds with low signal intensity with a significant number of pixels below the noise threshold level. The FTMS Booster X2 acquires the in-hardware phased time-domain transients that can be further directly converted into the absorption mode FT (aFT) mass spectra. The aFT mass spectra provide equal information to transients and are thus ideally suited for averaging at the post-acquisition stage. Our preliminary work demonstrates that signal averaging of Orbitrap transients significantly improves the frequency of detection (FOD), representing the proportion of total tissue voxels where the drug was detected, for peaks with low signal intensity. For instance, we found that FOD of emtricitabine increased from 4% for Orbitrap data (eFT mass spectra) to 29% for the aFT mass spectra. Data averaging using a 2x2 pixel square template further increased FOD to 57%, and 4x4 pixel averaging improved it to 85%. Comparatively, the image of a 100 nL spot of a 0.25 µg/mL emtricitabine solution constructed from Orbitrap eFT mass spectra (reduced profile) had a detectable response in 14 pixels, whereas it had 43 pixels using aFT mass spectra without averaging, and 108 pixels after applying a 4x4 pixel average. This work will be extended to assess how signal averaging enhances drug quantification. The limit of quantification will be evaluated for both the original and averaged signals using calibration standards spotted on blank tissues. Additionally, we will compare the cumulative ARV concentrations measured in dosed tissue sections by MSI to the quantification of ARVs in a serial section by conventional LC-MS analysis.
Novelty:
Enhanced sensitivity toward trace analytes through post-acquisition signal averaging of unreduced MSI data.
Preliminary Data:
Increase in emtricitabine frequency of detection from 4% for the original Orbitrap data to 85% for the 4x4 pixel averaging of the full profile data.
Contributing Authors:
Yury N. Desyaterik, Angela D. M. Kashuba, Konstantin O. Nagornov, Anton N. Kozhinov, Yury O. Tsybin, Elias P. Rosen

P-19

Dillman, Natalie
Johns Hopkins University School of Medicine, United States

Evaluation of A Novel Organophosphorus Nerve Agent Exposure Mouse Model by MALDI Imaging

Introduction:
A novel strain of genetically modified mice (KIKO) has been created with the aim of better mimicking the human condition as related to serum carboxylesterase (CaE) and acetylcholinesterase (AChE), which are key enzymes in organophosphate posioning. This model utilizes the C57BL/6J mouse strain with the mouse CaE and AChE knocked out and human AChE knocked in. This produces a mouse model which does not bind organophosphates through CaE, as well as more accurately mimics the activity of human AChE. To understand the distinctions among the wildtype (WT), CaE knockout (KO), and KIKO mouse strains, we are utilizing matrix-assisted laser desorption/ionization mass spectrometry imaging (MALDI-MSI) to investigate neurotransmitters, lipids, and proteins across the entire life span of the animals. The differences will be compared in KIKO versus WT or KO as well as male versus female for each genotype. We are investigating both brain and heart tissue from these animals as they contain the highest concentration of the AChE. These animals have the potential to be a more accurate model of organophosphate poisoning and evaluation of countermeasures as well as a novel model of neurodegeneration.
Method:
Heart and brain tissue were cryosectioned at 10-micron thickness onto ITO slides after collection from wildtype, knockout, and KIKO mice at 6-weeks, 14-weeks, and 40-weeks. Neurotransmitters were imaged on a Bruker RapifleX TOF/TOF in reflection-positive mode using gold nanoparticles as a matrix in 50% methanol as previously described. Tissues were imaged on a Bruker RapifleX TOF/TOF in reflectron positive mode at 50-micron spatial resolution. Lipids were imaged on a Bruker timsToF fleX MALDI-2 in positive and negative ion mode with CHCA (10mg/mL in 50% acetonitrile) as a matrix at 50-micron resolution.
Results:
No significant variations in lipid profiles were detected when comparing different strains or sexes at 14 weeks in either male or female animals when comparing KIKO to KO or WT by receiver operating characteristic (ROC) analysis. As expected, differences were observed between heart and brain. We are in the process of measuring more 14-week samples as well as measuring other time points. We have observed similar trends with 6-, 14-, and 40-week old mice where no neurotransmitters were significantly different between WT, KO, and KIKO. Notably, in the six-week-old mice as compared to the other age groups, variations in neurotransmitter levels were observed, aligning with expectations given their developmental stage. However, no discernible distinctions were observed between the WT and KIKO strains. Similarly, in the 14-week-old and 40-week-old mice, no significant differences were found in neurotransmitters between strains or sexes. Interestingly, despite gene expression data indicating a decrease in AChE, all three genotypes at all ages had the same amount of choline, indicating that despite the lower expression of AChE, the human enzyme maintains the same balance of choline within the KIKO system. To gain deeper insights into the underlying reasons for the divergent treatment responses observed in the strains, additional data will be collected by examining variations in enzymes and metabolites. This analysis aims to explore potential differences in the metabolic pathways and enzymatic activities between the strains and sexes, further elucidating the factors influencing their divergent reactions to treatments.
Novelty:
Using MALDI-TOF for analyzing a novel mouse model for organophosphorus poisoning
Preliminary Data:
Significant differences in lipids and neurotransmitters are not observed between the wild type and novel mouse models.
Contributing Authors:
Dillman N., Crawford, R., Tressler C., Carriero, S., Wadsworth, B., & Cadieux C.L.

P-20

Djambazova, Katerina
Vanderbilt University, United States

Multimodal Molecular Imaging Reveals Alterations to Lipid Profiles in Human Diabetic Nephropathy Kidney Tissue

Introduction:
Diabetic Nephropathy (DN) is a serious complication that can develop in patients with late-stage type 2 diabetes and is the leading cause of end-stage renal disease. Molecular alterations, such as heavy lipid deposition in kidneys, are common in patients with DN, however, the molecular makeup and the sites of these alterations are not well documented. Matrix-assisted laser desorption ionization imaging mass spectrometry (MALDI IMS) allows for the untargeted mapping of biomolecule distributions in tissue sections for molecules ranging from small metabolites to intact proteins. Here, we utilize multimodal molecular imaging, including MALDI IMS, histological stains, and multiplexed immunofluorescence (MxIF) to reveal lipid alterations due to DN that can be correlated with known tissue features and cell types.
Method:
Human kidney samples embedded in optimal cutting temperature (OCT) gel from the network for Pancreatic Organ Donors with Diabetes, in collaboration with Novo Nordisk, were cryosectioned at 5µm thickness and mounted onto indium tin oxide-coated slides. Sections were washed with chilled isotonic ammonium formate solution to remove OCT and salt. Matrix (4-(dimethylamino)cinnamic acid (DMACA)) was sublimed onto the tissue surface using an in-house developed sublimation device. MALDI IMS data were acquired in both polarities at 5µm or 10µm spatial resolution using a Bruker timsTOF FleX (Bruker Daltonics). Matrix was removed to perform MxIF to stain glomerular and tubular cell types, followed by a Periodic Acid Schiff (PAS) stain. Data analysis and visualization were performed using SCiLS and in-house developed software.
Results:
Diabetic nephropathy can cause significant abnormalities in the kidney structures and their functions. For example, glomeruli are the initial filtration units of the kidney, whose association with DN has been well documented in the literature. Glomeruli have been challenging to study with MALDI IMS due to their small size (<200µm); however, recent advancements in the field have allowed high spatial resolution MALDI IMS (≤ 10µm) to be routinely performed. Here, we acquired MALDI IMS, MxIF, and PAS stains of two DN and two control human kidney samples. MALDI IMS data were acquired in both positive and negative ionization modes at high spatial resolutions (5 and 10 µm). Liquid chromatography-tandem mass spectrometry (LC-MS/MS) was subsequently performed on serial tissue sections to aid in confident lipid analyte identification. Multimodal imaging data were acquired on the same tissue section and computationally registered to correlate molecular signals with known cells and histological structures. Preliminary data show that numerous lipids have different spatial distributions in DN and control samples. For example, lyso-phosphatidylcholine LPC(O-28:3) and sphingomyelin SM (18:1 2O/16:0), detected in negative ionization mode, have uniform intensity distributions within healthy glomeruli in the control tissues. In the DN samples, the ions showed varying intensities throughout the glomeruli, where higher intensities were observed at and beyond the outer glomerular perimeter. These lipids were also found to accumulate at distinct sites throughout the tubules and interstitial space. Utilizing the multimodal imaging pipeline, we identified that the ion distributions correlate with areas of significant glomerular and tubular injury, as confirmed by the PAS stains. High spatial resolution (5µm pixel size) MALDI IMS also revealed molecular heterogeneity within diseased glomeruli. Future work will focus on correlating the spatial distributions of these analytes to known cells and structures within kidney functional tissue units, such as the glomerulus.
Novelty:
Multimodal molecular imaging reveals distinct lipid profiles at sites of glomerular and tubular damage in diabetic nephropathy human kidney samples.
Preliminary Data:
Detailed histopathology and MxIF enable IMS data to be correlated to specific injury sites in human diabetic nephropathy kidney tissues.

Contributing Authors:
Katerina V. Djambazova1,2; Allison B. Esselman2,3, Heather H. Ward4, Claire Gibson4, Ellie Pingry1,2, Melissa Farrow2,5, Madeline E. Colley2,5, Lukasz G Migasz6, Jamie Allen1,2, Raf Van de Plas2,5,6, Jeffrey M. Spraggins1,2,3,5,7 1Department of Cell and Developmental Biology, Vanderbilt University, Nashville, TN, USA 2Mass Spectrometry Research Center, Vanderbilt University, Nashville, TN, USA 3Department of Chemistry, Vanderbilt University, Nashville, TN, USA 4Type 1 Diabetes & Kidney Disease, Global Drug Discovery, Novo Nordisk Research Center Seattle, Inc., Seattle, WA, USA 5Department of Biochemistry, Vanderbilt University, Nashville, TN, USA 6Delft Center for Systems and Control, Delft University of Technology, Delft, Netherlands 7Pathology, Microbiology and Immunology, Vanderbilt University Medical Center, Nashville, TN, USA

P-21

Duncan, Kyle
Vancouver Island University, Canada

A multimodal MSI pipeline to uncover metabolic heterogeneity in ovarian tumors

Introduction:

Tumors are a complex composition of cells that contain many microenvironments with unique metabolic profiles. Distinct local metabolisms within tumor microenvironments (TMEs) can impact the degree to which tumor infiltrating lymphocytes (TILs) can penetrate tumors, which results in immune 'hot' or 'cold' phenotypes that impacts overall patient survival. It is understood that immune cell infiltration improves survival outcomes, yet the precise reasons why TILs are present or absent in TMEs are still unclear. Herein, we investigate localized metabolic aberrations within the ovarian TME related to immune suppression using nanospray desorption electrospray ionization (nano-DESI) MSI. We merge nano-DESI spatial metabolomics data with matrix assisted laser desorption/ionization (MALDI) MSI to reveal metabolite heterogeneity within ovarian tumors and link metabolite profiles with immune cell infiltration.

Method:

Experiments were performed on OVCAR3 xenograft ovarian tumors with and without folate-receptor chimeric antigen receptor (CAR-T) t cell treatment. Resected tumors were embedded in CMC, snap frozen, sliced to 10-12 µm thick sections, and thaw mounted onto regular and ITO coated microscope slides. Nano-DESI imaging was performed using a custom-built platform coupled to an Exploris 120 Orbitrap mass spectrometer. The 150 µm OD and 50 µm ID primary and secondary capillaries in the nano-DESI platform, in combination with the MS duty cycle, yielded pixel dimensions ~ 150 µm x 10 µm. Serial sections were analyzed by matrix assisted laser desorption/ionization (MALDI) MSI using a tims-TOF flex in combination with HiPLEX immunohistochemistry mass tags for immune cell localization.

Results:

Methionine cycle metabolites are important mediators in ovarian cancer tumor driven immunosuppression. Specifically, it was found that tumor derived 1-methylnicotinamide suppressed targeted CAR-T based immunotherapies. Moreover, depletion of methionine enhanced T cell immune response. Yet the localization of methionine cycle intermediates in relation to TILs in heterogeneous tumors are unknown. We developed nano-DESI MSI methods to image methionine cycle intermediates in ovarian tumor tissue and relate quantitative MSI data to TIL localizations. A sample processing workflow was established for nano-DESI imaging OVCAR3 tumor sections. It was found that carboxymethyl cellulose (CMC) embedding material was ideal for retaining tumor tissue structural integrity without contributing signal background during MSI data acquisition. Using our custom build nano-DESI MSI platform, methionine cycle intermediates were profiled in positive ion mode. We found that most targeted metabolites were readily detected with nano-DESI MSI including methionine, s-adenosyl-methionine, nicotinamide, 1-methylnicotinamide, homocysteine, cysteine-threonine, serine, and cysteine. Nano-DESI MSI revealed unique regions-of-interest for each of these metabolites within the OVCAR3 tumors measured. We utilized a readily available 15N labelled amino acid mixture within the nano-DESI solvent to mitigate matrix effects and quantify extracted endogenous metabolites. Isotopically labeled methionine and serine are ideal internal standards for their endogenous analogues, however labeled standards of all analytes were not commercially available. Therefore, using standard solutions, we determined response factors for each methionine cycle intermediate with respect to all 15N amino acids in the prefabricated mixture. These data revealed the most suitable internal standard for each methionine cycle intermediate and facilitated quantitative nano-DESI MSI of all targeted metabolites, even when isotopically labeled internals standards were not available for purchase. We then combined quantitative nano-DESI MSI with MALDI and HiPLEX immunohistochemistry mass spectrometry to correlate methionine cycle intermediate abundance with immune cell localization. Ultimately, this proof-of-concept study provides the groundwork for studying metabolically derived tumor driven immunosuppression.

Novelty:

Combination of multimodal spatial metabolomics with localization of immune cells to help decipher tumor driven immunosuppression.

Preliminary Data:

Multimodal MSI of OVCAR3 ovarian tumor xenografts to investigate metabolic heterogeneity and tumor driven immunosuppression.

Contributing Authors:

Alora Keyowski, Bailey Maltesen, Nathalie Costie, Gillian Carleton, Angela Jackson, Julian Lum, Helena Petrosova, David Goodlett, Kyle Duncan

P-22

Dunne, Jaclyn
Medical University of South Carolina, USA

Evaluation of Antibody-Based Single Cell Imaging Techniques Coupled to Multiplexed Imaging of N-Glycans and Collagens by Matrix-assisted Laser Desorption/Ionization Mass Spectrometry Imaging

Introduction:
The extracellular matrix (ECM) is a proteinaceous component of the tissue microenvironment that impacts cell-cell and cell-matrix signaling. Many current spatial omics methods provide RNA or protein expression information with single cell resolution but lack connection with the extracellular microenvironment. Previous work in our lab has shown that both single cell signaling data and surrounding ECM information can be collected by combining single immunohistochemistry stains with ECM imaging. In this study, we examine several combinations of antibody-directed single-cell imaging modalities with Matrix-Assisted Laser Desorption/Ionization Mass Spectrometry Imaging (MALDI-MSI) to comprehensively assess both the cellular and extracellular microenvironment in clinically archived tissue.

Method:
Previously published methods for N-glycan and collagen analysis by MALDI-MSI were performed on formalin-fixed, paraffin-embedded (FFPE) tissue. Tissue imaging was done on a MALDI QTOF (timsTOF flex, Bruker) in positive ion mode over the m/z range 600-2500. Data visualization software (SCiLS 2022b, Bruker) was used to visualize image patterns. To image the entire microenvironment on a single tissue section we have coupled our MALDI-MSI workflows to other multiplexed spatial profiling methods. Combinations were tested on serial sections of tissues with either MALDI-MSI before or after the additional spatial techniques, which included Miralys™ Photocleavable Mass-tag (PC-MTs) Tissue Imaging Probes (AmberGen), GeoMx Digital Spatial Profiler (Nanostring), and Imaging Mass Cytometry (Fluidigm). Methods provided by the respective companies were used to apply antibodies/mass-tags.

Results:
MALDI-MSI of both N-glycans and extracellular matrix were completed either before or after each single cell modality. Effects on single cell modalities were investigated along with evaluation for peak intensity variation and introduction of imaging artifacts in the MSI data. Experiments were done on multiple tissues with a focus on breast cancer tissue. Workflows were purposefully utilized directly after each other in series using standardized protocols towards determining the optimal placement of each workflow, either before or after MALDI-MSI. Following AmberGen's MALDI-IHC protocols, a panel of 28 PC-MTs were applied to breast tissues, and we found that the signal of certain mass tags coupled to antibodies slightly decreases when MALDI-MSI techniques were done first. In this combination, MALDI-MSI data produced similar spectra and spatial localizations of N-glycan and ECM peptides regardless of method order. When MALDI-MSI and GeoMx Digital Spatial Profiling techniques were combined on a breast tissue microarray we saw a reduction in detection of fluorescent markers used to segment cell types and decreased expression in the GeoMx protein profiling. Although a similar distribution of N-glycan peaks was observed when GeoMx was done first, the intensities of these peaks were much lower. Imaging Mass Cytometry (IMC) was performed on breast tissue and IMC done first showed sharper single cell images compared to IMC after MALDI-MSI, which showed a decrease in signal for some antibodies. IMC completed first introduces artifacts in the MALDI-MSI ion images due to the CyTOF laser ablating a layer of the tissue. Overall, the data suggest that specific epitope binding may be diminished for each combination when MALDI-MSI is done prior to antibody/mass-tag application. Therefore, there is an optimal order for performing the single-cell modality and MALDI-MSI on the same tissue section.

Novelty:
MALDI-MSI can be combined with multiple antibody-directed single cell imaging modalities for enhanced investigation of clinically archived tissues.

Preliminary Data:
Analysis of N-glycan and extracellular matrix peptides may be combined with single cell imaging platforms for comprehensive tissue reporting.

Contributing Authors:
Jaclyn Dunne, Jake Griner, Martin Romeo, Jade Macdonald, Carsten Krieg, Mark Lim, Gargey Yagnik, Kenneth J. Rothschild, Richard R. Drake, Anand S. Mehta, Peggi M. Angel

P-23

Eisenberg, Seth
North Carolina State University, USA

Computational Approaches to MSI Data Analysis

Introduction:
The conventional data analysis workflow for mass spectrometry imaging involves annotating hundreds to thousands of measured m/z using an annotation software such as METASPACE. However, this often results in annotated background ions, and confidence scores (MSM) that are not internally consistent. Two computational tools are presented to improve the efficiency and accuracy of MSI data analysis. An ion classification tool (ICT) utilizing object-based image analysis was created to categorize ions as on-tissue or background, based on the number of detected objects after binary conversion. The molecular annotation confidence score (MACS) was developed to provide a confidence level for a molecular annotation based on fundamental mass spectrometry imaging metrics (mass measurement accuracy, spectral accuracy, and spatial distribution).
Method:
The ICT and MACS programs were written in MATLAB using commands available in the base code and in the add-on Image Processing Toolbox. Both tools were developed and optimized using data collected by infrared matrix-assisted laser desorption electrospray ionization (IR-MALDESI). The ICT performs binary conversion on an ion heatmap, creating objects in the image. Using image classification parameters, these ions are sorted into on-tissue (1-2 objects) or background ions (many randomly distributed objects). Using this list of on-tissue ions, MACS can calculate a confidence value associated with a pre-assigned annotation. The MACS is the product of functions evaluating the mass measurement accuracy, accuracy of predicted carbons, and spatial similarity of the monoisotopic ion (M) and first isotopic peak (M+1).
Results:
After development, the ICT program was tested on a representative sample with a random selection of 50 ions. The ICT successfully classified ions as on-tissue or background with 90% accuracy within seconds. The MACS program can generate a confidence level about an assigned molecular annotation for data collected on an on-tissue ROI or a whole tissue. The experimental m/z data is compared to the theoretical annotation m/z to determine an MMA score using a piecewise function. The experimental abundance data for the M and M+1 peaks are used to estimate the number of carbons in a molecule which is scored by measuring the difference from the theoretical number of carbons in the annotation. The M and M+1 heatmaps are compared using an SSIM tool, generating a score describing the similarity between the two heatmaps, where more confident annotations are given higher scores. When compared to the current standard for molecular annotation, METASPACE, significant differences in the assigned scores were observed. Annotations with very high MSM values (0.6-1.0 MSM) received similar MACS values. For moderately and low confident annotations (0.0-0.6 MSM), a wide range of MACS values were observed, both above and below the MSM values. When directly compared, the MACS values were more consistent with the confidence of an annotation.
Novelty:
The ICT and MACS programs can be utilized as an alternative method for MSI data analysis.
Preliminary Data:
ICT was created with 90% accuracy on 50 ions. MACS demonstrated more consistent and accurate annotation scores on 100 annotations.
Contributing Authors:
Kevan T. Knizner, David C. Muddiman

P-24

Ellis, Shane
University of Wollongong, Australia

Development of an atmospheric pressure laser desorption mass spectrometry imaging system coupled with plasma post-ionisation and trapped ion mobility

Introduction:
Despite the proven utility of conventional desorption/ionisation techniques used for mass spectrometry imaging (MSI) they are still limited in the sensitivity towards many analytes due to typically low ionisation efficiencies. In recent years a variety of post-ionisation techniques have been developed with the goal of ionising analytes not ionised by the initial ionisation process. These methods generally rely on generating a reactive chemical environment to promote additional charge transfer and include laser post-ionisation (MALDI-2) and plasma post-ionisation. In this work we have developed an atmospheric pressure laser desorption source coupled with plasma post-ionisation on a timsTOF mass spectrometer that results in high signal intensities for many metabolites and lipids at spatial resolutions as low as 10 micrometres.

Method:
A timsTOF Pro mass spectrometer (Bruker Daltonik) was coupled to the standard sample stage, laser and camera from the timsTOF Flex mounted externally to the instrument. Desorbed analytes were collected in a heated inlet capillary before entering the SICRIT ion source (Plasmion) where they are ionised by interaction with reactive species generating by the cold plasma prior to transfer into the vacuum region using the standard resistive glass capillary. The laser spot size is ~8 microns using energies that result in high analyte signals from tissue samples. Mammalian tissues were coated with DHA matrix via sublimation followed by recrystallisation whilst plant materials were analysed in the absence of an external matrix. Data was analysed using SCiLS lab software.

Results:
We optimised a variety of instrument parameters using both standards and liver homogenate tissue. The transit time setting which accounts for the time taken between the laser pulse and ions arriving at the analyser was increased from the 3 ms used for the standard vacuum MALDI source to 15 ms in this setup. The optimal inlet capillary temperature was analyte dependent and between 250-380˚C. For lipid imaging a temperature of 370˚C provided the best overall coverage. Remarkably and consistent with earlier studies using the same plasma ion source, lipid spectra closely resembled those obtained using MALDI-2 and were highly complementary to spectra measured using conventional MALDI. In positive-ion mode phosphatidylethanolamines, sterols and neutral glycosphingolipids such as hexosylceramides produced the most abundant signals with overall signal intensities matching those obtained using a standard MALDI-2 timsTOF Flex. The tissue imaging performance has been investigated using a variety of tissues including mouse and human brain tissue as well as pancreatic cancer tissue with high signal-to-noise data acquired in all cases from pixel sizes as low as 10 µm. The coupling with trapped-ion mobility (TIMS) is shown to provide additional chemical information by resolving many isobaric and isomeric species, including isomeric PE and demethylated PC. In many cases >8 mobility resolved features can be resolved and differentially imaged within a 0.2 Da mass window. We have utilised the TIMS to aid in the resolution of isotopologues from mice fed with D2O to study rates of lipid turnover within different brain regions. While an external matrix is beneficial for mammalian tissues by enabling the desorption of a broad range of analytes, plant and root samples containing higher endogenous UV absorption can be analysed without an external matrix and many metabolite species detected and imaged at 10 µm pixel size.

Novelty:
High sensitivity MSI using a new atmospheric pressure laser deposition ion source coupled with plasma post-ionisation and trapped ion mobility

Preliminary Data:
Lipid spectra resemble those acquired using MALDI-2 and MSI performance demonstrated using a variety of mammalian and plant tissue samples

Contributing Authors:
S.R. Ellis, J.A. Michael, J.KY. Lee, A. Don, M. Neihaus

P-25

Emmerson, Lauren
Vanderbilt University, United States

High specificity mapping of gangliosides in Staphylococcus aureus infected bone by MALDI TIMS imaging mass spectrometry

Introduction:
Osteomyelitis is a critical bone disease characterized by inflammation of bone tissue and is most frequently caused by Staphylococcus aureus infection. S. aureus gains access to the bone microenvironment and triggers an inflammatory response resulting in the formation of abscesses within the bone marrow. These abscesses and surrounding regions of tissue possess distinct molecular profiles, which can be characterized via matrix-assisted laser desorption/ionization (MALDI) imaging mass spectrometry (IMS). Specifically, the localization of gangliosides in S. aureus infected bone is identified with high sensitivity and specificity using MALDI imaging and trapped ion mobility (TIMS) mass spectrometry. Gaining further insight into the molecular mechanisms driving S. aureus-induced osteomyelitis is critical to inform future therapeutic and treatment options to improve the prognosis of affected patients.
Method:
C57BL6/J mice were subjected to osteomyelitis via intra-femoral injection of a derivative of S. aureus strain LAC that constitutively expresses a fluorescent reporter. Femurs were harvested and flash frozen 14 days post infection and subsequent embedding and cryosectioning was performed without fixing or decalcification as specified in Good et al. (10.1021/acs.analchem.1c04604). DHA (2,5-dihydroxyacetophenone) was sublimed and recrystallized. MALDI TIMS IMS data were collected at 10 um spatial resolution on a Bruker timsTOFfleX mass spectrometer. Fluorescence microscopy and hematoxylin and eosin staining provided morphological information and allowed for regions of the abscess to be annotated. Ion images were visualized via SCiLS(Bruker Daltonics) and ion mobility data were analyzed with DataAnalysis (Bruker Daltonics) and in-house tools.
Results:
Sample preparation of murine bone tissue for MALDI imaging, including sectioning and matrix application, was optimized to provide reproducible signal for a variety of lipid classes. One of these lipid classes is gangliosides, structurally defined by the presence of a ceramide backbone, oligosaccharide chains, and at least one sialic acid residue. The function of gangliosides in immune responses is not entirely understood, but this lipid class has been linked to infected tissues and immune response. Our data reveal the presence of gangliosides in dynamic and viable cell populations that border the necrotic bone marrow abscess, termed “abscess border”. GM1(42:2);O2 (m/z 1626.948), GM1-NeuGc(42:2);O2 (m/z 1642.940), and HexNAc-GM1(42:2);O2 (m/z 1830.026) are some examples of gangliosides detected in this outer fibrous abscess border. In a single m/z detected via MALDI IMS there could be multiple isomers with distinct distributions and unique biological implications. TIMS can be implemented to differentiate between ganglioside isomers in situ, such as a- and b- series gangliosides which vary based on the position of a sialic acid. This technology was leveraged in preliminary experiments to successfully differentiate the distribution of GM1a and GM1b isomers throughout murine kidney abscesses. The distributions of these isomers were monitored throughout the course of S. aureus kidney infection showing the temporal alteration in the ratio of GM1b/GM1a, which is hypothesized to reflect macrophage recruitment and activity near the infection site. Our TIMS imaging workflow was applied to the S. aureus osteomyelitis model to further interrogate ganglioside distributions in the bone marrow abscess border, and structural isomers were successfully separated to provide insight into their localization and unique biological functions.
Novelty:
MALDI TIMS IMS enables ganglioside isomer separation and provides unique distribution profiles of Staphylococcus aureus-induced bone infection.
Preliminary Data:
10um IMS of bone tissue showing localization of gangliosides around abscesses and separation of ganglioside isomers in kidney by TIMS.

Contributing Authors:
Lauren N. Emmerson1,2, Christopher J. Good1,3, Katerina V. Djambazova1,10, Lukasz G. Migas1,4, Raf Van de Plas1,4, James E. Cassat5,6,7,8, Jeffrey M. Spraggins1,2,3,5,8,9,10 1Mass Spectrometry Research Center, Vanderbilt University, Nashville, TN 2Chemical & Physical Biology Program, Vanderbilt University, Nashville, TN 3Department of Chemistry, Vanderbilt University, Nashville, TN 4Delft Center for Systems and Control, Delft University of Technology, Nashville, TN 5Department of Pathology, Microbiology, and Immunology, Vanderbilt University Medical Center, Nashville, TN 6Department of Pediatrics, Vanderbilt University Medical Center, Nashville, TN 7Department of Biomedical Engineering, Vanderbilt University, Nashville, TN 8Vanderbilt Institute for Infection, Immunology, and Inflammation, Vanderbilt University Medical Center, Nashville, TN 9Department of Biochemistry, Vanderbilt University, Nashville, TN 10Department of Cell and Developmental Biology, Vanderbilt University, Nashville, TN

P-40

Eshghi, Azad
Bruker Daltonics, Canada

High spatial resolution TIMS MALDI-2 imaging of Dhcr7-KO mice reveal changes in cholesterol biosynthesis

Introduction:
Cholesterol plays an essential role in brain development and aberrant biosynthesis can negatively impact structural integrity and functioning of the brain. Smith-Lemli-Opitz syndrome (SLOS), found to be caused by mutations in the DHCR7 gene, is one example of malfunctioning in the cholesterol biosynthetic pathway. The gene encodes for the enzyme 3β-hydroxysterol-Δ7-reductase (DHCR7) that catalyzes the last step of cholesterol synthesis. Previous studies with MALDI mass spectrometry imaging have demonstrated differences in sterol abundance and distribution in WT and Dhcr7-KO neonatal mouse brains. Here, we reproduced the previous work with improved spatial resolution, greater mobility separation and MALDI-2 to obtain higher sensitivity for sterols.

Method:
Thin 10 µm fresh frozen coronal mouse brain sections of neonatal (P0) Dhcr7-KO and WT mice were cyrosectioned and thaw-mounted on IntelliSlides. Prior to MALDI imaging, sections were desiccated and spray-coated with 2,5-DHAP using the M3+ Sprayer for lipid analysis. Imaging analysis was conducted on the timsTOF fleX M2 system at 20 µm spatial resolution with TIMS in both MALDI and MALDI-2 over m/z 300-1500 and mobility range 1/k 0 0.5 – 1.8 or m/z 300-930 and mobility range 1/k 0 0.7– 1.3 (targeting sterols) in positive ion mode and beam scan mode of 200 shots per pixel and mobility ramp of 300 ms. H&E staining was performed on the same sections post MALDI acquisition. Data visualization and statistical analysis was conducted in SCiLS Lab 2023a.

Results:
Initial experimentation was conducted to compare the sensitivity of sterols between MALDI-1 and MALDI-2. As expected, a greater overall sensitivity for sterols was observed with the MALDI-2 laser, with approximately five-to-ten-fold improvement for the targeted compounds: cholesterol, 7-DHD, 7-DHC, and desmosterol as dehydrated species [M-H 2O+H] +. The results matched the expected biological effects of Dhcr7-KO, where cholesterol is depleted and 7-DHD accumulates mostly in the KO, with high spatial localization in the white matter. TIMS separation of isomeric species, desmosterol and 7-DHC, both of which are precursors of cholesterol, was achieved, revealed unique endogenous abundance. Several lipids were also found to be more intense in the KO compared to the WT, most notably m/z 754.5342 (PC 32:1+Na), m/z 782.5637 (PC 34:1+Na) and m/z 810.5978 (PC 36:1+Na), while m/z 739.4641 (DG 42:12;O2+K), m/z 744.4909 (PC 30:0+K) and m/z 798.5321 (PC 34:1+K) were found to be more intense in the WT compared to the KO.

Novelty:
Mobility enabled MALDI-2 imaging of cholesterol biosynthesis intermediates in Dhcr7-KO samples.

Preliminary Data:
Off target effects of aberrant cholesterol biosynthesis

Contributing Authors:
Ethan Yang1; Azad Eshghi1; Amy Li2; Libin Xu2; Shannon Cornett1*

P-27

Hendriks, Tim
Maastricht MultiModal Molecular Imaging Institute (M4i), Netherlands

Development of a single section MALDI-MSI-LC-MS/MS workflow for proteomics and quantitative lipidomics

Introduction:
The visualization of molecular distribution within tissues is crucial for understanding the relationship between unique regions of interest. Fields as lipidomics, glycomics, and proteomics, are already being explored using existing mass spectrometry imaging (MSI) techniques. Whilst MSI allows for direct identification, it is often limited in detecting the most abundant molecules. To increase identifications, separate extraction experiments on consecutive tissue sections are required. We present a novel workflow that enables the detection, localization and identification of proteins and lipids as well as quantification of lipids in a human glioblastoma multiforme tissue. Our approach combines spatial information from MSI with non-targeted proteomics and lipidomics, as well as comparing direct lipid quantification via MALDI-MSI and LC-MS/MS on a single section.
Method:
For this study, we utilized human glioblastoma multiforme class IV (GBM). Tissue sections were sprayed with lipid-internal standards (Avanti Polar Lipids) and 2,5-dihydroxybenzoic acid. MALDI-2-MSI experiments were conducted on a timsTOF-fleX (Bruker) in positive-ionization mode with spatial resolution of 30µm. Segmentation data obtained from LipostarMSI (Molecular Horizon), allowed us to identify regions of interest, which were then isolated using laser-capture microdissection on an LMD7 (Leica). The isolated regions were subjected to a single methyl-tert-butyl-ether extraction. The apolar fraction was used for lipidomics analysis utilizing a Vanguish-Exploris480-Orbitrap in positive-ionization mode. The polar fraction was utilized for proteomics analysis using a Vanguish-QExactive-Orbitrap (Thermo). Lipid identification and quantification were performed using Lipostar (Molecular Discovery), and protein identification was accomplished using Proteome Discoverer (Thermo).
Results:
The MALDI-2-MSI results were analyzed using LipostarMSI and were normalized using TIC-normalization. Using a ratio-based quantification approach, lipids were quantified defined by the lipid class of the internal standard. Segmentation using K-means resulted in distinct segments corresponding to tumor, necrotic, and hypoxic regions, which were validated by a pathologist. The LMD cut sections were extracted and LC-MS/MS-based lipidomics was performed acquiring identification as well as quantification of lipid molecules. Within approximately 1 mm2 of tissue, the LMD- LC-MS/MS workflow successfully identified an average of 1200 lipids across various classes, including glycerophosphocholines, glycerophosphoethanolamines, ceramides, sphingomyelins, and triacylglycerols. Additionally, the proteomics analysis using the polar fraction of the same extraction resulted in the identification of an average of 1000 proteins. MSI quantification revealed lipid concentrations within the histologically defined regions-of-interest. MSI-based concentrations across the regions varied from approximately 1 pmol/mm2 to several hundred pmol/mm2 which were comparable to lipid concentations determined via LC-MS/MS. The difference in slide type showed that PEN-membrane slides resulted in the highest amount of identified lipids and proteins. IntelliSlides and ITO slides showed a decrease in identifications of approximately 30% and 50% respectively. The imaged sections showed a decrease of approximately 30% in identifications compared to the sections that were not subjected to mass spectrometry imaging. These findings highlight the capabilities of the MALDI-MSI-LC-MS/MS workflow, showcasing its potential in analyzing a single tissue section comprehensively.
Novelty:
Single section and extraction MSI-LC-MS/MS workflow for spatial proteomics and quantitative spatial lipidomics.
Preliminary Data:
The proposed workflow has the ability to detect, localize and identify proteins including quantify lipids from the same single section.
Contributing Authors:
Kasper K Krestensen, Giulia Sorbi, Sara Tortorella, Ron M.A. Heeren, Eva Cuypers

P-28

Esselman, Allison
Vanderbilt University, United States

Integrated Imaging Mass Spectrometry and Multiplexed Immunofluorescence for Molecular Imaging of Glomerular Cell Types

Introduction:
Diseases of the kidney, such as diabetic nephropathy, can alter cell types and diminish their ability to function properly. Glomeruli are spherical structures approximately 200 µm in diameter in the kidney that filter blood. They function through substructures made up of fenestrated capillaries, mesangium, basement membrane, and podocytes. To investigate molecular changes of glomeruli on a cellular level, we utilized high spatial resolution (5 µm pixel size) matrix-assisted laser desorption/ionization imaging mass spectrometry (MALDI IMS) to map the lipid content from hundreds of individual glomeruli and multiplexed immunofluorescence (MxIF) to stain glomerular cell types across human tissues. This multimodal approach allows for the discovery of lipidomic biomarker candidates for glomerular cell types using segmentation and interpretable machine learning.
Method:
Human kidney samples from the Cooperative Human Tissue Network at Vanderbilt University Medical Center were sectioned at 6 µm thickness and mounted onto indium tin oxide (ITO) glass slides. Autofluorescence microscopy was acquired to drive image co-registration and to automatically segment glomeruli. Samples were washed with ammonium formate coated with 4-(dimethylamino)cinnamic acid (DMACA) by sublimation. MALDI IMS data were acquired from hundreds of glomeruli using a Bruker timsTOF FleX (Bruker Daltonics) at 5 µm spatial resolution in negative ionization mode. The matrix was removed and MxIF was performed on the same tissue section with a panel of antibodies (4 cycles) that target cell types in glomeruli. Analysis was performed using in-house tools, including k-means clustering, classification, and Shapley additive explanations.
Results:
Rapid high spatial resolution MALDI IMS and MxIF were needed to uncover molecular profiles of glomerular cell types among hundreds of glomeruli in whole slide images of human tissue sections. A deep learning-based machine learning model was used to recognize and segment glomeruli based on autofluorescence microscopy images. The MALDI IMS experiment of hundreds of these segmented glomeruli in negative ion mode greatly reduced the acquisition time while providing the localization of lipids within the glomeruli. There were numerous detected lipids, including sphingomyelin (SM) 34:1, which showed increased intensity in some glomeruli, and phosphatidylserine (PS) 36:1, that increased among others in the same tissue section. These heterogeneous lipidomic profiles could be due to localized cellular changes. To link lipid distributions to specific cell types of glomeruli, MxIF was employed with a panel of 8 antibodies that were validated to work on tissue post-MALDI IMS acquisition. k-means clustering and image segmentation was then performed based on the fluorescence intensities of the antibodies to determine cellular localization and masks. The pixels of these cellular masks were aligned with MALDI IMS pixels, and interpretive machine-learning approaches were performed to uncover important biomarker candidates of each cluster. The integration of IMS with cell type-specific MxIF reveals distinct molecular markers of specific cell types within glomeruli. For example, PS 36:1 was a positively correlated biomarker for a cluster that had a high fluorescent intensity of the mesangial cell marker. This analysis can be used to characterize lipidomic profiles of glomerular cell types and study how these trends change with disease progression.
Novelty:
High spatial resolution microscopy-directed MALDI IMS and MxIF uncovers lipidomic profiles of glomerular cell types.
Preliminary Data:
Lipidomic biomarker candidates of glomerular cell types have been uncovered utilizing interpretable machine learning with MALDI IMS and MxIF data.
Contributing Authors:
Allison B. Esselman 1,2; Lukasz G. Migas 4; Felipe A. Moser 4; Léonore E. M. Tideman 4; Nathan Heath Patterson 1,3; Lukasz G. Migas 1,4; Martin Dufresne 1,3; Katerina V. Djambazova 1,5; Madeline E. Colley 1,3; Raf Van de Plas 1,3,4; Jeffrey M. Spraggins 1,2,3,5,6* 1 Mass Spectrometry Research Center, Vanderbilt University, Nashville, TN, USA 37232 2 Department of Chemistry, Vanderbilt University, Nashville, TN, USA 37232 3 Department of Biochemistry, Vanderbilt University, Nashville, TN, USA, 37232 4 Delft Center for Systems and Control, Delft University of Technology, Delft, The Netherlands 5 Department of Cell and Developmental Biology, Vanderbilt University, Nashville, TN, USA 37232 6 Department of Pathology, Microbiology and Immunology, Vanderbilt University Medical Center, Nashville, TN, USA 37232

P-29

FRACHE, Gilles
Luxembourg Institute of Science and Technology (LIST), Luxembourg.

Plug-and-play Atmospheric Pressure MALDI imaging module for Orbitrap high resolution mass spectrometers for reconstructed skin model investigations.

Introduction:
The interest in Mass Spectrometry Imaging (MSI) has been growing over the years and increasingly demanding (biomedical) applications are being investigated. Yet, Matrix-Assisted Laser Desorption/Ionization (MALDI) MSI instrumentation need to provide both precise localization, and unambiguous identification for (bio-)molecular ions. The presented experimental set-up takes benefit of the High-Resolution Accurate Mass measurement provided by the Orbitrap technology, combined with Atmospheric-pressure MALDI ionization, allowing for high resolution MSI in both mass and space. The latest generation Orbitrap Exploris 480 (Thermo Scientific) coupled to a plug-and-play APMALDI UHR ion source (Masstech) has been used to investigate skin models.
Method:
APMALDI HR MSI of skin samples was performed on platforms consisting of an atmospheric pressure MALDI source (MassTech AP MALDI UHR) fitted to Orbitrap HRMS systems (Thermo Fisher Scientific LTQ Orbitrap Elite and Exploris 480). Matrix application was performed using pneumatic sprayer (Sunchrom). Data visualization and interpretation was achieved using Multimaging (Imabiotech) and Lipostar (Molecular Horizon). Reconstructed human epidermis (RHE) were embedded and sliced by ultra cryo-microtomy and thaw mounted on conductive substrates before APMALDI MS imaging experiments.
Results:
The effects of various sample preparation steps on the molecular distributions of lipids and small metabolites in the biological tissue sections were evaluated. The replacement of human biopsies by in-vitro models (RHE) for the investigation of skin spatial metabolomics represents an analytical challenge to the dimension of RHE compared to real skin. With the enhanced sensitivity of the latest generation of Orbitrap instruments, APMALDI can provide MS imaging with high spatial resolution and high mass resolution. Additionally, such platform allows for a wide range of method including targeted, non-targeted, in-pixel DDA/DIA scans, as well as advanced incremental method adaptations using background exclusion/parent mass list inclusion using AcquireX workflows for consecutive imaging of adjacent sections on the latest generation of instruments. Such advanced imaging method can be directly correlated with LC/MS analyses of extracts of the same tissue sample for consolidated identifications on one single HRMS instrument. Among the presented examples, RHE cross sections were analysed to demonstrate the ability of the APMALDI Orbitrap Exploris setup to detect characteristic lipid composition for each skin layer with lateral resolution down to 5 micrometers.
Novelty:
Masstech APMALDI UHR Orbitrap MSI of epidermis models as a platform for skin metabolism studies.
Preliminary Data:
APMALDI Orbitrap imaging with lateral resolution 5 micrometers obtained for reconstructed skin models
Contributing Authors:
Maureen Feucherolles, William Le, Jérôme Bour, Carine Jacques, Hélène Duplan, Gilles Frache

P-30

Geier, Benedikt
Stanford University, School of Medicine, United States

A simplified system for a complex task - Imaging the metabolite landscape of a novel infection model

Introduction:
The site-specific metabolites bacteria produce during the infection of human tissues are largely unknown. Helicobacter pylori, a human-restricted pathogen, is the main risk factor for developing gastric cancer worldwide. It also thrives and persists in the harshest environment of the human landscape, evading stomach acid by navigating through the mucous layer, adhering to the epithelial junctions and growing as cell-associated microcolonies. Some H. pylori colonize deep in the gastric glands and form clonal populations on the surface of epithelial precursor and stem cells, causing inflammation and hyperplasia. Although these interactions indicate a potential site of carcinogenesis, the local metabolites facilitating colonization, persistence and disease progression at the host-pathogen interface remain largely unexplored.
Method:
Pinpointing the metabolites H. pylori produce during colonization of the proliferative epithelium required tight control of the infection and cellular-scale chemical imaging with high sensitivity. We integrated a novel infection model of human gastric organoids (gastroids), with matrix-assisted laser desorption/ionization mass spectrometry imaging (MALDI-MSI) and fluorescence microscopy for spatio-temporal metabolomics. To mimic the surface and gland niches of the gastric epithelium, we generated stem cell-rich gastroids from human stomach biopsies and synchronized their differentiation. By implementing a method to reverse organoid polarity, we exposed the epithelium's apical side for infection. Optimization of sample preparation and MSI parameters, for instance, through post-ionization, allowed us to resolve structure and chemistry of the bacterial microcolonies interacting with the human gastroids.
Results:
The human-derived gastroid infection model provided us with the host-specific cellular landscape H. pylori encounters when colonizing the stomach. Using fluorescently labeled reporter strains of H. pylori we located and mapped the bacterial microcolonies growing on the gastroids' surface. Identifying the location and state of infection in tissue cross-sections prior to MALDI-MSI was instrumental in correlating MALDI-MSI to specialized sites of infection. The radius of microcolonies on the epithelial surface spanned from ten to fifty micrometers, which required high-resolution MALDI-MSI at step sizes of five to ten micrometers. To boost ion intensities of minute microbial and host metabolites ionized from the small spots and to separate isomers, we chose a "MALDI2-tims-tof flex" to simultaneously apply post-ionization (MALDI2) and ion mobility during MSI. The increased signal intensity of the MALDI2 and the organoid model's reduced background of tissue chemistry revealed a subset of small molecules significantly enriched at the host-pathogen interface. The high-spatial-resolution of the MALDI-MSI enabled a targeted spatial analysis by performing spatial correlations between metabolite signals and the bacterial fluorescence on the organoid surfaces. The majority of metabolites specifically detected at the host-pathogen interface were lipids, including a previously unknown set of uniquely modified membrane lipids. Lipids serve as signaling molecules and building blocks of cellular membranes mediating host-pathogen interactions, including microenvironment adaptation and immune evasion. Our innovative approach of reconstructing the H. pylori-epithelial cell interface in a tightly controlled manner for multiplexed imaging of lipids and other small molecules at micrometer scales provides a distinctive insight into niche-specific metabolic interactions during microbial pathogenesis.
Novelty:
Integrating MALDI2-MSI with a human-based organoid infection model provides a tool for the discovery of site-specific metabolites during microbial infection
Preliminary Data:
Growing dataset of nearly 100 MALDI2-tims-tof flex and correlative IF Microscopy data of organoids and mice, infected and non-infected
Contributing Authors:
Benedikt Geier, Youlim Kim, Jessica A. Klein, Nannan Tao, Xiaowei V. Lu, Manuel Amieva

P-31

Ghezellou, Parviz
Justus Liebig University Giessen, Germany

Organoid mass spectrometry imaging at ultra-high lateral resolution

Introduction:
Organoids are laboratory-developed 3D organ models, originating from stem cells. They are gaining importance as research tools for, e.g., disease modeling, drug discovery, and personalized medicine. With the advancement of mass spectrometry imaging (MSI) instrumentation, this label-free analytical technique has become a powerful tool, capable of analyzing various biological samples, particularly tissues or single cells, with high mass resolution, mass accuracy, and lateral resolution. Here, we present a methodology and results that provide the metabolite spatial distribution in targeted organoids using an atmospheric-pressure scanning microprobe MALDI (AP-SMALDI) MSI setup with a lateral resolution of 1.5 µm at a mass resolution of more than 100 000.
Method:
Human cerebral and mouse intestinal organoids were generated and comprehensively characterized. The intestinal organoids were treated with the proinflammatory cytokine tumor necrosis factor-α (TNFα) and compared with untreated ones. Several sample preparation steps were applied to optimize the cryosectioning of organoids, maintaining the samples' integrity morphologically. The sections were thawed in a desiccator and subsequently covered with DHB (positive-ion mode) or 9AA (negative-ion mode) matrix using a SMALDIPrep pneumatic sprayer system (TransMIT GmbH, Giessen, Germany). MSI measurements were performed using an ultrahigh-resolution prototype AP-SMALDI ion source (TransMIT GmbH, Giessen, Germany), coupled with a Thermo Scientific Q Exactive mass spectrometer (Thermo Fisher Scientific, Bremen, Germany) at pixel sizes and laser spot sizes down to 1.5 µm in positive- and negative-ion mode.
Results:
We developed a reproducible sample preparation method for brain and intestinal organoid metabolite imaging using AP-SMALDI MSI. Preserving sample integrity (in native form morphologically) after sectioning is critical for MSI. Thus, 4% PFA was found as the optimal fixation method besides embedding the organoids in 15% gelatin before flash freezing and cryo-sectioning. However, care needs to be taken to avoid tissue cracking. We froze samples by suspending them in liquid-nitrogen-cooled isopropanol or just put them for short time at -20°C. Since the organoids are not easily distinguishable due to the embedding process at any point in the sample preparation process, histological staining after MSI analysis is required for proper visualization. Within a mass accuracy of ±2 ppm, we have detected and observed over a hundred lipid species in both, positive- and negative-ion mode, investigating protonated (H+), sodiated (Na+), potassiated (K+), and deprotonated (H-) species. Various software packages, e.g., Mirion and Metaspace, were used for data analysis and metabolite annotation. The distribution of lipid classes varied throughout organoid sections. For example, ceramide (Cer) species were recorded with high abundance in positive-ion mode in the lumen of the TNF-α treated intestine organoids. This suggests that TNF-α triggered a metabolic pathway that elevated endogenous ceramide levels and may activate the intrinsic apoptosis pathway. In the brain organoids, we observed that, e.g., phosphatidyl-ethanolamine (PE) and phosphatidyl-choline (PC) species were rather equally distributed within the organoids, unlike a number of phosphatidyl-serine (PS) species, which were only found around the organoid's outer edges. These findings, lipid profiling of distinct organoids imaged with ultra-high spatial resolution, demonstrate that the methodology and the prototype AP-SMALDI setup have the potential for further research on the localization of cell-type-specific metabolites and their function in organoid environments.
Novelty:
AP-SMALDI instrumentation for label-free molecular imaging of microscopic biological samples with high spatial resolution (1.5 µm), including 3D organoids.
Preliminary Data:
Various biomolecule classes and metabolites were detected and spatially visualized in organoids from different origins.
Contributing Authors:
Parviz Ghezellou, Elisa Badin, Max A. Müller, Svenja Pauer, Jasmin Ballout, Vinicius Pinho dos Reis, Eva Herker, Martin Diener, Kerstin Strupat, Bernhard Spengler

P-32

Glunde, Kristine
Johns Hopkins University School of Medicine, United States of America

FluoMALDI microscopy: matrix co-crystallization simultaneously enhances fluorescence and MALDI imaging

Introduction:
Fluorescence microscopy is frequently applied in spatial biological studies, enabling subcellular imaging of samples. Matrix-assisted laser desorption/ionization (MALDI) imaging is inherently multiplexed, enabling tissue imaging of various analytes simultaneously without prior knowledge of sample composition. In current workflows, autofluorescence microscopy is often performed prior to MALDI matrix coating and MALDI imaging, due to the belief that the matrix obscures and obstructs optical microscopy approaches. We developed FluoMALDI, a novel pipeline integrating fluorescence and MALDI imaging of the same matrix-coated sample, which is possible because co-crystallization of fluorophores with MALDI imaging matrices significantly enhances fluorophore brightness, amplifying innate tissue autofluorescence. This approach combines the high spatial resolution of fluorescence microscopy with the inherently multiplexed, versatile imaging capabilities of MALDI imaging.
Method:
Samples were prepared on indium-tin-oxide (ITO) slides and robotically sprayed (HTX sprayer) with 0.0016 mg/mm2 of MALDI matrix. Fluorescence microscopy was acquired following matrix application using widefield or confocal fluorescence microscopes (Olympus or Zeiss) at various excitation/emission wavelengths, followed by MALDI imaging on Bruker rapifleX. We used rhodamine-fluorophore-containing Sharpie® marker, or six other fluorophores, to draw or spot onto ITO slides, which were then coated with six different MALDI matrices separately to test the FluoMALDI workflow and measure fluorescence enhancement and co-crystallization. We next measured FluoMALDI using biological samples, including mouse brain cryo-sections. We tested how matrix density affects fluorescence enhancement and characterized matrix-fluorophore co-crystallization dynamically using fluorescence microscopy. Fluorescence and MALDI images were analyzed using ImageJ and flexImaging, respectively.
Results:
We report for the first time the counterintuitive and innovative discovery that (auto)fluorescence microscopy acquisition is enhanced and improved following MALDI matrix coating of fluorophores and tissue sections. Previously published protocols carried out fluorescence microscopy prior to matrix deposition, or on consecutive tissue sections without matrix. Our data clearly show that (auto)fluorescence signal enhancement occurs when MALDI matrices are deposited on fluorophore patterns or tissue sections. The matrix-induced autofluorescence enhancement of mouse brain sections resulted in greater clarity of histological features, including the hippocampal horn and cerebellum. Solvent alone did not cause any enhancement, while all tested matrix coatings resulted in fluorescence signal enhancements at the specific excitation (Ex) and emission (Em) wavelengths of each tested fluorophore. For rhodamine, the greatest fluorescence signal enhancements were detected for norharmane (nH) with 37-fold increase and α-Cyano-4-hydroxycinnamic acid (CHCA) with 30-fold increase. On mouse brain sections, matrix coating with 9-aminoacridine (9AA), CHCA, and nH resulted in autofluorescence enhancements of up to 2-fold in the green (Ex/Em=472nm/520nm) and red (Ex/Em=543nm/593nm) channel. Fluorescence enhancements increased with higher matrix density for all samples tested. FluoMALDI produced comparable fluorescence enhancements for several endogenous and exogenous fluorophores coated with various common MALDI imaging matrices, which worked equally well for widefield and laser-based confocal fluorescence microscopy systems. MALDI imaging was performed at various pixel sizes ranging from 5 to 50 micron, opening possibilities for FluoMALDI at microscopic scale. Extensive crystallization experiments using time-lapse video microscopy showed that fluorescence is enhanced through co-crystallization of fluorophores with MALDI matrices, localizing the fluorescence to co-crystals that are shaped differently than corresponding pure MALDI matrix crystals. FluoMALDI is a versatile new pipeline that significantly streamlines and enhances combined fluorescence and MALDI imaging approaches through the discovery that co-crystallization of fluorophores with MALDI matrices enhances their fluorescence signal intensities, thereby improving tissue autofluorescence contrast.
Novelty:
FluoMALDI integrates fluorescence and MALDI imaging of a single sample while enhancing (auto)fluorescence through co-crystallization of fluorophores with MALDI matrices
Preliminary Data:
Co-crystallization of fluorophores with MALDI matrices significantly enhances fluorophore brightness enabling amplification of innate tissue autofluorescence to guide MALDI imaging

Contributing Authors:
Xinyi Elaine Shen, Ethan Yang, Hoku West-Foyle, Dalton Brown, Cole Johnson, LaToya Roker, Caitlin Tressler, Ishan Barman, Scot Kuo, Kristine Glunde

P-33

Glunde, Kristine
Johns Hopkins University School of Medicine, United States of America

RaMALDI imaging: a novel multimodal imaging workflow integrating Raman spectroscopic and MALDI mass spectrometry imaging of a single sample

Introduction:
Multimodal tissue imaging techniques that integrate two modalities which complement each other, are powerful discovery tools. Efforts to combine Raman spectroscopic imaging (RSI) and MALDI mass spectrometry imaging (MSI) to extract a condensed image with the advantages of both modalities recently demonstrated the potential of providing spatially resolved, sensitive, specific biomolecular information. Although previous studies showed the correspondence between spectra and images of these two modalities, they have so far involved two separate sample preparations or consecutive tissue sections for RSI and MALDI-MSI, presenting discrepancies in samples, sample preparation, and resulting images. Additionally, such workflow requires extensive data processing for image registration. Here, we have developed RaMALDI, a streamlined workflow that integrates RSI and MALDI-MSI of a single sample.
Method:
We developed the RaMALDI workflow that enables both RSI and MALDI-MSI measurements on a single slide. Since RSI is typically performed on quartz slides, while MSI uses indium-tin oxide (ITO) slides and a MALDI matrix layer covering the sample, we first confirmed that RSI signal-to-noise ratios did not compromise when samples (Sharpie® markings) were prepared on ITO slides sprayed with 1,5-diaminonapthalene (DAN) at 0.0016 mg/mm2 density. We also tested five other common MALDI imaging matrices. Once optimized, we tested the RaMALDI workflow with three different types of biological samples – cryo-sectioned mouse liver homogenate, kidney tissue, and brain tissue. Measurements were performed using RSI followed by MALDI-MSI on the same tissue section. RSI and MSI data were processed independently.
Results:
Multimodal molecular imaging that combines RSI and MALDI-MSI overcomes the limitations of each single approach. However, various challenges to incorporating this multimodal imaging approach exist at multiple steps in the procedure. Particularly, imaging the same sample with a single preparation method is hardly explored due to compatibility issues between substrates, disparities in sample preparation protocols, and difficulties with matching data formats. To these challenges, here we demonstrate for the first time RaMALDI imaging, a streamlined, integrated multimodal imaging workflow of RSI and MALDI-MSI, which is performed on a single sample and uses a single sample preparation protocol by spraying DAN (or other) matrix onto a tissue section placed on an ITO slide. We demonstrate that RaMALDI works with both non-biological (Sharpie® drawings on ITO slide) and biological samples (mouse liver, kidney, and brain tissue sections) at various spatial resolutions (5 µm-100 µm), and that it simplifies the overall multimodal imaging procedure and the integration of molecular information acquired consecutively by RSI and MALDI-MSI from the same sample. We carefully show that DAN matrix, as opposed to five other MALDI imaging matrices, does not interfere with the acquired RSI signals, and that RSI acquisition prior to MALDI imaging of the same sample does not have any measurable effects on MALDI-MSI data quality. We also observed that MALDI matrix application to tissue sections prior to RSI acquisition protected the sample from degradation, as shown by repeated RSI measurements which demonstrated that Raman signal intensity was stable for at least up to 72 hours following matrix deposition. The presented RaMALDI is advantageous because it allows for analysis of a single tissue section with both modalities, reducing sample amounts needed, and significantly streamlines the multimodal approach, ultimately enabling highly multiplexed molecular imaging discoveries in tissue- and cell-based biomedical research.
Novelty:
We developed an integrated Raman and MALDI imaging workflow on a single tissue section using a single preparation method
Preliminary Data:
We demonstrate the RaMALDI workflow which combines Raman and MALDI-MSI on a single tissue section using a single preparation method
Contributing Authors:
Jeong Hee Kim, Ethan Yang, Caitlin M. Tressler, Xinyi Elaine Shen, Tae-Hun Hahm, Dalton R. Brown, Cole C. Johnson, Ishan Barman, Kristine Glunde

P-34

Godfrey, Trevor
Baylor College of Medicine, United States

Metabolic Signatures Differentiate Embryonal Hepatoblastoma and Pediatric Hepatocellular Carcinoma

Introduction:
Hepatoblastoma (HB) is the most common pediatric cancer of the liver and accounts for 1% of all pediatric cancers. Pediatric hepatocellular carcinoma (pHCC) is a rare but severe pediatric liver cancer. Children diagnosed with HB are assigned a risk-associated treatment group based on various clinical observations; most HB patients are designated as low or very low risk. Children diagnosed with pHCC are considered high-risk and have a poor survival rate. There is a clinical need to identify molecular differences between HB and pHCC to assist with diagnosis and risk stratification and identify molecular targets for future treatment regimes. As metabolism is a strong indicator of cancer phenotype, we characterize the metabolic differences between HB and pHCC using mass spectrometry imaging.

Method:
Flash-frozen HB and pHCC patient samples obtained from Texas Children's Hospital were analyzed using desorption electrospray mass spectrometry imaging (DESI-MSI). Samples were embedded in 2% carboxymethylcellulose, sectioned, and mounted on a glass slide. Serial sections were analyzed in negative ion mode on a Xevo G2-XS QTof mass spectrometer made by Waters. We used 80% methanol and 20% acetone as the spray solvent. The DESI sprayer geometry was optimized on mouse brain tissue to maximize signal intensity. The analyzed samples were stained with hematoxylin and eosin. Each slide was annotated by a pathologist that demarcated confirmed the sample histology as either pHCC or embryonal HB. These regions were used to extract MS data for analysis.

Results:
Using DESI-MSI, we performed an initial characterization of the metabolic and lipid heterogeneity in pHCC and HB patient samples. Specifically, we analyzed differences between the embryonal subtype of HB and pHCC. In these samples, we observed rich molecular profiles containing hundreds of metabolites. Most of these metabolites were lipids, including phosphatidylinositols (PI), phosphatidylserines (PS), phosphatidylglycerols (PG), phosphatidylethanolamines (PE), diacylglycerols (DG), ceramides (Cer), cholesterol esters (CE), sterols (ST), and fatty acids (FA). In addition, other small metabolites were observed in the spectra including ascorbic acid, glutamate, and xanthine. PCA analysis showed clear separation between embryonal HB and pHCC samples. PCA loading plot analysis showed the strong contribution of several fatty acids and lipids to the separation of embryonal HB and pHCC. We utilized significance analysis of microarray (SAM) statistical testing to identify metabolites that were specifically upregulated in either embryonal HB or pHCC. Metabolites identified with SAM correlated well with peaks identified in the PCA loading plot. The top fifteen metabolites more abundant in embryonal HB patient samples included 10 lipids (PS, PG, PE, PI, DG), 4 sterols (CE, ST), and one fatty acid (FA). The top fifteen metabolites found to be more abundant in pHCC patient samples included six lipids (PI, PS, PE, Cer), four lyso lipids (LPE, LPI, LPG), three fatty acids (FA), and one sterol (CE). These results suggest an increase in cholesterol containing compounds in embryonal HB and an increase in fatty acids in pHCC. Lipid abundance seemed to shift to contain more lyso lipids (lipids with one fatty acid tail removed) in pHCC compared to embryonal HB. The Molecular patterns identified in these subtypes will be a step towards creating a predictive model which could then help diagnose and assign risk for embryonal HB and pHCC patients.

Novelty:
Application of DESI-MSI to analyze metabolic signatures of hepatoblastoma and pediatric hepatocellular carcinoma samples.

Preliminary Data:
Our preliminary data shows clear differences in the metabolic signature of embryonal HB and pHCC patient samples.

Contributing Authors:
Trevor M. Godfrey, Andres F. Espinoza, Sarah E. Woodfield, Sanjeev A. Vasudevan, Livia S. Eberlin

P-35

Goncalves, Juliana
Institute of Pathology, Germany

Utilizing Mass Spectrometry Imaging to predict patient's treatment response from bladder resections.

Introduction:
Urothelial bladder cancer is responsive to immune checkpoint inhibitor (ICI) treatment. However, when monotherapy is applied only a minority of patients respond. Therefore, combining ICI treatment with other modalities such as radiation together with molecular preselection of patients who are likely to respond are potential avenues to optimize ICI regimens further. This clinical study combined radiation with ICI treatment in the neoadjuvant setting as a therapeutic option in bladder cancer. We employed mass spectrometry imaging to evaluate pre- and post-therapeutic resection specimen of the patients submitted to this treatment approach to identify molecular features that, upon diagnosis, can estimate the patient's success to this treatment. The outcome was compared with DNA/RNA sequencing.
Method:
Following clinico-pathological, and next generation sequencing, the samples (n=48), were adhered to an ITO glass slide. After deparaffinization and re-hydration, the samples were submitted to tryptic digestion, followed by matrix application using an HTX TM sprayer. The mass spectrometry proteomic data was recorded using a RapifleX MALDI-TOF instrument (Bruker) in the m/z range 600-3200. Following data acquisition, the tissue sections were stained using hematoxylin and eosin, and scanned using a digital slide scanner (Aperio AT). Regions of interest (invasive as well as non-invasive tumor and stroma from the previous tumor site) were annotated by a board-certified pathologist. The data was divided into groups according to the patient's treatment response: responder and non-responder. Data analysis was carried out using SCiLS Lab.
Results:
Invasive carcinomas obtained from patients who responded to the treatment exhibit a distinct mass spectrometry profile when compared to non-invasive carcinoma samples. Collagen α-2(I) chain (m/z = 868.44, 1645.65, and 2056.90) and collagen α-1(I) chain precursor (m/z = 2705.17 and 2869.27), with a ROC-AUC of 0.62 - 0.66, showed higher expression in the invasive carcinoma. Conversely, when comparing treatment responders with non-responders, it was observed that higher expression of COL1A2 and COL1A1 was associated with the non-responder group. Regarding the non-invasive carcinoma, overexpression of histones (H2, H3, and H4) and Keratin, type 2 cytoskeletal 7 (KRT7) was identified. However, a greater number of tryptic peptides from KRT7 was detected in the non-responder subgroup. Nevertheless, in order to accurately determine the significance of KRT7 in tumor invasiveness, a dedicated quantitative analysis needs to be performed. On the other hand, the feature with the highest expression in treatment responders was m/z 1032.59, corresponding to Histone H3. Further investigation of the tissue distribution of the identified fragments revealed that overexpression of histone H3 correlated with the histological annotations of the tumor region in responders. In contrast, expression of COL1A1 was nearly absent in this section of the tissue, while in the tumor region of the non-responder patient, COL1A1 expression was stronger and correlated with the morphology of the tumor region. Although the results obtained from the various techniques employed, including DNA sequencing, RNASeq data, methylome data, and proteomic data, yielded a wide range of information, they collectively point towards the involvement of keratin-associated pathways, collagen-related pathways, and genes associated with histone methylation.
Novelty:
Invasive carcinomas obtained from patients who responded to the treatment exhibit a distinct mass spectrometry profile when compared to non-invasive carcinoma samples. Collagen α-2(I) chain (m/z = 868
Preliminary Data:
Histone H3 is overexpressed in the tumor of responders while COL1A1 was almost absent but highly expressed in the non-responders.
Contributing Authors:
Juliana P. L. Gonçalves, Wilko Weichert, Nicole Pfarr, Kristina Schwamborn

P-36

Grayson, Amy
Biomolecular Sciences Research Centre, Sheffield Hallam University, United Kingdom

Establishment of a living skin equivalent model of atopic dermatitis

Introduction:
Atopic dermatitis (AD) is a chronic inflammatory skin disease characterised by epidermal barrier dysfunction and inflammation dominated by the increased expression of Th2 cytokines. To explore treatments for AD, a representative living skin equivalent (LSE) model of AD was created and challenged with the addition of skin microbes.
Method:
A representative full-thickness in-vitro human skin model of AD was produced by stimulation of commercially available LSE constructs with a combination of interleukins over the maturation phase. Once the skin cells of the native LSE models and AD LSE models had matured, the surface of the models was inoculated with pooled microbiota collected from healthy participants to replicate the microbiota of human skin.The microorganisms associated with the normal and AD skin models were characterised using culture-based and culture-independent methods. Desorption electrospray ionisation mass spectrometry imaging (DESI-MSI) was performed to investigate the expression of lipids within the native and AD-representative skin constructs cultured with or without the addition of skin microbiota.
Results:
Microbiological analysis showed that the surface of the normal and AD model skin becomes populated with human skin-derived aerobic and anaerobic microorganisms. DESI-MSI analysis identified the presence of a variety of lipids within the epithelial layer of native and AD-representative LSE constructs cultured in the presence and absence of skin microbiota.
Novelty:
This study supports the production of a representative in-vitro model of atopic dermatitis with the addition of skin microbiome.
Preliminary Data:
DESI-MSI analysis is a powerful tool for investigating the expression of lipids in in-vitro skin models.
Contributing Authors:
A. K. Grayson1, J. Newton1, S. Forbes1, T. J. Smith1, M. Li2, J. Mao2 , M. R. Clench1 1. Biomolecular Sciences Research Centre, Sheffield Hallam University, Sheffield, UK, S1 1WB 2. Colgate−Palmolive Company, 909 River Road, Piscataway, NJ 08855, USA

P-37

Grey, Gus
University of Auckland, New Zealand

Imaging of ion and metabolite transport and metabolism in the ocular lens with mass spectrometry

Introduction:
In the absence of a blood supply, the ocular lens remains transparent through the operation of a microcirculation that delivers nutrients and removes waste products from the lens nucleus. As we age, this system is perturbed, which may lead to lens cataract. Globally, lens cataract is the leading cause of preventable blindness, yet the only 'cure' is surgical implantation of a synthetic lens. A better understanding of normal lens transport and cataract formation is required if novel therapies are to be developed. To that end, imaging mass spectrometry (MALDI and LA-ICP) has been used to map uptake and metabolism of exogenous ions and molecules, and bioinformatic tools developed to characterise spatial uptake and metabolism in normal lenses and in an aging lens model.
Method:
Bovine lenses were incubated from 5 min-20h in artificial aqueous humour containing stable isotopically-labelled (SIL) lens nutrients (glucose, glutathione), pharmaceuticals, or using ion replacement where rubidium (Rb) has replaced potassium. Axial cryosections (20um) from were analysed by negative (metabolites) and positive (pharmaceuticals) mode MALDI-FT-ICR imaging mass spectrometry (IMS), or LA-ICP-MS (for elemental analysis). Time-point data were combined using a novel analysis pipeline written in R, and the mummichog algorithm incorporated to automatically annotate and map metabolic activity regions.
Results:
For lens nutrients, the major site of uptake in the normal lens was the peripheral epithelium and lens equator, as evidenced by MALDI IMS. Metabolic pathways such as 'glycolysis and gluconeogenesis' were most active in this region. Initial ion influx as measured by Rb was also localised to the lens equatorial region. In contrast, uptake profiles and rates of transport throughout the lens for pharmaceuticals were different to nutrients, and between different pharmaceutical classes. The effect of artificial lens aging on lens nutrient and pharmaceutical uptake will be discussed.
Novelty:
IMS can be utilised in developing future therapeutic interventions that exploit lens physiological biochemistry to delay the onset of cataract.
Preliminary Data:
Comparison and contrast of ionic and molecular transport in the ocular lens.
Contributing Authors:
Angus C. Grey, George Guo, Dingchang Shi, Yann Tenier, Luis Knight, Paul J. Donaldson

P-38

Hahm, Tae-hun
Johns Hopkins University, Howard county

Optimization of slide-scanning fluorescence microscopy-guided MALDI imaging of a single, fully prepared sample

Introduction:
Fluorescence microscopy, a widely used technique in spatial biological studies, plays a crucial role in visualizing and studying biological structures. We have recently developed FluoMALDI, a novel pipeline that integrates slide-scanning fluorescence microscopy and matrix-assisted laser desorption/ionization (MALDI) imaging within a single sample. FluoMALDI is based on the discovery that MALDI matrix co-crystallization with endogenous tissue fluorophores significantly enhances innate tissue autofluorescence. Here we have examined the effects of slide-scanning fluorescence microscopy on MALDI matrix crystals and MALDI imaging outcomes to determine and minimize possible adverse effects of fluorescence microscopy. Our findings show that slide-scanning fluorescence microscopy can be utilized on fully prepared MALDI imaging samples to structurally-anatomically guide MALDI imaging acquisition from a single, fully prepared sample.
Method:
Frozen tissues were cryo-sectioned on indium-tin-oxide (ITO) slides and robotically sprayed with 0.0016 mg/mm2 MALDI matrix using HTX M3+ sprayer, followed by fluorescence imaging on widefield, slide-scanning fluorescence microscopes (Olympus, Molecular Devices) at several or single wavelength(s). Subsequently, MALDI imaging was conducted on Bruker rapifleX or timsTOF fleX MALDI imaging instruments. Frozen mouse brain, heart, and liver tissues were utilized for FluoMALDI analysis on ITO slides, which were individually coated with three different MALDI matrices to assess the FluoMALDI workflow. Specifically, we investigated the effects of wavelength and exposure time during fluorescence microscopy on matrix co-crystals and MALDI imaging. Crystals were measured using polar and light microscopy (Olympus). Fluorescence and MALDI images were analyzed using ImageJ and SCiLS Lab, respectively.
Results:
We report for the first time that slide-scanning fluorescence microscopy for the purpose of structurally-anatomically guiding MALDI imaging acquisition, requires fluorescence microscopy optimization because adverse effects on matrix co-crystals and MALDI images may occur. We deposited 9-aminoacridine, norharmane, or α-cyano-4-hydroxycinnamic acid onto separate brain tissue sections. Next, we covered the right half of each brain tissue section with an aluminum foil and performed slide-scanning fluorescence imaging using three different wavelengths: blue (DAPI filter set), green (GFP filter set), and red (TRITC filter set). Following fluorescence imaging, we removed the cover and conducted MALDI imaging of the entire sample. Our MALDI imaging data revealed that the total ion count (TIC) intensities in the mouse hippocampus regions of the left brain halves which were exposed to the three fluorescence wavelengths, were more than 10% lower than those of the right halves which were not exposed to the three fluorescence wavelengths. Microscopic analysis revealed distinct alterations in matrix crystal shapes resulting from irradiation with three fluorescence wavelengths in the left, fluorescence-exposed brain halves only. To minimize such adverse effects of fluorescence microscopy acquisition on MALDI imaging data in the FluoMALDI pipeline, we optimized several parameters. First, we reduced the exposure time for each wavelength and conducted slide-scanning fluorescence microscopy using a single wavelength only. By implementing this approach, we observed that the TIC intensities in MALDI imaging from the left hippocampus region, which was solely exposed to green or red light during fluorescence imaging, were equal to those of the corresponding right hippocampus region which was not exposed to fluorescence microscopy prior to MALDI imaging for all three matrices tested so far. We are currently further testing and optimizing fluorescence microscopy-guided MALDI imaging, expanding our study across various tissues, as well as different MALDI matrices and fluorescence microscopy systems.
Novelty:
We optimized slide-scanning fluorescence microscopy to guide MALDI imaging in the FluoMALDI pipeline to mitigate adverse effects of fluorescence microscopy
Preliminary Data:
We acquired comparative fluorescence and MALDI imaging data for optimizing slide-scanning fluorescence microscopy-guided MALDI imaging in the FluoMALDI pipeline

Contributing Authors:
Tae-Hun Hahm (Johns Hopkins University School of Medicine, thahm2@jh.edu), Avishi Garg (Johns Hopkins University School of Medicine, agarg21@jhu.edu), Hoku West-Foyle (Johns Hopkins University School of Medicine, hwestfo1@jhmi.edu), Dalton Brown (Johns Hopkins University School of Medicine, dbrow273@jhmi.edu), Cole Johnson (Johns Hopkins University School of Medicine, njohn114@jhu.edu), Caitlin Tressler (Johns Hopkins University School of Medicine, ctressl3@jhmi.edu), Scot Kuo (Johns Hopkins University School of Medicine, skuo@jhu.edu), Kristine Glunde (Johns Hopkins University School of Medicine, kglunde1@jhmi.edu)

P-39

Heintz, Dimitri
Plant Imaging Mass Spectrometry, CNRS, IBMP, France

MALDI imaging analysis of pollutant in biosolids coming from waste water treatment plants

Introduction:
Biosolids, which are treated sewage sludges, are the entry point of heavy metals (HMs) and persistent organic pollutants (POPs) in the food web by application to agricultural land. Biosolids properties are beneficial to more and more applications for reuse, which necessitates a rapid and safe examination of their toxic content. The heterogeneous structure and content of biosolids makes their analysis difficult. To date, there is no unique method for identifying and assaying the variety of toxic compounds in biosolids: the analysis of HMs is done by ICP-MS and POPs analysis is mainly covered by two complementary methods (GC-MS and LC-MS). We propose a new approach for the rapid and safe analysis of biosolids using MALDI-MSI.
Method:
1g biosolid has been solubilized in 1ml methanol/water (90:10). Drop by drop déposited on a MALDI ITO glas slide (previously covered by conducitve tape). MALDI Imaging FT-ICR 7 Tesla has been made on biosolids coming from different representative waste water treatment plant. Micropollutant were identifed using Metaboscape and SCILS and NORMAN data base interrogation. Metabolites were validated (Schymanski level 1) by MS/MS and standard confirmation.
Results:
We developped a novel method that allows rapid and safe analysis of non-cohesive solid biological samples using matrix assisted laser desorption ionization (MALDI) mass spectrometry imaging (MSI). We chose biosolid samples and performed the nontargeted screening of heavy metals (HMs) and persistent organic pollutants (POPs) as a proof of concept of our methodology. We applied our methodology to biosolids, which are heterogeneous non-cohesive solids, byproducts resulting from anthropogenic activities, produced by waste wastewater treatment plants. Biosolids are composed of human faeces, urine but also all waste from household activity. and many other things depending on the treatments undergone
Novelty:
MALDI imaging for a rapid screen of pollutant in solid soil like samples
Preliminary Data:
MALDI imaging more rapid than LC-MS/MS combined to GC-MS and ICP-MS
Contributing Authors:
Claire Villette, Loïc Maurer, Adrian Wanko, Dimitri Heintz

P-40

Eshghi, Azad
Bruker Daltonics, Canada

High spatial resolution TIMS MALDI-2 imaging of Dhcr7-KO mice reveal changes in cholesterol biosynthesis

Introduction:
Cholesterol plays an essential role in brain development and aberrant biosynthesis can negatively impact structural integrity and functioning of the brain. Smith-Lemli-Opitz syndrome (SLOS), found to be caused by mutations in the DHCR7 gene, is one example of malfunctioning in the cholesterol biosynthetic pathway. The gene encodes for the enzyme 3β-hydroxysterol-Δ7-reductase (DHCR7) that catalyzes the last step of cholesterol synthesis. Previous studies with MALDI mass spectrometry imaging have demonstrated differences in sterol abundance and distribution in WT and Dhcr7-KO neonatal mouse brains. Here, we reproduced the previous work with improved spatial resolution, greater mobility separation and MALDI-2 to obtain higher sensitivity for sterols.

Method:
Thin 10 µm fresh frozen coronal mouse brain sections of neonatal (P0) Dhcr7-KO and WT mice were cyrosectioned and thaw-mounted on IntelliSlides. Prior to MALDI imaging, sections were desiccated and spray-coated with 2,5-DHAP using the M3+ Sprayer for lipid analysis. Imaging analysis was conducted on the timsTOF fleX M2 system at 20 µm spatial resolution with TIMS in both MALDI and MALDI-2 over m/z 300-1500 and mobility range 1/k 0 0.5 – 1.8 or m/z 300-930 and mobility range 1/k 0 0.7– 1.3 (targeting sterols) in positive ion mode and beam scan mode of 200 shots per pixel and mobility ramp of 300 ms. H&E staining was performed on the same sections post MALDI acquisition. Data visualization and statistical analysis was conducted in SCiLS Lab 2023a.

Results:
Initial experimentation was conducted to compare the sensitivity of sterols between MALDI-1 and MALDI-2. As expected, a greater overall sensitivity for sterols was observed with the MALDI-2 laser, with approximately five-to-ten-fold improvement for the targeted compounds: cholesterol, 7-DHD, 7-DHC, and desmosterol as dehydrated species [M-H 2O+H] +. The results matched the expected biological effects of Dhcr7-KO, where cholesterol is depleted and 7-DHD accumulates mostly in the KO, with high spatial localization in the white matter. TIMS separation of isomeric species, desmosterol and 7-DHC, both of which are precursors of cholesterol, was achieved, revealed unique endogenous abundance. Several lipids were also found to be more intense in the KO compared to the WT, most notably m/z 754.5342 (PC 32:1+Na), m/z 782.5637 (PC 34:1+Na) and m/z 810.5978 (PC 36:1+Na), while m/z 739.4641 (DG 42:12;O2+K), m/z 744.4909 (PC 30:0+K) and m/z 798.5321 (PC 34:1+K) were found to be more intense in the WT compared to the KO.

Novelty:
Mobility enabled MALDI-2 imaging of cholesterol biosynthesis intermediates in Dhcr7-KO samples.

Preliminary Data:
Off target effects of aberrant cholesterol biosynthesis

Contributing Authors:
Ethan Yang1; Azad Eshghi1; Amy Li2; Libin Xu2; Shannon Cornett1*

P-41

Henkel, Corinna
Bruker Daltonics GmbH & Co.KG, Germany

MALDI HiPLEX-IHC Imaging in combination with SpatialOMx enhances information content in glioblastoma heterogeneity analysis

Introduction:
Glioblastoma is the most common and a highly malignant primary brain tumor with five-year survival rates below 10 %. Glioblastomas are characterized by high levels of heterogeneity within the tumor cells and the tumor microenvironment, which consists of blood vessels and necrotic cells intermingled with differentiated and stem-like tumor cells. Tumor heterogeneity influences chemotherapy resistance and local cancer cell dissemination, both connected to a high recurrence rate of > 90%. Disturbed metabolism has been reported in glioblastoma, however the spatial context that allows assessment of intratumor heterogeneity and the tumor microenvironment have hardly been studied.
Method:
Fresh frozen tissue sections from three glioblastoma patients and one astrocytoma patient were measured by mass spectrometry imaging, first acquiring information from the lipids followed by antibody based MALDI HiPLEX-IHC Imaging. Images were acquired on a timsTOF fleX MALDI-2 with 20 µm spatial resolution. TIMS ion mobility was used for the lipid imaging. Bulk tumor tissue from the same patient was homogenized and lipids were extracted via MTBE phase separation and measured via LC-MS/MS and TIMS ion mobility (4D-Lipidomics) on the timsTOF fleX. MetaboScape was used for annotation of MALDI-imaging data using m/z values in combination with the measured collisional cross sections.
Results:
MALDI HiPLEX Imaging based on cell type specific antibodies revealed different cellular compositions in the four brain tissue samples. Glia cells were more evenly distributed over the tissue and showed variation between the four samples compared to immune cells. CD4 T-cells were more intense in the tumor tissue areas, while macrophages partially colocalized with collagen 1 in round structures, which we hypothesize to be areas of stem cells. One glioblastoma tumor contained many B-cells, which are rarely studied in this tumor type. Some lipids and metabolites were co-localized with macrophages, B-cells and astrocytes indicating cell-type specific molecular compositions. Lipid mass spectrometry imaging showed spatial heterogeneity in the tumor microenvironment as well as inside the tumor areas.
Novelty:
SpatialOMx and MALDI HiPLEX Imaging allowed detailed assessment of intratumor heterogeneity and the tumor microenvironment, which are both relevant to glioblastoma recurrence and therapy success.
Preliminary Data:
SpatialOMx in combination with MALDI HiPLEX-IHC Imaging can demonstrate spatial and cell-type specific lipid analysis
Contributing Authors:
Corinna Henkel1, Signe Frost Frederiksen1, Matthias Szesny1, Jörg Bartsch2, Kate Stumpo3, Melanie Föll4, Oliver Schilling4 1Bruker Daltonics GmbH & Co.KG, Bremen, Germany 2 Department of Neurosurgery/Lab, Faculty of Medicine, Philipps-University, Marburg, Germany 3 Bruker Scientific LLC, Billerica, MA 01821, USA 4Institute of Surgical Pathology, Faculty of Medicine – University of Freiburg, Germany

P-42

West, Connor
Bruker, United States of America

Software workflow and statistical analysis tools for evaluating multiomics MALDI MSI studies

Introduction:
Matrix assisted laser desorption/ionization mass spectrometry imaging (MALDI MSI) is an established analytical method for both targeted and untargeted spatial profiling in lipidomics, metabolomics, proteomics, and glycomics studies. Moreover, by using multiple acquisitions from the same tissue sample with different protocols, multiomics studies can be performed that allow for the investigation of spatial correlations between the distribution patterns of, for example, proteins, lipids, and glycans. We present a unified software workflow for performing such multiomics MSI data analyses, allowing one to apply state-of-the-art visualization tools and computational analysis algorithms to such multiomics datasets. Several application examples highlight the value and flexibility of this workflow.

Method:
MALDI MSI data was acquired using various protein, lipid, and glycan imaging protocols. The multiomics data analysis workflow consists of a) importing each dataset into a proprietary format, b) co-registering one or more source datasets with a target dataset based on corresponding optical or ion images, c) extracting spectral features from the source dataset(s) and mapping them to the target dataset spot raster, and d) applying standard visualization and statistical analysis tools for joint evaluation of the different -omics studies. In addition, a scripting API makes the multiomics data available for customized analysis or reporting workflows, or for integration with third party software. All software components are available as part of a commercial MSI software package (SCiLS Lab).

Results:
The described workflow was successfully applied to several multiomics studies: 1. In a targeted MALDI imaging study, a panel of photocleavable mass-tagged antibodies against 13 different protein markers were used to acquire highly specific spatial distribution images of these proteins at a lateral resolution of 20µm (MALDI HiPLEX-IHC). This protocol was applied to a fresh frozen mouse brain section and combined with untargeted lipid imaging data from the same section. Spatial co-localization analysis yielded specific lipid signals showing high spatial correlation to some of the protein antibodies, including myelin, synapsin-1, and amyloid beta. 2. Targeted MALDI HiPLEX-IHC imaging of a fresh frozen glioblastoma xenograft sample using a 5-plex panel of photocleavable mass-tagged antibodies was combined with untargeted lipid imaging from the same section, both acquired at 20µm lateral resolution. Joint multiomics analysis and visualization of both datasets revealed spatial correlation between certain lipid species imaged in the untargeted acquisition and antibody markers from the targeted protein imaging study. 3. In a multi-glycomics study, N-glycan imaging from a human colorectal cancer FFPE tissue section was combined with mucin-domain O-glycopeptide imaging facilitated by the mucin-selective protease StcE. For different compartments of the tumor, spatial correlation analysis enabled highlighting of respective co-localized O- and N-glycan species, thus providing more insight into the glycobiology of these tumors.

Novelty:
A unified data analysis workflow allows applying state-of-the-art visualization and analysis tools to various types of multiomics studies.

Preliminary Data:
The multiomics imaging workflow enabled us to quantitatively analyze spatial correlations between different molecular domains, yielding additional insights into the biology of the investigated tumors.

Contributing Authors:
Tobias Boskamp Sören Deininger Mark Lim Gargey Yagnik Natalie Agar Sylwia Stopka Rick Drake Stacy Malaker Rachel Stubler Kenneth Rothschild Katherine Stumpo

P-43

Ísberg, Ólöf Gerdur
Vanderbilt University, United States

Out-of-Sample Prediction Across Large-Scale IMS Datasets by Data-Driven Image Fusion

Introduction:
Matrix-assisted laser desorption/ionization imaging mass spectrometry (MALDI IMS) enables the untargeted, highly multiplexed mapping of a wide range of biomolecules, such as small metabolites, lipids, and proteins in situ. However, limitations in throughput and spatial resolution make performing MALDI IMS impractical for applications that require more than a few million pixels – e.g., high spatial resolution whole slide imaging (WSI) and 3-dimensional (3-D) molecular imaging. Herein, we assess the potential for data-driven image fusion to aid in advancing these two challenging application areas by providing predictions to complement classical ion measurements. By registering and fusing IMS and complimentary microscopy modalities, we aim to develop practical sampling methods that allow for robust ion distribution predictions across WSIs as well as 3-D volumes.
Method:
Human kidney tissue was cryosectioned at a 10-µm thickness and thaw mounted onto indium tin-oxide (ITO) coated glass slides. Autofluorescence microscopy (AF) images were acquired using EGFP, DAPI, and DsRed filters on a Zeiss AxioScan Z1slide scanner prior to MALDI matrix application. Samples were sublimated with a 2.5 mg/mL solution an aminated cinnamic acid analog. MALDI IMS was performed from m/z 300 to 1600 on a Prototype Bruker timsTOF Pro (Q-TOF) MS system (BrukerDaltonics, Bremen, Germany) in positive and negative ion modes. The images were collected with a 10 µm pixel size with 100 laser shots per pixel at 35% laser energy. Ion image data was visualized using SCiLS Lab Version 2023 and subsequently processed using an in-house processing pipeline.
Results:
A mock 3-D data set was collected to assess data-driven image fusion for out-of-sample prediction across serial human kidney whole slide images. All cryosections were collected with 10-µm thickness. Sets of 3 consecutive sections were collected for every 20 sections cut. Five 3-section sets were collected in total, with the first set including sections 1, 2, and 3, the second set including sections number 21, 22, and 23, and so on. For each set, every section was analyzed using AF microscopy to enable automated segmentation of nephron substructures using previously developed tools. The first section in each set was then analyzed using IMS in positive ion mode. A rectangular measurement region was analyzed with 10-µm pixel size resulting in ~1.2 million pixels, ensuring that all kidney structures were sampled (e.g., cortex, medulla, and vasculature). A similar analysis was performed on the third section of each set but in negative ion mode. These data are used to construct posIMS-AF and negIMS-AF fusion models in-section between MALDI IMS and AF/stained microscopy measurements, using in-house tools (http://fusion.vueinnovations.com/). These enable certain positive and negative mode ion species to be predicted on the basis of microscopy in the second tissue section of each 3-set, both at 10-µm and 5-µm pixel sizes. To assess ion distribution prediction, ground-truth IMS measurements were also collected on the second tissue section. Multiple measurement regions were collected from the medulla and cortex with both 10-µm and 5-µm pixel sizes, for both positive and negative ion modes. This approach was repeated on all five sets of tissue sections, after which all samples were stained with Periodic acid-Schiff (PAS) and imaged with brightfield microscopy. Fusion performance is assessed across all detected ions. These experiments will inform intelligent sampling methods to leverage data-driven image fusion to make large-scale 3-D tissue mapping more practical.
Novelty:
We investigate and evaluate how out-of-sample prediction based on data-driven image fusion can advance high-spatial-resolution IMS across 3-D tissue volumes.
Preliminary Data:
Out-of-sample IMS prediction of several known lipids from 5µm-pixel size to 1-µm resolution based on co-registered stained microscopy.
Contributing Authors:
Olof Gerdur Isberg, Lukasz G Migas, Melissa A Farrow, Madeline Colley, Jamie L. Allen, Haichun Yang, Mark P De Caestecker, Raf Van de Plas, and Jeffrey M Spraggins

P-44

Jia, Yifeng
University Oxford, United Kingdom

Optimisation on the new generation of microscope mode secondary mass spectrometry imaging

Introduction:
Mass spectrometry imaging (MSI) is a highly robust technology employed for the detection and characterization of mass and chemical distribution. It has found extensive utility in the fields of biology and diagnostics. Microscope mode MSI, in particular, showcases remarkable potential for large-scale clinical applications owing to its inherent high throughput advantage. However, the current limitations of low mass and spatial resolution significantly constrain the ability of MSI to achieve precise detection. To address this challenge, we have implemented a novel technique known as Post-Extraction Differential Acceleration (PEDA) in microscope mode Secondary Ion Mass Spectrometry (SIMS). This innovative approach enhances the mass resolution over a wide mass range, thereby enabling the realization of rapid MSI.

Method:
To enhance mass resolution, we implemented a voltage pulse on the extractor to optimize ion time-focusing along the Time-of-Flight (ToF) axis. By fine-tuning baseline and end voltages, and selecting precise trigger times, we achieved significant improvements. The pulse shape of the extraction voltage was modified to an exponential profile, providing varying accelerations for ions of different masses. Experimental results were validated through SIMION software simulations, and a genetic algorithm guided the optimization of PEDA voltage and pulse trigger timing. In terms of spatial resolution optimization, we employed two strategies: reducing lateral diffusion and increasing magnification. These factors are controlled by the voltage difference between the surface and extractor, as well as the Einzel lens voltage. Similar to the mass resolution optimization, the voltages were optimized using a genetic algorithm within the SIMION software and fine tuning experimentally.

Results:
In our high-throughput SIMS MSI setup, we integrated extraction optics, a commercially available C60+ primary ion beam (Ionoptika Ltd), a time-of-flight (ToF) tube, and a detector assembly consisting of a microchannel plate (MCP), scintillator, and Timpix3 camera, CCD camera, and Pixel Imaging Mass Spectrometry (PImMS) 1 camera. In the single-field PEDA, optimized differently at each individual mass, we achieved a mass resolution of 100 Da peak from 100 to 1600 Da using a step-shaped pulse. To optimize mass resolution for a range of masses, we applied an exponential pulse on the extractor plate. The mass resolution for a 399 Da mass peak was improved from 705 m/Δm to 6907 m/Δm, effectively resolving a previously confluent peak into three distinct mass peaks. The simulated results (conducted using SIMION software) were validated through experiments. These simulations confirmed the observed enhancements and indicated the potential for optimizing the mass range of the SIMS instrument to reach 2000 Da (ranging from 2000 Da to 4000 Da). Moreover, the theoretical maximum mass resolution in this optimized mass range was estimated to be 10,000. To demonstrate the spatial resolution, we used Rhodamine B as the sample, which was electro-sprayed through a nickel mesh with a grid size of 102 µm. The image was collected by an intensified CCD camera. With the optimization, the spatial resolution was increased from 23 µm to 12 µm. However, simulations indicate that the theoretical best spatial resolution can reach about 2 µm.

Novelty:
Fully optimisation of the new generation microscope mode secondary ion mass spectrometry imaging.

Preliminary Data:
Mass resolution of about 6900 at 399 Da, spatial resolution of about 12 µm.

Contributing Authors:
Yifeng Jia1, M. Elena Castellani12, Weiyu Kan1, Zoltan Takats2, Mark Brouard1, Felicia Green12

P-45

Johnson, Nicholas
Johns Hopkins University School of Medicine, USA

Innovative Software Solutions for Measuring Analyte Delocalization in MALDI Imaging

Introduction:
Matrix-assisted laser desorption/ionization (MALDI) mass spectrometry imaging (MSI) can be used to detect the spatial distribution of a wide range of analytes in tissue sections. As the spatial information provided by MALDI MSI is its primary advantage over non-imaging mass spectrometry approaches, preserving the localization of analytes throughout the MALDI MSI pipeline is of paramount importance. We have previously shown that delocalization of analyte signals in MALDI MSI depends on the method of matrix deposition. Our previous work evaluated the effects of matrix spraying parameters on delocalization, however, established methods of manually measuring delocalization were found to be imprecise. Here we developed a new software tool that measures delocalization and applied it to MALDI MSI experiments to minimize delocalization.
Method:
Fresh frozen heart, kidney, and brain tissues harvested from athymic nude mice were cryo-sectioned at 10 µm thickness onto indium tin oxide (ITO) slides using a Leica cryostat. Samples were sprayed with 10 mg/mL 1,5-diaminonapthalene (DAN) matrix in 50%, 70%, or 90% acetonitrile (ACN) with 0.2% trifluoroacetic acid (TFA) using an HTX M5 Sprayer. Sections were then imaged using a Bruker MALDI TOF/TOF rapifleX instrument running in reflectron positive mode with 100-micron raster, 100-micron m5 imaging laser, and mass range of m/z 0-3200. Delocalization was measured using a home-built software written in R that subsets MALDI imaging data into on-tissue and off-tissue sections, then measures the shortest distance from each point on the delocalization front to the tissue boundary.
Results:
To test our software, we re-analyzed data sets published in Tressler et al (JASMS 2021) which demonstrated the use of factorial design of experiments (DOE) to optimize spraying methods for matrix deposition in MALDI imaging. These data sets were re-analyzed using our home-built R-based software and compared with the published manual delocalization measurements. Our software measures delocalization along the entire tissue boundary rather than only at four representative averaged points as in the manual approach. For several of the tested matrix spraying conditions, we found a significant difference in the amount of delocalization when comparing manual with automated delocalization measurements. We then re-ran the DOE based on the automated delocalization measurements to determine new optimized spraying conditions. These re-analyzed DOE data show that tray temperature, flow rate, nozzle speed, and the combination of flow rate and nozzle speed were all key factors that affected the extent of delocalization. Previously, when basing the DOE optimization on manual delocalization measurements, only the first three factors were significant. Using our automated delocalization measurement software, we calculated a new optimized set of spraying parameters, which we tested experimentally, and which resulted in less delocalization than previously reported for DOE optimization based on manual delocalization measurements. One predominant theory suggests that higher water content in the solvent for matrix spraying leads to more analyte delocalization. To test this theory, we are currently working with data sets in which we are using our new software to measure the delocalization under different solvent conditions for matrix spraying. Our data indicate that not all analytes delocalize under the same solvent conditions for matrix spraying. We have selected four different peaks across the m/z range measured in four different organs for analysis with our delocalization software to understand the role of organ type and solvent composition on analyte delocalization.
Novelty:
New software tool that measures analyte delocalization in MALDI imaging to effectively optimize matrix spraying conditions and better understand delocalization
Preliminary Data:
Preliminary results show that different peaks react differently to changes in solvent composition.
Contributing Authors:
Cole Johnson, Ethan Yang, Nathan Riemann, Jason Fan, Eric Barton, Kristine Glunde, Caitlin Tressler

P-46

Jones, Caroline
Kratos Analytical Ltd., UK

Benchtop Matrix Assisted Laser Desorption Ionisation Mass Spectrometry Imaging (MALDI-MSI) of Human Tonsil Proteins using MALDI HiPLEX-IHC Probes

Introduction:
The human tonsil provides a rich site for the study of immune cell function with the potential to enhance research into autoimmune disease, food allergies, oncology and vaccination strategies amongst others. MALDI-based MS imaging has traditionally been the realm of high-end/high performance instrumentation. Here, we evaluate the performance of an entry-level MALDI imaging solution, in combination with the Miralys™ MALDI HiPLEX-IHC probes (AmberGen Billerica, MA), for precise mapping of immune cell populations within FFPE human tonsil tissue sections.

Method:
Prior to the mounting of tissue sections, ITO slides were coated with 20µl 50:50 Poly-L-lysine solution: H2O containing 0.07% IGEPAL-CO63. The mounted slides were immersed in a series of wash solutions (Ethanol: aqueous in varying concentrations) prior to antigen retrieval through exposure to 10mM citric acid. Following application of antibodies with novel photocleavable mass-tags (AmberGen, Billerica, MA) and subsequent coating with CHCA using a sublimation device (iM Layer, Shimadzu Corporation), tonsil sections were imaged in linear mode (50µm spacing) on a MALDI-8020 benchtop MALDI-TOF mass spectrometer (Shimadzu Corporation). Imaging files were processed using IonView software (Shimadzu Corporation).

Results:
In this work, we investigate the feasibility of multiplexed imaging analysis using a benchtop MALDI-TOF system. Using a panel of 6 biomarker probes, we are able to image the tonsil tissue sections with a stage step size of <100 µm . We have shown previously it is possible to achieve higher spatial resolution using this platform, although there are a number of factors that will influence the achievable spatial resolution including quality of tissue preparation, successful washing and antigen retrieval and matrix application. The use of the Miralys™ MALDI HiPLEX-IHC probes enables the study of much larger biomolecules within the target m/z range of the mass tags (m/z 1000-3000), overcoming the sensitivity issues associated with high mass intact protein MALDI imaging. We demonstrate that in this target mass range, the benchtop system is capable of resolving mass tags differing by only a few m/z. This is demonstrated using two mass tags differing by ~4Da.

Novelty:
Good quality, multiplexed protein imaging on an entry level MALDI-TOF MS system.

Preliminary Data:
Data demonstrating the capabilities of the benchtop system for high mass protein imaging of other sample types. Data acquisition for samples treated with the photocleavable mass-tags is in progress.

Contributing Authors:
Simona Salivo, Matthew Openshaw

P-47

Khajavinia, Amir
College of Pharmacy and Nutrition, University of Saskatchewan, Canada

Synthesis and characterization of nanodiamond-based MALDI matrices for the analysis of small molecules

Introduction:
In conventional matrix-assisted laser desorption ionization- mass spectrometry (MALDI-MS), the low-mass range of a spectrum is occupied with interfering peaks of the matrix, constituting its fragments, adducts, and cluster ions. The complexity of the spectra in the low-mass range limits the use of MALDI-MS for the analysis of low molecular weight (LMW) organic compounds. Immobilizing conventional matrices on the surface of nanoparticles has shown promising results for the MALDI-MS analysis of LMW analytes. In this study, we are designing new functionalized nanodiamonds (NDs) as MALDI matrices for the identification of LMW compounds, namely psychoactive compounds as model drugs. These matrices can theoretically be applied in MALDI imaging to increase the sensitivity of imaging applications.
Method:
Lysine-ND, lysyl-histidine-ND, and lysine/lysyl-histidine-ND are synthesized using our previously established protocols. The functionalized NDs were characterized using differential thermal gravimetric analysis. The particle size of the NDs was between 200-250 nm, and their zeta potential (i.e., surface charge) was between 20-30 mV measured using a Malvern Zetasizer Nano ZS instrument. A QSTAR® XL Hybrid MALDI-MS/MS System equipped with MALDI source will be used to test the synthesized NDs as MALDI matrices. Different concentrations of nanodiamonds, different spotting techniques, and solvents will be tested to optimize the analysis. Psychoactive compounds, namely psilocin, tetrahydrocannabinol (THC), and cannabidiol (CBD) are used to illustrate the utility of these novel matrices.
Results:
Initial MALDI-MS analysis using the lysine-NDs showed that the psychoactive compounds were detectable in the negative ion mode confirming the advantageous performance of functionalized NDs in MALDI analysis. The data revealed that the tested pharmaceuticals were favorably ionized in the negative ion mode, which is desirable when using biological samples as interferences from endogenous compounds are minimized in comparison with the more widely used positive ion-mode. The experimental conditions are currently being optimized by testing different solvents, different concentration combinations of the matrix and analyte, and different spotting techniques. In addition, NDs coupled with conventional matrices will be tested as MALDI matrices. The next step for this work will be testing these new matrices for the MALDI-MSI analysis of small molecules in animal tissues. In addition, NDs coupled with conventional matrices will be tested as MALDI matrices. The next step for this work will be testing these new matrices for the MALDI-MSI analysis of small molecules in biological samples.
Novelty:
New functionalized NDs are synthesized and tested for the analysis of psychoactive compounds in biological tissues for the first time.
Preliminary Data:
The functionalized nanoparticles were successfully engineered showing analyte signal in negative ionization.
Contributing Authors:
Amir Khajavinia, Iulia-Andreea Spataru, Ildiko Badea, Anas El-Aneed

P-48

Kittrell, Caroline
Medical University of South Carolina, United States of America

Establishing the Glycomic Profile of Immune Cell Clusters in Pancreatic Ductal Adenocarcinoma Tissues Using Combined MALDI MSI and MALDI IHC

Introduction:
Pancreatic cancer, one of the leading causes of cancer related mortality globally, has been suggested to have an immune quiescent tumor microenvironment. The lack of active immune cells within and surrounding pancreatic ductal adenocarcinoma (PDAC) tumors has been linked to the inability of immune checkpoint inhibitor therapy to provide curative results for patients with pancreatic cancer. Without a better understanding of immune cell population composition, metabolism, and activity within PDAC, it may be impossible to treat PDAC effectively with immunotherapy.
Method:
Utilizing histopathologic samples collected from patients with varying stages of PDAC, our lab has characterized the glycogen and N-linked glycan profile of immune cell clusters within and surrounding pancreatic tumors via MALDI-MSI. Candidate immune clusters were identified with Mayer's hematoxylin staining prior to PNGase F Prime digestion and MALDI-MSI. Glycogen deposits were identified by digestion with amylase. Additionally, we analyzed the cell composition of each immune cluster with photocleavable mass tags from AmberGen Inc. in highly multiplexed immunohistochemistry based on MALDI-MSI (MALDI-IHC). We selected antibodies targeting immune cell markers (CD3, CD8, CD11b, CD20, and CD68) and extracellular matrix components (E cadherin, Collagen 1A1, and actin αSmooth Muscle) specifically for this analysis.
Results:
We have found that high mannose and a diverse set of core fucosylated N-linked glycans are typical of immune cell clusters within and surrounding PDAC tumors. The presence of glycogen was evaluated for localization within the immune clusters and surrounding tumor microenvironment. Glycan colocalization was possible for immune cell clusters at the 60-micron level. Also, we have established that CD20+ B cells account for approximately 70% of the signal colocalized with these immune cell clusters within and surrounding pancreatic tumors based on MALDI-IHC. Signal from CD3+ T cells was also found to colocalize with predetermined immune cell clusters. In future studies we plan to link immune glycan profiles with progressive stages of pancreatic cancer and immunotherapy response.
Novelty:
A glycomic profile created via N-glycan and immunohistochemical analysis of immune clusters may be used as an immunotherapy response biomarker.
Preliminary Data:
We defined glycans typical of immune cell clusters in PDAC and described the immune cell composition of said clusters.
Contributing Authors:
Caroline Kittrell, Lyndsay Young, Jordan Hartig, Kameisha Rashford, Gargey Yagnik, Mark J. Lim, Kenneth Rothschild, and Richard Drake

P-49

Knizner, Kevan
North Carolina State University, USA

Automatic Z-Axis Correction for IR-MALDESI-MSI of Uneven Surfaces

Introduction:
Infrared matrix-assisted laser desorption electrospray ionization (IR-MALDESI) is a hybrid ionization source that combines the benefits of electrospray ionization (ESI) and matrix-assisted laser desorption/ionization (MALDI). The depth of focus of focused IR light is smaller than that of an ultraviolet light, making it more difficult to analyze intact and uneven samples in mass spectrometry imaging (MSI) studies. To ameliorate this, a chromatic confocal probe (CA probe) was installed in the IR-MALDESI source and used to measure the sample surface height at each coordinate of a region of interest (ROI). The height measurements were used to change the height of the stage to keep the sample surface within the depth of focus of the IR laser throughout the MSI analysis.
Method:
A chromatic confocal (CA) probe, a sensitive distance-measuring sensor, was incorporated into the NextGen IR-MALDESI source which contains a computerized three-dimensional translation stage. The sample surface is measured at each coordinate of a region of interest (ROI) by the CA probe. New functions were written for the MATLAB-based instrument control software (RastirZ) to record the height measurements and convert them into a guidance file that adjusts the Z-axis to compensate for the sample height variations and maintain the sample surface at the focal point of the laser throughout the MSI analysis. This process was automated with the addition of analyzing arbitrary spatial patterns with the Z correction enabled to reduce analysis time for MSI of uneven samples.
Results:
As a proof of concept, sectioned mouse liver on a tilted microscope slide to impose a constant height increase across the sample surface and was analyzed by IR-MALDESI with and without the automatic Z correction. The sample was measured at each location in a rectangular ROI by the CA probe, then analyzed by IR-MALDESI-MSI, which resulted in consistent spot sizes (~50 µm) and measured abundances of cholesterol ([M-H2O+H+]+ = m/z 369.3516) across the sample despite the height gradient when the Z correction was enabled. Irregular spot sizes and reduced signals were observed without Z correction. The ability to image arbitrary spatial patterns was combined with the Z correction for increased user-friendliness and reduced experiment time. This was validated by analyzing burn paper on a tilted glass microscope slide similar to the initial proof of concept experiment. An arbitrarily drawn bat was created from firing the laser at burn paper, where the resulting spot sizes were comparable across the entire ROI. A Prilosec tablet containing an imprinted "P" on its surface was chosen as a sample with a heterogenous height profile and was analyzed with and without Z correction. Triethyl citrate, part of the enteric coating of the pill, was detected homogeneously (RSD = 39%) when Z correction was enabled. In contrast, regions of low measured abundance and higher variation (RSD = 61%) were observed without Z correction because the sample surface height deviations exceeded the depth of focus of the laser. Finally, an intact hen liver was imaged with the auto Z correction to improve ablation-based 3D MSI. Height measurements were recorded for each new layer. This automation removes the need to pre-determine the depth resolution before analysis, nor does it require manually increasing the position of the z-axis between layers like in previous ablation-based 3D IR-MALDESI-MSI studies.
Novelty:
First method to automatically focus the sample surface during an IR-MALDESI-MSI analysis of uneven and intact samples.
Preliminary Data:
Automatic Z correction improved data generated by IR-MALDESI on mouse liver, a Prilosec tablet, and intact hen liver.
Contributing Authors:
Ying Xi, Kevan T. Knizner, Kenneth P. Garrard, David C. Muddiman

P-50

Krestensen, Kasper
M4i - Maastricht MultiModal Molecular Imaging Institute, The Netherlands

High resolution 14-plex MALDI-IHC on fresh frozen MALDI-MSI measured human brain tumour tissue

Introduction:
A novel technology is emerging, combining matrix-assisted laser desorption/ionization (MALDI), mass spectrometry imaging (MSI) and immunohistochemistry (IHC), to achieve highly multiplexed, targeted imaging of biomolecules in tissue. The new technique, MALDI-IHC, allows targeting of multiple molecules of interest using MALDI-MSI with no risk of overlapping antibody signals, in contrary to standard IHC. In this study, the multimodal capacities of MALDI-IHC are explored by comparing (1) MALDI-IHC on previously MSI-measured tissue sections with (2) unmeasured tissue sections. Furthermore, the applicability of MALDI-IHC is advanced by analysing fresh frozen brain tissue rather than FFPE tissue, comparing multiple brain tumour types and by pushing the spatial resolution to 5x5 µm pixel size.
Method:
Human fresh frozen brain tumour tissue sections (low grade glioma and gliobastoma) were stained with photocleavable mass-tagged antibodies targeting 14 brain tissue markers for multiplexing, both tumour and non-tumour specific, and analysed with MALDI-IHC. Images were acquired on a Bruker rapifleX MALDI Tissuetyper with a pixel size of 5x5 µm for high spatial resolution images. To investigate the multimodal capacities of MALDI-IHC, some tissue sections were measured with traditional MALDI-MSI on a Bruker rapifleX MALDI Tissuetyper with a pixel size of 30x30um, prior to MALDI-IHC staining.
Results:
Based on initial results, 10 out of 14 mass tags were successfully detected in the previously MALDI measured area and showed distinct and different spatial distributions within the tissue section. For example, while the mass tag targeting myelin basic protein showed a relatively homogenous distribution through the tissue, the mass tag for synapsin-1 showed areas of highly localised intensity in very few pixels at a time, scattered through the tissue. A similar 'spot-like' staining is observed with traditional immunohistochemistry targeting synapsin-1, corresponding with the targeted synaptic vesicles. A similar trend of small single-digit pixel clusters of high intensity was observed with the mass tag for amyloid-beta 42. While the mass tags were detected on both earlier MALDI measured and non-measured slides, the observed intensity of the MALDI-IHC measurement was significantly higher on slides not previously measured with MSI, however further experiments are needed to compare. With optimisation of the staining protocol conditions, it is expected to detect all 14 mass tags.
Novelty:
The effect of MALDI-MSI measurement prior to MALDI-IHC is shown on fresh-frozen brain tumour tissue at 5x5 µm spatial resolution.
Preliminary Data:
There is significant difference in MALDI-IHC intensity observed between previously MALDI-MSI measured and non-measured fresh frozen tissue sections.
Contributing Authors:
Kasper Krestensen, Eva Cuypers, Ron Heeren

P-51

Kubo, Akiko
Kobe University, Japan

MS imaging for short chain fatty acid of murine small intestine by on-tissue derivatization using N,N,N trimethyl-2-(piperazin-1-yl)ethan-1-aminium iodide (TMPA).

Introduction:
In the intestinal tract of organisms, there are long-chain fatty acids from the breakdown of lipids and short-chain fatty acids resulting from the activity of intestinal microorganisms. They are absorbed via intestinal epithelium and transported to the liver by the bloodstream. Short-chain fatty acids in the intestinal tract can be quantified by LC-MS and GC-MS, but due to their volatility and poor ionization efficiency, in situ visualization methods for imaging mass spectrometry have not been established. Therefore, we attempted to visualize short-chain fatty acids in fresh-frozen sections by on-tissue derivatization using N,N,N trimethyl-2-(piperazin-1-yl)ethan-1-aminium iodide (TMPA), which has quaternary ammonium group and 1-[Bis(dimethylamino)methylene]-1H-1,2,3-triazolo[4,5-b] pyridinium 3-Oxide Hexafluorophosphate (HATU), a reagent that condenses carboxylic acids with amines.
Method:
10-µm-thick fresh frozen sections of the small intestine of mice were prepared and dried in a cryostat chamber at -20°C. Derivatization reagents, containing TMPA (10 mM), HATU (5 mM), and 4-methylmorpholine (5 mM) in acetonitrile were applied to tissue sections. The derivatization reagent coated tissue sections were incubated in saturated acetonitrile gases at room temperature for 4 h. These were coated with the 1,5-Diaminonaphthalene (DAN) or 9-aminoacridine (9-AA) matrix. MSI analysis was performed using the iMScope QT atmospheric MALDI equipped with an optical microscope and the LCMS-9030 (Shimadzu). Tissue sections were stained with hematoxylin and eosin after MSI acquisition. Data analysis was performed using the IMAGEREVEAL MS (Shimadzu).
Results:
Short- and long-chain fatty acids in murine small intestine and intestinal contents were successfully derivatized by the on-tissue derivatization method and visualized by MS imaging. The basic derivatization was performed according to the methods of Sun et al., (Analytical chemistry 2020.92, 12126), but the composition of the reaction solution was modified by adding 4-methylmorpholine, an amine that does not react with carboxylic acids in the presence of HATU, to the reaction system. Since the short-chain carboxylic acids present in the intestinal tract are highly volatile, tissue sections were thaw mounted to ITO glass slides, dried in a cryochamber at -20°C, placed in conical tubes containing silica gel, and brought to room temperature. Then coated with the mixed derivatization reagent. Using this technique, short-chain fatty acids, which would otherwise volatilize under vacuum, were converted to nonvolatile quaternary amines, which were successfully detected by MALDI-MSI. Butyrate-TMPA and pentanoate-TMPA were detected primarily from the interior of the digestive tract, while lactate-TMPA and palmitate-TMPA were detected mainly in the villus in the small intestine. This reflects the absorption of lactic acid and long-chain fatty acids into the intestinal epithelium in the small intestine.
Novelty:
We have developed a method for MS imaging to visualize volatile short-chain fatty acids present in frozen tissue section.
Preliminary Data:
Short chain fatty acids butyrate-TMPA and pentanoate-TMPA were detected at gastrointestinal contents by MS imaging.
Contributing Authors:
Akiko Kubo (Kobe University) Kaoru Nakagawa, Manami Kobayashi(Shimadzu Corporation)

P-52

Leach, Gillian
University of Victoria, Canada

Workflow Optimization for Single-cell Metabolomic Profiling of Ovarian Cancer Cells

Introduction:
The application of transmission-mode Matrix-Assisted Laser Desorption/Ionization (t-MALDI) is one of the technological advancements that has enabled single-cell Mass Spectrometry Imaging (MSI). High-resolution t-MALDI images can have a pixel size of 1 µm, allowing collection of mass spectral information at the cellular level, while maintaining desired sensitivity. To address the present scarcity of established MSI workflows, this work describes development of an MSI method to metabolically type single cancerous cells. This method was develop using ovarian cancer tumors as a model. Future applications include characterization of cells in ascites, an abdominal fluid accumulation that is a common symptom of High-Grade Serous Ovarian Cancer (HGSOV). Ascites contains a mix of cancerous and healthy cells and is associated with poor patient prognosis.
Method:
Optimization was preformed on OVCAR3 tumours. Embedded tumours were cryosectioned (10-12 µm) and mounted onto Indium Tin Oxide (ITO) slides. The following matrices were tested in combination with different solvent preparations: 9-Aminoacridine (9AA), 2,5-Dihydroxybenzoic acid (DHB), α-Cyano-4-hydroxycinnamic acid (CHCA), and 1,5-Diaminonaphthalene (DAN). Matrix was deposited using a bespoke sublimation apparatus or an HTX M5 Sprayer (HTX Technologies). Data Acquisition was performed on a custom t-MALDI-2 source (Spectroglyph) consisting of transmission mode and coupled to a Q-Exactive Ultra-High Field Orbitrap (HF) mass spectrometer (Thermo Scientific). Data were collected using both MALDI Injector (Spectroglyph) and Tune (Thermo Scientific), and processed using ImageInsight (Spectroglyph). Datasets were uploaded to METASPACE for annotation. Tandem MS was used on select analytes to increase confidence of annotation.
Results:
Matrix mixes and application methods were optimized to achieve sufficient matrix density with minimized crystal size. DAN matrix protocols were successfully applied to yield <5 µm matrix crystals, while not affecting signal as to hinder annotation significantly. The Spectroglyph modified Orbitrap was used successfully in transmission geometry with a spot size of 1µm on OVCAR3 tumour sections to investigate metabolites relevant to ovarian cancer. Ablation quality was greatly influenced by alignment of the laser path and beam focus requiring these conditions to be tested before each analysis. Optimized instrumentation parameters were developed within the m/z range of 50-1000, with a focus on optimizing signal of m/z range of 100-500. Improvements in sample preparation and data acquisition yielded an abundance of spatially heterogeneous metabolites within the tumour microenvironment. METASPACE was used to successfully annotate several metabolites with ≤ 5% false discovery rate. Tandem MS was preformed to target several of the annotated metabolites to increase confidence of annotation. We are currently working on applying the workflow to single cells from OVCAR3 cell culture. Slide preparation for single cells as described by Cuypers and colleagues (PMID: 35413180) is being implemented and optimized for OVCAR3 single cells. The slides will be prepared and processed for MSI analysis (vide supra), with slight adaptations for single cells, such as 1µm step size. Biological and technical replicates will be used. Ultimately, we aim to collect mass spectra from over 100 individual cells to create a library of metabolomes. These data will be used to create an archetypal metabolome for OVCAR3 single cells, taking into consideration key distinguishing ions and relevant cancer metabolites. This workflow can then be applied to metabolically type other HGSOV-related cells and, further, to determine the cellular identities of ascites fluid cells.
Novelty:
Creating a metabolomic profile of ovarian cancer cells using single-cell analysis via a t-MALDI-2 source coupled to a Q-Exactive Orbitrap.
Preliminary Data:
A workflow has been optimized on OVCAR3 tumour sections.
Contributing Authors:
Gillian Leach Helena Petrosova Angela Jackson Gillian Carleton Ron M. A. Heeren Eva Cuypers Julian J. Lum Mikhail E. Belov David R. Goodlett

P-53

Lim, Mark
AmberGen Inc., USA

High-Plex, Multiomic and Multimodal Imaging of PANTHOS Neuronal Degeneration in Model Alzheimer's Transgenic Mouse Brain using MALDI-IHC

Introduction:
Alzheimer's Disease (AD) kills more people in the U.S. every year than breast and prostate cancers combined. Recent progress has been made in understanding AD pathology using transgenic AD mouse models, including 5XFAD-TRGL transgenic mice, where a fusion of the LC3 autophagosome marker with mRFP-eGFP is expressed selectively in neurons using a Thy1 promoter, enabling fluorescence imaging of relative pH in autophagy–lysosomal neuronal processes. This reveals that autophagy dysfunction arises from exceptionally early failure of autolysomal/lysosomal acidification, driving downstream AD pathogenesis. This process involves the formation in compromised, yet still intact neurons, of large autophagic waste-filled plasma membrane blebs which have a flower-like perikaryal rosette structure termed PANTHOS - Poisonous flower (ANTHOS).
Method:
To further explore the molecular composition of PANTHOS structures and proximal cells, we imaged brain tissue from 5XFAD-TRGL and other AD transgenic mouse models using a new, highly multiplex, multiomic and multimodal method termed MALDI-IHC. This method combines the relative strengths of mass spectrometry imaging (MSI) and immunohistochemistry by using novel photocleavable mass-tagged antibodies to probe the spatial location of a panel of intact proteins as well as to serve as markers of cell lineage. MSI was performed on a Bruker rapifleX Tissuetyper or timsTOF flex equipped with a microGRID accessory which enables 5 µm spatial resolution. Multiomic imaging combined untargeted label-free MSI with MALDI-IHC, and multimodal imaging combined fluorescence microscopy with MALDI-IHC, all performed on the same tissue section.
Results:
Results demonstrate the capability of combining fluorescence microscopy, label-free untargeted small molecule MSI and multiplexed MALDI-IHC based targeted protein imaging on the same tissue section to enable spatial biology analysis of many biomarkers from different "omic" classes, to help elucidate the mechanism of AD pathology. Workflows for multiomic imaging of small molecule metabolites and drugs along with intact proteins and glycans from different AD transgenic mouse brain models will be described. Moreover, co-registration will be shown of fluorescence-mRFP-eGFP-LC3 and MALDI-IHC images from the same tissue specimen to correlate PANTHOS structures with specific proteins using a >15-member neurological panel of PC-MT-antibody probes, including against β-amyloid, GFAP, NeuN, LC3 and Cathepsin D.
Novelty:
Photocleavable mass-tagged antibodies and lectins for high-plex, multimodal and multiomic MSI on the same specimen in novel transgenic Alzheimer's models.
Preliminary Data:
Highly multiplexed, multiomic and multimodal image data acquired from single tissue specimens of transgenic model AD mouse brain.
Contributing Authors:
Gargey Yagnik, Philip Stavrides, Ralph A. Nixon, Kenneth J. Rothschild and Mark J. Lim

P-54

Lin, Monica
University of Texas at Austin, United States

Mass Spectrometry Imaging Reveals Alterations in Protein and N-Glycan Molecular Signatures in Endometriosis Tissues

Introduction:
Endometriosis is a gynecological condition characterized by the uncontrolled growth of endometrial-like tissue outside the uterine cavity. Although highly prevalent, the biological mechanisms of endometriosis are poorly understood, and the disease is often misdiagnosed due to the current unavailability of pre-operative diagnostic methods. Thus, there is a critical need for studies which better characterize the dysregulated molecular mechanisms and expression of molecules in endometriosis to improve understanding of the disease and treatment of patients. Here, we investigate protein and N-glycan molecular signatures in eutopic endometrium and endometriosis lesions using matrix-assisted laser desorption ionization mass spectrometry (MALDI-MS) imaging. Overall, by characterizing molecular alterations in proteins and N-glycans, the results of this study provide insights into potential mechanisms involved in endometriosis pathogenesis.
Method:
Eutopic and ectopic endometrial tissues were collected from Seton Medical Center from patients undergoing endometriosis surgeries, flash frozen, and stored at -80°C. Tissue sections (12µm) were washed in ethanol (70%, 100%, 30 seconds), Carnoy's fluid (6/3/1ethanol/chloroform/acetic acid), ethanol, water, and ethanol. For intact protein analysis, imaging data was acquired on a Bruker RapifleX MALDI TOF/TOF mass spectrometer operated in linear positive ion mode from m/z 2000-24000. For N-glycan and tryptic peptide analyses, an on-tissue enzymatic digestion using PNGase F and trypsin was performed, respectively. N-glycan/peptide imaging data was acquired on a Bruker timsTOF fleX MALDI mass spectrometer in positive ion mode from m/z 600 to 3500. All imaging data was acquired at a spatial resolution of 50µm.
Results:
Intact protein imaging of ectopic endometriosis tissues revealed high relative abundances of neutrophil defensins (DEFA) 1, 2, and 3 localized to regions of endometrial glands and stroma. Concomitantly, endometrium tissues were observed to present higher detection and a more homogenous distribution of histone H4 and hemoglobin proteins alpha/beta. Comparing the peak area of the major proteins detected in endometriosis tissues, a significantly higher peak area for DEFA1, DEFA2, and DEFA3 was observed in endometriosis in comparison to endometrium (t-test; $p = 4.51\times10\text{-}5$ for DEFA2; $p = 6.73\times10\text{-}5$ for DEFA1; $p = 0.002$ for DEFA3). Further, a significantly higher average peak area was detected in endometrium tissues for histone H4 (t-test; $p = 0.04$), hemoglobin alpha (t-test; $p = 4.46\times10\text{-}8$), and hemoglobin beta (t-test; $p = 5.25\times10\text{-}11$). The increased abundance of neutrophil defensin proteins detected in regions of endometriosis lesions suggest a role of immune and inflammatory processes involved in endometriosis pathogenesis. Further, improved protein molecular coverage was achieved by analyzing tryptic peptide molecular profiles, revealing higher detection of tryptic peptides corresponding to extracellular matrix (ECM) proteins collagen and decorin in ectopic endometrial tissue. These findings suggest that interaction and adhesion of endometriotic cells with ECM proteins is a critical step in endometriosis development. Next, significance analysis of microarrays (SAM) was used to characterize alterations in N-glycan molecular profiles, revealing 51 significant m/z features to be altered in abundance in endometriosis lesions in comparison to eutopic endometrium. These alterations in N-glycan molecular profiles revealed significantly higher detection of fucosylated N-glycans and increased levels of branching from biantennary to tri- and tetraantennary structures in endometriosis lesions in comparison to eutopic endometrium. These results provide evidence that alterations in N-glycosylation machinery are involved in dysregulation of critical cellular and signaling processes and may contribute to endometriosis lesion development.
Novelty:
Protein and N-glycan molecular profiles of eutopic endometrium and endometriosis lesions were characterized to provide novel insights into endometriosis pathogenesis.
Preliminary Data:
Altered abundances in proteins and N-glycans were detected by MALDI imaging of endometriosis tissues to better characterize endometriosis disease mechanisms.
Contributing Authors:
Monica Lin, Erin H. Seeley, Suzanne Ledet, Christina Salazar, Michael T. Breen, Livia S. Eberlin

P-55

LU, Wenyun
Princeton University, United States

Acidic methanol treatment facilitates MALDI-mass spectrometry imaging of energy metabolism

Introduction:
Detection of small molecule metabolites (SMM), particularly those involved in energy metabolism using MALDI-mass spectrometry imaging (MSI), is challenging due to factors including ion suppression from other analytes present (e.g., proteins and lipids).
Method:
One potential solution to enhance SMM detection is to remove analytes that cause ion suppression from tissue sections before matrix deposition through solvent washes. Here, we systematically investigated solvent treatment conditions to improve SMM signal and preserve metabolite localization.
Results:
Washing with acidic methanol significantly enhances the detection of phosphate-containing metabolites involved in energy metabolism. The improved detection is due to removing lipids and highly polar metabolites that cause ion suppression and denaturing proteins that release bound phosphate-containing metabolites. Stable isotope infusions of [13C6]nicotinamide coupled to MALDI-MSI ("Iso-imaging") in the kidney reveal patterns that indicate blood vessels, medulla, outer stripe, and cortex. We also observed distinct ATP:ADP ratio across mouse kidney sections, reflecting regional differences in glucose metabolism favoring either gluconeogenesis or glycolysis. In mouse muscle, Iso-imaging using [13C6]glucose shows high glycolytic flux from infused circulating glucose in a type 2 fiber type (soleus) and relatively lower glycolytic flux in type 1 fiber type (gastrocnemius).
Novelty:
Improved detection of energy metabolites combined with isotope tracing provides an improved way to probe energy metabolism in vivo
Preliminary Data:
Acidic methanol wash improves the detection of phosphate-containing energy metabolites and is compatible with NEDC for analysis in negative ionization
Contributing Authors:
Wenyun Lu, Noel R. Park, Tara TeSlaa, Connor S.R. Jankowski, Laith Samarah, Melanie McReynolds, Xi Xing, Jessica Schembri, Morgan T. Woolf, Joshua D. Rabinowitz, Shawn M. Davidson

P-56

Mandic, Sara
Okayama University, Japan

Preparation and imaging of longitudinally sectioned C. elegans

Introduction:
In the past 50 years C. elegans has been used as a model organism for various kinds of biological studies, ranging from cell function to thermotaxis. This is possible due to the small size of the nematodes and their large brood sizes, making them very cost-effective and relatively easy to handle. Their size, however, makes them somewhat difficult to handle efficiently for an upcoming analytical technique, mass spectrometry imaging (MSI). The current work aims to create a new workflow allowing longitudinal sectioning of C. elegans, allowing their use for MSI analysis that can reveal the spatial distribution of a range of analytes for further elucidating molecular changes in the worms under various conditions.
Method:
To prepare the samples for imaging, a commercially available microfluidic device, Wormsheet, is used to align the nematodes. After alignment, an in-house developed and printed mould encloses the Wormsheet, allowing gelatine pouring to encapsulate the worms. The mould consists of two parts, resulting in a gelatine block with worms “sandwiched” in the centre. This block is then sectioned using a Leica cryotome and the sections are collected on ITO glass slides. The last preparation step consists of NEDC matrix deposition using the HTX-TM sprayer. Coated samples are analysed using Bruker rapifleX and solariX systems, for a combination of high-throughput analysis followed by further identification of worm-related signals. The final identification step utilises the LIPID MAPS database.
Results:
The sample preparation method described earlier, allowed for consistent preparation of C. elegans containing gelatine blocks. As a result of both tape markings and small air-pockets around the worms, it was possible to distinguish the exact positions of the worms during sectioning, allowing for more efficient preparation. The protocol also resulted in sections with multiple worms present and consecutive sections of the same worms being analysed. For matrix deposition, the HTX technologies Sublimator, as well as different conditions on the HTX-TM sprayer, were tested. HTX-TM sprayer at high deposition temperatures showed the most uniform and consistent deposition and extraction for NEDC. The samples were analysed in negative ion mode on both of the systems. The results showed an abundance of worm-related signals. The signals were tentatively identified as a variety of lipid species using the exact mass obtained on the solariX. For example, the signal present in all nematodes at m/z 466.2945 was denoted as a lysophospholipid, LysoPC (14:0/0:0) with a Δppm of 1 when compared to the theoretical mass of 466.2939. Additionally, when overlayed together, different lipid species showed complementary distributions, allowing for the determination of specific locations of these lipids within the analysed nematodes.
Novelty:
This methodology gives insight into the spatial distribution of analytes in C. elegans in longitudinal sections.
Preliminary Data:
Spatial distribution of lipid species in longitudinally sectioned C. elegans.
Contributing Authors:
Sara Mandic, Bryn Flinders, Michiel Vandenbosch, Ron M.A. Heeren, Masazumi Fujiwara

P-57

Marshall, Peter
GSK, UK

Exploring ionizability and adduct formation of pharmaceutical compounds in MALDI and MALDI-2 Mass Spectrometry Imaging with machine learning.

Introduction:
Drugs of interest can be undetected at physiologically relevant concentrations during MALDI imaging due to low ionisation efficiency and/or the interaction of the drug molecule with the local biochemical environment of the tissue. Insufficient sensitivity can be mitigated using post-ionisation (MALDI-2) but this may change the predominant ion type. In this work, we leverage a MALDI-MS imaging screen of 1,200 drug-like compounds under "simulated real life imaging" conditions to determine to what extent the ability of a compound to be ionised and which adducts are likely to be observed can be predicted based on a 2D chemical structure and it's physicochemical properties. In this context, we will explore whether we can link ionisation behaviour to specific parts of the chemical structure.

Method:
1µL droplets of compounds (10 µM in methanol) were spotted onto a specific position of a 16 µm-thick sections of rat liver homogenate. Samples were spray-coated with 2,5-dihydroxyacetophenone (DHAP) matrix. Positive and negative mode mass spectra were acquired with conventional and MALDI 2 on a prototype timsTOF fleX mass spectrometer (10 µm pixel size, 1,000 laser shots/pixel). The presence of an compound-ion was determined in MALDI and MALDI-2 for common ion types, ($[M^{\cdot *}]-$, $[M-H]-$, $[M^{\cdot *}]+$, $[M+H]+$) using isotope pattern matching, yielding 8 prediction endpoints. Two-dimensional chemical structures were digitally vectorised (Morgan fingerprint, 64-bit hash). Compounds were randomly assigned to train/test/validate groups and used to train the (hyper-) parameters of a machine learning model (Ensemble of Classifier Chains (ECC) based on Support Vector Machines (SVMs)).

Results:
The analytical sensitivity of MALDI Imaging for a structurally diverse set of 1,200 GSK compounds was determined using MALDI Mass Spectrometry Imaging (MALDI-1) and with laser-induced post-ionisation (MALDI-2). ~1,000 of the compound were detected by MALDI- or MALDI-2-MSI (950 in positive mode, 880 in negative mode, 500 in both), covering a wide structural and physicochemical property space. Our goal in this study is to predict which ion types would be expected for a given chemical compound based on its 2D chemical structure. Structures were standardized by de-salting and charge neutralization and a 'structural fingerprint' was generated. This fingerprint records the presence or absence of chemical features (e.g. functional groups), capturing the presence or absence of specific substructures in a fixed-length binary vector. The machine learning model was trained on the training subset using the test set for hyper-parameter to optimize its parameters and improve its generalization ability. The performance of the model was evaluated on the validation subset. Due to the high imbalance in the dataset, we report the Receiver Operating Characteristic Area Under the Curve (ROC-AUC) values as the most appropriate metric to report. An average ROC-AUC of >0.7 was achieved for the ion types considered, providing a chemoinformatics model with satisfactory predictive performance, especially considering the high imbalance seen in the training data. This indicates the model has effectively captured underlying relationships between the 2D chemical structures and ionisation. Using bulk physical-chemical properties as the feature vector showed significantly reduced predictive ability, indicating that bulk properties alone are not sufficient to predict ionisation behaviour. Restricting ourselves to linear models provides increased interpretability through inspection of the structural motifs most important for predicting ionisation behaviour. We compare these between adducts and after post-ionisation to generate clues to the mechanistic behaviour of MALDI & MALDI-2 ionisation.

Novelty:
The first structure based model for predicting MALDI ionisation behaviour.

Preliminary Data:
Predictive models have been trained on MALDI & MALDI-2 data from ~1200 compounds.

Contributing Authors:
Peter Marshall*1, Andrew D. Palmer1, Krischan A. Koerfer2, Hyundae Hong1, Jan Majer1, Klaus Dreisewerd2 and Jens Soltwisch2.
1GSK Research & Development - Stevenage (United Kingdom), 2Institute of Hygiene, University of Münster - Münster (Germany).

P-58

Marshall, Cody
Vanderbilt University, United States

Molecular Mapping of Alzheimer's Disease and Cerebral Amyloid Angiopathy (CAA) with MALDI IMS and IHC

Introduction:
Alzheimer's disease (AD) is the most common form of dementia with an estimated 6 million adults in the US diagnosed with the disease in 2020 and a predicted 13.85 million adults by 2060. The characteristic pathology of AD is extracellular Aβ-amyloid plaques. Cerebral amyloid angiopathy (CAA) co-occurs with AD and is characterized by Aβ-amyloid plaque deposition within the cerebrovasculature. The spatial scale and molecular complexity of cellular neighborhoods surrounding Aβ-amyloid extracellular and vascular plaques require high spatial resolution multimodal molecular imaging to understand AD and CAA development. Here we show methods for high spatial resolution matrix-assisted laser desorption/ionization (MALDI) imaging mass spectrometry (IMS) and immunohistochemistry (IHC) microscopy tuned for the study of AD and CAA.
Method:
Human brain tissues were fresh-frozen and embedded in 15% fish gelatin. Post-mortem human cortex tissues were cryosectioned at 10 µm thickness. An aminocinnamic acid analog matrix was sprayed onto the samples (0.5 µg/mm2) using a HTX M5 sprayer, and IMS data was acquired on a MALDI timsTOF flex (Bruker Daltonics). IHC was performed on serial sections, which are photobleached, fixed, and permeabilized. Collagen IV was used to stain vasculature. Thiazine red was used to stain Aβ-amyloid fibrils. IHC imaged with Zeiss AxioScan fluorescence slide scanner. IMS data were analyzed using DataAnalysis (Bruker Daltonics), SCiLS, and custom in-house software. Custom Napari plugins were used for multimodal image processing.
Results:
Methods have been developed to enable high spatial resolution MALDI IMS (10 µm pixel sizes) to be performed on post-mortem human brain tissues. Lipids from various lipid classes are observed with good sensitivity and spatial localization. For example, PS(40:6) (m/z 834.525) and SHexCer(d42:1) (m/z 906.631) are found to localize to the grey matter and white matter, respectively. Ganglioside GM3(d38:1) at m/z 1207.763 localizes to plaque features and the surrounding tissue microenvironment. Currently, all identifications are tentative based on mass accuracy, but work is underway to perform LC-MS/MS to validate all peak annotations. IHC following IMS shows neuropathological features, including extracellular Aβ-amyloid neuritic plaques in the grey matter suggesting AD in addition to Aβ-amyloid plaque deposits within brain vasculature, hallmarks of CAA. Serial sections of the frontal cortex were co-registered and overlaid to create high spatial resolution IMS and IHC multimodal data. Co-registration of IMS and IHC data collected from serial tissue sections was performed using autofluorescence images collected from of each tissue section. Briefly, IMS data were registered with accompanying autofluorescence images using the publicly available IMS MicroLink v0.1.7. Then autofluorescence images from serial sections and related IMS and IHC data were aligned using WSIreg 0.3.5. The resulting high-resolution multimodal imaging data was segmented for healthy vasculature regions and regions associated with CAA-diseased vasculature. This enabled spatial lipidomic comparisons to be made between tissue features, highlighting unique lipid profiles associated with localized regions of disease. 5 µm MALDI IMS experiments are currently underway to characterize the cellular environment of vessels diseased with CAA. Robust methods for high spatial resolution multimodal imaging are enabling the visualization of alterations to the molecular profiles near neuropathologies of AD and CAA. In addition, experiments with larger patient sample sizes are being performed.
Novelty:
Methods for high spatial resolution multimodal molecular imaging applied to AD and CAA human brain tissue.
Preliminary Data:
Intra and inter-sample comparisons of lipid profiles have been made between healthy and CAA vasculature from human brain tissue.

Contributing Authors:
Cody R. Marshall[1,2]; Claire F. Scott[2,3]; Lissa Ventura-Antunes[4,5]; Wilber Romero-Fernandez[5]; Alena Shostak [4,5]; Martin Dufresne[2,6]; Lukasz G. Migas[7]; Nathan H Patterson[2,4]; Raf Van de Plas[2,7]; Matthew S. Schrag[4,5]; Jeffrey M. Spraggins[1-3,6,8]

1. Chemical Physical Biology Program, Vanderbilt University School of Medicine, Nashville, TN, United States 2. Mass Spectrometry Research Center, Vanderbilt University School of Medicine, Nashville, TN, United States 3. Department of Cell and Developmental Biology, Vanderbilt University School of Medicine, Nashville, TN, United States 4. Vanderbilt University Medical Center, Nashville TN, United States 5. Department of Neurology, Vanderbilt University, Nashville, TN, United States 6. Department of Biochemistry, Vanderbilt University School of Medicine, Nashville, TN, United States 7. Delft University of Technology, Delft, Netherlands 8. Department of Chemistry, Vanderbilt University, Nashville, TN, United States

P-59

Martin, Roy
Waters, United States

Enhanced molecular coverage, resolution and speed for in-situ pharmaceutical tablet Imaging analysis by combining DESI and MALDI using multi-reflecting Q-Tof

Introduction:
Characterization of pharmaceutical tablets is important in the drug development process to ensure their quality and effectiveness. The traditional tablet dissolution method requires the use of LC-MS. However, this approach doesn't indicate the localisation of different components of the tablet formulation such as the active pharmaceutical ingredient (API) or excipients. Therefore, a method to directly analyse the tablet in-situ is required. MSI allows the analysis of samples without the need for dissolution. In this study, DESI and MALDI ion sources mounted on an ultra-high resolution Q-Tof spectrometer (up to 200,000 FWHM with a scan speed of up to 10 Hz) were used to evaluate the molecular coverage of the individual ionization techniques for the analysis of commercially available tablets

Method:
MSI experiments were carried out on a Q-oaTOF and multi-reflecting Q-Tof (MRT) mass spectrometer equipped with a DESI source. DESI spray conditions were set at 2 µL/min, 95:5 MeOH: water with 100 pg/µL leucine enkephalin. The N2 nebulising gas pressure was set at 10 psi and the stage speed was 500 µm/sec. The MRT was also equipped with a MALDI source. When the intermediate vacuum MALDI source was in operation, a solid-state diode-pumped Nd:YAG laser with a repetition rate of 1KHz was employed. α-Cyano-4-hydroxycinnamic acid (CHCA) matrix was sprayed using the HTX M5 (HTX Technologies) automated sprayer. All analyses were performed with a pixel size of 50 µm

Results:
Experiments were performed analysing commercially available tablets called Lysopain (20 mm diameter) without sugar 36 lozenges to suck. This tablet was chosen because of the flatness of the tablet and its compatibility with MSI analysis. The active ingredients are a mixture of small molecules, an API named cetylpyridinium chloride (C21H38ClN) and a protein-based molecule lysozyme hydrochloride. In DESI positive ion mode, the strongest signal detected from the tablet surface was m/z 304.29999 which corresponded to cetylpyridinim choloride [M-HCl+H]+ and was identified with a mass accuracy of 361 ppb. The distribution of the small molecule API was patchy with clusters of the API smaller than 600 x 600 µm on the surface of the tablet. Further signals with a similar distribution as [M-HCl+H]+ were identified in the ppb mass accuracy to be multimers of the small API such as [M2-HCl+H]+, [M3-HCl+H]+, [M4-HCl+H]+. Furthermore, multiply charged signals were detected with high charge states (+8 to +12) and were putatively identified as the domain C-type lysozyme protein. The distribution of the high charge states was also blotchy with clusters smaller than 300x 300 µm, localised differently to the small molecule API. In MALDI positive ion mode, the most intense signal was also cetylpyridinim choloride [M-HCl+H]+ with a mass accuracy of 330 ppb but no multimers or multiply charged species were detected. Similarly to DESI, the distribution of the cetylpyridinim choloride was patchy in small clusters across the tablet. Additional signals, unique to MALDI, that were ubiquitously distributed across the tablet were detected and remain to be putatively identified. Finally, all datasets were subjected to a Uniform Manifold Approximation and Projection (UMAP) algorithm using in-house software to automatically explore and perform unsupervised segmentation of pixels into clusters on similar spectral characteristics.

Novelty:
Complementarity of DESI and MALDI high resolution multi-reflecting Q-Tof (MRT) mass spectrometer with ppb mass accuracy for high identification confidence

Preliminary Data:
Images of Tablets

Contributing Authors:
Emmanuelle Claude, Wei Rao1, Laurent Bultel, Tristan Renaud, Joanne Ballantyne1

P-60

Matsuo, Ei-ichi
Shimadzu Corporation, Japan

Spatial Mapping of Lipids and Elements in Kidneys from Tissue-specific Adiponectin Knockout, Overexpressing and Wild Type Mice

Introduction:
Adiponectin is an important secretory protein, primarily produced in adipocytes. Higher levels of plasma adiponectin are associated with improved overall metabolic status and enhanced insulin sensitivity. The adipocyte is by far the most important source of adiponectin in circulation. However, expression can also be observed in the kidney. Our group has shown in previous work that adiponectin is renoprotective and accelerates functional recovery following renal injury. The in vivo relevance of renal adiponectin remains unclear. We therefore assessed the functional role of renal adiponectin by utilizing inducible kidney tubular cell-specific adiponectin overexpressing or kidney tubular cell-specific knockout mice. Here, we are characterizing the spatial distribution of lipids and elements of the kidneys of these mice using MALDI-TOF and LA-ICP-MS techniques.
Method:
MALDI-TOF imaging of 10 µm thick frozen kidneys from control, knock-out (KSPAKO) and overexpressing (KSPAPN) mice were thaw-mounted onto ITO coated glass slides. 9-aminoacridine (9-AA) was used as a MALDI matrix and was applied using an automated matrix vapor deposition system iMLayer (Shimadzu Corporation, Kyoto, Japan) at 0.9 µm film thickness. Negative-mode MS lipid analysis was carried out on an imaging mass microscope iMScope QT (Shimadzu Corporation) at 25 µm spatial resolution. Spatial elemental analysis was performed on a laser ablation system NWRimage (Japan Laser Corporation, Tokyo, Japan) coupled to an inductively coupled plasma mass spectrometry ICPMS-2030 (Shimadzu corporation) at 50 µm spatial resolution. Imaging data processing and differential analysis were performed using IMAGEREVEAL MS software package (Shimadzu corporation).
Results:
For semiquantitative assessment of lipids, three regions of interest (ROIs) were selected: medulla region, cortex, and the cortex-medulla (CM) transition area. We were able to observe a distributional impact of renal adiponectin on lipids levels that would go unnoticed in a conventional LC-MS analysis of kidney homogenate lipid extracts. Our analysis revealed that renal adiponectin deficiency triggers an upregulation of most ceramide derivatives in the medulla and in the transition area. These data are compatible with our previous findings indicating that adiponectin deficiency leads to a buildup of ceramide species. On the other hand, we discovered that fatty acids (FA), Sterols (ST), Acyl CoAs (CoA) and Phosphatidylinositol-phosphate (PIP) derivatives are up-regulated by adiponectin overexpression and decreased by adiponectin deficiency. Increased FA and CoA in KSPAPN kidneys could be associated to enhanced fatty acid oxidation. CoA itself displays strong bioactivity, including inhibition of critical metabolic enzymes, such as hormone-sensitive lipase. Moreover, PIP derivatives are critically involved in insulin signaling. Therefore, these adiponectin-mediated alterations of lipids exert a pivotal role on kidney function In the KSPAPN kidney. All the lipid IDs are putative based upon exact mass matches in LIPID MAPS. Further analysis of kidney cryosections from control and KSPAPN mice by LA-ICP-MS imaging at 50 µm spatial resolution, determined that Mn, Zn and Mo are preferentially distributed in the cortex and the CM region while Fe and Co are found to be concentrated in the cortex. P and Cu are ubiquitous in the tissue. P, Mn, and Mo were found elevated in KSPAPN kidney.
Novelty:
Comprehensive lipidomics by MALDI-TOF imaging in the kidney integrated with elements mapping by LA-ICP-MS.
Preliminary Data:
Distributional impact of renal adiponectin on lipids and elements levels.
Contributing Authors:
Ei-ichi Matsuo, Toshiharu Onodera, Koji Okuda, Shinichi Yamaguchi, Toshiya Matsubara, Philipp E. Scherer, and Ruth Gordillo

P-61

McHardy, Kate
Ionoptika Ltd, United Kingdom

Label-Free Molecular Imaging of Drug Permeation in Stratum Corneum Layer using Water Cluster Secondary Ion Mass Spectrometry (Water Cluster SIMS)

Introduction:
Mass spectrometry imaging (MSI) is a powerful tool for understanding drug molecule behaviour in skincare products. Water Cluster SIMS offers high-sensitivity imaging with reduced damage. It utilises ionised water clusters to sputter, generating fewer fragment ions compared to traditional ToF-SIMS, and generating a greater secondary ion yield, thus providing high sensitivity. This technique retains the advantages of high-spatial-resolution imaging presenting both surface and depth information. In this study, Water cluster SIMS was employed to observe the penetration and distribution of endogenous and exogenous compounds in commercial cosmetics and drugs in the skin using 2D and 3D imaging.
Method:
Two chemicals, commonly used in drugs and cosmetics, chlorhexidine digluconate and sodium ascorbyl phosphate, were selected. Each substance was applied to human skin for a duration of two hours. Afterwards, multilayer corneocyte flakes of stratum corneum (SC) were obtained using the skin stripping method. Analysis was performed using the J105 SIMS time-of-light secondary ion mass spectrometer (Ionoptika Ltd) with a 70kV (H2O)n beam, where n is in the range of 10,000-50,000, and a 40kV C60 beam. High-resolution images were acquired with a pixel size of less than 1 micron.
Results:
The results demonstrate the distribution and penetration of the drug molecules and other compounds within the structure of the stratum corneum through 2D and 3D images. Preliminary data suggest the possibility of chemical mapping to visualise the distributions in the skin layers and propose potential permeation routes of the drug molecules. The detailed images of the stratum corneum cells are visible in both 2D and 3D mass spectrometry ion images. This study aims to explore the sensitivity of Water Cluster SIMS in detecting commonly used drug compounds in human skin.
Novelty:
High-resolution imaging of drug molecules in human skin.
Preliminary Data:
Water Cluster SIMS can visualise drug compounds in human skin as 2D and 3D images.
Contributing Authors:
N. Sano, K. McHardy*, P. Blenkinsopp

P-62

Meuret, Cristiana
University of Washington, United States

Changes in brain glycan sulfation patterns drive neuroinflammation.

Introduction:
The brain's extracellular matrix (ECM) is comprised of sulfated glycoproteins, including chondroitin and dermatan sulfate glycosaminoglycans (CS/DS-GAGs). Sulfation addition to the CS/DS isomers is associated with isomer-specific biological functions, including charge molecule diffusion, protein-glycan interactions, and mechanical scaffolding in the brain. Loss of perineuronal nets (PNNs)—a CS/DS-GAG rich ECM structure that enmeshes GABAergic neurons involved in memory and cognition—have been reported in patients with Alzheimer's disease (AD) and mouse models of AD, as well as neuroinflammation. Moreover, we have previously shown that patients exhibiting AD clinicopathology had a significant increase in the monosulfated 6S-CS isomer. We predict that the increase in the 6S-CS isomer drives loss of stable PNNs via ECM remodeling and neuroinflammation.
Method:
Using an AAV1-[FLEX]on-mChst3-TA-EGFP viral construct, which overexpresses the 6S-CS sulfotransferase (Chst3) in the presence of Cre recombinase, we induced an increase in 6S-CS within PNN matrices surrounding hippocampal GABAergic neurons in Vgat-Cre mice (a mouse model that expresses Cre recombinant protein in GABAergic neurons). On the contralateral side, an AAV1-[FLEX]on-tdTomato control was used for comparison. Injections were performed using a 33g Hamilton syringe with 300nLs of virus and injected at 75nL/min. Histological outcomes for matrix and neuroinflammation included staining for stable PNN formation using Wisteria floribunda agglutinin (WFA), microgliosis using Iba1, and astrogliosis using GFAP. Confirmation of viral activity was performed by liquid chromatography and MALDI-imaging of the 6S-CS isomer throughout the brain tissue.
Results:
Fluorescent imaging of mouse brain tissue showed a striking induction of GFP+ neurons (488) on the ipsilateral hippocampus in association with the presence of AAV1-mChst3-EGFP, when compared to the tdTomato+ neurons (Cy3) observed on the AAV1-tdTomato contralateral side. There was an average increase in the 6S-CS isomer (1.6+/-<0.1% (mean+/-SE)) in whole hippocampal isolates by LC-MS/MS. This was spatially confirmed by MALDI-IMS performed on chondroitinase ABC (ChABC)-digested tissue slices sprayed with 9-aminoacridine (9-AA) matrix and imaged in negative mode. Specifically, MALDI-IMS revealed dense pixel coverage (20 µm/pixel) formed from the characteristic 6S-CS isomer fragmentation pattern (458>282 m/z) at 32 eV. The increase in 6S-CS overexpression was associated with a 39+/-12% decrease in WFA+ PNN structures, suggesting a reduction of PNNs surrounding GABAergic neurons within this brain region. Correlating to the loss of stable PNNs was a surprising increase in both microgliosis (Iba1; 1.8+/-0.3-fold increase, $p<0.05$) and astrogliosis (GFAP; 2.3+/-0.4-fold increase, $p<0.05$). We also observed the surprising appearance of WFA+ puncta on the 6S-CS overexpression ipsilateral hippocampus (2.8+/-0.8-fold increase, $p<0.05$) compared to the contralateral tdTomato control, which represent inclusion bodies previously linked to brain trauma. Taken together, we predict that brain upregulation of the 6S-CS isomer observed in patients with AD may drive both PNN loss and neuroinflammation.
Novelty:
Changes in brain glycan sulfation patterns directly induces PNN loss and neuroinflammation associated with Alzheimer's disease.
Preliminary Data:
We observed an increase in microgliosis and astrogliosis (neuroinflammatory markers) and loss of PNN structures in association with increased 6S-CS.
Contributing Authors:
Cristiana Meuret, Aarun Hendrickson, Asmit Kumar, Ingrid Redford, Jaden Le, Jarrad Scarlett, Miklos Guttman, Kimberly Alonge

P-63

Molloy, Kameron
Vanderbilt University, United States

High Sensitivity and Specificity IMS of Cerebrosides and Neutral Lipids

Introduction:
Matrix-assisted laser desorption/ionization imaging mass spectrometry (MALDI IMS) is a powerful tool for mapping the spatial distribution of biomolecules in tissue. However, advancements are still needed to improve sensitivity and molecular coverage for molecular classes that are difficult to ionize by MALDI. Two strategies that have been shown to enhance the detection of neutral lipids in a sample are: 1) salt deposition onto the sample and 2) the integration of laser post-ionization (MALDI-2). Previous studies have reported improved sensitivity with both techniques for various classes of neutral lipids and carbohydrates. Here, we assessed the performance of MALDI-2 and salt doping applied to various tissues, such as human and murine kidney and brain.
Method:
Human and murine tissues were cryosectioned at 10-µm thickness, thaw-mounted on indium tin oxide coated glass slides, and washed with either 150 mM ammonium formate containing or not, 66.7 mM of either potassium citrate or sodium citrate. Dihydroxyacetophenone acid (DHA), 2', 5'-dihydroxybenzoic acid (DHB), and 4-(dimethylamino)cinnamic acid (DMACA) were each sublimated on separate tissue sections. Lipids were extracted from serial sections using a modified methyl tert-butyl ether method and separated on a Premier UHPLC. MALDI IMS and LC-MS/MS experiments were performed on a timsTOF FleX. Data were analyzed using in-house developed tools for IMS and MS-DIAL for LC-MS/MS.
Results:
Methods for probing molecular classes not typically ionized and detected by MALDI are critical for comprehensive in situ mapping of lipids by IMS. A systematic comparison between MALDI and MALDI-2 on various organs revealed that MALDI-2 increased the sensitivity for a few classes of neutral lipids. As highlighted in previous studies, the MALDI matrix DHA contributed most to the efficiency of the MALDI-2 process. Cholesterol, hexosylceramides, and di- and tri-acylglycerols were detected more frequently with MALDI-2. The ions observed at m/z 425.377 and m/z 810.682, tentatively identified as a sterol (ST (30:3; O)) and a hexosylceramide (HexCer (42:2; O2)), respectively, are two examples of lipids only detected using MALDI-2. To maximize sensitivity and specificity, signal intensity was optimized for MALDI-2. In all cases, MALDI-2 performed best using few laser shots (~5 shots per pixel) and high laser energy. Complementary microscopy revealed that MALDI-2 conditions caused significant damage to the sample by ablating and puncturing the tissue. This is atypical of traditional MALDI experiments that used lower laser energy with a greater number of laser shots (50-200 shots per pixel). Further experiments are underway to assess various matrices at lower energies to enable both enhanced sensitivity by MALDI-2 and integrated multimodal studies performed in serial on the same tissue. In these studies, we are also comparing salt doping to MALDI-2 for ionizing neutral lipids and cerebrosides. Preliminary findings in murine brain tissue suggest that salt doping provides similar selectivity and sensitivity for these lipid classes to that of MALDI-2. Currently, experiments using various salt washes (e.g., potassium citrate, sodium citrate, and lithium citrate) combined with DMACA, DHA, or DHB sublimation are being done. These studies will provide robust methods for mapping lipid classes that often go undetected by MALDI IMS.
Novelty:
Comparison of MALDI-2 and salt doping for increased sensitivity and specificity of neutral lipids and cerebrosides.
Preliminary Data:
MALDI/MALDI-2 IMS of various tissues prepared with and without salt doping is used to optimize methods for imaging neutral lipids.
Contributing Authors:
Kameron R. Molloy1, 2; Madeline E. Colley2, 3; Martin Dufresne2, 3; Lukasz G. Migas2,4; Raf Van de Plas2,3,4; Jeffrey M. Spraggins1, 2, 3, 5, 6 1Department of Chemistry, Vanderbilt University, Nashville, TN 2Mass Spectrometry Research Center, Vanderbilt University, Nashville, TN 3Department of Biochemistry, Vanderbilt University, Nashville, TN 4Delft Center for Systems and Control, Delft University of Technology, Delft, Netherlands 5Department of Cell and Developmental Biology, Vanderbilt University, Nashville, TN 6Department of Pathology, Microbiology and Immunology, Vanderbilt University Medical Center, Nashville, TN

P-64

Nakagawa, Kaoru
Shimadzu Corporation, Japan

Distribution analysis of galanthamine, a plant alkaloid, by MS imaging

Introduction:
Plant alkaloids are used in various pharmaceuticals, such as anticancer drugs and analgesics. Among these plant alkaloids, galanthamine an Amaryllidaceae-type alkaloid with acetylcholinesterase inhibitor for the treatment of neurological diseases such as Alzheimer's disease. Although the chemical synthesis of galanthamine has been successfully achieved, Narcissus is the main source of its production. Research indicates that galanthamine content varies not only with the type of Narcissus, but also with the developmental stage and the part of the plant. Pharmaceutical companies are pursuing plant species with higher galanthamine content to increase pharmaceutical productivity. Therefore, we quickly confirmed the Narcissus in our study contained galanthamine using DPiMS QT. Subsequently, we analyzed the distribution of galanthamine by MS imaging (MSI) using the iMScope QT.

Method:
Narcissus tazetta with leaves growing to about 15 cm in length were used. Galanthamine was extracted with 50% EtOH aq. from freeze-dissolved leaves. The solution was analyzed via the DPiMS QT probe electrospray ionization kit and an LCMS quadrupole time-of-flight (QTOF) mass spectrometer (Shimadzu Corporation). Frozen leaves and bulbs were sliced to 30 µm thickness using a microtome and mounted on indium tin oxide (ITO) coated glass slides (Matsunami). These were coated with α-cyano-4-hydroxycinnamic acid (CHCA) via vapor deposition by using the matrix sublimation apparatus iMLayer (Shimadzu) at a thickness of 0.7 µm. MSI analysis was performed using an MSI system consisting of an LCMS-QTOF mass spectrometer connected to an iMScope QT atmospheric MALDI unit with a built-in microscope (Shimadzu).

Results:
Galanthamine was rapidly detected in the leaves extract solution using the DPiMS QT in only 12seconds. galanthamine could be identified by MSMS analysis and other compounds were also able to be detected and identified: lycorine and tazettine, bothalkaloids found in Narcissus. MS Imaging was performed on sections of leaves (in two locations) and bulbs with a spatial resolution of 25 µm for the entire section and 10 mm for the area observed under a microscope with a 10x objective lens. As a result, good MS images of galantamine, lycorine, and tazettine were obtained from all samples. The MSI of the bulbs showed that galantamine was distributed more in the leaves, but MSI of lycorine and tazettine did not confirm such a distribution, indicating that the regions of distribution differ depending on the type of plant alkaloid. In addition, this analysis of galanthamine distribution by MSI can identify regions with higher galantamine content and may contribute to an efficient determination of extraction regions for pharmaceutical manufacturing processes.

Novelty:
Distribution analysis by MSI is expected to contribute to improving the efficiency of pharmaceutical production from plant sources.

Preliminary Data:
This analysis of galanthamine distribution by MSI can identify regions with higher galantamine content.

Contributing Authors:
Kaoru Nakagawa; Tetsuo Iida; Shuichi Shimma; Manami Kobayashi

P-65

Nijs, Melanie
KU Leuven, Belgium

Hierarchical bi-clustering of mass spectrometry imaging data using recursive rank-2 non-negative matrix factorization

Introduction:
Mass spectrometry Imaging (MSI) is an advanced analytical technique that measures the abundance and spatial mapping of molecules present within a sample. One of the main challenges in MSI data analysis remains the complexity of the m/z-spectra caused by noise, matrix effects and other artifacts (Alexandrov et al., 2020). We observe that molecules with a high abundance suppresses those with lower m/z-ratios and can misdirect classical tools for data analysis, such as principal component analysis (PCA). Therefore, the observed significance of a molecule may not always be directly related to its abundance. In this work, we present a recursive rank-2 non-negative matrix factorization (rr2-NMF) algorithm that automatically returns spectral and spatial visualization of colocalized molecules, both highly and lowly abundant.

Method:
The proposed method performs a hierarchical inspection of the MSI of a tissue as it iteratively divides the data in two subclusters according to the similarity of the spectra, using the additive characteristic of NMF. We further examine two stopping criteria for the recursion: (i) a predefined depth of recursion, and (ii) convergence of the cosine similarity between the spectra of the pixels in each cluster. When the stopping criterion is met for a subcluster, the corresponding spectral and spatial distributions are plotted, together with a table containing the values of the peaks. To increase computational efficiency, we also provide a parallel implementation. We demonstrate performance and ease-of-use on MALDI-TOF MSI data from pancreatic tissues from healthy mice.

Results:
The results are easy-to-interpret spectral and spatial visualizations and demonstrate an increased level of detail compared to standard NMF (Nijs et al., 2021). The rr2-NMF algorithm starts from the full dataset and runs automatically until the stopping criterion is met. In contrast to previous analyses (Smets et al., 2019, Derwae et al., 2023) of our samples, rr2-NMF reveals detailed spatial and spectral distributions without parameter tuning or manual interaction. For the mouse pancreatic tissue, we detect known proteins present within the high abundances, including insulin (± 5800 Da) and the protein present in the acinar cells (± 6650 Da). Moreover, the method detects several molecules of interest with lower abundances, such as: ± 5821 Da, ± 5840 Da, 3923 Da, ± 3124 Da and ± 2901 Da, each of which exhibiting a particular spatial correlation. The spectral and spatial signatures of the clusters are confirmed by visualization of the ion images of the peak values. Our tool, implemented using Python's NMF package, performs unsupervised bi-clustering of the 1.6 GB sample in a few minutes, and allows for a 15% speed increase when executed in parallel. Finally, we compare the individual sample analyses with a multi-sample analysis across three pancreatic slices and demonstrate the scalability of the algorithm.

Novelty:
The proposed method already reveals detailed spatial and spectral distributions by tackling the dominance of the molecules in high abundance.

Preliminary Data:
Using rr2-NMF, we automatically detect relevant m/z-values in healthy mice pancreas and demonstrate scalability to multiple samples and bigger datasets.

Contributing Authors:
Etienne Waelkens (KU Leuven, Dept. Cellular and Molecular Medicine, Leuven, Belgium) Bart De Moor (KU Leuven, ESAT-STADIUS Leuven, Belgium)

P-66

Nikula, Chelsea
Sanofi, United States

Characterization of mRNA Vaccine Lipid Nanoparticle Biodistribution using a Multi-Modal Approach

Introduction:
Lipid nanoparticles (LNPs) as a mechanism for delivery of therapeutics has become a popular route for drug administration over the past 20 years. This is largely due to the ability of LNPs to protect the encapsulated drug, enable cellular uptake, and for the potential of targeted drug delivery through functionalization of surface lipids. In addition to their application in the delivery of small molecule therapeutics, LNPs have also recently been approved for use as a key component within multiple COVID-19 vaccine formulations.
Method:
In the development of new mRNA vaccines, the FDA and EMA recommend several studies to determine the biodistribution of mRNA, the carrier/delivery system, and the expressed protein. Matrix-assisted laser desorption/ionization mass spectrometry imaging (MALDI-MSI) is a technique which provides the spatial distribution of a variety of analytes including lipids, metabolites, drugs, and peptides within biological samples. Due to this, MALDI-MSI is very well suited to determine the biodistribution of the LNP carriers.
Results:
This work highlights the application of MALDI-MSI in combination with mRNA quantitation by RT-qPCR, protein expression using Luciferase-encoding mRNA, and lipid quantitation by LC-MS/MS to determine the spatial distribution of Sanofi mRNA LNPs and benchmarking mRNA LNPs in mice.
Novelty:
multi-modal approach to characterizing biodistribution of vaccine LNPs
Preliminary Data:
MALDI-MSI, RT-qPCR, protein expression, LC-MS
Contributing Authors:
Chelsea Nikula(1), Melody Li(1), Hui Wang(2), Kristen Randall(2), Sudha Sundaram(2), Katie Malley(3), Dinesh Bangari(3), Emanuele de Rinaldis(1), Lilu Guo(1), Bailin Zhang(1) 1 Precision Medicine and Computational Biology, R&D, Sanofi, Cambridge, MA, USA 2 Discovery Biology mRNA Center of Excellence, Vaccines, Sanofi, Waltham, MA, USA 3 Global Discovery Pathology, Translational In Vivo Models, Sanofi, Cambridge, MA, USA

P-67

Lanekoff, Ingela
Uppsala University, Sweden

Ion-to-image (i2i) – a new mass spectrometry imaging data analysis platform for continuous ionization techniques

Introduction:
Mass spectrometry imaging (MSI) needs efficient data processing pipelines to extract and generate information from very dense data sets. There is a multitude of different MSI modalities, yet there is currently no simple and free option to process Orbitrap data from imaging techniques with continuous data acquisition using automatic gain control (AGC). Here we present a new software application called ion-to-image (i2i) with a graphical user interface that is user-friendly. The i2i application supports both targeted and non-targeted data processing of the data set, region-of-interest analysis, scan filter selection, and quantitation. Together with the simple graphical user interface i2i enables efficient processing of continuously acquired MSI data.
Method:
The i2i application was written in MATLAB 2022a with the Bioinformatics Toolbox, Parallel Computing Toolbox, Image Processing Toolbox and MATLAB App Designer. Packages, including colormaps and special GUI functions, were downloaded from the MATLAB file exchange. The testing data set was generated from a mouse brain tissue section with pneumatically assisted nanospray desorption electrospray ionization (PA-nano-DESI) MSI on an Orbitrap Velos Pro set to 100 000 mass resolving power (at 400 m/z). The image had a total of 91 line scans, over 3.3 GB of raw data, and a pixel size of 20x75 µm.
Results:
For efficient data processing, all raw files from the imaging data set was converted to the open file format .mzML as centroids and read with an in-house made .mzML reader. The centroid data format is reduced compared to the continuous and enables data processing in real-time, being both memory efficient and highly responsive to the user. File loading from the 3.3 GB testing data set was completed in 92 seconds, corresponding to ~1 second per raw file (~14 MB), and extraction of m/z features for targeted analysis in milliseconds. The time for both file loading and feature extraction was found to correlate linearly with the file size. A large benefit of the i2i is that all scan filter information is simultaneously extracted. This makes it easy to select the desired scan filter for unique and complex data processing of images acquired using MSn, SIM, or polarity switching.
The i2i also includes a workflow for non-targeted analysis of MSI data sets that allows for unbiased comparison of tissue regions. Individual spectra are aligned by grouping all detected m/z together in feature groups. The feature groups can be filtered based on user-defined search parameters, including the minimum intensity, detection frequency, and fold change. The results show that 95% of all features in the test data set were grouped within less than 3.2 ppm mass error. In addition, it only takes 6 seconds to assign all feature groups from the test data set. Using the raw image of PC 34:1, we show that the number of false positive features is dependent on the parameter settings and can be minimized by adjusting the input parameters accordingly, thus increasing throughput and simplifying the workflow for non-targeted MSI.
Novelty:
We present a new i2i application for efficient image generation and data processing of MSI data acquired in continuous mode with AGC.
Preliminary Data:
-
Contributing Authors:
Johan Lillja1, Kyle D. Duncan1,2, Ingela Lanekoff1*

1 Department of Chemistry – BMC, Uppsala University, Uppsala, Sweden

2 AERL, Vancouver Island University, Nanaimo, VA, Canada

P-68

Okuda, Koji
Shimadzu Corporation, Japan

Immuno-elemental imaging by Laser Ablation – Inductively Coupled Mass Spectrometry (LA-ICP-MS) integrated with iMScope

Introduction:
Essential trace elements play crucial roles in the maintenance of health and prevention of the diseases. Although they are involved in many metabolic pathways, there has been few examples of observations on the dynamics of trace elements and their relationship to immunological functions throughout the body. Thymus is a lymphoid organ which plays a central role in immune responses. However, molecular dynamics of the thymic microenvironment and its relevance to autoimmune diseases remain largely unknown. We have developed a method, named thoracic Mass Spectrometry Imaging (tMSI), as a standard protocol of molecular imaging of whole-animal sectioning in various settings of mammals in vivo.
Method:
ICR mice and SJL/J mice were fed for the study of dexamethasone-induced immunosuppression, experimental autoimmune encephalomyelitis (EAE), respectively. J2N-k, known as cardiomyopathic hamster and its control, J2N-n hamsters at various weeks of age were also analyzed. Spectra were acquired using ICPMS2030 and iMScope (SHIMADZU), whereas ions were detected with a spatial resolution of 50 µm. IMAGEREVEALTM MS (1.30.0.11507) (SHIMADZU) was used for image and statistical analysis. Hematoxylin-Eosin staining was performed for identical and serial sections. In the current study, we have utilized laser ablation inductively coupled plasma mass spectrometry (LA-ICP-MS) for multi-modal tissue imaging technology to visualize the localization of P, Fe, Cu, Zn, and Rb in coronal sections of mouse and hamster thoracic tissue on a single slide.
Results:
Here we have successfully obtained multimodal imaging data with tMSI platform. In a single slide, bone marrow, thymus, lymph node, smooth muscle, skeletal muscle, heart, esophagus, trachea, lung, spinal cord, fat, arteriovenous vessels, and blood components could be observed. Integration of LA-ICP-MS and MALDI-MSI data sets delineates spatially resolved trace elements and metabolites directly from thoracic tissue samples. For example, iron and 2,3-BPG were mostly located intravascular areas where red blood cells resided. Especially, adopting uniform manifold approximation and projection (UMAP) method for tMSI well works on the classification of lymphoid organs strongly demarcated with Hematoxylin staining. As massive apoptotic cell death in the thymic cortex, necrotic cell death in the cardiac and skeletal muscle tissues, and lymphocyte trafficking into central nervous system were evidenced in dexamethasone induced mice, J2N-k hamsters, and EAE mice, respectively. As a result, known and unknown metabolomic and elemental factors were detected with multimodal approaches: massive cell death in the thymic cortex and medulla in DEX treated mice, lymphocyte trafficking from bone marrow into cardiac and skeletal muscles in J2N-k hamsters and ectopic immune cell infiltration from periphery into central nervous system in EAE mice with the current strategy.
Novelty:
LA-ICP-MS and iMscope with UMAP application gives us a new avenue to dissect an immuno-elemental aspect of the disease progression.
Preliminary Data:
Apoptotic and/or nectrotic cell death as well as immune cell trafficking process can be visualized with multimodal imaging technology.
Contributing Authors:
Koji Okuda1), Maiko Okamura2), Takushi Yamamoto1), Shinichi Yamaguchi1), Shuji Yamashita2), Masaya Ikegawa2) 1) SHIMADZU Co., Japan 2) Graduate School of Life and Medical Sciences, Doshisha University

P-69

Orekhov, Theodor
ICP RAS, Russia

Novel MALDI MS + FLIP approaches for verifying continuity of membranous structures and measurements of nucleus-cytoplasm exchange

Introduction:
Novel MALDI MS + FLIP approaches for verifying continuity of membranous structures and measurements of nucleus-cytoplasm exchange rates are proposed. Novel approaches for the measurements of lateral diffusion / molecular mobility and bindings using MALDI + FRAP hybridization are proposed.

Method:
FRAP (Fluorescence Recovery After Photobleaching) is a method for the diffusion kinetics measurements in living cells using fluorescence microscopy which allows to estimate quantitatively the two dimensional lateral diffusion in molecularly thin film containing fluorescent-labeled probes, or for single cell examination (i.e. the study of lateral mobility of cellular molecules). Fluorescence Loss in Photobleaching (FLIP) is a microscopic technique predominantly performed using laser scanning microscopy (e.g. for tagged protein local photobleaching by short, intensive laser excitation on CLSM platform) used for the studies on molecular mobility inside the cells and membranes. MALDI (Matrix-Assisted Laser Desorption / Ionization) is a soft ionization technique used in mass spectrometry, allowing for the analysis of biomolecules (biopolymers such as DNA, proteins, peptides and sugars) and large organic molecules (such as polymers, dendrimers and other macromolecules), which tend to be fragile and fragmented when ionized by more conventional ionization methods (according to encyclopedic definition). The above laser-based technique is readily compatible with MALDI and all above mentioned methods.

Results:
In this report we propose to design a new scheme for FRAP measurements based on a coordinate-positioning two-axis stage for MALDI imaging (from typical MALDI heads) and focusable laser sources with programmable microbeam / millibeam positioning. The method is appropriate for standard MALDI heads with nitrogen lasers (337 nm), excimer ArF (193 nm), KrF (248 nm), XeCl (308 nm) and frequency-tripled and quadrupled Nd:YAG lasers (355 nm and 266 nm, respectively). The method can also operate at non-conventional wavelengths, such as 532; 307, 317, 327, 347, and 357 nm (Ahn, 2012), according to the photobleachable carrier spectrum.

Novelty:
Novel MALDI MS + FLIP approaches for verifying continuity of membranous structures and measurements of nucleus-cytoplasm exchange rates are proposed.

Preliminary Data:
Many in situ MS-experiments were designed to obtain detailed information on the molecular-chemical basis of fluorescence recovery.

Contributing Authors:
T. Orekhov, A. Jablokow, O. Gradow

P-71

Petralia, Laudine
New England Biolabs, Inc., United States

Enzymatic release of parasite-specific glycans for MS imaging

Introduction:
Glycans, or carbohydrate chains attached to proteins or lipids, are widely distributed in nature and involved in a variety of biological processes, particularly in cellular communication. Broad glycosidases cleaving off the glycan from their carriers have proven valuable for glycomic studies. To date, only the peptide-N-glycosidase (PNGase) F releasing asparagine (N)-linked glycans from proteins has been used in mass spectrometry imaging (MSI) workflows, allowing major discoveries in malignant tissue N-glycosylation. PNGase A and Endoglycoceramidase (EGCase) would respectively allow MSI studies of N-glycans carrying α1-3 core-fucose and of glycosphingolipid (GSL) glycans. Both glycoconjugates are of high interest with GSL glycans being the major glycolipids found in animals, while N-glycans modified with α1-3 core-fucose are abundant in invertebrates and notably in parasitic helminths.
Method:
We applied a protocol established for PNGase F to release glycans from mammalian and non-mammalian tissues using PNGase A and EGCase. Fresh-frozen mouse livers and male Ascaris suum, a porcine nematode parasite, were sectioned in a cryostat and adjacent tissue sections were mounted on slides. Following washing, enzymes were applied to the slides using a TM-Sprayer™ and incubated at 37°C. Slides were scanned prior to being sprayed with α-Cyano-4-hydroxycinnamic acid matrix using the TM-Sprayer™ and imaged on a timsTOF flex instrument in positive ion-mode.
Results:
First, the ability of PNGase A to release mammalian N-glycans from mouse liver tissue sections was evaluated by comparison with PNGase F. Various incubation times, reaction buffers and enzyme concentrations were investigated to optimize the deglycosylation efficiency. Next, PNGase A was applied to A. suum sections previously treated with PNGase F, to release PNGase A-specific N-glycans expressed by the parasite. Similarly, we applied EGCase to both types of tissues since the use of this enzyme would permit the study of mammalian and parasitic GSL glycans in situ.
Novelty:
Initial use of glycosidases for MS imaging of relevant glycans
Preliminary Data:
NA
Contributing Authors:
Laudine M. C. Petralia[1], Edwin E. Escobar[1], Andrew Hanneman[1], Jeremy M. Foster[1] [1] New England Biolabs, Ipswich. MA, USA

P-72

Ponzoni, Adele Asia
Aliri, France

MALDI-FTICR-Mass Spectrometry Imaging untargeted spatial metabolomic analysis- Novel analysis approach for biomarker discovery in AS-associated Inflammatory Bowel Disease preclinical model

Introduction:
Ankylosing spondylitis (AS) is a chronic immune-mediated inflammatory disease, whose development is associated with HLA-B27, and primarily arises as spondylarthritis. AS-affected patients can also manifest inflammatory bowel disease (IBD), with a frequency of 5-10%. ERAP1 is the second most important identified locus in AS and its inhibition can be explored as a therapeutic approach. Identifying biomarkers in the compartments affected by the disease will help to assess molecular changes upon ERAP1-inhibitory treatment. We performed untargeted spatial metabolomic analysis on intestine samples from an AS preclinical model, using MALDI-Mass Spectrometry Imaging (MSI), and developed a data analysis approach aimed to highlight statistically relevant features. We performed MSMS fragmentation on the selected features to annotate them as biomarkers for the disease context.
Method:
Cecum and colon samples were collected from 18-weeks-old wildtype (wt) and HLA-B27 transgenic rats (n= 9 per group). 10µm-thick transversal cryosections were collected from each sample and spray-coated with DHB or 1,5-DAN matrices. Tissue imaging was performed at high spatial resolution, in positive and negative ion mode using a 7T-MALDI-FTICR mass spectrometer in full scan mode 75−1200 m/z. Following the acquisition, MALDI matrix was removed, and tissues were stained with hematoxylin-eosin (H&E) coloration. Data analysis, T-test (WT vs transgenic), clusters identification by KMEANS clustering on UMAP projection and morphometric analysis, were performed on MultimagingTM software. The features highlighted by the statistical analysis undergo MSMS fragmentation. The annotation was performed by comparing their fragmentation patterns with patterns available in open-source databases.
Results:
Segmentation of intestine layers was performed based on H&E coloration. Epithelial hyperplasia was observed in the samples from transgenic group. Colon and the cecum intestine showed great difference, in terms of features modulation, between wt and transgenic groups, when these were compared by statistical analysis. At the linear p-value and fold change threshold selected, 239 features in positive and 134 features in negative ion mode were significantly modulated in colon samples, and 274 features in positive and 315 features in negative ion mode were significantly modulated in cecum samples between the two groups. A batch integration step was implemented to remove the analytic bias between data obtained in separate run. This allowed for an improved cluster identification. Biological clusters separation was observed between wt and transgenic groups in both colon and cecum samples. Statistical analysis, i.e. T-test, was performed on the clusters characterizing the two groups, to highlight the features differentially modulated. By matching the results of these two approaches, 25 features in positive and 20 features in negative ion mode were highlighted in colon samples, and 35 features in positive and 15 features in negative ion mode were highlighted in cecum samples. Only a minority of features were shared by both colon and cecum samples. The MS/MS fragmentation patterns of these features were acquired, focusing on the region of signal's distribution, and multiple open-source databases were interrogated to annotate them as biomarkers, belonging to the class of metabolites and lipids. Morphometric analysis was further performed on the samples to improve the identification of modulated features between different histological and spatial regions.
Novelty:
Features were highlighted using a novel MSI-data analysis approach. Batch integration allowed the analysis of data from separated run.
Preliminary Data:
The workflow presented enabled spatial biomarker discovery, in a way specific to the disease context, from MSI data.
Contributing Authors:
Ponzoni Adele, Speca Silvia, Gerstenberg Amandine, Tomezyk Aurore, Gaudin Mathieu, Deprez-Poullain Rebecca, Launay David, Deprez Benoit, Ramos Corinne

P-73

Pope, Alexis
Vanderbilt University, United States of America

Mapping the lipid landscape of microbial biofilms by MALDI IMS

Introduction:
Microbial biofilms are surface-adhering communities encased in a protective extracellular matrix that often confer antibiotic resistance, host immune evasion, and high propensity for chronic infection. These emergent properties are due to the microbe-microbe interactions that give rise to organizational patterns and diverse functionality within biofilms. These intricate bacterial networks can be interrogated using matrix-assisted laser desorption/ionization (MALDI) imaging mass spectrometry (IMS) as it allows for spatial analysis of the molecular landscape, providing a deeper understanding of the biological drivers of pathogenesis and resistance. Here, we sought to leverage this technology to analyze biofilm heterogeneity within and between clinically relevant pathogens, such as Staphylococcus aureus, Pseudomonas aeruginosa, and Clostridioides difficile.
Method:
Biofilms were grown statically using filter discs on agar plates containing optimal media. Following incubation at 37C for 2-3 days, biofilms were frozen and embedded in a mixture of 5% carboxymethylcellulose(CMC) and 10% gelatin, cryosectioned at 10 µm thickness, and thaw mounted on indium tin oxide (ITO) poly-L-lysine coated slides. Samples used for lipid analysis were washed with 150 mM ammonium formate. Autofluorescence images were taken to determine morphological integrity prior to IMS experiments and for co-registration with complimentary microscopy. 4-dimethylamino cinnamic acid (DMACA) matrix was applied by sublimation and IMS data were acquired at 10 µm spatial resolution using MALDI timsTOF Flex (Bruker Daltonics). Data analysis was performed using SCiLS (Bruker Daltonics) and in-house software.
Results:
Bacterial biofilms (e.g., Staphylococcus aureus, Pseudomonas aeruginosa, and Clostridioides difficile) were grown using an in vitro filter disc assay. This static approach allowed for reproducibility and growth to maturity, as defined by consistent counts of colony-forming units (CFUs). We demonstrated that embedding using a CMC/gelatin mixture could adequately preserve biofilm morphology without interfering with MALDI IMS signal. Subsequent cryosectioning was possible at 10 µm thickness in an orientation exposing the interior elements of the biofilm. After washing of the sections with ammonium formate, sublimation of DMACA enabled highly sensitive lipid analysis with minimal delocalization. MALDI IMS was performed at 10µm spatial resolution in both positive and negative ion modes allowing for the detection of a wide range of lipid species. These include phosphatidylglycerol (PG), Lysyl-PG, cardiolipins (CL), phosphatidylcholine (PC), diacylglycerols (DG), and digalactosyldiacylglycerols (DGDG) which could be associated with specific regions of the biofilm. Current work is underway to validate lipid identities and to correlate molecular distributions to gradations in environmental factors such as nutrient accessibility.
Novelty:
MALDI IMS allows for spatial mapping of lipid distributions associated with distinct biofilm architecture across a variety of pathogens.
Preliminary Data:
10µm spatial resolution MALDI IMS showing lipid localization associated with morphological features unique to different microbial biofilms.
Contributing Authors:
Alexis Pope[1,2], Jeffrey A. Freiberg[4,5], Tess P. McNeely[4,5], Lukasz G. Migas[3], Madeline E. Colley[1,8], Raf Van de Plas[1,3], Eric P. Skaar[4,8], Jeffrey M. Spraggins[1,2,4-8] [1]Mass Spectrometry Research Center, Vanderbilt University, Nashville, TN; [2]Chemical & Physical Biology Program, Vanderbilt University, Nashville, TN; [3]Delft Center for Systems and Control, Delft University of Technology, Nashville, TN; [4]Department of Pathology, Microbiology, and Immunology, Vanderbilt University Medical Center, Nashville, TN; [5]Vanderbilt Institute for Infection, Immunology, and Inflammation, Vanderbilt University Medical Center, Nashville, TN; [6]Department of Cell and Developmental Biology, Vanderbilt University, Nashville, TN; [7]Department of Chemistry, Vanderbilt University, Nashville, TN; [8]Department of Biochemistry, Vanderbilt University, Nashville, TN

P-74

Preisler, Jan
Masaryk University, Czechia

Single-particle infrared laser ablation ICP MS for digital imaging of 3D cell aggregates

Introduction:
Conventional tools for immunohistochemical tissue imaging usually rely on confocal fluorescence microscopy (CFM), scanning/transmission electron microscopy (SEM/TEM), or laser ablation inductively coupled plasma mass spectrometry imaging (LA ICP MSI), sometimes termed imaging mass cytometry. We report a new laser ablation technique, single-particle infrared laser ablation (SPIRLA), employing a pulsed 2940 nm laser and a simple ablation cell for digital mapping biomarkers in tissues using gold nanoparticle (AuNP) tags. Unlike the conventional UV laser ablation systems, where nanoparticles are ablated, we are able to desorb intact nanoparticles and count them in the single-particle mode with an ICP mass spectrometer. This offers analogical advantages as photon counting compared to proportional light detection, including the detection limit of a single biomarker molecule.
Method:
The method is demonstrated by monitoring proliferating cells in 3D aggregates of human colorectal carcinoma HT29 cells. The 3D aggregate sections were labeled with primary biotinylated anti-Ki-67 monoclonal antibody and by streptavidin conjugates with 20 nm AuNPs or Alexa Fluor® 635 to image the Ki-67 antigen. The samples were ablated with an optical parametric oscillator (Opolette 2940, OPOTEK) in a laboratory-built IR ablation system connected to an ICP mass spectrometer (Agilent 7900, Agilent). For reference methods, a UV laser ablation system (LSX-213 G2+, Teledyne Photon Machines Inc.) equipped with a 213 nm Nd:YAG laser and laser scanning confocal microscope (TCS SP8; Leica Microsystems) were employed. Data were processed and visualized using a devoted program developed in the LabVIEW environment.
Results:
Using a simple ablation system with the 2940 nm laser, signals of intact AuNPs were generated from model samples by the ICP mass spectrometer running in the single-particle detection mode. The washout time of the ablation cell was ~70 ms, and the detection efficiency of AuNPs was 83%. This high percentage of detected AuNPs from surfaces is superior to existing laser ablation techniques and presents a tool with the ultimate detection limit of single biomarker molecules in tissues tagged with metal NPs. A set of sections from the equatorial part of a single 3D aggregate was imaged using conventional light microscopy, CFM, conventional UV LA ICP MSI, and SPIRLA ICP MSI. A reference CFM image of an aggregate section with Ki-67 labeled by Alexa Fluor® 635 conjugate shows the expected gradient of proliferating cell abundance decreasing gradually from the aggregate edge to its necrotic core. A similar trend is observed on images of an aggregate section with Ki-67 labeled by AuNPs from UV LA ICP MSI; significant background can be observed around the aggregate due to the nonspecific adsorption of AuNPs. Using SPIRLA ICP MSI, a sharp distribution map of the proliferation biomarker Ki-67 labeled with 20 nm AuNPs on an aggregate section was obtained. Thanks to the digital way of detection, units and low tens of AuNPs per pixel can be determined with an accuracy of one AuNP per pixel. Substituting proportional detection of photons or Au ions (in CFM or UV LA ICP MSI) with NP counting reduces digital noise and background signal of SPIRLA ICP MSI compared to both reference techniques. Furthermore, the use of IR laser substantially suppresses the desorption of AuNPs outside the tissue compared to the UV laser. With a multielement mass spectrometer, the technique has the potential for imaging multiple markers.
Novelty:
Digital tissue imaging with a single biomarker molecule detection limit based on a precise counting of gold nanoparticle tags.
Preliminary Data:
Multimodal images of proliferating cells in 3D cell aggregates using fluorescence microscopy, UV LA, and SPIRLA ICP MSI.
Contributing Authors:
Jan Preisler, Marek Stiborek, Lenka Jindřichová, Stanislava Meliorisová, Antonín Bednařík, Vadym Prysiazhnyi, Viktor Kanický, Jiří Kroupa, Pavel Houška, Barbora Adamová, Jarmila Navrátilová

P-75

Prentice, Boone
University of Florida, USA

Unraveling the Spatial Lipidome Using Gas-phase Ion/ion Reactions

Introduction:
The diverse array of chemical compounds present in tissue samples results in many isobaric (i.e., same nominal mass) and isomeric (i.e., same exact mass) compounds in imaging mass spectrometry experiments. Adequate separation and identification of these compounds is necessary to ensure accurate analyte annotation and avoid composite images comprised of multiple compounds. High-resolution accurate mass (HRAM) measurements are able to resolve these compounds in some instances, but HRAM measurements are not always feasible depending on the instrument platform and the desired experimental time scale. Alternatively, we have used ion/ion reactions to selectively react with desired classes of analytes. This reaction offers a rapid gas-phase fractionation approach that eliminates physical manipulation of the tissue for improved specificity in imaging mass spectrometry.

Method:
Gas-phase charge inversion ion/ion reactions are performed by alternatively injecting matrix-assisted laser desorption/ionization (MALDI)-generated lipid analyte ions generated from tissue surfaces and electrospray ionization (ESI)-generated reagent ions through a quadrupole mass filter and into a hexapole ion trap of a Fourier transform ion cyclotron resonance (FT-ICR) mass spectrometer (7T solariX, Bruker Daltonics). The MALDI-generate analyte ions are singly charged and the reagent ions are multiply charged and of the opposite polarity. A mutual storage ion/ion reaction period allows for the formation of charge inverted, lipid product ions. The product ions are then transferred to the ICR cell for subsequent dissociation and mass analysis.

Results:
We have developed instrumentation and novel gas-phase reactions to provide high levels of chemical resolution. These gas-phase transformations are fast, efficient, and specific, making them ideally suited for implementation into imaging mass spectrometry workflows. These workflows have enabled the identification of multiple sn-positional phosphatidylcholine (PC) isomers, the separation of isobaric phosphatidylserines and sulfatides, and the identification of fatty acid (FA) double bond isomers using a variety of charge transfer and covalent ion/ion reactions. For example, a charge inversion ion/ion reaction between protonated PCs and a 1,4-phenylenedipropionic acid (PDPA) reagent dianion was used to convert protonated PCs to anionic ion types and reveal up to five sn-positional isomers for each sum composition lipid, with the relative abundance of these isomers varying in abundance throughout rat brain tissue. Though phosphatidylcholines (PCs) are readily abundant in positive ion mode imaging mass spectrometry experiments, low energy collision induced dissociation (CID) of protonated PCs typically results exclusively in fragmentation of the lipid head group and gives no structural information on the fatty acyl chains. Following charge inversion to the negative ion mode via an ion/ion reaction with PDPA, CID of the PC anion readily produces fragment ions indicative of the FA tails present in the lipid. We have performed this reaction at every pixel in imaging mass spectrometry experiments to reveal significantly different relative spatial distributions of PC isomers within rat brain tissue, highlighting the importance of resolving isomers in imaging mass spectrometry experiments. We have also used ion/ion reactions to form divalent earth metal complexes with FAs to enable charge remote fragmentation upon CID and reveal double bond positions. This charge inversion ion/ion reaction was performed between fatty acid monoanions and magnesium tris-phenanthroline dications and resolved significant differences in palmitoleic and spienic FA isomer distributions in the dermis and sebaceous glands of human skin.

Novelty:
Gas-phase ion/ion reactions have been used to differentiate and identify isobaric and isomeric lipids in imaging mass spectrometry.

Preliminary Data:
Preliminary data are in the form of spatial profiling and imaging experiments revealing differential distributions of lipid isomers in tissues

Contributing Authors:
Boone M. Prentice

P-76

Pusparajah, Mathusha
Western University, Canada

Mass Spectrometry Imaging of Neurotransmitter Networks in DOX-Administered BRCA2 Knockout Mice Brains using FMP-10 Matrix

Introduction:
Germline breast cancer susceptibility gene 2 (BRCA2) mutations increase the risk of hereditary breast cancer. Doxorubicin (DOX) is an effective chemotherapy drug used to treat breast cancer; however, patients often experience DOX-induced cognitive impairment, also known as "chemobrain". Matrix-assisted laser desorption/ionization mass spectrometry imaging (MALDI-MSI) is a promising technique that maps the spatial distribution and relative abundance of molecules in brain tissue. The novel 2-fluoro-1-methyl pyridinium (FMP-10) reactive matrix, developed by TAG-ON, performs on-tissue chemical derivatization of phenolic hydroxyl, primary, and secondary amine groups to allow for easier ionization and identification of endogenous neurotransmitters in brain tissue. We applied the FMP-10 matrix to assess how DOX-administration alters neurotransmitter production and release in homozygous and heterozygous BRCA2 knockout mouse brains.
Method:
Female control and BRCA2 knockout mice are grown in a sterile, environment-controlled facility. At postnatal day 56, BRCA2 knockout mice are administered a single dose of DOX (10 mg/kg, i.p.), while the control mice are given vehicle (PBS). Brain tissues are collected 7 days post-treatment. A subset of brains is used for MALDI-MSI, while the remainder is used for quantitative (q)PCR and immunoblotting of DNA damage, apoptosis, and cell-cycle arrest markers. For MALDI-MSI, tissues are sectioned at the nucleus accumbens and hippocampus regions using a CM1850 Cryostat. The tissue sections are thaw-mounted onto a steel plate and sprayed with the FMP-10 matrix using a TM-Sprayer under optimized conditions. Mass spectrometric analyses are acquired using a Sciex 5800 MALDI TOF/TOF system.
Results:
Prior to imaging the DOX-administered BRCA2 knockout mice, we wanted to achieve optimal detection of neurotransmitter networks using the FMP-10 matrix, similar to that obtained by TAG-ON, with the instrumentation available at Western University. FMP-10 optimization trials were performed on wild-type mice brains by adjusting the TM-Sprayer nozzle temperature at which the FMP-10 matrix is sprayed on the tissue and the MALDI mass spectrometer laser intensity. We were able to conclude that when the FMP-10 matrix was sprayed at 85 °C and imaged at a laser intensity of 5100, we could detect up to 14 different neurochemicals in the tissue. We obtained high detection of neurotransmitters like dopamine, serotonin, γ-aminobutyric acid (GABA), and norepinephrine, as well as neurotransmitter metabolites like DOPAC, 3-MT, and 5-HIAL, and amino acids like L-histidine, L-phenylamine, L-cysteine, L-threonine, and L-serine, tyramine, and tryptamine. We applied this methodology to image the DOX-treated homozygous and heterozygous BRCA2 knockout mouse brains, and our MSI data revealed that DOX-administration can dysregulate major neurotransmitter levels in the NAcC brain region, contributing to the development of chemobrain. Through relative quantitation, we observed a statistically significant decrease in DA levels in WT+DOX, HET+DOX, and HOMO+DOX mice. Likewise, Antkiewicz-Michaluk et al. reported similar findings of a decrease in DA concentration in the frontal cortex, striatum, and hippocampus of rats following a single DOX injection. In addition, we observed a decrease in GABA and 5-HT due to DOX-administration; however, these results are not statistically significant, and more trials need to be conducted. Down-regulation of DA, GABA, and 5-HT was also observed in the NAcSh (Bregma 0.745 mm) and hippocampal regions (Bregma -2.255 mm) of these mice. Neurotransmitters are essential for normal cognitive functioning, and our results suggest that DOX-administration alters neurotransmitters, leading to impaired cognitive functioning.
Novelty:
Detecting and quantifying neurochemicals in DOX-treated BRCA2 knockout mice will help us understand how chemobrain develops in breast cancer patients.
Preliminary Data:
Decreases in dopamine, GABA, and 5-HT levels were observed in the nucleus accumbens core, shell, and hippocampus of DOX-treated mice.
Contributing Authors:
Mathusha Pusparajah, Juan Pablo Galindo Lazo, Berk Rasheed, Aman Singh, Krishna K. Singh and Ken K.-C. Yeung

P-77

Sato, Noriko
Hamamatsu University School of Medicine, Japan

Mass Spectrometry Imaging Reveals Alterations of 2-Arachidonoylglycerol in Brain Regions of Restraint-Stressed Mice after Traditional Herbal Medicine Administration.

Introduction:
The endocannabinoid 2-arachidonoylglycerol (2-AG) is elevated in response to chronic stress exposure. 2-AG has been implicated in anti-inflammatory and neuroprotective actions, relief of depressive symptoms, and reduced stress-induced anxiety behaviors. Using mass spectrometry imaging, our laboratory demonstrated that 2-AG levels increase in the brain tissue of mouse models subjected to chronic restraint stress. Furthermore, certain traditional herbal medicines, utilized in Japan for centuries, are known to counteract stress and cognitive decline. However, their exact mechanisms of action remain elusive. In this study, we investigated the changes in 2-AG distribution in the brain of chronic restraint stress mouse models following the administration of traditional herbal medicines known for their anti-stress and cognitive enhancement properties.
Method:
In this study, mice were divided into four groups: a control group receiving water, and three other groups each receiving a different type of traditional herbal medicine. They were restrained for 30 min in a 50 mL-centrifuge tube for eight consecutive days. On the eighth day, before the stress exposure, the control group was orally administered water, while each of the three treatment groups received their respective traditional herbal medicine. Subsequent imaging of the coronal brain sections of all groups was conducted using desorption electrospray ionization mass spectrometry imaging (DESI-MSI).
Results:
Imaging by DESI-MSI was performed on the 8th day after the start of chronic restraint stress, immediately after the last restraint stress after water or traditional herbal medicine administration. The results showed that for the water-treated control group, 2-AG accumulation was observed in the forebrain, similar to our previous report. On the other hand, for the three traditional herbal medicine (Yokukansan, Ninjin'yoeito, and Kamikihito) -treated groups, the signal intensity and distribution of 2-AG in the mouse brain was different from that of the water-treated control group. Also, the distribution of 2-AG precursors, 1-oleoyl-2-arachidonoyl-sn-glycerol (OAG) and 1-stearoyl-2-arachidonoylglycerol (SAG), was different from that of the control group.
Novelty:
We first analyzed 2-AG distribution in the brain after the administration of traditional herbal medicine to the restraint stress model mouse.
Preliminary Data:
DESI-MSI imaging of traditional herbal medicine components obtained in the measurement of traditional herbal medicines.
Contributing Authors:
Noriko Sato, Qing Zhai, Ariful Islam, Islam Md Monirul, Takumi Sakamoto, Yutaka Takahashi, Tomohito Sato, Hirotaka Kushida, Masashi Hiramoto, Takashi Matsumoto, Tomoaki Kahyo, and Mitsutoshi Setou

P-78

Sato, Tomohito
Hamamatsu University School of Medicine, Japan

Comparative Analysis of Three MSI Platforms for the Imaging of Cyclosporin A on Mouse Tissues

Introduction:
Cyclic peptides, with molecular weights ranging from 500 to 2000, are categorized as medium-sized molecules. Medium-sized molecules, with their ability to infiltrate cells like small molecule drugs and bind to specific molecules similar to large molecule drugs, are emerging as a promising therapeutic strategy for targeting intracellular lesion molecules. To accurately detect and identify trace molecules in tissues, Mass Spectrometry Imaging (MSI) platforms require both robust sensitivity and fine spatial resolution. In this study, the iMScopeTM QT (Shimadzu, Japan), also known as the newly developed atmospheric pressure matrix-assisted laser desorption/ionization (AP-MALDI), was applied to cyclosporin A (CsA) imaging and compared to other MSI platforms.
Method:
CsA standards were spotted onto mouse tissue sections mounted on slide glasses at various concentrations. Experiments were performed across four MSI platforms, AP-MALDI-QToF, MALDI Fourier transform ion cyclotron resonance (FT-ICR), desorption electrospray ionization quadrupole time-of-flight (DESI-QToF), and DESI- triple quadrupole (DESI-TQ). For AP-MALDI-QToF and MALDI-FT-ICR, α-Cyano-4-hydroxycinnamic acid (CHCA) was deposited using iMLayer (Shimadzu, Japan). For each device, conditions were optimized specifically for CsA imaging, and detection sensitivity was compared for imaging CsA on mouse tissue.
Results:
After applying different concentrations of CsA on mouse tissues, we assessed the detection sensitivity of each platform. In three platforms except for DESI-TQ, CsA was detected as [M+H]+, [M+Na]+, and [M+K]+. Across all three platforms, the ion with the potassium adduct for CsA, [M+K]+ exhibited the strongest detection signal. On the other hand, in DESI-TQ, cyclosporine was most strongly detected with the ammonium adduct ion. Our results indicated that concentrations of ≥0.5 µg/mL were detected with AP-MALDI-QToF, ≥2 µg/mL with DESI-QToF, and a more substantial ≥10 µg/mL with MALDI-FT-ICR. It was suggested that AP-MALDI-QToF is a promising option for imaging medium-sized cyclic peptides, such as CsA.
Novelty:
The fact that the imaging of cyclic peptides is performed using the newly developed AP-MALDI instrument.
Preliminary Data:
Tissue imaging of CsA-treated mice measured using each MSI platform.
Contributing Authors:
Tomohito Sato, Ariful Islam, Md Muedur Rahman, Takumi Sakamoto, Yutaka Takahashi, Tomoaki Kahyo, and Mitsutoshi Setou

P-79

Satoh, Takaya
JEOL Ltd., Japan

The improvement of qualities of mass images using a machine learning model trained scanning electron microscope images and its application to statistical analysis.

Introduction:
The matrix-assisted laser desorption/ionization imaging mass spectrometry (MALDI-MSI) is used to visualize the localization of proteins, peptides, metabolites, and drugs on the sample surface. One of the issues of MALDI-MSI is the relatively low SN ratio of extracted images. It is due to the ununiform matrix applied to the sample surface or low ion intensities from limited pixel regions. We have developed a method to improve the quality of extracted mass images using the machine learning model (hereafter called AI noise filter) trained scanning electron microscope images to solve the issue. The AI noise filter was also applied as a pretreatment of vertex component analysis (VCA), a type of statistic analysis.

Method:
The AI noise filter was created by the following procedure. Our machine learning model was created based on a conditional generative adversarial networks (cGAN), a supervised method. First, about 3,000 high-quality secondary electron images were prepared as training data. Then, low-quality images were created by adding shot noise following the Poisson distribution to the high-quality images at several levels of SN ratio settings. With paired low-quality and high-quality images, we trained the machine learning model that converts low-quality images to high-quality images. The procedure for applying this machine learning model trained scanning electron microscope images to MALDI-MSI was developed. The MALDI-MSI measurements were performed by JMS-S3000 “SpiralTOF™-plus 2.0” (JEOL Ltd.).

Results:
The performance of the AI noise filter was tested with two samples. The first was the permanent red pen, which includes compounds that can ionize without a matrix compound. The mass image of minor components, which have 0.1% ion intensity of the base peak in the average mass spectrum, was used for the test. We have compared the improvement of the image qualities of the AI noise filter, binning processing, and Gaussian filter. Gaussian filtering and binning processing can also remove noise to some extent but blur structures' contours. On the other hand, when the AI noise filter was used, denoising preserved the shapes of the image structure while improving the SN ratio. The second sample was a mouse brain tissue section. The 2,5-DHB was applied with an airbrush to observe lipids. More than 100 mass images were extracted from the high-mass resolution MALDI-MSI data. All the extracted mass imaging data were processed by AI noise filter, binning processing, and Gaussian filter. After that, we performed VCA analysis on all the processed data to find the characteristic parts from the mass image. As a result, we have found that the AI noise filtering processes before VCA analysis are much more effective than binning or Gaussian filtering. The VCA analysis can easily find the mass peaks contributing to the separation of characteristic parts.

Novelty:
Development of AI noise filter for improving the mass image qualities and its application to VCA analysis.

Preliminary Data:
The AI noise filter improved the quality of mass images and was effectively used to preprocess VCA analysis.

Contributing Authors:
Takaya Satoh

P-80

Schwamborn, Kristina
Institute of Pathology, TU Munich, Germany

Predictive proteomics in head and neck squamous cell carcinoma using mass spectrometry imaging

Introduction:
Head and neck squamous cell carcinoma (HNSCC) has high incidence and recurrence rates. From previous studies, we observed that the morphologic pattern known as tumor budding (TB) and a grading system based on TB and cell nest size (referred to as the cellular dissociation grading; CDG) exhibited a significant association with downregulation of immune cell infiltrate (CD3, CD8, and FoxP3-positive T-cells) as well as low expression of HLA and INF- γ. These findings suggest that morphologic patterns like TB and CDG, along with tumor stroma, hold promise as potential biomarkers for immunotherapy. We have investigated HNSCC tissue heterogeneity using mass spectrometry imaging (MSI) to identify potential molecular markers for a better disease stratification.
Method:
Following clinico-pathological, next generation sequencing, and immunological evaluations, the samples (n=48), assembled in four TMAs, were adhered to ITO glass slides. After deparaffinization and re-hydration, the samples were submitted to tryptic digestion, followed by matrix application using an HTX TM sprayer. The mass spectrometry proteomic data was recorded using a RapifleX MALDI-TOF instrument (Bruker) in the m/z range 600-3200. Following data acquisition, the tissue sections were stained using hematoxylin and eosin, and scanned using a digital slide scanner (Aperio AT). Regions of interest (tumor and stroma) were annotated by a board certified pathologist. Data analysis was carried out using SCiLS Lab. Features of interest where identified from MS/MS on-tissue fragmentation. Further validation using IHC was carried out.
Results:
Upon investigating the differences between the stroma and tumor composition, we discovered that approximately 23% of the 529 features examined in this study exhibited an ROC-AUC of over 80%, indicating the distinct nature of the tissues. Notably, m/z 1043.55 displayed a strong correlation with the epithelial regions. To assess tumor grading, we divided the patient cohort into three distinct grades. Principal component analysis revealed noticeable distinctions between grade 3 and grade 1 tumors. Here we identified molecular features from COL1A2, COL1A1, and H2B1, which were overexpressed in tumors with higher grades. Furthermore, a correlation was observed between higher tumor budding and the overexpression of three peptide fragments. When analyzing the correlation of immunologic variables with molecular alterations, we found significant associations between FAT1 mutation and high density intraepithelial CD3+ (p=0.025), CD8+ (p=0.005), and FoxP3+ (p=0.042) TIL infiltrate, as well as high density stromal CD8+ TIL infiltrate (p<0.001). We also investigated MSI proteomic signatures with TILs based on FAT1 mutation. ROC-AUC analysis revealed no significant proteomic differences in the CD3 positive epithelial regions. However, for the stroma, notable proteomic differences between CD3 positive and CD3 negative samples were identified through ROC-AUC analysis, including m/z 1585.8 (AUC=0.672), m/z 1781.9 (AUC=0.685), m/z 1079.7 (AUC=0.685), and m/z 1751.8 (AUC=0.685). Regarding CD3, CD8, and FOXP3, the PCA plots indicated distinct differences. However, these differences do not appear to stem from individual features, but rather from a group of features. Therefore, further exploration of these correlations through machine learning techniques is warranted. Our results show great promising in paving the way to include MALDI imaging as potential biomarker analysis method for ICI therapies but as well as for “conventional” or targeted therapy studies and patient prognostication based on morphomolecular and proteomic data.
Novelty:
Preliminary study for the use of MSI as a potential fast approach to assist with therapy decision for HNSCC patients.
Preliminary Data:
Identification of protein features that correlate with high tumor grading and with elevated tumor budding in HNSCC.
Contributing Authors:
Juliana P. L. Gonçalves, Nicole Pfarr, Wilko Weichert, Melanie Boxberg, Kristina Schwamborn

P-81

Scott, Claire
Vanderbilt University, United States

Characterizing the lipid and cellular landscape of Alzheimer's disease white matter hyperintensities

Introduction:
White matter hyperintensities (WMH) are brain lesions associated with Alzheimer's disease (AD) visible during MRI scans. Uncovering the molecular underpinnings of AD-associated brain tissue features such as WMH will lead to better understanding of the disease and effective treatment strategies. Molecular imaging of AD tissues via targeted immunofluorescence (IF) microscopy can reveal critical cell types and neuropathological features across tissue sections. MALDI IMS can be used for untargeted molecular mapping of human brain tissue sections. Whole brain lipid levels are altered in AD, and here we will examine how lipids are impacted within WMH in situ. We establish a multimodal imaging workflow that combines IF and MALDI IMS to comprehensively study cellular and molecular landscapes of human brain tissue.

Method:
Upon completion of T2-weighted-Fluid-Attenuated Inversion Recovery (T2-FLAIR) magnetic resonance imaging (MRI), FFPE AD and control human brain tissue samples were sectioned at 15µm thickness and mounted onto indium tin oxide (ITO) glass slides. Sections imaged using IF were photobleached prior to application of antibodies and subsequent imaging on a Zeiss Axioscan.Z1 slide scanner. Sections imaged with MALDI IMS were washed with 150 mM ammonium formate and sublimed with 10 mg of DMACA using an in-house developed sublimation device. MALDI IMS data were acquired at 10µm spatial resolution in positive and negative ionization on a Bruker timsTOF FleX (Bruker Daltonics). Data analysis was performed using SCiLS, ZEN microscopy software, and in-house software.

Results:
We are developing multimodal imaging workflows for human brain tissue, like those we have previously established for human kidney, that combine MRI, IF, and MALDI IMS. Incorporating MRI scans into our multimodal workflow provides clear distinction between WMH and normal appearing white matter (NAWM), allowing for inter- and intra-donor comparisons to be made between areas and WMH and NAWM. Initial validation of the growing panel of IF antibodies is underway. These markers are capable of mapping features within the brain, such as astrocytes, axons, myelin basic protein, activated microglia, blood vessels, tau tangles, and neuropil threads. Antibodies, such as Neurofilament 200, GFAP, and MBP, have been validated using control human brain tissue, confirming sensitivity and specificity, and determination of any background staining by omitting the primary antibody as a negative control. Antibody concentration has been adjusted to achieve optimal signal/noise ratio in human brain tissue. Microscopy images give cellular context to molecular data acquired with MALDI IMS. Whole-brain lipid levels have been found to be altered in those diagnosed with AD and we will examine how lipids are impacted within WMH. Experiments on samples of WMH and NAWM brain tissue from a 61-year-old male with AD were conducted at 10 µm spatial resolution with a scan range of m/z 200-2500 in negative ion mode. The number of common annotated peaks found in both samples was 243, while 78 peaks were unique to the NAWM, and 148 were unique to the WMH. Among the 243 shared peaks, various lipid species such as [SHexCer (42:1;O2)-H]- (m/z 890.638) were present at lower ion intensity in the WMH than the NAWM, while other lipid species such as [PA (36:1)-H]- (m/z 701.5132) were present at higher ion intensity in the WMH than the NAWM.

Novelty:
Combining MALDI IMS with IF allows for detailed mapping of the cellular and molecular landscape of Alzheimer's disease WMH.

Preliminary Data:
Co-registered MRI, IF, and negative ion mode MALDI IMS data reveal lipidomic differences between WMH and NAWM.

Contributing Authors:
Claire F Scott 1,2; Wilber Romero Fernandez 4; Cody R Marshall 2,3; Lukasz G Migas 7; Martin Dufresne 2,5; Angela Kruse 1,2; Katerina V Djambazova 1,2; Allison B Esselman 2,6; Matthew S Schrag 4; Raf Van de Plas 2,7; Jeffrey M Spraggins 1-3,5,6. 1Department of Cell and Developmental Biology, Vanderbilt University, Nashville, TN; 2Mass Spectrometry Research Center, Vanderbilt University, Nashville, TN; 3Chemical Physical Biology Program, Vanderbilt University School of Medicine, Nashville, TN; 4Department of Neurology, Vanderbilt University, Nashville, TN; 5Department of Biochemistry, Vanderbilt University, Nashville, TN; 6Department of Chemistry, Vanderbilt University, Nashville, TN; 7Delft University of Technology, Delft, Netherlands

P-82

Seneviratne, Herana Kamal
University of Maryland, Baltimore County, United States

MALDI mass spectrometry imaging reveals highly localized region-specific alterations of brain lipid metabolism across male and female mice

Introduction:
Lipids are vital as signaling molecules and structural components in the brain. The brain is a highly heterogeneous organ and its neuroanatomical regions are rich in complex lipids, such as sphingolipids (sphingomyelins, ceramides, sulfatides, cerebrosides, and gangliosides), glycerophospholipids, and cholesterol. Recent studies have shown that there is an association between altered lipid levels and an increased risk of adverse effects in the central nervous system. However, our current understanding of sex-specific alterations in brain lipid metabolism is incomplete.
Method:
With this in mind, we employed a high-resolution matrix-assisted laser desorption/ionization mass spectrometry imaging (MALDI MSI) coupled with tandem mass spectrometry to assess region-specific alterations in brain lipid metabolism in mice. For these, we used healthy adult C57BL/6J male and female mice (n=3). Freshly harvested brain tissues were snap frozen and coronal sections (10 µm thickness) were prepared using a cryostat. For lipid imaging, 2,5-dihydroxybenzoic acid was utilized as the matrix at a concentration of 15 mg/mL.
Results:
MALDI tissue imaging experiments revealed highly localized specific lipid precursors and metabolites belonging to a range of classes, including sphingomyelins, ceramide phosphates, phosphatidylcholines, glycerophosphoinositols, phosphatidylethanolamines, hexosyl ceramides, and sulfatides across male and female brain sections. Interestingly, lipid precursors (phosphatidylcholines and sphingomyelins) and their metabolites (lysophosphatidylcholines and ceramides) exhibited distinct localization in the hippocampus, thalamus, hypothalamus, corpus callosum, and cortex. Although phosphatidic acid 39:1 and 39:5 exhibited similar localization patterns in both male and female brains, male brain sections exhibited distinct enrichment of lysophosphatidylcholine 24:1 in the corpus callosum and fiber tracts. Further, phosphatidylcholine 32:3, 32:2, and 34:6 were more abundant in the hippocampus and cortex regions of male mice.
Novelty:
Application of MALDI Mass spectrometry imaging coupled with tandem mass spectrometry to assess region-specific alterations in brain lipid metabolism.
Preliminary Data:
Taken together, our results reveal novel lipid localization patterns highlighting region- and sex-specific differences in brain lipid composition and metabolism.
Contributing Authors:
Nav Raj Phulara, Farhan Augustine, Weihong Lin, Herana Kamal Seneviratne

P-83

Shimma, Shuichi
Osaka University, Japan

Enzyme histochemistry using mass spectrometry imaging

Introduction:
Investigating enzymatic process distribution in organisms is vital for understanding biological phenomena. Immunohistochemistry and in situ hybridization are commonly used for enzyme distribution evaluation, but they lack efficient enzyme activity visualization. Enzyme histochemistry enables localized visualization by administering a specific substrate to initiate enzymatic reactions on tissue sections. A chromogenic response occurs when the substrate interacts with the reaction's by-products or products, allowing detection and visualization. However, this technique is limited to enzymes with artificial substrates capable of generating color reactions through hydrolysis or oxidation-reduction processes. Recently, enzyme histochemistry using mass spectrometry imaging (MSI) has gained attention. It provides a novel advantage by directly ionizing substrate-enzyme reactions in tissues, allowing simultaneous detection of substrate and product. This poster will elucidate an innovative MSI-based approach to enzyme histochemistry, showcasing practical application examples.
Method:
In MSI-based enzyme histochemistry, the careful choice of substrates assumes significance. This presentation entailed visualizing the localization of enzyme reactions concerning acetylcholinesterase, choline acetyltransferase, and glutamate decarboxylase. The substrates employed for each enzyme were acetylcholine-d9, choline-d9, and glutamate-d3. The substrate solutions were applied via spray onto the surface of the sample sections and incubated for the designated duration. Subsequently, the matrix was introduced, followed by the execution of MSI.
Results:
The visualization of the acetylcholinesterase reaction in the mouse brain revealed its activity in the striatum, midbrain, and hypothalamus. Similarly, choline acetyltransferase exhibited activity specifically in the striatum of the mouse brain. When visualizing the mouse spinal cord, the reaction was observed to be active in the nerve roots originating from the spinal cord. Examination of glutamate decarboxylase in legumes and barley demonstrated a significant level of GABA production in the young roots. Additionally, in barley, the utilization of high-resolution imaging unveiled the occurrence of the reaction within the aleurone layer.
Novelty:
MSI-based enzyme histochemistry enables simultaneous detection and localization of substrate-enzyme reactions, offering an innovative approach.
Preliminary Data:
MSI-based enzyme histochemistry has demonstrated its applicability across a diverse range of enzymes.
Contributing Authors:
Shuichi Shimma

P-84

Shrestha, Bindesh
Waters Corporations, United States

Mass Spectrometry Imaging of metabolites using both untargeted and targeted MS systems with Desorption Electrospray Ionization (DESI)

Introduction:
Mass Spectrometry Imaging (MSI) methods, such as Desorption Electrospray Ionization (DESI), have emerged as powerful tools for determining the spatial distribution of metabolites and lipids within tissues. However, the complexity of tissues and the decreasing amounts of analytes sampled with higher spatial resolution pose challenges for the detection and quantitation of many low-abundant metabolites. DESI MSI is widely recognized for mapping small molecules from tissue sections without any sample preparation when combined with high-resolution mass spectrometers for untargeted imaging. On the other hand, tandem quadrupole instruments are known for their exceptional sensitivity and specificity in targeted applications using multiple reaction monitoring (MRM).

Method:
In this study, we present a comprehensive approach for investigating the distribution of small molecules. We utilized untargeted, discovery, MS mode with DESI on an ultrahigh-resolution Multi-Reflectron Time-of-Flight system (SELECT SERIES™ MRT mass spectrometer) to image a wide range of metabolites with a mass accuracy better than 500 ppb. We also performed targeted MS imaging, in MRM mode, of selected molecules on a tandem quadrupole MS (XEVO™ TQ Absolute mass spectrometer). Both experiments were conducted using the same DESI XS source with a high-performance sprayer at 2 µL/min solvent composition of 98:2 methanol:water containing 0.1% formic acid and 200 pg/µL of Leu-enkephalin.

Results:
The majority of metabolites and lipids were successfully imaged with high mass accuracy using the untargeted discovery imaging on the MRT MS. For targeted MS imaging with MRM, the tandem quadrupole demonstrated its capability to image the molecules through fragmentation, thereby providing a more confident identification. While the selectivity of the DESI MRT system, with its ultrahigh resolution (200,000 FWHM), enabled the filtering out of interferences, the DESI TQ system with its MRM transition's selectivity exhibited superiority as no signals were detected outside the tissue section. This finding highlights the enhanced specificity of the targeted approach for imaging MS. This integrated approach enables comprehensive analysis of metabolite and lipid distributions in tissues, providing valuable insights into their spatial localization and potential functional roles.

Novelty:
Untargeted and targeted imaging using Desorption Electrospray Ionization (DESI)

Preliminary Data:
Mass Spectrometry Imaging of metabolites using both untargeted and targeted MS systems with Desorption Electrospray Ionization (DESI)

Contributing Authors:
Bindesh Shrestha, Mark Towers, Hernando Olivos, Anthony Midey, and Emmanuelle Claude

P-85

Maneta, Stefania
Imperial College London, United Kingdom

Single-Cell Omics and Mass Spectrometry Imaging Using Laser Desorption – Rapid Evaporative Ionisation Mass Spectrometry

Introduction:
The robust and reproducible metabolomic and lipidomic characterization of individual cells has been a long-standing goal in the field of mass spectrometry. Mass Spectrometry Imaging (MSI) provides a potential answer to this challenge through various techniques (such as Matrix Assisted Laser Desorption Ionisation (MALDI) or Desorption ElectroSpray Ionisation (DESI)) that can routinely achieve single-cell resolution in MSI data. Here we present our novel method, Laser Desorption – Rapid Evaporative Ionization Mass Spectrometry (LD-REIMS) as a new method for single-cell omics works. REIMS was initially a technique for characterizing bulk tissues (even in vivo environments), microbial colonies, food products, and cells. With the utilization of purpose built imaging platforms using 3-micron lasers we were able to use the novel ionization method to enable single-cell resolution imaging without the need of prior sample preparation. Here we present our work in the development of the technique, and single-cell imaging application to perform metabolomic profiling and histologically classifying various human cancerous samples, animal models, and cell and organoid samples using metabolic information.
Method:
The instrument consists of a prototype REIMS source installed on a Xevo G2-XS QToF (Waters) mass spectrometer. Home-built motorized 2D XY (Prosolia and Thorlabs) stages coupled with laser optics were used as a sampling platform for all imaging experiments. The generated aerosol was aspirated from near the focal optics using a 1.5 mm long PTFE tubing. The REIMS source was configured in ”direct inlet” mode, and a Tee piece was used to supply 0.1 ml/min 2-propanol as a matrix solution. The iKnife experiments were performed using a prototype handpiece coupled with a Covidien ForceTriad diathermy generator. Intelliguide CO2 laser (Omniguide) at 10600nm, Opolette HE2731 OPO laser (Opotek), 2700–3100nm, and prototype picosecond infrared laser (operating at 3000 nm wavelength, 500kHz frequency and around 200 nJ/pulse energy) were used to map the laser parameters. Fresh frozen Porcine liver, mouse, and rat brain samples (sectioned to 12 µm thickness and mounted on standard superfrost microscope slides) were used for optimizing and characterizing the setup. Fresh frozen and Formalin-Fixed, Paraffin Embedded (FFPE) Human colorectal tissues and tissue microarrays, and breast cancer samples were used for human tissue imaging. A2480 and OVCAR4 ovarian cancer cell line samples were used for single-cell experiments.
Results:
The molecular coverage of the Laser Desorption – REIMS is comparable to the iKnife data and other imaging techniques, numerous metabolites and lipids were observed during experiments. Using the animal tissues, the laser fluences and spot sizes were optimized. The spot size achieved with our setup after optimization was 70µm with the CO2 laser, around 25µm with the OPO laser, and 10µm with the picosecond laser, fluence at the ablation point was found to be around 5 J/cm2 with the commercial lasers and 1 e-1J/cm2 with the picosecond setup. Using oversampling techniques, 20 µm imaging was achieved using the nanosecond OPO laser on mouse brain samples, providing close to single-cell resolution images. Due to the superior beam quality of the picosecond laser, <10µm raster imaging was possible, proving the capacity to do single-cell resolution imaging. The short picosecond pulsed laser also enhances the sensitivity of the technique by two orders of magnitude compared to the commercial OPO laser. The obtained metabolic profiles were used to match the histological status of the tissue, and the method allows a robust and reproducible acquisition of molecular pathological data, which shows a good correlation with the histopathological status of tissues. Human colorectal cancer and breast cancer models were tested with the method. A multiomics LD-REIMS imaging study was also performed on FFPE colorectal Tissue MicroArray (TMA) slides, the setup was compared with and without xylene treatment samples and no significant differences were found between the two, proving the method to be true sample-preparation free method for analyzing FFPE samples and larger cohorts of samples are under analysis for the large-scale study. The method was also tested in transmission mode using cell models. Compared to Reflection -mode optics (where the laser is focused to the glass-slide mounted tissue from the side of the tissue) transmission mode setup allows the utilization of shorter focal distance optics at the cost of the power loss caused by the IR absorption of the glass slide, which absorbs around 25% of the energy. The transmission mode setup allows the acquisition of data from single cells from 3D culturing media. Organoid models were acquired within a matrigel environment and imaging data was successfully collected from sectioned organoid models.

Novelty:
Sample preparation-free ambient ionization imaging technique, that can provide single-cell resolution imaging data.
Preliminary Data:
Results on systems characterization, imaging data on various human, animal and cell lines, fresh frozen and FFPE processed.
Contributing Authors:
Daniel Simon (1) (2) Yuchen Xiang (1) Ronan Battle (1) Stefania M. Stavrakaki (1) Helen Huang (1) Kenneth Robinson (2) Lauren Ford (1) Robert Murray (1) Zoltan Takats (1) (2) (1) Imperial College London, London, United Kingdom (2) Rosalind Franklin Institute, Harwell, United Kingdom

P-86

Sisley, Emma
University of Birmingham, England

Tissue Washing Improves Native Ambient Mass Spectrometry Imaging of Membrane Proteins

Introduction:
Nano-desorption electrospray ionisation (nano-DESI) is an ambient MS imaging technique which allows in situ analysis of proteins and their complexes directly from tissue, providing both structural and spatial information. Until recently, the approach was applied exclusively to the analysis of soluble proteins; however, there is a drive for new techniques which enable analysis of membrane proteins. Here we present a tissue washing method, combined with an increased detergent concentration in our sampling solvents, that has allowed us to detect and image membrane proteins directly from rat brain and kidney tissue.
Method:
Nano-DESI MSI was performed using a home-built ion source coupled to an Orbitrap Eclipse mass spectrometer. Thin tissue sections (10 µm) from fresh frozen rat brain or kidney were thaw mounted onto glass slides. Tissue sections were washed 3x using 200 mM of ammonium acetate while control samples were left unwashed. Nano-DESI imaging experiments were conducted using 200 mM ammonium acetate + 2x the critical micelle concentration (CMC) of the detergent C8E4. Proteins of interest were identified through in-situ top-down HCD fragmentation.
Results:
Method development was initially performed using brain tissue. Introducing a washing step prior to nano-DESI and sampling with 2x CMC yielded a range of newly detected signals compared to mass spectra collected from unwashed tissue. These new proteins were fragmented resulting in the identification of two membrane proteins, VDAC1 and VAMP2 from the brain. VDAC1 is a beta barrel membrane protein located in the outer membrane of mitochondria while VAMP2 is a single pass membrane protein found in synaptic vesicles. In addition to integral membrane proteins, tissue-washing enabled detection of membrane-associated proteins. RAB3a was identified and found to be modified with hydrophobic S-geranylgeranyl groups on the two cysteine residues at its C-terminus. These hydrophobic lipid anchors are important for membrane localisation. Rab3a was also observed to have GDP non-covalently bound suggesting that washing does not necessarily disrupt non-covalent interactions. MS imaging was performed and showed that the membrane proteins retain their spatial distribution after washing. The RAB3A and other membrane associated proteins were also observed to have distinct spatial distributions showing the tissue washing approach to be compatible with MS imaging. Soluble proteins such as ARF3, that were easily observed with 0.5x CMC of detergent (and no washing), were observed to be delocalised. The workflow was also applied to sections of rat kidney. MSI of the kidney tissue yielded similar results. A range of proteins (20.3 – 51.7 kDa) showed distinct distributions. Actin, a soluble protein, was identified in the mass spectra but in the MS image was shown to be delocalised.
Novelty:
Tissue washing and increased detergent concentration enables ambient MSI of membrane proteins in a range of tissues.
Preliminary Data:
Mass spectrometry imaging and identification of membrane proteins in rat brain and kidney tissue
Contributing Authors:
Oliver J. Hale Helen J. Cooper

P-87

Spangenberg, Philippa
Department of Immunodynamics, Institute for Experimental Immunology and Imaging, Medical Research Centre, University Hospital Essen, Essen, Germany, Germany

Identification of tissue niche-specific molecular signatures by mass spectrometry imaging

Introduction:
Tissues contain a plethora of different niches, where a dynamic cellular crosstalk shapes physiological and pathological processes. Under inflammatory conditions, tissue niches can influence immunological mechanisms such as immune cell recruitment by releasing chemotactic signals, that attract immune cells to the site of infection. Identification of molecular signatures specific to these tissue microenvironments is crucial to better understand the immunological mechanisms that regulate immune cell migration and function. Mass spectrometry imaging (MSI) enables the spatial mapping of molecules within tissue sections, providing a means to identify niche-specific molecules. However the identification of such molecules in raw MSI data remains challenging. Here we present a new analysis pipeline to investigate tissue niche-specific molecular signatures in MSI data.
Method:
We performed MSI on consecutive 8 µm-thick tissue sections from uropathogenic Escherichia coli (UPEC)-infected and control urinary bladders (n=10) of female mice. MSI experiments were conducted on a timsTOF fleX MALDI-2 instrument (Bruker Daltonics) at a pixel size of 5 µm. MSI data were pre-processed by smoothing, peak picking, alignment, matrix/artifact removal, peak filtering, and normalization. Statistical analysis, dimensionality reduction and machine-learning-based algorithms were used to extract and visualize tissue niche-specific molecules. Immunofluorescence (IF) staining was performed on adjacent sections which were incubated with antibodies against epithelial cells and neutrophils (EpCAM-1 and Ly6G) and imaged on a Zeiss AxioScan.Z1. MSI and IF data were registered via symmetric normalization implemented in the Advanced Normalization Tools (ANTs) library.
Results:
We developed a pipeline which integrates bioinformatic methods for data pre-processing and analysis. The pre-processing workflow takes raw MSI files as input, processes all files in parallel, and outputs the processed data in imzML format along with various quality control visualizations for each step. All processing steps are automated in a pipeline integrated into the workflow management system Snakemake, which enables reproducible and scalable data analyses. Within the pre-processing workflow non-tissue-related pixels and non-informative ions are removed to enhance data quality for subsequent analysis. Therefore we use the spatial coherence measure and developed a UMAP-based clustering approach. The analysis workflow takes the pre-processed imzML data as input and extracts tissue niche-specific molecules by using statistical analysis, dimensionality reduction and machine-learning-based algorithms. We used this pipeline to analyze MSI data of UPEC-infected vs control urinary bladder sections of female mice. With our pipeline we could identify distinct pixel clusters within the infected urothelium which highly express triacylglycerols. Furthermore, the analysis revealed that several ether-linked phospholipids are upregulated in the infected bladder and are in spatial proximity to the identified urothelial cluster. We performed immunofluorescence staining on consecutive sections which were incubated with antibodies against neutrophils. We integrated the microscopy data with the MSI data through image registration. By correlating the MSI signals to the microscopy images, we could show that the identified phospholipids are co-localized to neutrophils.
Novelty:
We integrate and optimize existing bioinformatic methods into an automated workflow capable of extracting tissue niche-specific molecular signals.
Preliminary Data:
Preliminary MSI data of UPEC-infected vs control bladder sections showed significant molecular changes between the two groups.
Contributing Authors:
Philippa Spangenberg, Sebastian Bessler, Sascha D. Krauß, Jenny Bottek, Lars Widera, Stephanie Thiebes, Devon Siemes, Jianxu Chen, Abdelrahman Elskhawy, Jens Kleesiek, Jens Soltwisch, Olga Shevchuk, Matthias Gunzer, Klaus Dreisewerd, Daniel R. Engel

P-88

Spathies, Jacquelyn
Vanderbilt University, United States

Lipidomic characterization of mucosal and submucosal regions along the zebrafish gastrointestinal tract using High-Resolution MALDI Imaging mass spectrometry

Introduction:
The gastrointestinal tract (GI) of adult zebrafish contains heterogeneous cell populations such as mucin-secreting goblet cells that help create a mucosal barrier similar to humans. This barrier is the first line of defense against infection and is heavily impacted during inflammation and injury. Molecular imaging technologies, such as imaging mass spectrometry (IMS), can be co-registered with microscopy data to determine the molecular profiles of specific tissue regions and cell types along the zebrafish GI tract, including the mucus layer. Herrin, we characterize the lipidomic profile of the mucosal and submucosal regions along the zebrafish GI tract based on IMS, fluorescence, and stained microscopy.

Method:
Matrix-assisted laser desorption ionization time-of-flight IMS (MALDI TOF IMS) was performed using a timsTOF Flex (Bruker Daltonics) for lipidomic analysis of zebrafish GI tract. Experiments were done on a transgenic GFP-tagged Claudin 15-like a (cldn15la:GFP) and wild-type zebrafish. Three fish per group were euthanized at >90 days post fertilization, GI tracts were collected, and samples were frozen in 100% an isopentane/dry ice slurry and embedded in 10% fish gelatin. Sections were sectioned at a thickness of 10 um, and pre-IMS fluorescent images were taken (Zeiss Axio Scan.Z1). An aminated cinnamic acid analog matrix was applied using an in-house sublimation apparatus. Images were then analyzed using SCILS (Bruker Daltonics) and in-house software.

Results:
In this study, we developed a MALDI IMS workflow for the analysis of dissected GI tract of adult zebrafish. Sample processing and preparation were optimized to enable high spatial resolution IMS at 10 um. Unsupervised machine learning was performed, revealing multivariate lipid profiles of sub-mucosal and mucosal regions within the tissue based on k-means clustering and segmentation. Utilizing the genetic tractability of zebrafish, experiments were done on a transgenic Cldn15la:GFP zebrafish line containing a fluorescently labeled intestinal-specific membrane protein. The tg(Cldn15la:GFP) line allowed for improved examination of the cellular and luminal arrangements within the GI tract. Microscopy data from transgenic fish was used to validate the molecular localization data generated from IMS experiments. Alcian blue staining of acidic mucosal sugars was done on post-IMS sections to provide additional confirmation that the lipid profiles assigned to these regions are in reference to the mucosal barrier. Smaller lipids, such as sterols or cholesterol classes, localize to the mucosal region, while the sub-mucosal region has a higher abundance of glycerophospholipids. Future LC-MS/MS experiments will be done to confirm the exact lipids present in these two tissue regions. These methods will be used to study shifts in the lipidomic profiles of mucosal and sub-mucosal regions during bacterial exposure to better understand how these shifts contribute to bacterial growth and expansion.

Novelty:
Discovering lipidomic profile of mucosal and sub-mucosal regions along the zebrafish GI tract using integrated microscopy and high-resolution MALDI IMS

Preliminary Data:
High spatial resolution IMS can characterize the lipid distribution along the mucosal and sub-mucosal regions of the zebrafish GI tract.

Contributing Authors:
Jacquelyn Spathies, Caitlin C. Murdoch, Eric P. Skaar, Jeffrey M. Spraggins

P-89

Towers, Mark
Waters Corporation, United kingdom

Towards In-Vitro Diagnostic Imaging of HepaRG Spheroids by DESI-Tandem Quadrupole MS.

Introduction:
During the development stages for novel pharmaceutical compounds there is the requirement for in-vivo dosing for efficacy and safety assessment. With the introduction of the 3R's concept, scientists have been constantly improving in-vitro tests, allowing for a more informed candidate selection and elimination process prior to animal study requirement. Until recently in vitro studies have focused primarily on 2D cell cultures, however there is a growing interest in 3D models that better mimic the micro-environment within an organism. In particular, 3D liver models such as HepaRG spheroids have been developed to investigate drug-induced liver injury (DILI). Here we show targeted high sensitivity DESI imaging analysis; mapping drug and drug-metabolite localization within the HepaRG spheroids.

Method:
HepaRG spheroids were cultured for 7 days, after which they were dosed at typical therapeutic levels, with either; perhexiline, carbamazepine or warfarin. Perhexiline was dosed at between 10 µM and 0.004 µM, carbamazepine and warfarin were dosed at 1000 µM and 0.4 µM. Approximately 72 hrs After dosing the spheroids were moved to storage at 4 ºC. Prior to analysis the spheriods were washed 1XPBS. Spheroids were spotted onto polylysine coated glass slides and dried for 5 mins in a desiccator prior to analysis. A 1 µL PBS blank was also spotted. Samples were analyzed using a Waters™ Xevo™ TQ Absolute tandem quadrupole mass analyzer fitted with a Waters DESI XS source using the high performance sprayer.

Results:
The candidate pharmaceutical compounds were selected based on DESI ionization efficiency of the target compound and observed cytotoxicity at typical study dosing levels. To observe the progressive hepatotoxic effect of each drug, the spheroids were cultured in media spiked at various concentrations: covering typical expected dosing levels in-vitro. This feasibility study aims to demonstrate that DESI-MS provides a suitable platform for imaging spheroids and that drugs and their metabolites can be detected within the spheroids, due to the high sensitivity provided by targeted tandem quadrupole mass spectrometry. Spheroid analysis using a Q-ToF mass spectrometer provides a screening application where the living tissue can clearly be distinguished from the necrotic core and biological changes can be investigated between control and dosed tissue. By combining the two techniques, a comprehensive data set can be generated mapping drug penetration, metabolite production and biological changes within e.g. the lipid profile. The workflow includes peak list generation for each tissue region, enabling statistical analysis for discovery of target marker compounds. Imaging software was used to create visual overlays of the marker compounds, clearly demonstrating the distribution of each molecule within the spheroid. Perhexaline was imaged down to the 0.04 µM dosing level, warfarin to 1µM and Carbamazepine to 4µM. In addition, the metabolites Cis-Hydroxy-Perhexiline, 10-OH Warfarin and 7-OH Warfarin, were also observed and localisation within the spheroid visualised. This work demonstrates that spheroids can be imaged by DESI either using a QToF style mass spectrometer for a general screening approach or with a more targeted tandem quadrupole instrument for increased selectivity and sensitivity of preselected analytes of interest. For Research Use Only. Not for use in diagnostic procedures.

Novelty:
Enhanced analyte selectivity and sensitivity, spheroid imaging using a DESI inlet coupled to a tandem quadrupole mass spectrometer.

Preliminary Data:
DESI XS inlet on a Xevo TQ Absolute provides a sensitive tool for imaging drug and drug-metabolite distribution within spheroids.

Contributing Authors:
Lisa Reid(1), Alicia Rosell-Hidalgo(2), Kirsten Headspith(2) 1) Waters Corporation, Wilmslow, Cheshire, UK. 2) Cyprotex Ltd., Alderley Park, Cheshire, UK

P-90

Trinklein, Timothy
University of Illinois Urbana-Champaign, United States

Three-dimensional tissue biochemical mapping with cell-type specificityvia an integrative deep learning-based mass spectrometry imaging pipeline

Introduction:
A novel integrative experimental and computational mass spectrometry imaging (MSI) framework is introduced to address several key issues in 3D biochemical tissue mapping. First, the pipeline is shown to increase the throughput of acquiring Fourier transform (FT)-MSI by 15-fold via deep learning-based reconstruction. Second, multimodal image registration is used to correct geometric deformations in tissue sections. Finally, we integrate data from thousands of isolated single cells from the same tissue and map the chemical profile of single cells back to their spatial origin via a learning-based computational approach.
Method:
To enhance the throughput of FT-MSI of many tissue sections, select sections are imaged with long transients while the remaining sections are imaged at high throughput with short transients. The entire dataset was reconstructed using a deep neural network designed to learn and recover low-dimensional embeddings of the high-resolution data. Next, thousands of single cells are dissociated from adjacent tissue sections and profiled by FT-MS also reconstructed by a similar deep-learning-based method. A Union-of-Subspaces (UoSS) model is used to map dictionaries of single-cell clusters to the tissue maps. Registration of brain sections to a magnetic resonance imaging (MRI) atlas enables geometric deformation correction for volumetric reconstruction while further allowing single-cell data to be assigned to brain-region-specific locations.
Results:
Our approach is validated on two tissue types: rat brain (coronal and sagittal sections) and rat pancreas. Three-dimensional mapping of the rat brain was achieved with 50 µm lateral resolution and 16 µm sections with over 1,000 lipid features detected. Serial MSI sections were successfully registered to an MRI atlas, allowing 3D visualization of biomolecular distributions. A total of 13,566 single cells from five brain regions were chemically profiled and mapped back to the tissue of origin. This enabled us to localize lipid profiles to specific brain regions. A total of 344 lipids were cross-annotated and used to generate 18 single cell clusters. Both cluster-specific and brain region-specific lipid organization was discovered. For instance, hexosylceramide was found in higher levels in the brainstem, thalamus, and superior colliculus, while ceramides and sphingomyelins were more abundant in the corpus callosum and the corticofugal pathway. To demonstrate generalizability to other tissue types and chemical compounds, rat pancreas sections were imaged along with thousands of single cells. Peptide and lipid signals provided spatial contextualization for single cells within pancreatic islets simultaneous with high-throughput volumetric imaging. In summary, we demonstrate high-throughput, multiscale biochemical profiling of the 3D tissues. Large-scale single-cell biochemical profiles can be mapped to spatial locations in tissue in concert with high-resolution tissue FT-MSI, providing unprecedented insight into the intricate biochemical organization of tissues.
Novelty:
This method jointly learns two coupled networks to discover and recover low-dimensional embeddings of high-dimensional data for high-resolution reconstruction from short transients. Computationally integrating dissociated single-cell profiles and tissue i
Preliminary Data:
Data for deep learning-based reconstruction of rat brain sections is given. Results of single cells mapped to tissue-specific regions are shown.
Contributing Authors:
Yuxuan Richard Xie, Timothy J. Trinklein, Daniel C. Castro, Stanislav S. Rubakhin, Jonathan V. Sweedler*, Fan Lam*

P-91

Vallianatou, Theodosia
Uppsala University, Sweden

Spatial metabolic mapping of the aging brain with mass spectrometry imaging

Introduction:
Thorough metabolic profiling of specific brain regions in early aging may reveal pathophysiological mechanisms and identify potential neuropharmacological targets associated with the onset of cognitive decline. By using positive ionization mode mass spectrometry imaging (MSI), we have previously mapped multiple neurochemical alterations, including catecholamines and indoleamines, cholinergic pathway metabolites, cerebrosides and antioxidants, associated with early aging in various mouse brain regions. Furthermore, we have investigated the interaction between aging and the response to tacrine-induced acetylcholinesterase inhibition, a well-characterized therapeutic approach for dementia treatment. In this study, we utilized negative mode MSI expanding our understanding of brain senescence towards other classes of lipids and metabolites. Hence, we aim at establishing a comprehensive spatial metabolic platform associated with brain aging.
Method:
We used matrix-assisted lased desorption/ionization (MALDI) MSI to perform untargeted spatial metabolomics on brain tissue from 12-weeks (n=8) and 14-months (n=8) old mice. Half of the mice in each age group were administered tacrine and half the vehicle. 9-amino acridine (9AA) and N-(1-naphthyl) ethylenediamine dihydrochloride (NEDC) were used as the MALDI matrices. Ultrahigh mass resolution experiments were performed in a Fourier-transform ion cyclotron resonance (FTICR) mass spectrometer and high lateral resolution analysis on selected tissue sections was performed in a timsTOF instrument. Metabolite identification and structural validation was performed in the FT-ICR and, in specific cases, with Desorption electrospray ionization (DESI)/QQQ instrumentation.
Results:
With our negative ionization mode MSI approach, we imaged a wide range of brain metabolites (m/z 80-1500), including, among others, taurine, aspartate, glutamate (Glu), glutamine (Gln), N-acetyl-aspartate, N-acetyl-aspartyl-glutamate, beta-citryl-glutamate, ascorbic acid, glutathione, purine and pyrimidine nucleotides and multiple lipid classes (sphingolipids, sulfatides, phosphoethanolamines, lysophospholipids). Multivariate data analysis and three-way ANOVA (factors: age-treatment-brain region) revealed a significant overall aging effect. Aging and tacrine administration were associated with increased Gln/Glu ratio, an indicator of neural/glial function. Several sulfatides, localized in the white matter, were altered (increased or decreased) with aging, while levels of lysophosphatidic acids decreased with age, especially in cortex, striatum and hippocampus.
Novelty:
Together with our previous findings, we have uncovered region-specific unique metabolic changes leading to establishing predictive models for brain ageing.
Preliminary Data:
Early aging affects multiple brain metabolic pathways in a region-specific manner.
Contributing Authors:
Theodosia Vallianatou, Anna Nilsson, Tina Angerer, Per Svenningsson, Per E. Andrén

P-92

Van Ardenne, Jacqueline
Vanderbilt University, United States

Multimodal Imaging of Host-Pathogen Interactions in Staphylococcus aureus Infections

Introduction:
Staphylococcus aureus (S. aureus) is an opportunistic pathogen that is the leading cause of death associated with bacterial infections worldwide. Severe infections are often associated with bacterial dissemination through the bloodstream, which allows S. aureus to seed infections in peripheral tissues and form abscesses. Models for interactions between host immune cells and bacteria resulting in these abscesses have largely been characterized on a cellular level. The bacteria persist in the center of the abscess, surrounded by viable and necrotic immune cells. However, specific molecular changes in both host and pathogen during abscess progression are not well understood. Multimodal imaging provides a unique opportunity to interrogate molecular profiles in tandem with cellular-level changes to characterize host-pathogen interactions.

Method:
Female C57BL/6J mice were infected with S. aureus Newman and sacrificed humanely 5 days post infection. Kidneys were flash frozen on an isopentane/dry ice slurry and embedded in 2.6% carboxymethylcellulose. 5 µm thick serial sections from kidneys were obtained with Leica Biosystems CM3050S cryostat and thaw mounted onto microscope slides. 4-(dimethylamino)cinnamic acid matrix was applied to the sections with an in-house sublimation apparatus. MALDI IMS data was obtained in negative ionization mode using a Bruker timsTOF fleX with 5 µm pixel size. Histological stains, including Gram and hematoxylin and eosin, and immunofluorescence were performed on serial sections. The stains, immunofluorescence, and IMS data were co-registered using IMS Microlink and WSIreg, and regions were annotated in QuPath for further computational analysis.

Results:
High spatial resolution matrix-assisted laser desorption/ionization imaging mass spectrometry (MALDI IMS) of infected tissue sections enables attribution of m/z features to specific tissue functional units (FTUs), as well as infection-associated pathology such as the bacterial colonies and abscessed regions. Serial sections of histological stains, immunofluorescence, and MALDI IMS data were co-registered, such that annotations from any of the imaging modalities could be applied to all serial sections to identify correlations between molecular distributions and tissue features. Specific FTUs which are responsible for blood filtration in the kidney (e.g. glomeruli and vasculature) were selected for comparison due to the role blood flow plays in bacterial dissemination during infection. Using these methods, we evaluated the changes in molecular profiles of a variety of regions, including glomeruli, distal tubules, S. aureus bacteria, and abscesses due to infection. For example, a GM3 ganglioside which is intense in the glomeruli of healthy kidney tissue, is absent in glomeruli near the abscesses. These glomeruli were identified as sclerotic in the hematoxylin and eosin (H&E) stain of serial tissue sections. Further computational analyses, such as k-means clustering, can be used to identify subpopulations of these various tissue features based on their molecular profiles. k-means clustering of MALDI IMS data corresponding to the abscesses demonstrated heterogeneity within and between distinct abscesses. Evaluation of serial H&E stains revealed that the abscess is comprised entirely of viable and necrotic neutrophils at 5 days post-infection. However, subpopulations of these neutrophils cannot be identified within H&E stains. On the other hand, k-means clustering uncovered regions of neutrophils with distinct molecular profiles that are enriched in phosphatidylinositol species. Through analysis of the co-registered data, these regions seem to be associated with Splendore-Hoeppli identified in the Gram stain, which is thought to be debris resulting from interactions between host immune cells and invading pathogens.

Novelty:
Multimodal imaging reveals molecular and cellular changes in abscesses and surrounding FTUs resulting from host-pathogen interactions.

Preliminary Data:
H&E, Gram stains, immunofluorescence and IMS were collected from serial sections, co-registered, annotated, and analyzed with various methods, including k-means.

Contributing Authors:
Jacqueline M. Van Ardenne, Lukasz G. Migas, Kyle T. Enriquez, Madeline E. Colley, Allison B Esselman, Katherine N. Gibson-Corley, Raf Van de Plas, Eric P. Skaar, Jeffrey M. Spraggins

P-93

Wahl, Daniel
University of Michigan, USA

Metabolic rewiring in human brain cancer

Introduction:
Metabolic adaptation can promote oncogenic phenotypes in glioblastoma (GBM), but the metabolic pathways utilized by GBM and how they differ from the pathways utilized in normal cortex are poorly understood. Here, we utilize *in vivo* stable isotope tracing in mice and patients with glioblastoma to define carbon fate and metabolic rewiring in cancer.

Methods:
We infused uniformly-labeled ^{13}C glucose into mice bearing orthotopic GBM patient-derived xenografts or into patients undergoing surgical resection for likely GBM. Tumor and cortex were physically separated in mice by fluorescence-guided microdissection. In humans, samples of enhancing tumor, non-enhancing tumor and normal cortex were separated intraoperatively using MRI guidance. Samples were subsequently analyzed by liquid chromatography mass spectrometry and MALDI imaging mass spectrometry to determine the downstream metabolic fates of infused ^{13}C glucose.

Results:
Of eight patients infused with $^{13}C_6$-glucose, six were confirmed to have GBM while the others had non-GBM high grade gliomas. In mice and in patients, glucose-derived carbon effectively entered glycolysis and labeled glycolytic intermediates equivalently in tumor and cortex. Compared to GBM tissue, cortical tissue preferentially oxidized glucose-derived carbon in the TCA cycle and used glucose-derived carbon to synthesize the neurotransmitter GABA. Cortical tissue utilized glucose-derived carbon to synthesize the amino acid and neurotransmitter precursor serine, while GBM tissue preferentially derived serine from extracellular sources. By contrast, GBM preferentially utilized glucose-derived carbon for the synthesis of metabolites required for growth: purines, pyrimidines and NAD^+/NADH. These studies are the first measurements of numerous metabolic pathways in human brain cancer and cortex and suggest that GBMs suppress the physiologic utilization of glucose carbons for ATP and neurotransmitter generation and instead use these carbons to synthesize the biomolecules they need to proliferate. Consistent with this hypothesis, eliminating dietary serine in mice slowed GBM PDX growth and forced tumors to synthesize serine from glucose, which in turn lowered tumor nucleotide and NAD^+/NADH levels. Dietary serine depletion had minimal effects on cortical metabolism, consistent with glucose being the primary serine source in the normal brain.

Novelty:
These first direct measurements of metabolic pathway activity in human and mouse brain cancer reveal adaptive metabolic rewiring and new therapeutic targets.

Contributing Authors:
Andrew J. Scott[1,2,*], Anjali Mittal[3,4,5,*], Baharan Meghdadi[5], Sravya Palavalasa[1], Abhinav Achreja[2,3,4,6], Alexandra O'Brien[1], Ayesha U. Kothari[1], Donna M. Edwards[1], Zhe Wu[7], Jiane Feng[7], Kari Wilder-Romans[1], Vijay Tarnal[8], Nathan Qi[7], Costas A. Lyssiotis[2,7,9,#], Wajd N. Al-Holou[2,10,#], Deepak Nagrath[2,3,4,5,#,&], Daniel R. Wahl[1,2,#,&]

1Department of Radiation Oncology, University of Michigan, Ann Arbor, MI, USA
2Rogel Cancer Center, University of Michigan, Ann Arbor, MI, USA
3Laboratory for Systems Biology of Human Diseases, University of Michigan, Ann Arbor, MI, USA
4Biointerfaces Institute, University of Michigan, Ann Arbor, MI, USA
5Department of Chemical Engineering, University of Michigan, Ann Arbor, MI, USA
6Department of Biomedical Engineering, University of Michigan, Ann Arbor, MI, USA
7Department of Molecular and Integrative Physiology, University of Michigan, Ann Arbor, MI, USA
8Department of Anesthesiology, University of Michigan, Ann Arbor, MI, USA
9Department of Internal Medicine, Division of Gastroenterology, University of Michigan, Ann Arbor, MI, USA
10Department of Neurosurgery, University of Michigan, Ann Arbor, MI, USA

P-94

Vandenbosch, Michiel
Maastricht University, Nederland

A multimodal imaging approach to study the effects of L-asparaginase within solid tumors

Introduction:
Asparagine plays a crucial role in the growth and survival of tumor cells at various stages of tumor progression. It is a non-essential amino acid that can be obtained from dietary sources or synthesized from aspartic acid by an enzyme called asparagine synthetase. Numerous cancer cell types do not express asparagine synthetase and therefore have a particularly high dependency on external sources of asparagine. Asparlas is a drug designed to treat acute lymphoblastic leukemia, comprising the enzyme L-asparaginase. This enzyme aids in cancer growth inhibition by breaking down asparagine. Despite its effectiveness in treating various forms of leukemia, the extent of its efficacy in solid tumors is still largely unknown.
Method:
Fresh frozen liver tumors were cryosectioned. To enhance the sensitivity of asparagine analysis, an on-tissue chemical derivatization involving 4-hydroxy-3-methoxycinnamaldehyde was refined. Following derivatization, a solution of 2,5-dihydroxybenzoic acid in 70% methanol and 0.2% trifluoroacetic acid was applied to the tissue section using an M3+ sprayer (HTX technologies). MALDI-MSI (Matrix-Assisted Laser Desorption/Ionization Mass Spectrometry Imaging) data was obtained using a timsTOF-flex instrument (Bruker), allowing for simultaneous visualization of Asparlas, asparagine, and the lipid profile within a single analysis. Tumor, stroma, and healthy tissue regions were identified based on region-specific lipid markers, with confirmation provided by histological staining. Additionally, an immunohistochemistry protocol was optimized on consecutive sections to detect asparagine synthetase using a rabbit polyclonal anti-asparagine synthetase primary antibody (ProteinAtlas).
Results:
In this study, we conducted a comprehensive analysis to investigate the distribution and impact of L-asparaginase (Asparlas) in xenografted solid tumors . By generating ion images of various lipids, we were able to observe distinct distributions within the tissue, enabling characterization of tumor, stromal, and healthy regions. These latter were confirmed by subsequent histological staining. Notably, samples treated with Asparlas exhibited notable changes in distribution compared to those injected with the vehicle alone. In the untreated group, asparagine was primarily concentrated within the tumor regions. However, administration of Asparlas resulted in effective depletion of asparagine, as evidenced by the altered distribution. Conversely, the distribution of aspartic acid showed the opposite trend, confirming the mechanism of action of Asparlas. These findings indicate the promising potential of Asparlas as a treatment for solid tumors. However, it should be noted that residual asparagine was still detectable, suggesting that solid tumor cells may also acquire asparagine from their microenvironment, potentially through the release of asparagine by stromal cells. Furthermore, we optimized an immunohistochemistry staining method to examine the distribution of asparagine synthetase. This allowed us to investigate the relationship between asparagine synthetase expression and the sensitivity/resistance to Asparlas treatment. In conclusion, our multimodal imaging approach presented significant potential for studying the effects of L-asparaginase treatment. It provided valuable insights into the distribution patterns of asparagine and the relationship between asparagine synthetase expression and response to Asparlas.
Novelty:
A multimodal imaging approach was set up to visualize an L-asparaginase as well as its effect within solid tumors.
Preliminary Data:
For the first time, the distribution as well as the effect of L-asparaginase was studied in solid tumor.
Contributing Authors:
Laura van der Vloet, Pierre Barbier Saint Hilaire, Christophe Bouillod, Georges Da violante, Emre Isin, Ron M.A. Heeren, and Michiel Vandenbosch

P-95

Wali, Syeda Nazifa
Purdue University, United States

Imaging of isomeric metabolites in biological tissues with a nano-DESI timsTOF system

Introduction:
The ability to measure spatial distributions of metabolites in biological tissues is critical to understanding biochemical pathways involved in both health and disease. However, the presence of isobaric and isomeric species makes it difficult to unambiguously determine metabolite localization in tissues. Ion mobility mass spectrometry (IM-MS) enables high-speed gas phase separation of ions based on their collisional cross sections (CCS). When integrated with imaging platforms, IM substantially improves the chemical specificity of metabolite imaging by separating isobaric and isomeric species. Herein, we use a nano-DESI imaging platform coupled to the timsTOF instrument for the analysis and visualization of isomeric metabolites in biological tissue with ion mobility mass spectrometry imaging (IM-MSI).
Method:
Frozen 18 µm-thick sections of 13-month-old wild type (WT) mouse brain tissues were used for the analysis. A nano-DESI platform is coupled to the timsTOF Pro to enable high-resolution ion mobility separation in MSI experiments. Imaging experiments of mouse brain tissues were performed using acetonitrile spiked with suitable internal standards as a working solvent. For the amino acid isomers, online derivatization with fluorenylmethyloxycarbonyl chloride (Fmoc-Cl) was performed to improve trapping efficiency and to increase the m/z of the metabolites. Initially, the ion mobility was calibrated within the 0.5-1.0 range to observe the species present. Afterwards, the instrumental settings were optimized by narrowing the ion mobility range and increasing the ramp time to obtain high ion mobility resolution within the calibrated range.
Results:
The timsTOF was calibrated in the lower ion mobility region and the instrumental settings were optimized to increase the intensity of the species in the lower m/z region. Nano-DESI line scans were performed on mouse brain tissue to detect potential isomeric metabolites using IM-MS . High-resolution ion mobility resolution settings were used to resolve the isomeric pairs. For the annotation of the detected peaks, standard solutions were prepared, and their ion mobilities were compared with species detected in tissues. For example, the isomeric betaine and valine, which are ionized either as protonated species at m/z 118.0868 or as sodium adducts at m/z 140.0687 cannot be distinguished in MS. However, they have different CCS values and can be differentiated using high-resolution ion mobility separation. The required IM resolution for this isomeric pair is ~200. Meanwhile, IM features observed for the peaks at m/z 401.2664 and 417.2402 were tentatively assigned as sodium and potassium adducts of 1-arachidonylglycerol and 2-arachidonylglycerol. We also observed several other isomeric metabolite pairs and confirmed their identities by comparing their CCS with the standards. Subsequent imaging experiments of IM-separated ions of leucine and isoleucine provided insights into their spatial localization on mouse brain tissue. A good correspondence between the results obtained for several known isomeric metabolites and literature data validates our approach. IM-MSI is a powerful discovery tool for the untargeted spatial localization of metabolites in biological systems.
Novelty:
High-resolution ion mobility coupled with nano-DESI MSI enables imaging of isomeric metabolites in biological tissue.
Preliminary Data:
Ion mobility nano-DESI was used for the detection and imaging of isomeric species present in biological tissues.
Contributing Authors:
Syeda Nazifa Wali, Lixue Jiang, Julia Laskin

P-96

Wallace, Elizabeth
Medical University of South Carolina, United States

A MALDI mass spectrometry imaging N-glycome atlas and analytic pipeline for human normal and cancer tissues

Introduction:
N-glycosylation is an abundant post-translational modification of most cell-surface proteins. The presence of N-glycans aid in crucial cellular functions like protein folding, protein localization, cell-cell signaling, and immune detection. As different tissue types display different N-glycan profiles, changes in N-glycan compositions occur in tissue-specific ways when cells become cancerous. However, no comparative atlas resource exists for documenting changes in the N-glycomes of multiple normal and cancerous human tissue types. The goal of this study was to create such an atlas and to demonstrate the usefulness of code to analyze MALDI-MSI data efficiently and accurately in a way that can be used in graphing pipelines or analytic tools.
Method:
We used MALDI mass spectrometry imaging (MSI) to look at two custom formalin-fixed paraffin-embedded (FFPE) tissue microarrays (TMAs) containing fifteen tissue types. For each patient tissue, there were samples of both normal and tumor tissues. Using established MALDI MSI workflows and existing N-glycan databases, the N-glycans present in each tissue core were spatially profiled and peak intensity data compiled for comparative analyses. A multi-enzymatic approach allowed for further information on structural composition, using EndoF3 to confirm core fucose and stabilization chemistry to distinguish sialic acid linkages. Analysis was performed using R and functions were written for in-depth analysis, starting with Bruker's SCiLS program to create a data analysis pipeline. Data will also be available in METASPACE.
Results:
The most abundant glycans seen in every tissue were the biantennary glycan with a core fucose at 1809.64 m/z and the same glycan structure without a core fucose at 1663.58 m/z, with triantennary, bisected, and sialylated forms of these glycans making up most of the top glycans across the tissues. High mannose glycans tended to be elevated in cancer, as did polylactosamine, multiantennary, and paucimannose glycans. Biantennary and hybrid glycans tended to be lower in cancer, and glycans containing an N-Acetylglucosamine (GlcNAc) bisect varied by tissue type with no clear trend. We also observed that multiantennary glycans with a core fucosylation in particular tended to be increased in cancer, though no overall changes in core fucosylation proved significant. We also looked at sialylation in depth and observed that, although there were no strong overall trends for α2,3 vs. α2,6 linkage abundance changes between normal and cancer, when one type of linkage was high in the normal, it was low in cancer, and vice versa. Additionally, we noted that α2,3 linked sialic acids were more abundant in tissues overall. All of these results were analyzed and graphed using custom code in R. Overall, this study has demonstrated key trends in cancer and shown the overall trends of glycan structures in different tissue types and their cancer. It also demonstrates the use of our code to analyze data from SCiLS in an efficient pipeline for streamlined analysis and consistent graphing.
Novelty:
An atlas like this has not been created before. We have created and demonstrated code for efficiently analyzing MALDI-IMS data.
Preliminary Data:
This study reports structural information on a wide scale for both normal tissue types and cancers in those tissues.
Contributing Authors:
Elizabeth N. Wallace1, Connor A. West1, Grace Grimsley1, Colin T. McDowell1, Xiaowei Lu1, Evelyn Bruner2, Kiyoko F. Aoki-Kinoshita3; Anand S. Mehta1, Peggi M. Angel1, and Richard R. Drake1 1Medical University of South Carolina, Department of Cell & Molecular Pharmacology & Experimental Therapeutics, Charleston SC 2Medical University of South Carolina, Department of Pathology and Laboratory Medicine, Charleston SC 3Soka University, Department of Bioinformatics, Tokyo, Japan

P-97

Weber, Andreas
Institute for Surgical Pathology, Medical Center, University of Freiburg, Freiburg, Germany, Germany

Mass spectrometry imaging of a large cohort of rare intrahepatic cholangiocarcinoma deploying tissue micro arrays

Introduction:
Intrahepatic cholangiocarcinoma (ICC) is a rare and aggressive type of cancer that originates from the bile ducts within the liver. It accounts for approximately 8-10% of all cholangiocarcinoma cases. It poses significant challenges in early detection and treatment due to its asymptomatic nature and aggressive behaviour. Understanding ICC at the spatio-molecular level is crucial for developing effective diagnostic methods and therapies. The analysis of the spatial abundance of biomolecules present in tumor tissue leads to insights regarding intratumor heterogeneity and the composition of the tumor microenvironment.
Method:
Here, we present a spatially resolved mass-spectrometric analysis of a large ICC cohort of 70 patients with patient-matched tumor and tumor-adjacent tissue samples deploying tissue micro arrays (TMA s) with 409 cores. Employing a MALDI TOF with a spatial resolution of 50 µm allowed a high precision of the molecular distribution. Tryptic peptide imaging was performed to elucidate the spatial distribution of proteins. Data preprocessing was carried out using an automated workflow within the Galaxy framework, ensuring consistent and reproducible data treatment. Hematoxylin and eosin (H&E) staining was conducted post measurement to visualize tissue morphology. Pathologists provided annotations in the H&E images to precisely delineate regions of interest. To extract meaningful insights from the data, supervised machine learning algorithms were used.
Results:
The application of supervised spatial shrunken centroids (SSC) algorithm yielded a notable classification accuracy, demonstrating the efficacy of this approach in discerning distinct biomolecular patterns. In the comparison between tumor and tumor-adjacent liver tissue, a prominent peptide originating from collagen 1 emerged as the most discriminative feature. This finding highlights the robust presence of locally distributed extracellular matrix (ECM) components in ICC, indicative of its desmoplastic nature. This observation aligns with the known association of ICC with enhanced stromal reactions. The utilization of Neural Network (NN)-based models on H&E images further enhanced our ability to delineate morphological variations across the tissue sections. As a next step, we aim to refine our analysis by performing detailed annotations of vital tumor areas and ECM regions. This focused annotation strategy will facilitate the development of more precise classifiers, enabling the identification of subtle molecular signatures associated with specific microenvironmental components. To augment our findings, we intend to integrate existing immunohistochemistry (IHC) stainings with the MALDI imaging data. To achieve this, we are aiming at the development of an automatic coregistration workflow. This innovative approach will enable the seamless fusion of histological and molecular information.
Novelty:
The novelty of this analysis lies in its unprecedented spatial insights into a large cohort of rare ICCs.
Preliminary Data:
Metabolite mass spectrometry imaging on adjacent tissue slices was carried out and will be integrated with the peptide dataset.
Contributing Authors:
Andreas Weber - Institute for Surgical Pathology, Medical Center, University of Freiburg, Freiburg, Germany Bálint András Barta - Institute for Surgical Pathology, Medical Center, University of Freiburg, Freiburg, Germany Pia Hönscheid – Institute of Pathology, University Hospital Carl Gustav Carus at the Technische Universität Dresden, Germany Konrad Kurowski - Institute for Surgical Pathology, Medical Center, University of Freiburg, Freiburg, Germany Sai Srikanth Lakkimsetty - Khoury College of Computer Sciences, Northeastern University, Boston, MA, USA Olga Vitek - Khoury College of Computer Sciences, Northeastern University, Boston, MA, USA Peter Bronsert - Institute for Surgical Pathology, Medical Center, University of Freiburg, Freiburg, Germany Melanie Christine Föll - Institute for Surgical Pathology, Medical Center, University of Freiburg, Freiburg, Germany

P-98

Hulahan, Taylor
Medical University of South Carolina, United States

Unique Extracellular Matrix Proteomic Niches of Ductal Carcinoma in Situ and Invasive Breast Cancer by Matrix-Assisted Laser Desorption/Ionization Imaging

Introduction:
Ductal carcinoma in situ (DCIS) is a non-invasive breast cancer that is often treated similarly to invasive breast cancer (IBC) with surgery and radiation therapy. However, only a small and unpredictable subset of patients progress to IBC, leading to significant overtreatment. Reliable prognosticators are needed that can stratify patients into those who will progress to IBC (progressors) and those that do not (non-progressors). Contemporary work has focused on the tumor microenvironment for its prognostic value, specifically stromal differences between progressors and non-progressors. Here, we spatially investigate the molecular regulation of fibrillar collagen domains within DCIS and IBC pathologies with the long-term goal of developing a stromal signature that predicts progression to IBC and strives to limit the overtreatment of DCIS.
Method:
A comparative analysis of extracellular matrix peptide signatures between DCIS and IBC pathologies was performed using a 22-lumpectomy sample cohort derived from 17 different patients defined as pure DCIS (n=9), mixed DCIS-IBC (n=8), and pure IBC (n=4). We leveraged our well-established method of extracellular matrix (ECM)-targeting spatial proteomics using Matrix-assisted Laser Desorption/Ionization-Quadrupole Time-Of-Flight (MALDI-QTOF) imaging followed by high-resolution mass-accuracy proteomics for peptide identification. Altogether, this combined approach permits the reporting of collagen types and their post-translational modifications including 40 other extracellular matrix (ECM) proteins involved in the regulation of collagen fibers. Following MALDI-QTOF imaging of the entire lumpectomy specimen, four lumpectomies underwent higher resolution imaging of individual, pathologist-defined DCIS (n=38) and IBC (n=17) lesions.
Results:
Over 1000 putatively identified peaks were linked to pathological annotations or adjacent regions. Segmentation analysis of 843,210 pixels revealed 12 hierarchal uniquely localized proteomic groups with specific clusters coinciding with histopathological features and pathological annotations. Of these peaks, 43 were found to have significantly different intensity profiles between DCIS and IBC pathologies by non-parametric, two-tailed t-test ($p<0.05$) within the eighteen-lumpectomy subset. Eight of these differentially expressed peptides were identified as fibrillar collagen sequences within annotated triple helical regions and many contained post-translationally modified sites. These fibrillar collagen sequences had the ability to discriminate between DCIS and IBC pathologies by area under the receiver operating curve (AUROC)≥0.75 and Wilson/Brown t-test ($p<0.05$). To determine if proximity to IBC influenced the proteomic profile of DCIS pathologies, mixed DCIS-IBC lumpectomies (n=4) with DCIS lesions varying distances from the invasive cancer field were examined for ECM proteomic field effects in relation to distance from invasive region. Notably, DCIS lesions within invasive regions had a more similar proteomic profile to IBC than DCIS lesions located more distally from the IBC region via principal component analysis and hierarchical clustering. Analysis of individual DCIS lesions within the four-lumpectomy subset used for higher-resolution analysis similarly demonstrated that lesions closer to invasive areas had a more similar representation of proteomic clusters via segmentation analysis as well as more comparable average peak intensity profiles of distinct peptides linked to proteins associated with breast cancer progression and survival outcomes. Overall, the data suggest that unique collagen signatures characterize DCIS and IBC pathologies. These signatures could be useful for understanding recurrence and progression to IBC in a subset of high-risk DCIS patients. Further investigation of the spatial distribution of the collagen proteome within DCIS pathologies and relative to clinical outcome is needed.
Novelty:
Use of extracellular matrix signatures to distinguish ductal carcinoma in situ risk to progression.
Preliminary Data:
This study differentiates ductal carcinoma in situ lesion pathology with increased invasive cancer risk by molecular composition of collagen.
Contributing Authors:
Taylor S Hulahan, Elizabeth N Wallace, Shelley Hwang, Laura Spruill, Jeffrey R Marks, Richard R Drake, Peggi M Angel

P-99

Wiedemann, Katja Rebecca
Institute of Inorganic and Analytical Chemistry, Justus Liebig University, Giessen, Germany, Germany

Applying HR AP-SMALDI MSI to visualize parasite infection-driven spatially resolved metabolic changes in infected tissues

Introduction:
When a parasite enters its host, it depends entirely on the host organism to survive. However, parasite establishment and nutrient scavenging activates the host's defense mechanisms. Therefore, infections result in measurable changes in the composition and distribution of metabolites in host tissue, especially when in direct contact with the parasite. Understanding such changes and their underlying parasite–host interactions is crucial for identifying new drug targets. Imaging both organisms simultaneously in the same tissue sample can deliver important insights into processes occurring in vivo. Additionally, finding infection-specific marker signals can help to further understand parasite–host interactions.
Method:
MSI: AP-SMALDI5 AF ion source (TransMIT GmbH, Giessen, Germany), 10 µm pixel size, Thermo Scientific Q Exactive HF Orbitrap (Thermo Fisher Scientific (Bremen) GmbH, Germany), mass resolution R = 240,000 at m/z 200. Cryosections of 20 µm thickness were coated with matrix using an ultrafine pneumatic sprayer (SMALDIPrep, TransMIT). For positive-ion mode, DHB (2,5-dihydroxybenzoic acid) and DHAP (2,5-dihydroxyacetophenone), for negative-ion mode DAN (1,5-diaminonaphthalene) and also DHAP were used. LC-MS/MS: Dionex Ultimate 3000 UHPLC (Thermo Fisher Scientific), ACQUITY UPLC HSS T3 1.8 µm reversed-phase column (100 X 2.1 mm) (Waters), Thermo Scientific Q Exactive HF-X Orbitrap (Thermo Fisher Scientific). Nano-HILIC-MS/MS: Thermo Scientific UltiMate 3000 RSLCnano System, Accucore 150 amide-HILIC column (0.075 mm x 150 mm), Thermo Scientific Q Exactive HF-X Orbitrap.
Results:
We studied two different parasite–host models. On the one hand, we investigated the lipid distribution in bovine skin tissue, infected with cysts stages of the apicomplexan parasite Besnoitia besnoiti. On the other hand, we investigated hamster liver samples containing Schistosoma mansoni eggs. For both systems, characteristic infection markers were found with significant changes in signal intensities when compared to control samples. Additionally, we were able to image the lateral distribution of infection markers and found accordance with biological structures as identified in optical images of the analyzed tissues. In the skin of B. besnoiti-infected cattle, parasite-formed cysts were visible to the naked eye. MS images showed both, enrichment and depletion of distinct lipid species inside the cysts. Also, some lipids proved characteristic for cyst walls. In schistosomiasis, S. mansoni eggs are deposited in the hamster liver, which leads to granuloma formation around the eggs. Due to the high-lateral-resolution capability of the AP-SMALDI5 AF ion source (egg size = 100-200 µm), we could visualize both, the trapped eggs in MS images and the changes in lipid as well as glycosphingolipid (GSL) distributions in granulomatous tissue. Therefore, a GSL database was created in a first step by preparing extracts for subsequent nano-HILIC-MS/MS experiments. In total, over 60 glycosphingolipids were identified, 47 of which were fully characterized with respect to their saccharide composition and ceramide backbone moiety. Statistical upregulation of most identified GSLs already indicated their involvement in granuloma formation. Additionally, we observed a substructure in formed granulomas, concerning lipids and GSLs. For example, ether-phosphatidylethanolamines were mainly found in the outer part of the granulomas. Ultra-high resolution MALDI MSI measurements with 3 µm step size were performed on a prototype AP-SMALDI ion source, revealing a substructure of S. mansoni eggs with a GSL species only distributed on the egg surface.
Novelty:
Simultaneous mass spectrometric imaging of parasites and their hosts using high resolution in mass and space.
Preliminary Data:
-
Contributing Authors:
Katja R. Wiedemann1, David Luh1, Stefanie Gerbig5, Parviz Ghezellou1, Alejandra Peter Ventura1, Martin Roderfeld2, Elke Roeb2, Christoph G. Grevelding3, Liliana M. R. Silva3, Carlos Hermosilla3, Anja Taubert3, Kerstin Strupat4, Bernhard Spengler1,5 1Institute of Inorganic and Analytical Chemistry, Justus Liebig University, Giessen, Germany 2Gastroenterology, Justus Liebig University, Giessen, Germany 3Institute of Parasitology, Justus Liebig University, Giessen, Germany 4Thermo Fisher Scientific (Bremen) GmbH, Bremen, Germany 5TransMIT GmbH, Giessen, Germany

P-100

Yamaguchi, Shinichi
Shimadzu Corp, Japan

How should we segment the MS image area?

Introduction:
We explore the segmentation approach for MS image areas. While segmentation based on known information poses no issues, determining it from measured data presents challenges. Clustering using MS image data encounters two main problems: the curse of dimensionality and determining the number of clusters. Several proposed methods address these concerns. One potential solution is reducing dimensionality by applying false (pseudo)-coloring with UMAP. In this poster, we discuss clustering techniques for false-color images, focusing on the possibility of obtaining a reasonable cluster count through mathematical methods.
Method:
Data A thoracic portion frozen section of the mouse MSI was performed using an atmospheric pressure MALDI–QIT-TOF . Data Processing This data was reduced to 3 dimensions space by using UMAP.
Results:
Different methods yielded different numbers of clusters, but the Elbow method and HDBSCAN matched estimates below 128. Consequently, determining the "correct" number of clusters from the data is challenging. Even with the same data, researchers select different cluster numbers and ROIs. Instead of focusing on the number of regions, it would be more constructive to establish an interactive trial-and-error method for researchers to explore the data's distribution of interest. Extracting ROIs based on an overview image that represents the data's characteristics is desirable. The use of UMAP to create a false-color image is suitable for this purpose.
Novelty:
False color and Segmentation by UMAP
Preliminary Data:
N/A
Contributing Authors:
Shinichi Yamaguchi1, Masaya Ikegawa2
1Shimadzu Corporation, Kyoto, Japan; 2Doshisha University, Kyoto, Japan

P-101

Ye, Lan
UHN PMCRT, Canada

Rapid classification of Lung Cancer Types by Picosecond Infrared Laser Mass Spectrometry (PIRL-MS): A comprehensive evaluation across various tissue models

Introduction:
The diversity in prognosis, treatment response, and overall survival across lung cancer types necessitates rapid and precise diagnosis. Although current approaches involve histologic evaluations, immunohistochemistry, and molecular assays, their turnaround times often span several days. Ambient analysis with Picosecond InfraRed Laser (PIRL) ablation soft ionization mass spectrometry (MS) is a potential tool for rapid lung cancer identification. With just ~10-second sampling and analysis duration, this technique offers rapid and precise detection and classification of lung cancer types through molecular signatures.
Method:
Immortalized and patient derived lung cancer cell lines, xenografts and organoids thereof, and banked primary human samples of adenocarcinoma, squamous cell carcinoma, small cell carcinoma and large cell carcinoma (155 specimens) were subjected to Picosecond InfraRed Laser (PIRL) with sampling time not exceeding 10 seconds. Tissue molecular content in the form of a gas plume was captured and analysed by a Xevo-G2-XS quadrupole Time of Flight (qToF) mass spectrometer. Repeat sampling and investigation using multivariate statistical analysis methods such as Principal Component Analysis Linear Discriminate Analysis (PCA-LDA) was performed to build a training set. Model validation was performed by blind sample analysis of patient derived xenografts and primary human samples.
Results:
Proof-of-principle sampling revealed distinct m/z markers specific to each lung cancer and tissue type. Patient derived xenografts resembled primary human tissue most closely with organoids coming a close second. The accuracy of predictions for banked tissue was close to 90% with sensitivity and specificity of blind sample detection as well as determination of the molecular identities of lung cancer classifying m/z values with chromatography and high-resolution mass spectrometry currently on going. This illustrates the potential of our methodology for accurate lung cancer classification, and further suggests xenografts developed from immortalized lung cancer cell lines to have limited utility in classifying primary patient tissue.
Novelty:
Rapid 10-second PIRL-MS can potentially guide surgical decisions in real time and serve as an intraoperative tool enhancing the diagnosis speed.
Preliminary Data:
PIRL-MS molecular profiles were discovered that can distinguish different classes of lung cancer tumours.
Contributing Authors:
Lan Anna Ye, Michael Woolman, Francis Talbot, Alexa Fiorante, Yuki Sata, Fumi Yokote, Nicholas Bernards, Michael Cabanero, Howard J. Ginsberg, and Arash Zarrine-Afsar

P-102

Young, Reuben
University Of Wollongong, Australia

Imaging lipids in single cells and tissues using histological dyes for ambient laser desorption and plasma ionisation

Introduction:
For organoid tissues to fulfil complex functions, discretely organised cell types are fit with unique physical and chemical properties. Lipids are a diverse class of biomolecule that are known to contribute to cellular property differences, such as membrane structure and signalling. As such, correct characterisation of lipid chemical structures and designation of molecular profiles to specific cells and cell structures is paramount to our understanding of cell biology and disease. To achieve this, conventionally both optical imaging and mass spectrometry imaging are combined. However, combining these techniques without partially sacrificing data quality is not trivial. To circumvent this, herein we describe a technique that uses histological dyes as the desorption-matrix for MALDI-MSI in parallel with microscopy imaging.
Method:
Fresh-frozen organ tissues were sectioned and thaw-mounted to standard glass microscopy slides. Cells were partially cultured on-slide and chemically fixed using 4% PFA. Both tissues and cells were stained using histological dyes, such as haematoxylin and cresyl violet, and a modified staining technique that avoids delipidation of cell structures. Subsequently, sample slides underwent bright field microscopy imaging prior to positive polarity MALDI-MSI at 10 or 50 micrometre spatial resolution using a timsTOF Pro mass spectrometer fit with a modified 355 nm MALDI source capable of atmospheric pressure desorption and plasma ionisation. Decoupling the desorption and ionisation processes allows for histological stains to desorb tissue and cell lipids separately to their downstream-ionisation using a low-temperature plasma source.
Results:
Commensurate MALDI-MS lipid image quality and spectral intensity was observed from the application of matrix-assisted and dye-assisted techniques to tissues and cells. The dye-assisted approach resulted in high-intensity signals for many lipid species, including phospholipids and glycosphingolipids, and displayed minimal lipid delocalisation as was seen by the close correlation between ion images and tissue morphology. Additionally, owing to the absence of matrix and matrix cluster features from the mass spectra, lipid signal-to-noise was shown to be improved with dye-assisted desorption compared to matrix-coated samples. This consequently allowed for the observation of lipid species not commonly seen in positive polarity mass spectrometry, such as protonated phosphatidylinositol. The ability to micrograph the stained cells and tissues prior to MALDI-MSI and laser ablation allowed for high quality optical images to be obtained. Additionally, as the removal of matrix and lipids from the samples using organic solvents was not required, high-fidelity correlation between optical images and MALDI-MS images was maintained without the presence of commonly arising defects such as tissue curling and cracking. Comparison between tissue micrographs from the modified histological staining technique and conventional staining workflows revealed minimal loss of qualitative data able to be drawn from the modified staining process. Although not conventional, the staining of cells provided a higher degree of contrast in the brightfield microscopy images and displayed no translocation of cells across the slide.
Novelty:
Cutting-edge ambient pressure MALDI source with plasma ionisation allows for decoupled desorption and ionisation events, which expands matrix molecule selection.
Preliminary Data:
The use of histological dyes as the desorption-matrix for MALDI-MSI streamlines sample preparation and improves optical and MALDI-MS image correlation.
Contributing Authors:
Reuben S. E. Young, Shane R. Ellis

P-103

Zawadzka, Malgorzata
University of Oslo, Norway

Towards Mass Spectrometry Analysis of Organoids and Gastruloids

Introduction:
A nano desorption electrospray ionization mass spectrometry (nanoDESI-MS) platform will be developed in-house and optimized to studying organoids and gastruloids. Organoids are self-organized 3D organ-like structures, derived from e.g. stem cells. Organoids are however significantly less structured and mature than their human equivalents. Gastruloids constitute a distinct group of organoid models that recapitulate a gastrulation. In this fundamental developmental process, the cells in the zygote reorganize themselves into a discernable organism profile. The data obtained with the nanoDESI-MS is to be correlated with Raman spectrometry to monitor spatial distribution of metabolites, morphogenetic and signaling pathways to develop a deeper understanding of organoid development and stem cell biology.
Method:
NanoDESI platform is built based on the established protocol with modifications to achieve high flexibility and high spatial resolution. The nanoDESI platform is coupled to an Orbitrap Mass Spectrometer. Nanoemitters are produced in-house using the gravity-assisted self-termination etching process with hydrofluoric acid, and coated with SnO2 using atomic layer deposition to ensure conductivity. For comparison with commercially available mass spectrometric imaging, a Bruker timsTOF fleX instrument with MALDI-MSI was used. Matrix was applied using Tessem Lab protocol: 20mg/ml 2,5-dihydroxybenzoic acid in 70% methanol + 0.1% trifluoric acetic acid, 10 passes. Samples were embedded in 2% carboxymethylcellulose, dried in Leica cryostat chamber and cut into 10 µm slices. Slides (dedicated Bruker's Intellislides) were precooled in -20 °C in a cryostat chamber.
Results:
For in-house nanoDESI, a functioning platform was built and tested. A liquid bridge was obtained in positive ionization mode and desorption of the analyte from the slide was observed. Next steps involve also improving desorption, optimizing flow and creating stable liquid bridge, as well as producing images of samples. When employing MALDI MSI, first MS images of 7 day-old gastruloids were obtained and correlated with DAPI (4',6-diamidino-2-phenylindole) staining and scanned images. Liver organoids require different sample preparation as it was impossible to slice the samples with preserving the structure. The spatial resolution of 20 µm was not sufficient to obtain detailed images in this experiment what confirms the need of method with higher spatial resolution to analyze gastruloids. Collected images give however a good indication of potential finding using MSI. This pilot subproject gave us good basis for optimization of all steps in the process, from sample preparation, through matrix application to collecting images. In the next stages, images of steatotic and normal liver organoids will be analyzed with DESI and MALDI MSI in the Waters laboratory with the goal of mapping metabolite distribution. The imaging will be also performed on organoids exposed to per- and polyfluoroalkyl substances (PFAS) compounds as a first step in mapping organic pollutions in various cells using organoids and gastruloids as models in cooperation with the Norwegian Institute of Public Health.
Novelty:
Imaging gastruloids in different stages of development. Single cell resolution imaging of liver organoids derived from induced pluripotent stem cells.
Preliminary Data:
MALDI images obtained from mouse gastruloids (embryonic organoids).
Contributing Authors:
Jon Erlend Haavaag (master student) working together with Ph.D student Malgorzata Zawadzka on the construction and optimization of the nanoDESI-MS platform. Alexandra Aizenshtadt has prepared liver organoids and Sergei Ponomartcev has prepared mice gastruloids. Jorunn Stamnæs performed MALDI imaging analysis of the gastruloids and data handling in the National network of Advanced Proteomics Infrastructure. Hanne Røberg-Larsen, Steven Ray Wilson and Stefan Krauss are project supervisors and PIs in the UiO:Life sSience Convergence Environment Integrated technology for trackning organoid morphogenesis.

P-104

Zhang, Wanqiu
Aspect Analytics, Belgium

Pipeline for spatial multi-omics data integration for investigating transcriptomic and lipid heterogeneity in prostate cancer

Introduction:
Recent advances in spatial omics enable detailed molecular analyses of cells and tissues in their native state. Combined multiple spatial omics approaches are needed because individual assays capture a subset of molecular content, but this presents several bioinformatic challenges. First, spatial omics assays are usually conducted on different tissue sections, requiring dataset co-registration. Secondly, these technologies measure across a range of spatial resolutions. Lastly, software and bioinformatics tools for combined visualisation and exploration of multiple spatial omics datasets are generally lacking. We describe a spatial multi-omics dataset integration pipeline enabling co-registration and granularity matching, allowing for combined visualisation and downstream analysis. This pipeline was applied to mass spectrometry imaging (MSI) and spatial transcriptomics (ST) measurements of human prostate cancer (PCa).

Method:
Matched prostate tumour and normal biopsies (8 x normal, 8 x tumour) were collected from PCa patients (n = 8) who had undergone radical prostatectomy, snap frozen, and stored at -80°C. Cryosections (10 µm) were used for ST (Visium Spatial Gene Expression platform, 10X Genomics) and MALDI-2 MSI analysis. MALDI-2 MSI for lipids was performed on an Orbitrap Elite mass spectrometer (Thermo Fisher Scientific) in positive ion mode at 30 µm spatial resolution. Tissue sections were coated with DHB using an M5 sprayer (HTX Technologies). The ST and MSI-measured sections were H&E stained according to recommended protocols, and then digitised for pathologist annotations. Co-registration was performed using a non-rigid registration algorithm (Aspect Analytics NV).

Results:
We built a spatial multi-omics integration pipeline and applied it to two commonly used spatial omics modalities: ST, using the Visium Spatial Gene Expression platform, and spatial lipidomics, via MALDI-2 MSI. As these modalities are conducted on separate tissue sections, the first step was to co-register the datasets. Since both ST and MSI include H&E staining of tissue sections in their workflows, we used the stained images to link the ST and MSI data together. First, a couple of representative images of the MSI data were computed (via e.g., UMAP) to co-register to the respective H&E image. Next, the MSI-slide H&E was registered to the H&E corresponding to the ST data. Finally, we directly linked the MSI with the ST data, via a shared spatial coordinate system. We applied Gaussian weighting to account for differences in spatial resolution between the ST and MSI data (55 µm and 30 µm, respectively), thus obtaining a representative aggregated lipid spectrum associated with each ST spot, and matched spatial readouts. Detailed pathology annotations conducted on high-resolution microscopy images were transferred to the shared ST-MSI spatial coordinates. Our approach therefore allows simultaneous visualisation and exploration of five different modalities:

- Gene transcript distributions,
- Lipid distributions,
- H&E-stained image from the section used for ST,
- H&E-stained image from the section used for MSI, and
- Pathologist annotations delineating different histopathological regions in the samples.

The shared coordinate system allows for combined MSI and ST data analysis such as unsupervised approaches (e.g., clustering, and non-negative matrix factorization) and correlation analysis of gene and lipid expression, which can be linked to specific histopathological regions in PCa samples.

Novelty:
We developed a pipeline for spatially integrating multi-omics datasets, allowing direct comparison between different modalities., and enabling integrated downstream analysis.

Preliminary Data:
Development of a bioinformatic pipeline which can be applied to investigate spatial biochemical trends, such as correlated genes and lipids.

Contributing Authors:
Wanqiu Zhang1,2, Xander Spotbeen3, Sebastiaan Vanuytven4,5, Sam Kint4,5, Tassiani Sarretto6,7, Fabio Socciarelli8, Jose Ignacio Alvira Larizgoitia5,9, David Wouters5,9, Gabriele Partel5, Alice Ly2, Maria José Q. Mantas2, Thomas Gevaert10, Wout Devlies10,11, Katy Vandereyken4,5, Steven Joniau10,11, Massimo Loda8, Bart De Moor1, Thierry Voet4,5, Alejandro Sifrim5,9, Shane Ellis6,7, Marc Claesen2, Nico Verbeeck2, Johannes Swinnen3 Author affiliations: 1STADIUS Center for Dynamical Systems, Signal Processing and Data Analytics, Department of Electrical Engineering (ESAT), KU Leuven, Kasteelpark Arenberg 10, 3001 Leuven, Belgium 2 Aspect Analytics NV, C-mine 12, 3600 Genk, Belgium 3 Laboratory of Lipid Metabolism and Cancer, KU Leuven and Leuven Cancer Institute (LKI), Leuven, Belgium 4 Laboratory of Reproductive Genomics, Department of Human Genetics, KU Leuven, Leuven, Belgium 5 KU Leuven Institute for Single Cell Omics (LISCO), KU Leuven, Leuven, Belgium 6 Molecular Horizons and School of Chemistry and Molecular Bioscience, University of Wollongong, Northfields Ave, Wollongong, NSW 2522 Australia 7 Illawarra Health and Medical Research Institute, Northfields Ave, Wollongong, NSW 2522 Australia 8 Department of Pathology and Laboratory Medicine, Weill Cornell Medical College, New York, NY, USA 9 Laboratory of Multi-omic Integrative Bioinformatics, Department of Human Genetics, KU Leuven, Leuven, Belgium 10 Department of Urology, University Hospitals Leuven, Leuven, Belgium 11 Department of Development and Regeneration, KU Leuven, Leuven, Belgium.

P-105

Manoli, Eftychios
Imperial College London, United Kingdom

Molecularly Aware Robotics for Surgery (MARS) – A Novel Mass Spectrometry-Assisted Robotic Platform for Precise Surgical Interventions

Introduction:
Rapid Evaporative Ionisation Mass Spectrometry (REIMS), a mass spectrometric tool, has recently been successfully utilized in surgical settings to accurately identify cancerous and healthy tissues in-vivo. Coupling such molecular-level diagnostic tools with robotic surgery platforms provides significant potential for delivering precise and autonomous diagnostic and therapeutic interventions during tumour removal surgeries. Our group developed a laser ablation-compatible endoscopic robotic platform to assist an integrated REIMS system, where the real-time diagnostic information from mass spectrometry is also applied to guide the robotic device, enabling real-time tissue classification and 3D tissue map generation intraoperatively. This abstract demonstrates the development and application of this Molecularly Aware Robotics for Surgery platform, highlighting its potential for advancing surgical precision and accessibility.

Method:
For precise surgical ablation and real-time tissue mapping in minimally invasive surgery, a novel hybrid robotics platform, incorporating a soft hydraulic robotic platform and an electrothermally actuated fibre-based robot is developed. This platform utilizes a visual servoing system for its motion control, enabling the controlled delivery of CO2 laser fibre (Omniguide, USA) for tissue ablation, as well as the collection of the generated surgical aerosols. Molecular analysis of aerosols employs a mass spectrometer (Xevo G2-S QToF, Waters Corporation, USA), coupled with a REIMS source. The real-time tissue classification information, analyzed using a statistical model (Principal Component Analysis – Linear Discriminant Analysis), is used as the feedback for the closed-loop control of the robotic platform to perform further ablation and data collection.

Results:
This work combined two novel robotic platforms, a visual tracking system, a laser ablation device, and a REIMS system. The successful integration of the two robotics systems enabled their coordinated motion through commands exchanged between their respective controllers. The hybrid robot's small dimension end effector (1.7mm diameter) and flexibility enable its operation in challenging access surgical sites, such as transoral or transvaginal surgery for cancer removal. The vision and REIMS systems guided the hybrid robot to demonstrate an ablation scanning strategy on ex-vivo cancerous mouse skin tissue samples: a large-size raster scan by the hydraulic robot was coupled with continuous line scanning of the fibre robot to cover the gap between the adjacent raster lines in a short time. The hydraulic robot covered a motion range of 5x5cm2, while the fibre robot exhibited precision lower than 100µm. The tissue classification model of mouse skin samples was built in advance using the REIMS. During the robotic laser ablation, tissue types were identified in real-time. This generated tissue information was combined with estimated end effector pose information from the computer vision system to create point cloud tissue maps, which presented visually accurate results, validating the capability of the MS-assisted robot for precise tissue mapping. As part of future work, we will separate the target tissue into two: one for histopathological analysis to generate a ground truth to compare with the robotic system's generated tissue map. Additionally, we conducted a cadaver study in a transoral surgical environment, yielding preliminary results that demonstrate the applicability of the robotic system. We are currently enhancing the control and design of the robotic platform to enable semi-autonomous surgery, aiming to preserve healthy tissue while ensuring complete tumour resection. To validate these functionalities, we are planning a gynecological pilot study focused on cervical cancer removal.

Novelty:
A mass spectrometry-assisted robotic platform enables the creation of high-precision diagnostic tissue maps in challenging access surgical sites intraoperatively.

Preliminary Data:
Tissue classification model of mouse skin samples and generated diagnostic tissue maps.

Contributing Authors:
Jinshi Zhao (1) Daniel Simon (1, 2) Mark Runciman (1) Haozheng Xu (1) Chi Xu (1) Mohamed Abdelaziz (1) Eftychios Manoli (1) James Higginson (1) James McKenzie (1) Maria Paraskevaidi (1) Apostolia Galani (1) Stamatia Giannarou (1) George Mylonas (1) Zoltan Takats (1, 2) Burak Temelkuran (1, 2) (1) Imperial College London, London, United Kingdom (2) Rosalind Franklin Institute, Harwell, United Kingdom

P-106

Zhou, Weiwei
National Physical Laboratory, United Kingdom

Scylla: A multi-modal compatible and vendor-independent ambient mass spectrometry imaging platform with high-speed sensor data streaming and pixel-wise data traceability

Introduction:
Ambient mass spectrometry imaging (AMSI) is a powerful group of analytical techniques which enables MS data acquisition directly on sample surface under atmospheric environment. AMSI is frequently limited by the inflexibility of homebuilt ad-hoc software which is significantly costly to maintain, modify, and upgrade its components. This is particularly prominent when needing to switch between different modalities. Similarly, MS proprietary software are only capable of performing predetermined modes of operation in a manual way. Additionally, sensor data streaming and storage are not available in any MS software. We report the development, application, and technical evaluation of Scylla, a multi-modal compatible LabVIEW-based AMSI control and monitoring platform, which provides vendor-independent flexibility, comprehensive sensor data streaming capability, and pixel-wise image quality traceability.
Method:
The fundamental architecture of Scylla is a modular multiple-loop Queue Message Handler application framework, which executes multiple subroutines in parallel at different delays and rates while retaining inter-module communication. Scylla offers unique advantages so that each physical or functional module is decoupled to the rest of the framework and readily modifiable. Generic Hardware Abstraction Layer is written to simplify the switching process between hardware components from different vendors. Scylla also operates a dedicated high-speed sensor data streaming module, which logs data from peripheral devices (energy meter, motor readout, thermocouple, etc.). Sensor data are then used to facilitate the image data conversion and pixel-wise data quality interrogation. Scylla has been applied to multiple AMSI source setup including IR-REIMS, IR-LDI-PPI, and AP-UV-MALDI.
Results:
Scylla performance is evaluated at various levels of sample and instrumental complexities. Within a single modality, off-tissue total ion intensity showed excellent level of stability over 18-hour experimental time. PCA results also suggested the absence of time-dependent signal instability. To evaluate data reproducibility, the left and right parts of an axial-symmetrical coronal mouse brain image were used as training and testing data set, respectively, to test the fitted Linear Discriminant Analysis (LDA) classifier model based on training (left) k-means results. Predicted testing (right) data demonstrated a high level of symmetry to the training (left) data and a good agreement with the k-means obtained using whole brain. Single ion images (SII) showed high signal-to-noise ratio where numerous lipid species were detected in the 700-900 mass range. Distinct anatomical features are visible through SII and k-means segmentation. To evaluate the robustness of Scylla performance across modalities, streamed sensor data, which were acquired from vendor-independent peripheral devices for different modalities, were examined against image quality. From sensor data heatmaps, it was visible that streamed sensor data accurately captured subtle dynamic changes during experiments, which can be used to facilitate datacube reconstruction, and to interrogate image quality retrospectively. An even more evidential example was demonstrated when comparing MS image against pixel-resolved IR-laser parameters heatmaps. To evaluate the consistency of Scylla generated data from similar samples under significantly different conditions, a recently (2022) acquired coronal mouse brain image was used to fit a LDA classifier model, which was then used to predict k-means segmentation of an unrelated sagittal mouse brain image acquired in 2019 on a different MS instrument. It can be noted that, not only the predicted segmentation was in a good agreement with those obtained using its own spectra, but the cluster identities, manifested as anatomical regions, also correlate prominently between the two.
Novelty:
Scylla is the first universal interface for AMSI with multi-modal compatibility evaluated on diverse fresh-frozen tissue samples and hardware combinations.
Preliminary Data:
Excellent signal stability, data reproducibility, and spectral quality. Robust sensor data streaming. Consistency between data acquired under significantly different conditions.

Contributing Authors:
Weiwei Zhou1, Efstathios Elia1, Rory T. Steven1, Alex Dexter1, Zoltan Takats2, Josephine Bunch1,2* 1 National Centre of Excellence in Mass Spectrometry Imaging, Chemical and Biological Science Department, National Physical Laboratory, Teddington, TW11 0LW, UK 2 Faculty of Medicine, Department of Metabolism, Digestion and Reproduction, Imperial College London, London, SW7 2AZ, UK * Corresponding author: josephine.bunch@npl.co.uk

P-107

Zickuhr, Greice Michele
University of St Andrews, United Kingdom

Evaluation of DESI-MSI for integration into histopathology workflows for biomarker discovery.

Introduction:
DESI-MSI has the potential to be a valuable translational and investigative tool for biomarker studies. Its application in histology workflows uses adjacent sections for histological analysis and immunophenotyping, thus limiting spatial co-registration. We report a workflow that uses a single tissue section to obtain high molecular and phenotypical information suitable for image analysis. The integration of DESI-MSI, with high MeOH content as the desorption solvent and a heated transfer-line, with H&E, PAS, multiplex immunofluorescence, and immunohistochemistry results in a rich unambiguous tool for correlation of metabolic markers and phenotypic features.
Method:
Human kidney sections (10 µm thickness) were analysed by DESI XS MSI (Xevo G2 QToF, Waters) at 20 x 20 µm pixel size varying scan speeds (10, 20 or 30 scans/sec) and the heated transfer-line temperature (at 150 or 450 oC). Data were acquired in negative ionization mode between m/z 50 – 1200, processed and analysed in HDI® (Waters). Post-DESI sections were histochemically stained (H&E and PAS) to identify morphological features. A multiplex immunofluorescence panel comprising Nucblue™ and antibodies against p57 and PFKFB3 was applied to the same sections. Fluorophores were stripped and a further immunohistochemistry panel of vimentin and pan-cytokeratin antibodies was applied. Images were obtained at 20x resolution (Zeiss Axioscan scanner) and analysed by HALO® AI (Indica Labs).
Results:
DESI-MSI analysis using the novel heated transfer-line at 450 oC yields higher lipid signal intensities when compared to 150 oC. In the range of m/z 600 – 900, 450 oC resulted in an overall intensity increase of 1.8-fold with 98:2 MeOH:H20 as the desorption solvent. At the compromise of increased sensitivity, the heat generated by the transfer-line and the solvent from the sprayer results in coagulation of proteins in the tissue confirmed by histological assessment by an experienced kidney pathologist of the sections post-DESI acquisition with H&E and PAS staining. Both histological stains reveal more extracellular matrix and intra-tubular protein contents in tissue sections submitted to DESI when compared to control sections (room temperature and DESI not-scanned but kept in the box). The same pattern was observed in the immunofluorescence results with an increased signal intensity of protein biomarkers of tissues scanned by DESI with higher transfer-line temperatures. Despite the difference in intensities, tissue features were recognizable in all four staining procedures applied to the tissue post-DESI scanning. In addition to the assessment and confirmation of overall tissue morphology and basement membranes integrity provided by H&E and PAS staining, with the immunofluorescence and immunohistochemistry panels we identified kidney features such as podocytes, glomeruli and different tubules, and applied image analysis software to generate images. These results combined indicate that a single tissue section can be submitted to DESI-MSI analysis and a combination of histological techniques, with no loss of epitopes and spatial information.
Novelty:
Evaluation of DESI-MSI to enable metabolic profiling and colocalization of phenotypic features from a single tissue section for biomarker discovery.
Preliminary Data:
Technical and biological replicates for DESI-MSI experiments followed by a panel of four different histology assessments.
Contributing Authors:
Greice Michele Zickuhr; Dr Alison Dickson; Prof David Harrison; Dr In Hwa Um
Dr Alison Dickson;
Prof David Harrison;
Dr In Hwa Um

P-108

Zoratto, Samuele
TU Wien, Austria

Quantifying the distribution of endogenous lipids in skin – bridging the gap between MS imaging and Lipidomics

Introduction:
While MALDI MSI provides high-resolution spatial distribution of analytes, it still struggles to provide reliable quantitative information, especially for endogenous compounds. This limits our ability to fully understand the complexities of biological systems like skin tissue. Here, we propose an approach that employs a gelatin-based medium to establish an external matrix-matched calibration function for selected analytes, to quantify skin's endogenous lipids. In particular, we explored ionization effects related to acyl chain length and those from different matrices, such as tissue and tissue surrogates. The presented method aims to bridge the gap between MALDI MSI and in-depth lipidomic analysis.

Method:
Lipid calibrant solution (LipCAL) is comprised of 1,2-dihexanoyl-sn-glycero-3-phosphocholine (DHPC), 1,2-dilauroyl-sn-glycero-3-phosphoethanolamine (DLPE), 1,2-dipalmitoyl-sn-glycero-3-phosphocholine (DPPC), 1,2-distearoyl-sn-glycero-3-phosphoethanolamine (DSPE), and 1,2-diarachidoyl-sn-glycero-3-phosphocholine (16:0 PC). LipCAL was prepared as stock and diluted to appropriate concentration levels before mixing it with gelatin and depositing it on ITO slides. Lipids were analyzed as sole standard compounds, as a mixture, in solution, and within the gelatin medium. Gelatin blocks with different LipCAL concentrations were cryosectioned and mounted on microscopic slide; several sectioning thicknesses were investigated. All analyses are conducted in positive ion mode on a 7T scimaX FTICR MRMS (Bruker) equipped with a dual ESI/MALDI source. For MALDI MSI 1,5-Diaminonaphthalene was used as matrix.

Results:
Currently, MALDI MSI is known to be, at best, a semi-quantitative analytical technique. Hence, we propose an approach to quantify endogenous lipids by MALDI MSI with a particular focus on skin. Five carefully selected lipids, with diverse headgroups and acyl chain lengths, were embedded into a gelatin medium at varying concentrations to create an external matrix-matched calibration function. With its skin-like properties, the gelatin medium simulates the matrix effects, ranging from ion suppression to influences on ionization efficiency, as typically observed in skin tissue. To test the fidelity and robustness of the proposed approach, we performed systematic investigations at different lipid concentration levels either alone, combined, or mixed with gelatin. Isolated and combined lipids were investigated via direct infusion ESI FTICR MS. When mixed in gelatin, the isolated or combined lipids were analyzed via MALDI FTICR MSI. At first, the mixture was spotted before hardening on a glass slide and then analyzed. Later, the mixture was cured, frozen, sectioned, and mounted on a slide. Multiple thickness settings were explored. Furthermore, we compared these analyses with recent results (IMSC 2022) from skin equivalents. In those previous experiments, a lipid standard solution (LipSTD) comprised of 1,2-dinonanoyl-sn-glycero-3-phosphocholine (DNPC), DPPC, and 1-palmitoyl-2-arachidonoyl-sn-glycero-3-phosphocholine (PAPC), was used to dope skin equivalents (SE, 3D cell cultures) with and without fibroblasts. SEs were exposed to 0/80 J/cm2 UVA radiation to generate oxidized PAPC (oxPAPC) species, thereby altering LipSTD levels. External calibration was then performed directly from the standard applied on the glass slide without considering matrix effects. These results can now be used to better understand ion suppression and matrix ionization efficiencies for in tissue quantification. Lastly, oxPAPC quantitative information can be derived and compared to previous results. The authors thank the Federal Ministry of the Republic of Austria and CHANEL Parfums et Beauté for financial support.

Novelty:
We developed a new approach to quantify endogenous lipids in skin sections by MALDI MSI.

Preliminary Data:
Preliminary results support our gelatin-based calibration approach as a tool for the quantitative analysis of lipids via MALDI MSI.

Contributing Authors:
Samuele Zoratto, Christopher Kremslehner, Florian Gruber, Martina Marchetti-Deschmann

P-109

Castellani, Elena
University of Oxford, UK

Development of a High Throughput Microscope Mode Secondary Ion Imaging Mass Spectrometer

Introduction:
Secondary Ion Mass Spectrometry (SIMS) is a surface-analysis mass-spectrometric technique in which a primary ion beam irradiates a solid sample, hence releasing secondary ions that are then collected by a mass analyser. SIMS is one of the key ionisation techniques in Mass Spectrometry Imaging (MSI), in which a primary ion beam is used to visualize the spatial distribution of the sample, thus considerably expanding the analytical sensitivity of conventional mass spectrometry. By coupling a defocused primary ion beam with stigmatic ion optics and a position-sensitive detector, SIMS imaging can be performed in microscope mode. In this work, we combined a pulsed ion extraction technique, Pulsed Extraction Delayed Acceleration (PEDA), and multi-mass ion imaging, with a fast CMOS detector with high time resolution, thus allowing for the simultaneous analysis of large sample areas with high mass and spatial resolution resolution.

Methods:
A defocused beam of C60+ ions, produced by a primary ion gun initially developed for microprobe mode SIMS imaging, was combined with novel extraction optics and a multichannel-plate/phosphor screen detector assembly. Optimal voltage conditions for each component were obtained via simulations with SIMION, an ion trajectory software, using a Genetic Algorithm (GA). A secondary electron detector was used to acquire beam profile images and to ensure that the beam defocussed in a uniform manner. The spatial resolution was tested by recording microscope mode MS images of Rhodamine B samples sprayed through a metal grid using a Pixel Imaging Mass Spectrometry (PImMS) camera, which is equipped with a fast time-stamping device with time resolution of 12.5 ns. Hence, PImMS is capable of recording not only intensity information, but also time of flight. The mass resolution was instead tested on metal samples by measuring the leading edge of a reference mass peak, recorded using both a photomultiplier tube and the PImMS camera.

Novelty:
Coupling of microscope mode SIMS imaging with secondary ion mass spectrometry and pulsed extraction of the secondary ions.

Preliminary data:
A highly defocused C60+ primary ion beam was achieved by lowering the voltage on a focusing lens stack on the ion gun. The beam profile was studied via secondary electron imaging, which showed that the ion beam maintained an even coverage over several millimetres of the sample surface, making it suitable for microscope mode MSI. Moreover, the primary beam was probed at different positions along the x and y coordinates using two sets of deflectors, thus ensuring the beam had even flux across the whole sample. The combination of stigmatic optics and a pulsed extraction of the secondary ion beam allowed for the retention of both time of flight and spatial information at the detector. SIMION simulations ensured that, despite changing the ion extraction field, the secondary ion beam could still reach the centre of the detector. Photomultiplier tube mass spectra of metal samples were recorded using both positive and negative polarity, showing great accord with literature. The time resolution, measured as the 20%-80% portion of the leading edge of the most abundant mass peak, was approximately 10 ns, which roughly corresponds to the rise time of the scintillator used to transform the ion signal into photons. Microscope mode images of Rhodamine B dye sprayed through metal grids of different sizes gave a spatial resolution of 23.8 ± 8.2 µm, over an area of ~1.86 mm2. This value for spatial resolution is in great accord with simulations and results achieved with another microscope mode imaging mass spectrometer, which instead uses matrix assisted laser desorption-ionisation (MALDI) as the ionisation method. These results show that microscope mode SIMS imaging is a promising technique for the rapid simultaneous analysis of multiple composite samples, with potential applications on samples of biological and biomedical interest.

Contributing Authors:
M. Elena Castellani,1,2 Yifeng Jia,1 Anya Eyres,1 Natasha Smith,1 Michael Burt,1 Josephine Bunch, 2 Zoltan Tákats 2, Mark Brouard 1 and Felicia Green 2
Affiliations:
1. Department of Chemistry, University of Oxford, Chemistry Research Laboratory, Oxford, OX1 3TA
2. Rosalind Franklin Institute, Harwell Campus, Didcot, OX11 0QX